Chikungunya virus nonstructural protein 1 as an antiviral target

Kovacikova, K.

Chikungunya virus nonstructural protein 1 as an antiviral target

Kristina Kovacikova

The research described in this thesis was performed at the Department of Medical Microbiology of the Leiden University Medical Center, Leiden, the Netherlands and was funded by the Marie Sklodowska-Curie ETN European Training Network “ANTIVIRALS” (EU grant agreement 642434).

ISBN: 978-94-6416-510-4
Cover design: Barbora and Jaroslav Sebes
Lay-out: Publiss | www.publiss.nl
Print: Ridderprint | www.ridderprint.nl

Chikungunya virus nonstructural protein 1 as an antiviral target

Proefschrift

ter verkrijging van
de graad van doctor aan de Universiteit Leiden,
op gezag van rector magnificus prof. dr. ir. H. Bijl,
volgens besluit van het college voor promoties
te verdedigen op dinsdag 20 april 2021
klokke 15:00 uur

door

Kristina Kovacikova
geboren te Zilina, Slowakije
in 1991

Promotor

Prof. dr. E. J. Snijder

Co-promotor

Dr. M. J. van Hemert

Leden promotiecommissie

Prof. dr. A. Geluk
Prof. dr. F. J. M. van Kuppeveld (Utrecht University)
Dr. T. Ahola (University of Helsinki)
Dr. S. Myeni

Table of contents

Everything will be okay in the end. If it's not okay, it's not the end.
-statement attributed to John Lennon (1940 – 1980)-

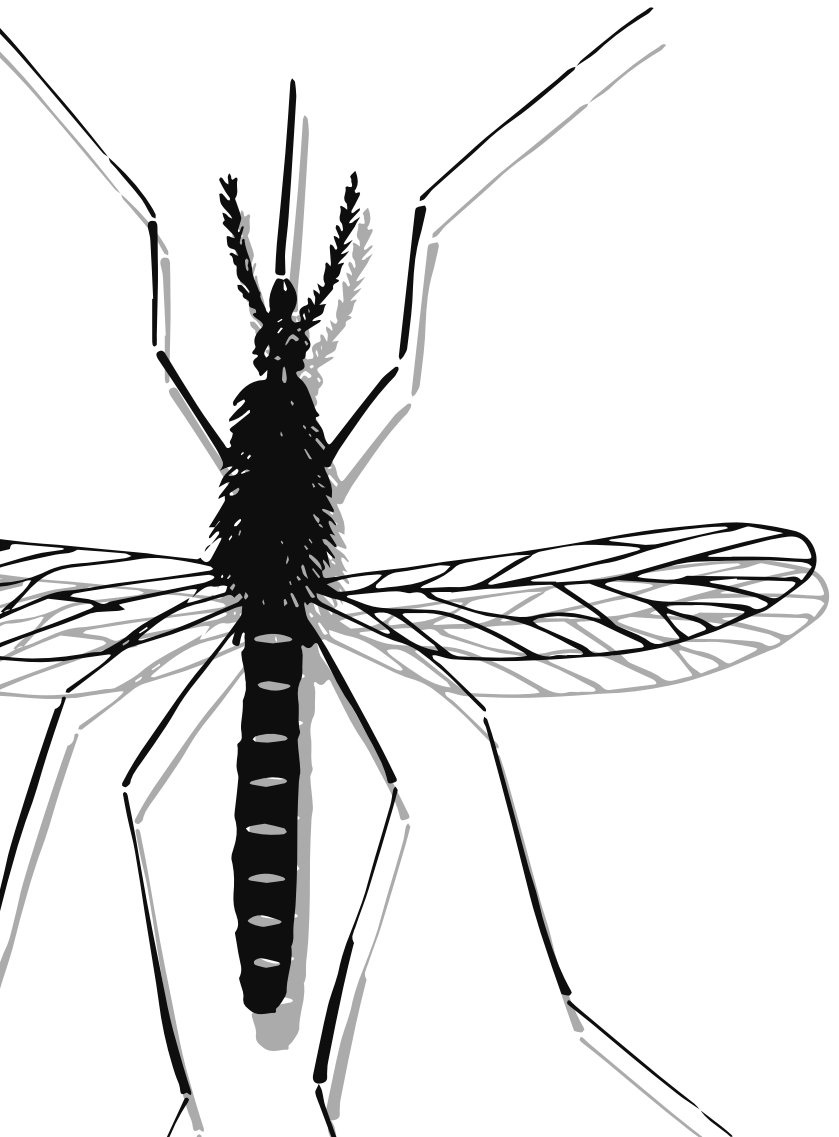

CHAPTER 1

General Introduction

Alphaviruses as human pathogens

The vast majority of (re)emerging viral infectious diseases are caused by viruses with an RNA genome. Among these, arthropod-borne (arbo)viruses are especially important, since they can result in high morbidity and mortality of people and livestock. They alternate between vertebrate and invertebrate hosts which makes their replication cycles unique and fundamentally different from those of single-host RNA viruses. Mosquito-borne alphaviruses are divided into arthritogenic and encephalitic alphaviruses. The arthritogenic alphaviruses include chikungunya virus (CHIKV), Semliki Forest virus (SFV), Sindbis-like viruses (SINV), Mayaro virus (MAYV), o'nyong-nyong virus (ONNV), Barmah Forest virus (BFV) and Ross River virus (RRV), among others, and are a major cause of infectious arthritis-like disease worldwide. They are typically endemic in Africa, South and Southeast Asia, parts of Central and South America as well as southern and northern Europe. The encephalitic alphaviruses include Venezuelan equine encephalitis virus (VEEV), Eastern equine encephalitis virus (EEEV) and Western equine encephalitis virus (WEEV). These viruses circulate in Central, South and North America. While relatively rare in humans, they can cause one of the most severe acute viral infections with neurological symptoms. These viruses can also be spread by aerosols, and therefore their potential misuse for biological warfare is of great concern, which is why they are currently placed on the US Select Agents and Toxins list.

The first symptom of an infection with arthritogenic alphaviruses is a febrile illness, which can progress to rheumatic disease, described as polyarthralgia and/or polyarthritis and can be chronic and debilitating. CHIKV was originally isolated in 1952/1953 from the serum of a febrile patient in the present-day Tanzania (1). It is likely that CHIKV epidemics occurred before this period but were misdocumented as dengue fever outbreaks (2). CHIKV is genetically closely related to ONNV, which has so far been geographically restricted to the African continent. CHIKV and ONNV infections cause similar symptoms, which is reflected in the native African names for CHIKV and ONNV that mean "that which bends up" and "weakening of the joints", respectively.

CHIKV persists in sylvatic or enzootic cycles in sub-Saharan Africa, where the transmission occurs between multiple forest-dwelling *Aedes* spp. mosquitoes and non-human primates (NHPs). In sylvatic cycles, humans are considered incidental hosts and are sporadically infected by a spillover from sylvatic vectors. Initially, phylogenetic

studies identified two enzootic CHIKV lineages: West African and East/Central/South African (ECSA) (3). An Asian lineage, likely to have originated from the ECSA lineage, was first isolated in 1958 and implicated in outbreaks in India and Southeast Asia during the 1960s (4). In both Africa and Asia, CHIKV epidemics occurred with intervals of 7 to 20 years between the 1950s and 2000s. The Indian Ocean lineage (IOL), a descendant of the ECSA lineage, was responsible for the explosive CHIKV outbreak in coastal Kenya in 2004, from where it spread over several Indian Ocean islands and subsequently to large parts of South and South East Asia. Since then, it has caused recurrent and sometimes large epidemics, especially in the Indian subcontinent and in Southeast Asia (5, 6).

Like for other arboviruses such as ONNV, Zika virus (ZIKV) and dengue virus (DENV), humans are not considered dead-end hosts and the human-mosquito-human transmission cycle is responsible for sustaining high CHIKV transmission rates in the human population (7). Prior to 2005, *Ae. aegypti* was recognized as the only vector for CHIKV transmission in urban areas. The amino acid substitution A226V in the E1 glycoprotein (E1-A226V), which was first detected during the La Reunion epidemic in 2005-2006, led to a resurgence of the outbreak on this island and facilitated virus transmission by *Ae. albopictus* (8). After 2006, CHIKV has expanded into the temperate regions of the world via infected air travellers and in part due to its enhanced ability to infect *Ae. albopictus* mosquitoes, which – for example- resulted in recent European outbreaks in Italy in 2007 and 2017 (9, 10) and in France in 2010, 2014 and 2017 (11-13) (Fig. 1). In late 2013, on the Island of St. Martin in the Caribbean, autochthonous CHIKV transmission was reported for the first time in the Americas (14). The outbreak was caused by a CHIKV strain belonging to the Asian lineage that had been circulating in the urban cycle at least since the 1950s (15). Interestingly, Brazil has experienced two independent introductions of CHIKV strains. Since 2014, strains belonging to the Asian lineage and to the ECSA genotype have been co-circulating in the Brazilian territory (16).

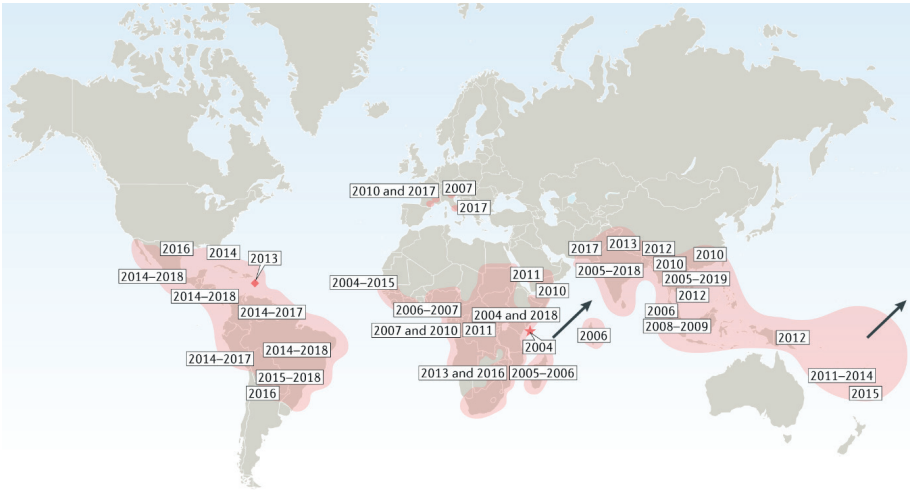

Figure 1: Emergence and spread of the 2004-2020 CHIKV epidemic. In 2004, CHIKV re-emerged on Lamu Island, in Kenya (red star). The epidemic expanded in Africa and spread eastwards across Indian Ocean islands and in Asia. CHIKV reached the Americas in late 2013, when the first autochthonous transmission was reported on the St. Martin Island in the Caribbean (red diamond). From there, CHIKV spread into Central and South America. Throughout the CHIKV epidemic, small regional outbreaks have also occurred in Italy and France and southern USA. Reused with permission from (17).

Disease manifestations, clinical outcome and economic impact of CHIKV infection

CHIKV typically causes a self-limiting febrile illness known as chikungunya fever (CHIKF) associated with potentially chronic debilitating joint and muscle pain. CHIKV outbreaks are characterized by high attack rates, with up to 30 – 75% population being affected with CHIKV at a time (18). Most CHIKV infections are symptomatic and the number of people who develop symptoms is on average higher than for those infected with flaviviruses, for example. The incubation period for CHIKV infection ranges from 2 to 7 days. The onset of fever is often very abrupt and the fever typically lasts up to 7 days. In some cases, the clinical symptoms can resemble those of diseases caused by other arthropod-borne agents, such as DENV. Polyarthralgia usually develops around the same time and primarily affects the peripheral joints such as fingers, toes, wrists, elbows and knees. Some individuals also develop an itchy maculopapular skin rash, affecting mainly the torso and the extremities (19). The disease is associated with high morbidity, but is rarely fatal. In general, patients with chronic CHIKV recover

within 3 – 24 months (20). However, the La Reunion epidemic brought to light atypical manifestations such as severe neurological complications, including encephalitis and Guillain-Barre syndrome (21). Such forms of CHIKF are less frequent and limited to subgroups of patients like the elderly, the very young and people with underlying comorbidities (22, 23). Infections acquired via mother-to-child transmission, first reported during the La Reunion outbreak, can be fatal or involve severe neurological sequelae in foetuses and young infants (24). The economic impact of CHIKV is high, especially given the burden of disease and related consequences for work and school absenteeism. There is an immediate cost to the patient due to lost productivity and associated treatment costs.

CHIKV genome structure and replication cycle

CHIKV is a small, enveloped (+) strand RNA virus that belongs to the Old Word (Semliki Forest virus-like) group of arthritogenic alphaviruses within the *Togaviridae* family. The CHIKV genome comprises a single-stranded RNA genome of 11,800 nucleotides, with a 5' 7-methylguanosine cap and a 3' poly-A-tail. The genome contains two open reading frames (ORFs) that are flanked by 5' and 3' untranslated regions (UTRs) (25). The 5' UTR comprises 76 nucleotides while the 3' UTR contains as many as 526 nucleotides. In addition, a third UTR of 68 nucleotides is found between the two ORFs and carries a promoter sequence to direct the transcription of the 26S subgenomic RNA (26). The first ORF, constituting approximately the 5' two-thirds of the genome, encodes for nonstructural proteins 1-4 (nsPs) that are part of the viral replicase complex. The second ORF, which is expressed from the 26S mRNA, covers the 3' one-third of the genome and encodes for six proteins: capsid (C), E1, E2, E3, 6K and transframe (TF) protein (27), the latter being a product of-1 ribosomal frameshifting in the sequence encoding the 6K protein (Table 1). The CHIKV virion is formed by a glycoprotein shell enclosing a host-derived lipid bilayer and an icosahedral nucleocapsid composed of 240 units of C proteins. The CHIKV envelope carries 80 sets of spikes, each made up of three E1-E2 heterodimers (28).

Table 1: CHIKV proteins and their functions

Protein	Function	Reference
nsP1	guanine-N7-methyltransferase	(42)
	guanylyltransferase	(43)
	membrane association	(44)
nsP2	nucleoside triphosphatase	(45)
	RNA 5' triphosphatase	(46)
	helicase	(47)
	protease	(48)
	innate immune evasion/host shut-off	(49, 50)
nsP3	ADP-ribosylhydrolase	(51, 52)
	replication	(53)
nsP4	RNA-dependent RNA polymerase	(54, 55)
	terminal adenylyltransferase	(56)
C	nucleocapsid formation	(37)
E1	membrane fusion	(57, 58)
E2	receptor binding	(59)
E3	particle assembly	(60)
6K	ion channel	(61, 62)
TF	(particle assembly)	(39)

CHIKV enters cells via E2-mediated attachment to a host cell receptor (Fig. 2). The matrix remodelling-associated protein 8 (Mxra8) has been identified as a receptor for multiple arthritogenic alphaviruses (29). Glycosaminoglycans (GAGs), which are expressed on many susceptible cell types, also serve as an attachment factor and aid CHIKV entry into the cells. Following viral attachment to the cells, viral particles are internalized mainly by clathrin-mediated endocytosis. Endosomal acidification triggers conformational changes in the viral glycoproteins which lead to the insertion of the E1 fusion loop into the host membrane (30). The membrane fusion process occurs rapidly and is highly dependent on the presence of cholesterol (31). Following release into the cytoplasm, the incoming viral RNA (vRNA) gets directly translated to produce the P1234 replicase polyprotein precursor. Nevertheless, only about 10% of the translation events produce the full P1234 polyprotein precursor, whereas the rest yields a P123 polyprotein (25). To produce P1234, translational readthrough has to occur due to the presence of an opal (UGA) stop codon between the nsP3- and nsP4-coding sequences, which is thought to regulate the levels of nsP4 (32). The P1234 polyprotein precursor is cleaved in *cis* into P123 and nsP4 by a protease domain in

nsP2. P123 together with nsP4 forms an 'early replication complex', which is short-lived, synthesizes a full-length (-) strand vRNA (33) and induces the formation of virus replication compartments termed spherules. Spherules serve as the sites for vRNA replication and are initially targeted to the plasma membrane by the nsP1 portion of P123, while later during infection they form endosome-like compartments in the cytosol (34), also called virus-induced type 1 cytophathic vacuoles (CPV-1) (35, 36). Later in the replication cycle, P123 gets further cleaved in *trans* into the individual nsPs, which can assemble into a nsP1-4 'late replication complex'. The nsPs can be

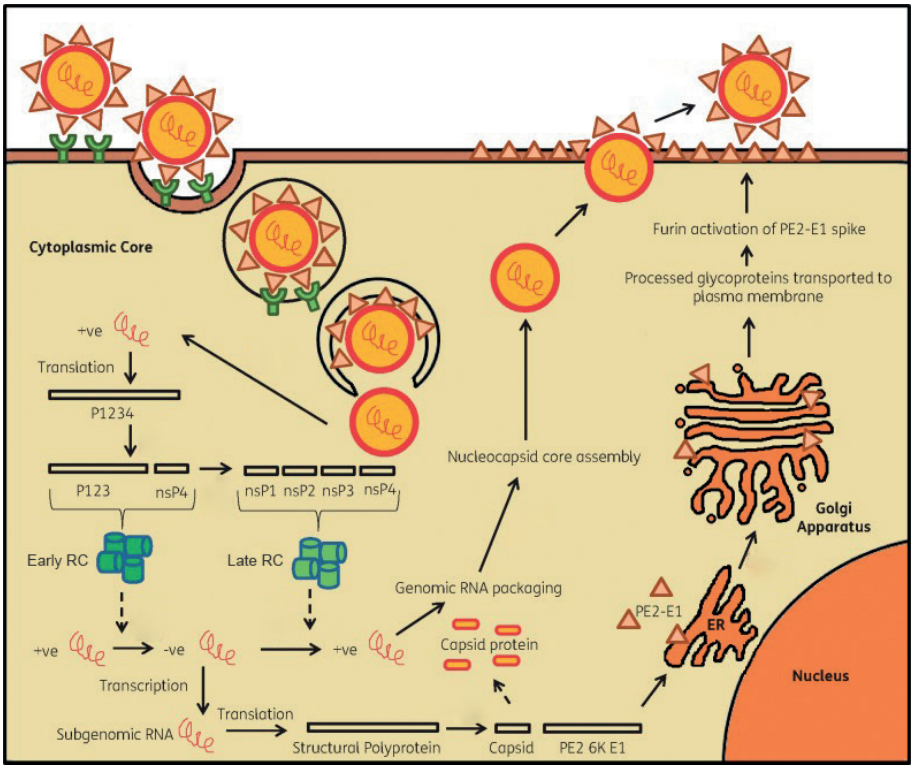

Figure 2: CHIKV replication cycle. In short, CHIKV enters cells mainly via clathrin-mediated endocytosis upon which the nucleocapsid is released into the cytosol. The incoming vRNA is translated to produce P1234 polyprotein precursor, which is first cleaved into P123 and nsP4 and forms an early RC, and then fully processed nsP1-4 form a late RC. The early RC is responsible for the synthesis of (-) strand vRNA and spherule formation while the late RC carries out the synthesis of genomic (+) strand vRNA and 26S subgenomic (+) strand vRNA. Following translation of the structural polyprotein derived from the 26S subgenomic (+) strand vRNA, the C protein is autocatalytically cleaved and forms a nucleocapsid upon interaction with newly synthesized genomic (+) strand vRNA. The E1 and E2 glycoproteins undergo a series of post-translational modifications in the Golgi secretory pathway, following which they assemble at the host plasma membrane. Finally, the CHIKV nucleocapsid acquires a host-derived lipid bilayer with E1 and E2 glycoproteins upon release from the host cell. Adapted from (63).

found at the neck of spherules, which harness dsRNA intermediates in order to protect them from detection by the cytoplasmic innate immune sensors. The late replication complex is responsible for the synthesis of genomic (+) strand vRNA and 26S subgenomic (+) strand vRNA. The 26S subgenomic (+) strand vRNA encodes the structural polyprotein C-E3-E2-6K(TF)-E1. Following autocatalytic cleavage of the C protein from the structural polyprotein (37), the C protein in the cytosol interacts with newly synthesized genomic (+) strand vRNA to initiate the formation of nucleocapsids (38). Subsequent synthesis of the structural polyprotein generates a majority product E3-E2-6K-E1 and a minority product E3-E2-TF due to ribosomal frameshifting (27, 39). A signal sequence in the N-terminal region of E3 directs the major and minor structural polyproteins to host secretory pathways where they get modified. Cleavage by host proteases results in pE2 (E3-E2); 6K or TF; and E1 (40). During the transit through the Golgi secretory pathway, E1 and E3-E2 undergo conformational changes and post-translational modifications including palmitoylation, N-linked glycosylation and E3 release due to host furin cleavage. At the late phase of infection, type 2 cytophathic vacuoles (CPV-2) transport E1 and E2 glycoproteins from the *trans*-Golgi network to the plasma membrane (41). Finally, fully formed nucleocapsids carrying full-length (+) strand genomic RNA assemble at the plasma membrane with mature E1 and E2 glycoproteins to form a mature virion, which is released from the host cell (33).

Immunopathology of CHIKV infection during the acute phase

Upon a bite of an infected mosquito, CHIKV primarily replicates in dermal fibroblasts. From the skin, the virus migrates to other parts of the body via the lymphatic system until it reaches the bloodstream. Through the bloodstream, CHIKV reaches joint, muscle and bone tissue, which represent the main sites linked to the most commonly observed clinical manifestations (Fig. 3). While the clinical course of CHIKV infection is rather well-documented, molecular details on how precisely CHIKV causes disease are not well understood. Many of the antiviral responses that are involved in immunopathology are also essential for the clearance of viral infection, which has important implications for the development of therapeutics.

During acute chikungunya fever, patients experience peak viremia at day 2 after the initiation of symptoms. The viremia declines sharply during days 3 and 4, and becomes undetectable by day 5 (64). CHIKV reaches a high viral load during the acute

phase of infection (> 10^6 to 10^{10} viral particles per millilitre of blood), with particularly high titres in the elderly. The strong decline in viremia before the generation of potent neutralizing antibodies is consistent with an important role for the early interferon (IFN) response. The recapitulation of CHIKV infection in a mouse model with abrogated IFNα/β signalling resulted in severe CHIKV infection (65). Type I IFNs, such as IFNα or IFNβ, are highly efficient in limiting CHIKV replication. To counteract the host IFN response, alphaviruses have evolved suppression and evasion mechanisms, for example by eliciting a nsP2-mediated host transcriptional shutoff in infected cells (66, 67). Interestingly, the anti-alphaviral activity of type I IFNs is less effective at lower temperatures. The peripheral disease of limbs and extremities appears to be a consequence of enhanced CHIKV replication in these sites, owing to their slightly lower body temperature (68).

Experimental evidence suggests that fibroblasts could be the principal source of type I IFNs during CHIKV infection (69). Skeletal muscle, joint and dermal fibroblasts are the primary sites of CHIKV replication early in infection (70). The presence of Mxra8 on a vast array of different cell types (71) indicates that monocytes, macrophages, endothelial cells or nerve cells can also serve as a potential reservoir. The acute phase of CHKV infection in humans results in increased pro-inflammatory cytokines including interleukin 6 (IL-6), monocyte chemotactic protein 1 (MCP-1), IFNα, IFNγ, IFNγ-induced protein 10 (IP-10) and monokine induced by IFNγ (MIG) (72, 73). Some of these molecules serve as chemokines and are responsible for recruiting leukocytes to the sites of infection and triggering cellular responses.

High plasma levels of IFNγ, IL-4, IL-7 and IL-12p40 are associated with the onset of adaptive immunity. The primary response to acute CHIKV infection is also characterized by a strong up-regulation of $CD8^+$ cytotoxic T cells (74) and the development of neutralizing antibodies (Abs). Neutralizing anti-CHIKV IgM Abs develop as early as 4 days after the onset of symptoms and play the predominant neutralizing role in the first phase of infection (75). Neutralizing anti-CHIKV IgG Abs, consisting primarily of the IgG3 isotype, are usually detected when the virus is cleared (7-10 days after the onset of symptoms) and persist for many years. A robust IgG3 response is linked to a more severe acute phase but reduces the likelihood of developing persistent arthralgia (76). These observations indicate that the adaptive immune response plays an important role in controlling CHIKV-induced arthritis, further suggesting a direct link between viral infection and joint inflammation (77) (Fig. 3). The acute symptoms usually resolve within 2 weeks, but incapacitating arthralgia may linger for weeks to months and in some cases even years.

Mechanisms of CHIKV persistence and tissue inflammation during a chronic phase

Chronic chikungunya arthritis (CCA) is often described as a rheumatic syndrome as the pathogenesis of CCA and rheumatoid arthritis may involve similar mechanisms. Long-lasting arthralgia, in particular, is a clinical sign that distinguishes CHIKV from DENV infection. Up to 40% of infected patients ultimately develop CCA. The increased probability of developing CCA depends on predisposing factors such as comorbidities (e.g. diabetes), older age (>35-45 years for joint pain), and high viremia and severe disease during the acute phase (78).

CHIKV infection is cytopathic and results in direct tissue injury. Alphavirus-associated arthritides are predominantly caused by mononuclear cells such as monocytes and macrophages, with some contribution of B cells, T cells and natural killer (NK) cells (17). Studies in a macaque model indicate that macrophages are the likely main cellular reservoir of persistent CHIKV. At later stages of infection, CHIKV was found to persist in joints, muscles, lymphoid organs and liver for at least 3 months after viral inoculation (79). In addition, musculoskeletal cells and fibroblasts have also been shown to harbour persistent viral RNA (80). CHIKV persistence in these target sites is likely responsible for the long-lasting disease symptoms. There are several ways in which pathogenic CHIKV can establish persistence, such as by evasion of neutralizing antibodies produced by B cells (81) or by evasion of antiviral $CD8^+$ T cell immunity (82). CHIKV-apoptotic blebs, among others, have also been implicated in virus persistence by allowing the virus to escape the host immune response and infect neighbouring cells (83). CHIKV-induced arthropathies likely emerge from innate and adaptive immune responses stimulated by the virus and/or viral material (RNA or protein) in joint tissues (84). Strikingly, researchers have struggled to isolate infectious virus from patients with chronic disease. One study reported the isolation of CHIKV RNA and protein from synovial macrophages of 1 patient 18 months after infection (85), illustrating the difficulty to obtain infectious virus from chronic patients.

CCA has been associated with increased circulating levels of pro-inflammatory cytokines including IL-6, granulocyte macrophage colony-stimulating factor (GM-CSF), IFNα and IL-17 (86). In CCA, plasma levels of IL-6 and GM-CSF have been found to be significantly higher in patients with persistent arthralgia compared to those who recovered (87). CHIKV-infected monocytes in the later stage of infection are the major source of pro-inflammatory mediators IFNα, IL-12, CC-chemokine ligand 2 (CCL2)

and CXC-chemokine ligand 10 (CXCL10) (88), while macrophages produce mostly IL-6 and tumour necrosis factor (TNF) (89). A major challenge for the field has been the identification of proinflammatory immune mediators that could be targeted with therapeutics without compromising their antiviral functions.

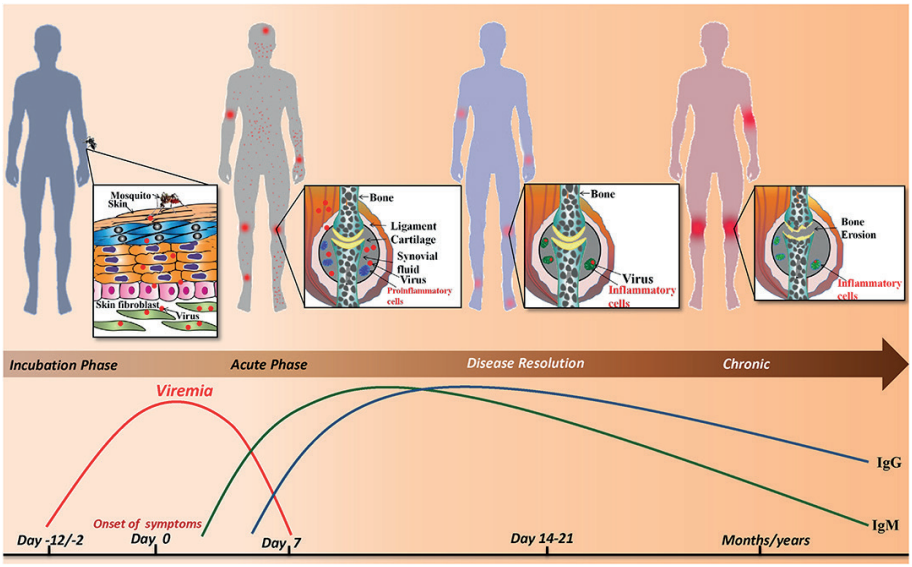

Figure 3: The clinical course of CHIKV infection. Following a bite of an infected mosquito, CHIKV primarily replicates in dermal fibroblasts from where it spreads to the rest of the body via the lymphatic system and the bloodstream. CHIKV mostly affects large synovial joints such as the knee and the elbow and the main clinical symptoms include fever, maculopapular rash and joint and muscle pain. The high viral load is initially controlled by the host innate immune response, while later during the infection it correlates with the development of neutralizing IgM and IgG antibodies. Despite the robust host immune response, viral particles can persist in the synovial fluid of the joints, which can result in severe pathology lasting months to years. Reused with permission from (90).

Current treatment and a historical perspective on CHIKV antiviral development

Treatment for CHIKF relies on supportive care, short-term opioid analgesics, paracetamol or acetaminophen, and non-steroidal anti-inflammatory drugs (NSAIDs). However, NSAIDs need to be prescribed with caution in patients with a suspected DENV infection, given the possible haemorrhagic complications (91). As the pathogenesis of CCA is not well understood, treatment of patients has remained empirical. In the absence of evidence-based treatment, clinicians often prescribe a variety of anti-inflammatory drugs, in addition to symptomatic treatment with

NSAIDs. Such inflammation suppressing agents include corticosteroids, chloroquine, hydroxychloroquine, sulfasalazine, methotrexate and immune-modulating therapies targeting proinflammatory mediators or T cell responses (reviewed in (92, 93)). So far only three trials examined a therapeutic approach to treat CHIKF in humans. In the early 1980s, a first pilot study to evaluate the efficacy of a potential CHIKV treatment using chloroquine phosphate was conducted. The 20-week treatment program of a small cohort of 10 patients with a daily dose of 250 mg improved the condition in 7 out of the 10 patients (94). In 2007, however, a study on La Reunion Island disproved the benefits of chloroquine treatment on relieving CHIKV symptoms (95). Chloroquine was also tested in an exploratory intervention trial against a commonly used NSAID meloxicam, but failed to prove efficacy in treating musculoskeletal pain and arthritis in patients with acute CHIKV infection (96). The current stages of CHIKV small-molecule antiviral drug development will be discussed in Chapter 2.

Non-small molecule-based inhibitors: treatment with monoclonal (m) Abs and nucleic acids

Besides small-molecule inhibitors, treatment with mAbs has been used as a powerful strategy for the short-term treatment of emerging viral diseases. Neutralizing CHIKV mAbs can block CHIKV entry, fusion and release. The advantage of passive immunization is that mAbs can be administered to any age, high-risk or immunocompromised population due to their safety. However, the high cost associated with the manufacturing of recombinant mAbs represents the biggest obstacle for their development. Several potent human and mouse anti-CHIKV mAbs were shown to be protective against CHIKV *in vivo* (reviewed in (97)). They can be given prophylactically or administered post-exposure to limit CHIKV spread and reduce symptoms in infected individuals. More research is needed to investigate the ability of mAbs to prevent CHIKV persistence in joint tissues. Given the high mutation rate of alphaviruses, escape mutants can develop following treatment with mAbs during acute phase, a problem that can also be encountered during treatment with small-molecule inhibitors. This problem may be overcome by administration of a combination of mAbs targeting different epitopes. One study showed that escape mutants from combination antibody therapy are clinically attenuated (98), arguing for the use of combination therapy in preventing the emergence of drug resistance. Modern approaches rely on the injection of nucleic acids (DNA or RNA) encoding Ab sequences for *in vivo* production of recombinant Abs.

These approaches obviate the need for complex manufacturing and save costs. For instance, a study describing the use of CHKV24 mRNA-encoded mAb formulated in a lipid nanoparticle for treatment of CHIKV-infected mice and NHPs reported protection against arthritis and musculoskeletal disease (99).

CHIKV vaccine development

CHIKV vaccines have been in development for over 50 years, but the efforts intensified only in the past decade with a total of eight promising candidates in Phase I, Phase II and one vaccine candidate currently entering Phase III clinical trials. Considering that CHIKV antigenic diversity is limited and infection may lead to long-lasting immunity, developing a CHIKV vaccine seems to be particularly attractive. Importantly, reciprocal cross-protection after infection with other alphaviruses such as MAYV (100) or ONNV (101) has been reported in animal models, potentially increasing the success of such a vaccine in low-income countries with a high disease burden. Nevertheless, a licensed vaccine against CHIKV is not available thus far. The global market for a CHIKV vaccine has been estimated to be approximately €500 million annually (17). For comparison, the global influenza vaccine market today has on average still a ten-fold higher market value.

Researchers have used various platforms to develop a CHIKV vaccine, including inactivated viral vaccines, live-attenuated virus (LAV) vaccines, recombinant viral-vectored vaccines, virus-like particle (VLP) vaccines, subunit vaccines and nucleic acid-based vaccines. Several CHIKV LAV vaccine candidates have been produced with either mutations, deletions or modifications in CHIKV nonstructural or structural proteins (102-108). In general, LAV vaccines can stimulate stronger and longer-lasting immune response at the cost of lower safety due to the risk of reversion to virulence.

The first CHIKV vaccine tested in volunteers, an isolate from a patient in Thailand named CHIKV strain AF15561, was formalin-inactivated and developed by scientists at the Walter Reed Army Institute of Research, USA (109). An attenuated CHIKV clone selected by passaging strain AF15561 18-times in MRC-5 cells, called CHIKV 181/clone 25 (110), was then tested for safety and immunogenicity in a Phase I trial and entered Phase II clinical trials in 2000 (111). The development of this LAV vaccine was discontinued due to virus-specific side effects, including arthralgia, in approximately 8% of the vaccinees and due to the low incidence of the disease at the time. Studies in mice indicated that the attenuation of CHIKV vaccine strain 181/25 relies on two

mutations in the E2 glycoprotein T12I and G82R (112). Mechanistically, the mutation G82R likely promotes the interaction of the positively charged amino acids within E2 with the negatively charged GAGs (113).

In CHIKV recombinant virus-vectored vaccine development, measles vector has been widely used as a replicating vector owing to its remarkable safety and efficacy. A live-attenuated recombinant viral vectored vaccine comprising the Schwarz vaccine strain of measles virus (MV) engineered to express CHIKV structural proteins has recently been announced to progress into Phase III clinical trials. The CHIKV RNA sequence in this vaccine is derived from strain 06-49 belonging to the ECSA lineage, which was isolated from a patient during the La Reunion outbreak. This vaccine, MV-CHIK, is highly immunogenic and protects mice (114) and NHPs (115) from lethal challenge with CHIKV. In a randomised, double-blind, placebo-controlled Phase I trial the MV-CHIK induced highly neutralizing anti-CHIKV Abs in healthy adults, even in the presence of pre-existing vector immunity (116). After two immunisations, the patients reached a 100 % seroconversion rate. The MV-CHIK vaccine also elicits cross-neutralizing immune response to the CHIKV vaccine strain 181/25, which is based on an Asian lineage isolate. In a randomised, double-blind, placebo-controlled and active-controlled Phase II trial conducted in Europe, healthy volunteers aged 18-55 years were subjected to a dose of control vaccine, MV-CHIK or measles prime and MV-CHIK via the intramuscular route (ClinicalTrials.gov Identifier: NCT02861586). MV-CHIK demonstrated an excellent safety and tolerability in this trial (117) and became the first CHIKV vaccine to enter a Phase III clinical trial.

Another candidate vaccine that entered Phase II clinical trials consists of non-replicating chikungunya VLPs developed at the National Institutes of Health, USA. The VLP vaccine (VRC-CHKVLP059-00-VP) elicited high titre of neutralizing anti-CHIKV Abs in a NHP model of CHIKV infection and protected from disease (118). In a Phase I study with healthy volunteers, the vaccine was well-tolerated and immunogenic, with a second booster vaccination reaching a 100 % seroconversion rate, similar to the MV-CHIK vaccine (119). In a Phase II clinical trial conducted among healthy adults aged 18-60 years in Central America, the study volunteers were subjected to two intramuscular injections given 28 days apart and followed for 72 days (ClinicalTrails.gov Identifier: NCT02562482). The VLP vaccine was well tolerated and demonstrated good safety (120). There is good evidence that a vaccine made against one genotype elicits cross-protective immune response against all CHIKV genotypes, as demonstrated by a study in which recipients of the VLP vaccine developed cross-reactive neutralizing anti-

CHIKV Abs to 9 CHIKV strains belonging to all 3 genotypes (121). On the basis of the promising Phase II results, both MV-CHIKV and CHIKV VLP vaccines have been granted the priority medicines status by the European Medicines Agency.

Vector control strategies

The global population at risk of mosquito-borne infections such as CHIKV, DENV or ZIKV is expanding due to changes in distribution of two key vectors: *Ae. aegypti* and *Ae. albopictus.* Their worldwide distribution is largely driven by the presence of suitable climate and human movement. Until a vaccine or therapeutic treatment for CHIKF becomes available, people living in the world's most affected areas have to rely on vector control to limit the contact with virus-carrying mosquitoes. Traditional methods in controlling vector-borne diseases use larvicides and insecticides, but their use has become less effective due to the emergence of insecticide resistance and the inability of insecticides to penetrate house walls, where many adult female mosquitos rest and feed (6). Modern strategies of mosquito control include the Sterile Insect Technique to generate transgenic sterile male *Ae. aegypti* mosquitoes. This lethality-based approach essentially reduces the mosquito population and, as such, possibilities for viral transmission (122). More elegant strategies have used a maternally-inherited bacterial endosymbiont called *Wolbachia*, which has a strain-specific effect. For example, *Ae. aegypti* mosquitoes transinfected with the wMel and wMelPop strains resulted in reduced CHIKV transmission (123, 124). On the other hand, *Ae. albopictus* is a natural carrier of two strains of *Wolbachia*, wAlbA and wAlbB, which have no effect on CHIKV infection (125). Interestingly, when the wMel strain was introduced into the *Ae. albopictus* mosquitoes in the presence of the natural strains, reduction of CHIKV transmission was observed (126). Together with other mitigation strategies such as behavioural and protective measures, including wearing long-sleeved clothing, vector control has become crucial in diminishing the impact of CHIKV infection on human lives in affected areas. However, mosquito control programs are not highly efficient in outbreak containment. Antiviral treatment represents the most effective control measure during outbreak situations as will be discussed in Chapter 2.

Thesis outline

This thesis describes the identification and characterization of several new classes of CHIKV nsP1-targeting inhibitors. It begins by describing the selection of antiviral compounds through rational drug design and antiviral drug screening, proceeds with detailed molecular *in vitro* studies to identify the viral target of selected compounds and concludes with molecular docking studies on the CHIKV nsP1 cryo-EM structure.

Chapter 2 contains a comprehensive literature review on CHIKV small-molecule inhibitors. It further discusses relevant topics in modern CHIKV antiviral drug discovery including the choice of cell lines and animal models for CHIKV antiviral research.

Chapter 3 describes the identification of 6'-fluorinated-aristeromycin and 6'- fluorinated-homoaristeromycin analogues as novel CHIKV inhibitors. The ability of these compounds to inhibit CHIKV cytopathic effect, reduce viral load and their cytotoxicity in mammalian cells are reported.

Chapter 4 represents a mode of action study of 6'-β-fluoro-homoaristeromycin and 6-fluoro-homoneplanocin A in CHIKV-infected cells. It describes the identification of CHIKV nsP1 as the target of these antiviral compounds in cell-based assays and *in vitro* enzymatic assays with purified SFV nsP1.

Chapter 5 is a mode of action study of a novel class of CHIKV small-molecule inhibitors called CHVB. It characterizes the antiviral effect of these compounds on several CHIKV clinical isolates and identifies CHIKV nsP1 as the antiviral target of the CHVB series. Antiviral activity is confirmed using *in vitro* enzymatic assays with VEEV and SFV nsP1.

Chapter 6 explores the relationships between CHIKV nsP1 mutants that are resistant to different classes of nsP1-targeting compounds. It describes molecular docking of selected CHIKV nsP1 inhibitors on a recently solved CHIKV nsP1 cryo-EM structure and provides interpretations with regard to their mode of action.

Chapter 7 discusses the key findings of this thesis in a broader context and emphasises their implications for future CHIKV antiviral research.

References

1. Robinson MC. 1955. An epidemic of virus disease in Southern Province, Tanganyika Territory, in 1952-53. I. Clinical features. Trans R Soc Trop Med Hyg 49:28-32.
2. Powers AM, Logue CH. 2007. Changing patterns of chikungunya virus: re-emergence of a zoonotic arbovirus. J Gen Virol 88:2363-77.
3. Powers AM, Brault AC, Tesh RB, Weaver SC. 2000. Re-emergence of Chikungunya and O'nyong-nyong viruses: evidence for distinct geographical lineages and distant evolutionary relationships. J Gen Virol 81:471-9.
4. Volk SM, Chen R, Tsetsarkin KA, Adams AP, Garcia TI, Sall AA, Nasar F, Schuh AJ, Holmes EC, Higgs S, Maharaj PD, Brault AC, Weaver SC. 2010. Genome-scale phylogenetic analyses of chikungunya virus reveal independent emergences of recent epidemics and various evolutionary rates. J Virol 84:6497-504.
5. Charrel RN, de Lamballerie X, Raoult D. 2007. Chikungunya outbreaks--the globalization of vectorborne diseases. N Engl J Med 356:769-71.
6. Weaver SC, Lecuit M. 2015. Chikungunya virus and the global spread of a mosquito-borne disease. N Engl J Med 372:1231-9.
7. Petersen LR, Powers AM. 2016. Chikungunya: epidemiology. F1000Res 5.
8. Schuffenecker I, Iteman I, Michault A, Murri S, Frangeul L, Vaney MC, Lavenir R, Pardigon N, Reynes JM, Pettinelli F, Biscornet L, Diancourt L, Michel S, Duquerroy S, Guigon G, Frenkiel MP, Brehin AC, Cubito N, Despres P, Kunst F, Rey FA, Zeller H, Brisse S. 2006. Genome microevolution of chikungunya viruses causing the Indian Ocean outbreak. PLoS Med 3:e263.
9. Rezza G, Nicoletti L, Angelini R, Romi R, Finarelli AC, Panning M, Cordioli P, Fortuna C, Boros S, Magurano F, Silvi G, Angelini P, Dottori M, Ciufolini MG, Majori GC, Cassone A. 2007. Infection with chikungunya virus in Italy: an outbreak in a temperate region. Lancet 370:1840-6.
10. Venturi G, Di Luca M, Fortuna C, Remoli ME, Riccardo F, Severini F, Toma L, Del Manso M, Benedetti E, Caporali MG, Amendola A, Fiorentini C, De Liberato C, Giammattei R, Romi R, Pezzotti P, Rezza G, Rizzo C. 2017. Detection of a chikungunya outbreak in Central Italy, August to September 2017. Euro Surveill 22.
11. Delisle E, Rousseau C, Broche B, Leparc-Goffart I, L'Ambert G, Cochet A, Prat C, Foulongne V, Ferre JB, Catelinois O, Flusin O, Tchernonog E, Moussion IE, Wiegandt A, Septfons A, Mendy A, Moyano MB, Laporte L, Maurel J, Jourdain F, Reynes J, Paty MC, Golliot F. 2015. Chikungunya outbreak in Montpellier, France, September to October 2014. Euro Surveill 20.
12. Calba C, Guerbois-Galla M, Franke F, Jeannin C, Auzet-Caillaud M, Grard G, Pigaglio L, Decoppet A, Weicherding J, Savaill MC, Munoz-Riviero M, Chaud P, Cadiou B, Ramalli L, Fournier P, Noel H, De Lamballerie X, Paty MC, Leparc-Goffart I. 2017. Preliminary report of an autochthonous chikungunya outbreak in France, July to September 2017. Euro Surveill 22.
13. Grandadam M, Caro V, Plumet S, Thiberge JM, Souares Y, Failloux AB, Tolou HJ, Budelot M, Cosserat D, Leparc-Goffart I, Despres P. 2011. Chikungunya virus, southeastern France. Emerg Infect Dis 17:910-3.

14. Cassadou S, Boucau S, Petit-Sinturel M, Huc P, Leparc-Goffart I, Ledrans M. 2014. Emergence of chikungunya fever on the French side of Saint Martin island, October to December 2013. Euro Surveill 19.
15. Lanciotti RS, Valadere AM. 2014. Transcontinental movement of Asian genotype chikungunya virus. Emerg Infect Dis 20:1400-2.
16. Nunes MR, Faria NR, de Vasconcelos JM, Golding N, Kraemer MU, de Oliveira LF, Azevedo Rdo S, da Silva DE, da Silva EV, da Silva SP, Carvalho VL, Coelho GE, Cruz AC, Rodrigues SG, Vianez JL, Jr., Nunes BT, Cardoso JF, Tesh RB, Hay SI, Pybus OG, Vasconcelos PF. 2015. Emergence and potential for spread of Chikungunya virus in Brazil. BMC Med 13:102.
17. Suhrbier A. 2019. Rheumatic manifestations of chikungunya: emerging concepts and interventions. Nat Rev Rheumatol doi:10.1038/s41584-019-0276-9.
18. Suhrbier A, Jaffar-Bandjee MC, Gasque P. 2012. Arthritogenic alphaviruses--an overview. Nat Rev Rheumatol 8:420-9.
19. Hossain MS, Hasan MM, Islam MS, Islam S, Mozaffor M, Khan MAS, Ahmed N, Akhtar W, Chowdhury S, Arafat SMY, Khaleque MA, Khan ZJ, Dipta TF, Asna SMZH, Hossain MA, Aziz KS, Mosabbir AA, Raheem E. 2018. Chikungunya outbreak (2017) in Bangladesh: Clinical profile, economic impact and quality of life during the acute phase of the disease. PLoS Negl Trop Dis 12:e0006561.
20. Paixão ES, Rodrigues LC, Costa MDCN, Itaparica M, Barreto F, Gérardin P, Teixeira MG. 2018. Chikungunya chronic disease: a systematic review and meta-analysis. Trans R Soc Trop Med Hyg 112:301-316.
21. Oehler E, Fournier E, Leparc-Goffart I, Larre P, Cubizolle S, Sookhareea C, Lastere S, Ghawche F. 2015. Increase in cases of Guillain-Barre syndrome during a Chikungunya outbreak, French Polynesia, 2014 to 2015. Euro Surveill 20.
22. Arpino C, Curatolo P, Rezza G. 2009. Chikungunya and the nervous system: what we do and do not know. Rev Med Virol 19:121-9.
23. Gerardin P, Couderc T, Bintner M, Tournebize P, Renouil M, Lemant J, Boisson V, Borgherini G, Staikowsky F, Schramm F, Lecuit M, Michault A. 2016. Chikungunya virus-associated encephalitis: A cohort study on La Reunion Island, 2005-2009. Neurology 86:94-102.
24. Gerardin P, Barau G, Michault A, Bintner M, Randrianaivo H, Choker G, Lenglet Y, Touret Y, Bouveret A, Grivard P, Le Roux K, Blanc S, Schuffenecker I, Couderc T, Arenzana-Seisdedos F, Lecuit M, Robillard PY. 2008. Multidisciplinary prospective study of mother-to-child chikungunya virus infections on the island of La Reunion. PLoS Med 5:e60.
25. Khan AH, Morita K, Parquet Md Mdel C, Hasebe F, Mathenge EG, Igarashi A. 2002. Complete nucleotide sequence of chikungunya virus and evidence for an internal polyadenylation site. J Gen Virol 83:3075-84.
26. Wong KZ, Chu JJH. 2018. The Interplay of Viral and Host Factors in Chikungunya Virus Infection: Targets for Antiviral Strategies. Viruses 10.
27. Firth AE, Chung BY, Fleeton MN, Atkins JF. 2008. Discovery of frameshifting in Alphavirus 6K resolves a 20-year enigma. Virol J 5:108.
28. Voss JE, Vaney MC, Duquerroy S, Vonrhein C, Girard-Blanc C, Crublet E, Thompson A, Bricogne G, Rey FA. 2010. Glycoprotein organization of Chikungunya virus particles revealed by X-ray crystallography. Nature 468:709-12.

29. Zhang R, Kim AS, Fox JM, Nair S, Basore K, Klimstra WB, Rimkunas R, Fong RH, Lin H, Poddar S, Crowe JE, Jr., Doranz BJ, Fremont DH, Diamond MS. 2018. Mxra8 is a receptor for multiple arthritogenic alphaviruses. Nature doi:10.1038/s41586-018-0121-3.
30. van Duijl-Richter MK, Hoornweg TE, Rodenhuis-Zybert IA, Smit JM. 2015. Early Events in Chikungunya Virus Infection-From Virus CellBinding to Membrane Fusion. Viruses 7:3647-74.
31. Hoornweg TE, van Duijl-Richter MK, Ayala Nunez NV, Albulescu IC, van Hemert MJ, Smit JM. 2016. Dynamics of chikungunya virus cell entry unraveled by single virus tracking in living cells. J Virol doi:10.1128/jvi.03184-15.
32. Li G, Rice CM. 1993. The signal for translational readthrough of a UGA codon in Sindbis virus RNA involves a single cytidine residue immediately downstream of the termination codon. J Virol 67:5062-7.
33. Strauss JH, Strauss EG. 1994. The alphaviruses: gene expression, replication, and evolution. Microbiol Rev 58:491-562.
34. Gorchakov R, Garmashova N, Frolova E, Frolov I. 2008. Different types of nsP3-containing protein complexes in Sindbis virus-infected cells. J Virol 82:10088-101.
35. Frolova EI, Gorchakov R, Pereboeva L, Atasheva S, Frolov I. 2010. Functional Sindbis virus replicative complexes are formed at the plasma membrane. J Virol 84:11679-95.
36. Kujala P, Ikaheimonen A, Ehsani N, Vihinen H, Auvinen P, Kaariainen L. 2001. Biogenesis of the Semliki Forest virus RNA replication complex. J Virol 75:3873-84.
37. Melancon P, Garoff H. 1987. Processing of the Semliki Forest virus structural polyprotein: role of the capsid protease. J Virol 61:1301-9.
38. Owen KE, Kuhn RJ. 1996. Identification of a region in the Sindbis virus nucleocapsid protein that is involved in specificity of RNA encapsidation. J Virol 70:2757-63.
39. Snyder JE, Kulcsar KA, Schultz KL, Riley CP, Neary JT, Marr S, Jose J, Griffin DE, Kuhn RJ. 2013. Functional characterization of the alphavirus TF protein. J Virol 87:8511-23.
40. Lobigs M, Garoff H. 1990. Fusion function of the Semliki Forest virus spike is activated by proteolytic cleavage of the envelope glycoprotein precursor p62. J Virol 64:1233-40.
41. Soonsawad P, Xing L, Milla E, Espinoza JM, Kawano M, Marko M, Hsieh C, Furukawa H, Kawasaki M, Weerachatyanukul W, Srivastava R, Barnett SW, Srivastava IK, Cheng RH. 2010. Structural evidence of glycoprotein assembly in cellular membrane compartments prior to Alphavirus budding. J Virol 84:11145-51.
42. Cross RK. 1983. Identification of a unique guanine-7-methyltransferase in Semliki Forest virus (SFV) infected cell extracts. Virology 130:452-63.
43. Ahola T, Kaariainen L. 1995. Reaction in alphavirus mRNA capping: formation of a covalent complex of nonstructural protein nsP1 with 7-methyl-GMP. Proc Natl Acad Sci U S A 92:507-11.
44. Spuul P, Salonen A, Merits A, Jokitalo E, Kaariainen L, Ahola T. 2007. Role of the amphipathic peptide of Semliki forest virus replicase protein nsP1 in membrane association and virus replication. J Virol 81:872-83.
45. Rikkonen M, Peranen J, Kaariainen L. 1994. ATPase and GTPase activities associated with Semliki Forest virus nonstructural protein nsP2. J Virol 68:5804-10.

46. Vasiljeva L, Merits A, Auvinen P, Kaariainen L. 2000. Identification of a novel function of the alphavirus capping apparatus. RNA 5'-triphosphatase activity of Nsp2. J Biol Chem 275:17281-7.
47. Gomez de Cedron M, Ehsani N, Mikkola ML, Garcia JA, Kaariainen L. 1999. RNA helicase activity of Semliki Forest virus replicase protein NSP2. FEBS Lett 448:19-22.
48. Hardy WR, Strauss JH. 1989. Processing the nonstructural polyproteins of sindbis virus: nonstructural proteinase is in the C-terminal half of nsP2 and functions both in cis and in trans. J Virol 63:4653-64.
49. Akhrymuk I, Kulemzin SV, Frolova EI. 2012. Evasion of the Innate Immune Response: the Old World Alphavirus nsP2 Protein Induces Rapid Degradation of Rpb1, a Catalytic Subunit of RNA Polymerase II. J Virol 86:7180-91.
50. Göertz GP, McNally KL, Robertson SJ, Best SM, Pijlman GP, Fros JJ. 2018. The Methyltransferase-Like Domain of Chikungunya Virus nsP2 Inhibits the Interferon Response by Promoting the Nuclear Export of STAT1. J Virol 92.
51. McPherson RL, Abraham R, Sreekumar E, Ong SE, Cheng SJ, Baxter VK, Kistemaker HA, Filippov DV, Griffin DE, Leung AK. 2017. ADP-ribosylhydrolase activity of Chikungunya virus macrodomain is critical for virus replication and virulence. Proc Natl Acad Sci U S A 114:1666-1671.
52. Abraham R, Hauer D, McPherson RL, Utt A, Kirby IT, Cohen MS, Merits A, Leung AKL, Griffin DE. 2018. ADP-ribosyl-binding and hydrolase activities of the alphavirus nsP3 macrodomain are critical for initiation of virus replication. Proc Natl Acad Sci U S A 115:E10457-e10466.
53. LaStarza MW, Lemm JA, Rice CM. 1994. Genetic analysis of the nsP3 region of Sindbis virus: evidence for roles in minus-strand and subgenomic RNA synthesis. J Virol 68:5781-91.
54. Hahn YS, Grakoui A, Rice CM, Strauss EG, Strauss JH. 1989. Mapping of RNA-temperature-sensitive mutants of Sindbis virus: complementation group F mutants have lesions in nsP4. J Virol 63:1194-202.
55. Sawicki D, Barkhimer DB, Sawicki SG, Rice CM, Schlesinger S. 1990. Temperature sensitive shut-off of alphavirus minus strand RNA synthesis maps to a nonstructural protein, nsP4. Virology 174:43-52.
56. Tomar S, Hardy RW, Smith JL, Kuhn RJ. 2006. Catalytic core of alphavirus nonstructural protein nsP4 possesses terminal adenylyltransferase activity. J Virol 80:9962-9.
57. Gibbons DL, Ahn A, Chatterjee PK, Kielian M. 2000. Formation and characterization of the trimeric form of the fusion protein of Semliki Forest Virus. J Virol 74:7772-80.
58. Wahlberg JM, Bron R, Wilschut J, Garoff H. 1992. Membrane fusion of Semliki Forest virus involves homotrimers of the fusion protein. J Virol 66:7309-18.
59. Smith TJ, Cheng RH, Olson NH, Peterson P, Chase E, Kuhn RJ, Baker TS. 1995. Putative receptor binding sites on alphaviruses as visualized by cryoelectron microscopy. Proc Natl Acad Sci U S A 92:10648-52.
60. Lobigs M, Zhao HX, Garoff H. 1990. Function of Semliki Forest virus E3 peptide in virus assembly: replacement of E3 with an artificial signal peptide abolishes spike heterodimerization and surface expression of E1. J Virol 64:4346-55.

61. Gaedigk-Nitschko K, Schlesinger MJ. 1990. The Sindbis virus 6K protein can be detected in virions and is acylated with fatty acids. Virology 175:274-81.
62. Lusa S, Garoff H, Liljestrom P. 1991. Fate of the 6K membrane protein of Semliki Forest virus during virus assembly. Virology 185:843-6.
63. Ching KC, L FPN, Chai CLL. 2017. A compendium of small molecule direct-acting and host-targeting inhibitors as therapies against alphaviruses. J Antimicrob Chemother doi:10.1093/jac/dkx224.
64. Carey DE, Myers RM, DeRanitz CM, Jadhav M, Reuben R. 1969. The 1964 chikungunya epidemic at Vellore, South India, including observations on concurrent dengue. Trans R Soc Trop Med Hyg 63:434-45.
65. Couderc T, Chretien F, Schilte C, Disson O, Brigitte M, Guivel-Benhassine F, Touret Y, Barau G, Cayet N, Schuffenecker I, Despres P, Arenzana-Seisdedos F, Michault A, Albert ML, Lecuit M. 2008. A mouse model for Chikungunya: young age and inefficient type-I interferon signaling are risk factors for severe disease. PLoS Pathog 4:e29.
66. Frolova EI, Fayzulin RZ, Cook SH, Griffin DE, Rice CM, Frolov I. 2002. Roles of nonstructural protein nsP2 and Alpha/Beta interferons in determining the outcome of Sindbis virus infection. J Virol 76:11254-64.
67. Breakwell L, Dosenovic P, Karlsson Hedestam GB, D'Amato M, Liljestrom P, Fazakerley J, McInerney GM. 2007. Semliki Forest virus nonstructural protein 2 is involved in suppression of the type I interferon response. J Virol 81:8677-84.
68. Prow NA, Tang B, Gardner J, Le TT, Taylor A, Poo YS, Nakayama E, Hirata TDC, Nakaya HI, Slonchak A, Mukhopadhyay P, Mahalingam S, Schroder WA, Klimstra W, Suhrbier A. 2017. Lower temperatures reduce type I interferon activity and promote alphaviral arthritis. PLoS Pathog 13:e1006788.
69. Schilte C, Couderc T, Chretien F, Sourisseau M, Gangneux N, Guivel-Benhassine F, Kraxner A, Tschopp J, Higgs S, Michault A, Arenzana-Seisdedos F, Colonna M, Peduto L, Schwartz O, Lecuit M, Albert ML. 2010. Type I IFN controls chikungunya virus via its action on nonhematopoietic cells. J Exp Med 207:429-42.
70. Ziegler SA, Lu L, da Rosa AP, Xiao SY, Tesh RB. 2008. An animal model for studying the pathogenesis of chikungunya virus infection. Am J Trop Med Hyg 79:133-9.
71. Zhang R, Kim AS, Fox JM, Nair S, Basore K, Klimstra WB, Rimkunas R, Fong RH, Lin H, Poddar S, Crowe JE, Jr., Doranz BJ, Fremont DH, Diamond MS. 2018. Mxra8 is a receptor for multiple arthritogenic alphaviruses. Nature 557:570-574.
72. Teng TS, Kam YW, Lee B, Hapuarachchi HC, Wimal A, Ng LC, Ng LF. 2015. A Systematic Meta-analysis of Immune Signatures in Patients With Acute Chikungunya Virus Infection. J Infect Dis 211:1925-35.
73. Kelvin AA, Banner D, Silvi G, Moro ML, Spataro N, Gaibani P, Cavrini F, Pierro A, Rossini G, Cameron MJ, Bermejo-Martin JF, Paquette SG, Xu L, Danesh A, Farooqui A, Borghetto I, Kelvin DJ, Sambri V, Rubino S. 2011. Inflammatory cytokine expression is associated with chikungunya virus resolution and symptom severity. PLoS Negl Trop Dis 5:e1279.
74. Wauquier N, Becquart P, Nkoghe D, Padilla C, Ndjoyi-Mbiguino A, Leroy EM. 2011. The acute phase of Chikungunya virus infection in humans is associated with strong innate immunity and T CD8 cell activation. J Infect Dis 204:115-23.

75. Chua CL, Sam IC, Chiam CW, Chan YF. 2017. The neutralizing role of IgM during early Chikungunya virus infection. PLoS One 12:e0171989.

76. Kam YW, Simarmata D, Chow A, Her Z, Teng TS, Ong EK, Renia L, Leo YS, Ng LF. 2012. Early appearance of neutralizing immunoglobulin G3 antibodies is associated with chikungunya virus clearance and long-term clinical protection. J Infect Dis 205:1147-54.

77. Hawman DW, Stoermer KA, Montgomery SA, Pal P, Oko L, Diamond MS, Morrison TE. 2013. Chronic joint disease caused by persistent chikungunya virus infection is controlled by the adaptive immune response. J Virol 87:13878-88.

78. van Aalst M, Nelen CM, Goorhuis A, Stijnis C, Grobusch MP. 2017. Long-term sequelae of chikungunya virus disease: A systematic review. Travel Med Infect Dis 15:8-22.

79. Labadie K, Larcher T, Joubert C, Mannioui A, Delache B, Brochard P, Guigand L, Dubreil L, Lebon P, Verrier B, de Lamballerie X, Suhrbier A, Cherel Y, Le Grand R, Roques P. 2010. Chikungunya disease in nonhuman primates involves long-term viral persistence in macrophages. J Clin Invest 120:894-906.

80. Young AR, Locke MC, Cook LE, Hiller BE, Zhang R, Hedberg ML, Monte KJ, Veis DJ, Diamond MS, Lenschow DJ. 2019. Dermal and muscle fibroblasts and skeletal myofibers survive chikungunya virus infection and harbor persistent RNA. PLoS Pathog 15:e1007993.

81. Hawman DW, Fox JM, Ashbrook AW, May NA, Schroeder KMS, Torres RM, Crowe JE, Jr., Dermody TS, Diamond MS, Morrison TE. 2016. Pathogenic Chikungunya Virus Evades B Cell Responses to Establish Persistence. Cell Rep 16:1326-1338.

82. Davenport BJ, Bullock C, McCarthy MK, Hawman DW, Murphy KM, Kedl RM, Diamond MS, Morrison TE. 2020. Chikungunya Virus Evades Antiviral CD8(+) T Cell Responses To Establish Persistent Infection in Joint-Associated Tissues. J Virol 94.

83. Krejbich-Trotot P, Denizot M, Hoarau JJ, Jaffar-Bandjee MC, Das T, Gasque P. 2011. Chikungunya virus mobilizes the apoptotic machinery to invade host cell defenses. FASEB J 25:314-25.

84. Poo YS, Rudd PA, Gardner J, Wilson JA, Larcher T, Colle MA, Le TT, Nakaya HI, Warrilow D, Allcock R, Bielefeldt-Ohmann H, Schroder WA, Khromykh AA, Lopez JA, Suhrbier A. 2014. Multiple immune factors are involved in controlling acute and chronic chikungunya virus infection. PLoS Negl Trop Dis 8:e3354.

85. Hoarau JJ, Jaffar Bandjee MC, Krejbich Trotot P, Das T, Li-Pat-Yuen G, Dassa B, Denizot M, Guichard E, Ribera A, Henni T, Tallet F, Moiton MP, Gauzere BA, Bruniquet S, Jaffar Bandjee Z, Morbidelli P, Martigny G, Jolivet M, Gay F, Grandadam M, Tolou H, Vieillard V, Debre P, Autran B, Gasque P. 2010. Persistent chronic inflammation and infection by Chikungunya arthritogenic alphavirus in spite of a robust host immune response. J Immunol 184:5914-27.

86. Chow A, Her Z, Ong EK, Chen JM, Dimatatac F, Kwek DJ, Barkham T, Yang H, Renia L, Leo YS, Ng LF. 2011. Persistent arthralgia induced by Chikungunya virus infection is associated with interleukin-6 and granulocyte macrophage colony-stimulating factor. J Infect Dis 203:149-57.

87. Dupuis-Maguiraga L, Noret M, Brun S, Le Grand R, Gras G, Roques P. 2012. Chikungunya disease: infection-associated markers from the acute to the chronic phase of arbovirus-induced arthralgia. PLoS Negl Trop Dis 6:e1446.

88. Her Z, Malleret B, Chan M, Ong EK, Wong SC, Kwek DJ, Tolou H, Lin RT, Tambyah PA, Renia L, Ng LF. 2010. Active infection of human blood monocytes by Chikungunya virus triggers an innate immune response. J Immunol 184:5903-13.

89. Nayak TK, Mamidi P, Sahoo SS, Kumar PS, Mahish C, Chatterjee S, Subudhi BB, Chattopadhyay S, Chattopadhyay S. 2019. P38 and JNK Mitogen-Activated Protein Kinases Interact With Chikungunya Virus Non-structural Protein-2 and Regulate TNF Induction During Viral Infection in Macrophages. Front Immunol 10:786.

90. Srivastava P, Kumar A, Hasan A, Mehta D, Kumar R, Sharma C, Sunil S. 2020. Disease Resolution in Chikungunya-What Decides the Outcome? Front Immunol 11:695.

91. Simon F, Javelle E, Oliver M, Leparc-Goffart I, Marimoutou C. 2011. Chikungunya virus infection. Curr Infect Dis Rep 13:218-28.

92. Marti-Carvajal A, Ramon-Pardo P, Javelle E, Simon F, Aldighieri S, Horvath H, Rodriguez-Abreu J, Reveiz L. 2017. Interventions for treating patients with chikungunya virus infection-related rheumatic and musculoskeletal disorders: A systematic review. PLoS One 12:e0179028.

93. Mostafavi H, Abeyratne E, Zaid A, Taylor A. 2019. Arthritogenic Alphavirus-Induced Immunopathology and Targeting Host Inflammation as A Therapeutic Strategy for Alphaviral Disease. Viruses 11.

94. Brighton SW. 1984. Chloroquine phosphate treatment of chronic Chikungunya arthritis. An open pilot study. S Afr Med J 66:217-8.

95. De Lamballerie X, Boisson V, Reynier JC, Enault S, Charrel RN, Flahault A, Roques P, Le Grand R. 2008. On chikungunya acute infection and chloroquine treatment. Vector Borne Zoonotic Dis 8:837-9.

96. Chopra A, Saluja M, Venugopalan A. 2014. Effectiveness of chloroquine and inflammatory cytokine response in patients with early persistent musculoskeletal pain and arthritis following chikungunya virus infection. Arthritis Rheumatol 66:319-26.

97. Jin J, Simmons G. 2019. Antiviral Functions of Monoclonal Antibodies against Chikungunya Virus. Viruses 11.

98. Pal P, Fox JM, Hawman DW, Huang YJ, Messaoudi I, Kreklywich C, Denton M, Legasse AW, Smith PP, Johnson S, Axthelm MK, Vanlandingham DL, Streblow DN, Higgs S, Morrison TE, Diamond MS. 2014. Chikungunya viruses that escape monoclonal antibody therapy are clinically attenuated, stable, and not purified in mosquitoes. J Virol 88:8213-26.

99. Kose N, Fox JM, Sapparapu G, Bombardi R, Tennekoon RN, de Silva AD, Elbashir SM, Theisen MA, Humphris-Narayanan E, Ciaramella G, Himansu S, Diamond MS, Crowe JE, Jr. 2019. A lipid-encapsulated mRNA encoding a potently neutralizing human monoclonal antibody protects against chikungunya infection. Sci Immunol 4.

100. Webb EM, Azar SR, Haller SL, Langsjoen RM, Cuthbert CE, Ramjag AT, Luo H, Plante K, Wang T, Simmons G, Carrington CVF, Weaver SC, Rossi SL, Auguste AJ. 2019. Effects of Chikungunya virus immunity on Mayaro virus disease and epidemic potential. Sci Rep 9:20399.

101. Partidos CD, Paykel J, Weger J, Borland EM, Powers AM, Seymour R, Weaver SC, Stinchcomb DT, Osorio JE. 2012. Cross-protective immunity against o'nyong-nyong virus afforded by a novel recombinant chikungunya vaccine. Vaccine 30:4638-43.

102. Plante K, Wang E, Partidos CD, Weger J, Gorchakov R, Tsetsarkin K, Borland EM, Powers AM, Seymour R, Stinchcomb DT, Osorio JE, Frolov I, Weaver SC. 2011. Novel Chikungunya Vaccine Candidate with an IRES-Based Attenuation and Host Range Alteration Mechanism. PLoS Pathog 7:e1002142.

103. Chan YH, Teo TH, Utt A, Tan JJ, Amrun SN, Abu Bakar F, Yee WX, Becht E, Lee CY, Lee B, Rajarethinam R, Newell E, Merits A, Carissimo G, Lum FM, Ng LF. 2019. Mutating chikungunya virus non-structural protein produces potent live-attenuated vaccine candidate. EMBO Mol Med doi:10.15252/emmm.201810092.

104. Zhang YN, Deng CL, Li JQ, Li N, Zhang QY, Ye HQ, Yuan ZM, Zhang B. 2019. Infectious Chikungunya Virus with a Complete Capsid Deletion: a New Approach for CHIKV Vaccine. J Virol doi:10.1128/jvi.00504-19.

105. Hallengard D, Kakoulidou M, Lulla A, Kummerer BM, Johansson DX, Mutso M, Lulla V, Fazakerley JK, Roques P, Le Grand R, Merits A, Liljestrom P. 2014. Novel Attenuated Chikungunya Vaccine Candidates Elicit Protective Immunity in C57BL/6 mice. J Virol 88:2858-66.

106. Piper A, Ribeiro M, Smith KM, Briggs CM, Huitt E, Nanda K, Spears CJ, Quiles M, Cullen J, Thomas ME, Brown DT, Hernandez R. 2013. Chikungunya virus host range E2 transmembrane deletion mutants induce protective immunity against challenge in C57BL/6J mice. J Virol 87:6748-57.

107. Wang E, Kim DY, Weaver SC, Frolov I. 2011. Chimeric chikungunya viruses are nonpathogenic in highly sensitive mouse models but efficiently induce a protective immune response. J Virol 85:9249-52.

108. Nougairede A, De Fabritus L, Aubry F, Gould EA, Holmes EC, de Lamballerie X. 2013. Random codon re-encoding induces stable reduction of replicative fitness of Chikungunya virus in primate and mosquito cells. PLoS Pathog 9:e1003172.

109. Harrison VR, Eckels KH, Bartelloni PJ, Hampton C. 1971. Production and evaluation of a formalin-killed Chikungunya vaccine. J Immunol 107:643-7.

110. Levitt NH, Ramsburg HH, Hasty SE, Repik PM, Cole FE, Jr., Lupton HW. 1986. Development of an attenuated strain of chikungunya virus for use in vaccine production. Vaccine 4:157-62.

111. Edelman R, Tacket CO, Wasserman SS, Bodison SA, Perry JG, Mangiafico JA. 2000. Phase II safety and immunogenicity study of live chikungunya virus vaccine TSI-GSD-218. Am J Trop Med Hyg 62:681-5.

112. Gorchakov R, Wang E, Leal G, Forrester NL, Plante K, Rossi SL, Partidos CD, Adams AP, Seymour RL, Weger J, Borland EM, Sherman MB, Powers AM, Osorio JE, Weaver SC. 2012. Attenuation of chikungunya virus vaccine strain 181/clone 25 is determined by two amino Acid substitutions in the e2 envelope glycoprotein. J Virol 86:6084-96.

113. Silva LA, Khomandiak S, Ashbrook AW, Weller R, Heise MT, Morrison TE, Dermody TS. 2014. A single-amino-Acid polymorphism in chikungunya virus e2 glycoprotein influences glycosaminoglycan utilization. J Virol 88:2385-97.

114. Brandler S, Ruffie C, Combredet C, Brault JB, Najburg V, Prevost MC, Habel A, Tauber E, Despres P, Tangy F. 2013. A recombinant measles vaccine expressing chikungunya virus-like particles is strongly immunogenic and protects mice from lethal challenge with chikungunya virus. Vaccine 31:3718-25.

115. Rossi SL, Comer JE, Wang E, Azar SR, Lawrence WS, Plante JA, Ramsauer K, Schrauf S, Weaver SC. 2019. Immunogenicity and Efficacy of a Measles Virus-vectored Chikungunya Vaccine in Nonhuman Primates. J Infect Dis doi:10.1093/infdis/jiz202.

116. Ramsauer K, Schwameis M, Firbas C, Mullner M, Putnak RJ, Thomas SJ, Despres P, Tauber E, Jilma B, Tangy F. 2015. Immunogenicity, safety, and tolerability of a recombinant measles-virus-based chikungunya vaccine: a randomised, double-blind, placebo-controlled, active-comparator, first-in-man trial. Lancet Infect Dis 15:519-27.

117. Reisinger EC, Tschismarov R, Beubler E, Wiedermann U, Firbas C, Loebermann M, Pfeiffer A, Muellner M, Tauber E, Ramsauer K. 2019. Immunogenicity, safety, and tolerability of the measles-vectored chikungunya virus vaccine MV-CHIK: a double-blind, randomised, placebo-controlled and active-controlled phase 2 trial. Lancet 392:2718-2727.

118. Akahata W, Yang ZY, Andersen H, Sun S, Holdaway HA, Kong WP, Lewis MG, Higgs S, Rossmann MG, Rao S, Nabel GJ. 2010. A virus-like particle vaccine for epidemic Chikungunya virus protects nonhuman primates against infection. Nat Med 16:334-8.

119. Chang LJ, Dowd KA, Mendoza FH, Saunders JG, Sitar S, Plummer SH, Yamshchikov G, Sarwar UN, Hu Z, Enama ME, Bailer RT, Koup RA, Schwartz RM, Akahata W, Nabel GJ, Mascola JR, Pierson TC, Graham BS, Ledgerwood JE. 2014. Safety and tolerability of chikungunya virus-like particle vaccine in healthy adults: a phase 1 dose-escalation trial. Lancet doi:10.1016/s0140-6736(14)61185-5.

120. Chen GL, Coates EE, Plummer SH, Carter CA, Berkowitz N, Conan-Cibotti M, Cox JH, Beck A, O'Callahan M, Andrews C, Gordon IJ, Larkin B, Lampley R, Kaltovich F, Gall J, Carlton K, Mendy J, Haney D, May J, Bray A, Bailer RT, Dowd KA, Brockett B, Gordon D, Koup RA, Schwartz R, Mascola JR, Graham BS, Pierson TC, Donastorg Y, Rosario N, Pape JW, Hoen B, Cabié A, Diaz C, Ledgerwood JE. 2020. Effect of a Chikungunya Virus-Like Particle Vaccine on Safety and Tolerability Outcomes: A Randomized Clinical Trial. Jama 323:1369-1377.

121. Goo L, Dowd KA, Lin TY, Mascola JR, Graham BS, Ledgerwood JE, Pierson TC. 2016. A Virus-Like Particle Vaccine Elicits Broad Neutralizing Antibody Responses in Humans to All Chikungunya Virus Genotypes. J Infect Dis 214:1487-1491.

122. Phuc HK, Andreasen MH, Burton RS, Vass C, Epton MJ, Pape G, Fu G, Condon KC, Scaife S, Donnelly CA, Coleman PG, White-Cooper H, Alphey L. 2007. Late-acting dominant lethal genetic systems and mosquito control. BMC Biol 5:11.

123. Moreira LA, Iturbe-Ormaetxe I, Jeffery JA, Lu G, Pyke AT, Hedges LM, Rocha BC, Hall-Mendelin S, Day A, Riegler M, Hugo LE, Johnson KN, Kay BH, McGraw EA, van den Hurk AF, Ryan PA, O'Neill SL. 2009. A Wolbachia symbiont in Aedes aegypti limits infection with dengue, Chikungunya, and Plasmodium. Cell 139:1268-78.

124. van den Hurk AF, Hall-Mendelin S, Pyke AT, Frentiu FD, McElroy K, Day A, Higgs S, O'Neill SL. 2012. Impact of Wolbachia on Infection with Chikungunya and Yellow Fever Viruses in the Mosquito Vector Aedes aegypti. PLoS Negl Trop Dis 6:e1892.

125. Mousson L, Martin E, Zouache K, Madec Y, Mavingui P, Failloux AB. 2010. Wolbachia modulates Chikungunya replication in Aedes albopictus. Mol Ecol 19:1953-64.

126. Blagrove MS, Arias-Goeta C, Di Genua C, Failloux AB, Sinkins SP. 2013. A Wolbachia wMel transinfection in Aedes albopictus is not detrimental to host fitness and inhibits Chikungunya virus. PLoS Negl Trop Dis 7:e2152.

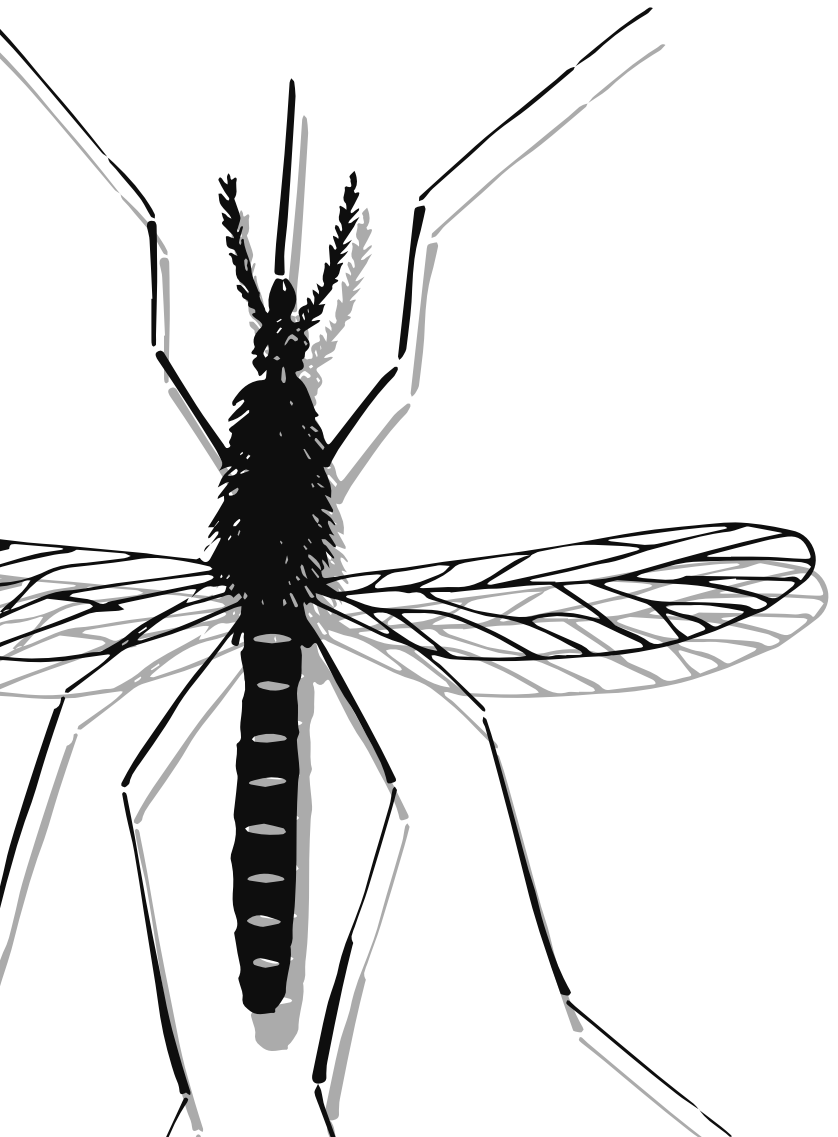

CHAPTER 2

Small molecule inhibitors of Chikungunya virus: mechanisms of action and antiviral drug resistance

Kristina Kovacikova and Martijn J van Hemert

Department of Medical Microbiology, Leiden University Medical Center, 2333ZA, Leiden, The Netherlands

Antimicrob Agents Chemother. 2020 Nov 17;64(12):e01788-20

Abstract

Chikungunya virus (CHIKV) is a mosquito-transmitted alphavirus that has spread to more than 60 countries worldwide. CHIKV infection leads to a febrile illness known as Chikungunya fever (CHIKF), which is characterized by long-lasting and debilitating joint and muscle pain. CHIKV can cause large-scale epidemics with high attack rates, which substantiates the need for development of effective therapeutics suitable for outbreak containment. In this review, we highlight the different strategies used for developing CHIKV small-molecule inhibitors, ranging from high-throughput cell-based screening, *in silico* screens and enzymatic assays with purified viral proteins. We further discuss the current status for the most promising molecules including *in vitro* and *in vivo* findings. In particular, we focus on describing host and/or viral targets, mode of action and mechanisms of antiviral drug resistance and associated mutations. Knowledge of the key molecular determinants of drug resistance will aid selection of the most promising antiviral agent(s) for clinical use. For these reasons, we also summarize the available information about drug-resistant phenotypes in *Aedes* mosquito vectors. From this review, it is evident that more of the active molecules need to be evaluated in pre-clinical and clinical models to address the current lack of antiviral treatment for CHIKF.

Introduction

Chikungunya virus (CHIKV) is a mosquito-borne alphavirus belonging to the *Togaviridae* family that can cause explosive epidemics of acute and chronic arthritis in humans. The main vectors responsible for its transmission are the day-biting *Aedes aegypti* and *Aedes albopictus* mosquitoes. CHIKV was first isolated from a febrile patient in 1952/1953 in what is currently Tanzania (1). In the following years it caused periodic local outbreaks in Africa and Asia. In 2004, CHIKV re-emerged in coastal Kenya (2), from where it spread to immunologically naïve populations in La Reunion island, surrounding Indian Ocean islands and South Asia during 2005-2006. During this outbreak, a new CHIKV variant harbouring the A226V amino acid substitution in the E1 glycoprotein was isolated (3), which-unlike earlier isolates- was more efficiently transmitted by the *Aedes albopictus* mosquitoes that are abundant in the temperate regions of the Americas, Europe and Africa. In late 2013, CHIKV caused the first locally-transmitted outbreak on the Caribbean island of St Martin (4), resulting in more than 2.5 million cases across Central and South America in the period between 2014-2017 (https://www.paho.org/hq/index.php?option=com_topics&view=rdmore&cid=5927&Itemid=40931&lang=en). In Europe, the first autochthonous outbreak was described in Italy in 2007 (5) and since then renewed CHIKV transmission has occurred in Italy in 2017 (6) and southern France in 2010, 2014 and 2017 (7-9).

Chikungunya fever (CHIKF) typically begins with a sudden onset of fever 3 to 7 days after a bite of an infected mosquito, followed by symptoms like rash, myalgia and polyarthralgia. Polyarthralgia is mainly symmetrical and peripheral, affecting the small joints of wrists, ankles and phalanges, as well as the larger joints such as the knee and the elbow (10). The patients usually report incapacitating pain that can last for weeks to months. CHIKF treatment has been focused entirely on relieving patients' symptoms with analgesics, antipyretics and anti-inflammatory agents. Nevertheless, some of these drugs can have serious side effects upon prolonged use. The current lack of clinically approved therapeutics and adequate control measures for CHIKF warrants the development of safe and effective antiviral therapy.

In this review, a comprehensive overview of small-molecule inhibitors of CHIKV is presented in Tables 1-4 grouped by the approach by which they were identified. Table 1 and 2 contain inhibitors that were identified by cell-based screening, Table 3 contains compounds identified by *in silico* approaches and Table 4 lists compounds that were identified in enzymatic assays. It is important to note that the values presented in Tables 1-4 are not directly comparable as the experimental parameters/setup vary

between studies: e.g. the use of different virus isolates, multiplicity of infection (MOI), readouts [virus-induced cytopathic effect (CPE) vs titers vs qRT-PCR], time of harvest, type mouse models. Since this review focuses on small-molecule inhibitors, we have not included siRNA-mediated gene silencing approaches.

Strategies for anti-CHIKV drug discovery and design

Considering the global distribution of CHIKV and its mosquito vectors, the potential for additional spread and its impact on human health, the development of preventive measures is imperative. Several approaches have been used for identification of potential CHIKV inhibitors, including cell-based high-throughput screening (HTS) campaigns, rational and structure-based drug design using crystal structures or homology modelling of viral proteins. One of the conventional approaches for CHIKV drug discovery uses cell-based screening with readouts that measure CPE. The CPE reduction assay screens can provide information on antiviral activity of compounds and their cytotoxicity can be assessed in parallel on uninfected cells in the same plate. Such screens are often deployed to test known clinically approved drugs, in a process referred to as drug repurposing. The advantages of this route are decreased costs related to drug approval and an accelerated process to potential licensing of the compound. Due to increased computational power, HTS has emerged recently as an efficient process for screening thousands of compounds from large compound libraries including FDA-approved and novel molecules. The emergence of computer-aided drug design has also greatly contributed to the development of CHIKV inhibitors. These approaches are based on the structure of a viral protein to perform *in silico* virtual screens. Compounds identified by *in silico* computer-based screening can be further optimized by acquiring an understanding of the compound's structure-activity relationship (SAR) and improved derivatives can be synthesized for validation in enzymatic and cell-based assays. However, the computer-aided design for compounds targeting the CHIKV replicase is limited because, thus far, only the structures of the N-terminal and C-terminal region of nonstructural protein 2 (nsP2), representing the RNA helicase and protease domains, respectively, and the N-terminal macrodomain of nsP3 have been resolved (11-13). More opportunities for molecular docking studies arise from CHIKV structural proteins, as the structures for the envelope (E) proteins and the capsid (C) protein have been determined. Although the crystal structures for complete CHIKV nsPs are not yet available, researchers have used various purification

methods to obtain enzymatically active recombinant nsPs for use in cell-free assays. Validation of compounds originating from *in silico* virtual screens in enzymatic assays with purified proteins is especially important for confirmation of target specificity. In cell-based assays, resistance selection in the presence of (suboptimal concentrations of) compound has been widely used to identify the viral target of compounds. Tables 1 and 2 provide a comprehensive overview of all resistance mutations that have been identified so far, information which -together with cross-resistance studies- can aid in the elucidation of the mode of action of compounds that might be identified in future screening efforts. Besides the compound's mode of action, an understanding of molecular determinants of resistance can provide useful information about the virus replication cycle and pathogenesis.

Compounds targeting CHIKV entry and egress

The alphavirus virion is composed of a nucleocapsid core with T=4 icosahedral symmetry surrounded by a host-derived lipid bilayer which is decorated with 80 trimeric spikes of E1-E2 heterodimers (14-16). The E2 protein mediates viral entry by attachment to the receptors on the cell surface (17). This process is followed by clathrin-mediated endocytosis which delivers the viral particle to the early endosomes (18). The low pH in the endosomal compartment triggers conformational changes in the E1-E2 heterodimer and results in the insertion of the E1 fusion protein into the endosomal membrane. More specifically, the E1 glycoprotein is converted from a nonfusogenic form to a highly stable fusogenic E1 homotrimer (19, 20). This event will ultimately create a fusion pore and release the nucleocapsid into the cytosol. Compounds that exhibit antiviral activity against entry, fusion and egress of CHIKV are listed in Table 1.

Envelope protein E1

Obatoclax, an anti-cancer compound, was found to inhibit CHIKV infection early in the replication cycle by neutralizing the acidic endosomal environment required for fusion. The L369I mutation in domain III of the E1 fusion glycoprotein conferred at least partial resistance to obatoclax and generated resistant viruses with enhanced fusogenic potential (21).

Envelope protein E2

Arbidol/umifenovir has been licensed as an anti-influenza agent in both Russia and China and inhibits a wide-range of viruses. Arbidol inhibits early stages of the CHIKV replication cycle, which was confirmed by selection of an arbidol-resistant variant carrying a G407R mutation in the structural polyprotein (22), which corresponds to a G82R mutation in the E2 glycoprotein. This mutation also causes attenuation of the CHIKV vaccine strain 181/25, presumably by increasing interactions with glycosaminoglycans on the host cell surface (23). Arbidol derivatives with increased potency and selective inhibition of CHIKV have been developed, but the precise mechanism of action of these compounds remains unresolved (24).

Suramin is an approved drug for treatment of parasitic infections in humans and was shown to inhibit CHIKV entry in three independent studies (25-27). The compound likely influences CHIKV attachment to cells and may prevent conformational changes of the E1/E2 heterodimer that are required for viral fusion. Selection of suramin-resistant variants revealed that the mutations N5R and H18Q in the E2 glycoprotein cause some resistance to the compound. Molecular docking with the mature CHIKV spike suggested that suramin interacts with the N-terminal loop and domain A in the E2 glycoprotein, an interaction that would negatively affect virion binding to the receptor (28). Suramin treatment of C57BL/6 mice infected with different clinical isolates of CHIKV ameliorated CHIKV-induced foot swelling, inflammation and cartilage damage (29).

Capsid protein

Picolinic acid was found to bind to the hydrophobic pocket of the C protein, which might inhibit the C protein's interaction with the cytoplasmic domain of the E2 glycoprotein. The antiviral activity of picolinic acid was also confirmed in CHIKV-infected cells, although the inhibitory concentration was rather high for clinical applications (30).

6K

The 6K protein belongs to the family of viroporins or ion channel-forming proteins. It is a highly hydrophobic protein with membrane fusogenic properties. Viroporins allow for movement of small molecules and ions across membranes, which can be important during viral entry, replication and egress. The potential of 6K to serve as a therapeutic target is illustrated by the drug amantadine, a well-known influenza inhibitor that

targets the ion-channel forming M2 protein of influenza viruses (31). Amantadine inhibited ion channel activity and altered particle morphology in biophysical systems. Mechanistically, 6K likely needs to interact with E2 for its delivery to the plasma membrane where it forms an ion channel. The antiviral effect of amantadine on CHIKV was also confirmed in infected cells (32).

Drugs targeting CHIKV entry with an uncharacterized mode of action

Chloroquine (CHL) is an old anti-malarial drug with a broad range of antiviral activities against a variety of viruses. CHL had been deployed in clinical trials long before its anti-CHIKV activity was established in cell culture. The rationale for this unusual strategy was that CHL had conferred benefits in lessening joint inflammation in patients with rheumatoid arthritis during trials in the late 1950s (33). The efficacy of CHL phosphate was first investigated in a small patient cohort, which led to an alleviation of patient symptoms and justified its further use for the treatment of CHIKV-associated arthritis (34). However, the benefits of CHL for the treatment of acute CHIKV infection were disproved in the "CuraChik" trial conducted during the 2005-2006 La Reunion epidemic (https://clinicaltrials.gov/ct2/show/NCT00391313). Moreover, CHL-treated patients had more frequent complaints of arthralgia compared to placebo recipients (35). In an Indian trial during the 2006 CHIKV epidemic, CHL also did not yield benefits in relieving symptoms of musculoskeletal pain and arthritis compared to the commonly used non-steroidal anti-inflammatory drug meloxicam (36). These and other studies supported the hypothesis that CHL might enhance viral replication, which was later demonstrated *in vivo* in CHL-treated BALB/c mice infected with another arthritogenic alphavirus, Semliki Forest virus (37). In CHIKV-infected cells, CHL seems to block or delay virus internalization depending on the time of treatment. It is effective at early stages of viral infection, likely by impairing cell-virus surface interactions and blocking endosomal acidification (38).

Doxycycline is a tetracycline antibiotic used for treatment of bacterial infections that has also shown promising anti-CHIKV activity. It was postulated that the anti-CHIKV activity of doxycycline is directed towards viral entry rather than viral replication. Docking studies with the CHIKV nsP2 cysteine protease and E2 glycoprotein indicated that the compound could bind to both these viral targets. However, cell-based assays confirmed that doxycycline inhibits viral entry, likely by impairing conformational changes in the E2 glycoprotein. Treatment of adult ICR mice with doxycycline alone did not result in an improved outcome in comparison with combination treatment with ribavirin (39).

Curcumin is a turmeric plant extract that has been used for treatment of gastrointestinal disorders in Asia. The antiviral effect of curcumin on CHIKV has been demonstrated using pseudotyped viral particles (40) and subsequently a study using wild-type CHIKV showed that curcumin reduces the infectivity of CHIKV particles and their binding at the cell surface (41). A CHIKV insect cell fusion inhibition assay was used to screen for fusion inhibitors and identified two compounds, niclosamide and nitazoxanide, as prospective CHIKV inhibitors. In other assays both compounds were confirmed to inhibit CHIKV entry and suppress cell-to-cell transmission (42).

Apigenin, a natural compound with a 5,7-dihydroxyflavone structure, has shown moderate anti-CHIKV activity. Flavonoids have been previously reported to suppress the entry pathway of members of other virus families. However, the flavonoids tested against CHIKV, among which apigenin was the most potent, strongly inhibited CHIKV replicon levels and had no effect in an SFV entry assay (43), suggesting they do not target entry. Synthetic flavaglines such as FL3 were based on a class of naturally occurring plant compounds with activity in the low nanomolar range. FL3 inhibited CHIKV infection at the entry step by serving as a prohibitin ligand and disrupting the interaction between CHIKV and the prohibitin receptor (44).

Compounds targeting CHIKV replication

The incoming alphavirus genomic RNA is translated into two polyproteins: P123 and P1234. P123 is the more abundant of the two and P1234 arises as a result of the translational read-through of an opal stop codon (with about 10 % efficiency) at the end of nsP3 coding sequence (45). These polyproteins are processed by the protease domain of nsp2. Cleavage intermediates as well as fully cleaved individual viral nsPs play specific roles in CHIKV (-) and (+) strand RNA synthesis. The functions of nsPs have been largely characterized by using recombinant viruses with mutations in nsPs, in biochemical assays and by *in silico* identification of enzymatic sequence motifs. CHIKV inhibitors targeting individual nsPs are described in Tables 2, 3 and 4.

Nonstructural protein 1 (nsP1)

Alphavirus nsP1 (535 amino acids) is a viral mRNA capping enzyme with guanine-N7-methyltransferase (MTase) and guanylyltransferase (GTase) activities responsible for capping of the 5’ ends of the newly synthesized genomic 42S mRNA and 26S subgenomic (sg) mRNA. The MTase catalyses the transfer of the methyl group from

S-adenosylmethionine (SAM) to the N7 position of a GTP molecule, forming m^7GTP and releasing S-adenosylhomocysteine (SAH) as by-product (46). The GTase binds the m^7GTP and forms a covalent intermediate, m^7GMP-nsP1, while releasing a pyrophosphate (PPi) (47). The m^7GMP is then transferred to the 5'-diphosphate RNA, which is generated through the RNA 5' triphosphatase activity of nsP2 (48), to create a methylated cap structure at the 5' terminus. This cap structure is essential for viral mRNA translation and prevents mRNA degradation by host 5'-exonucleases. The middle part of nsP1, spanning the amino acid residues 245 to 264, contains an amphipathic helix responsible for association of the alphavirus replication complex with membranes (49). Specifically, the presence of the amphipathic helix and palmitoylated cysteines 417-419 (50) allows nsP1 and nsP1-containing replication complexes to anchor to cholesterol-enriched membrane microdomains (51). Importantly, site-directed mutagenesis of conserved residues in alphavirus nsP1 indicated that abrogation of nsP1 enzymatic activities is detrimental for virus replication (52).

In recent years, the number of reports describing an inhibitory effect of molecules specifically targeting nsP1 functions has substantially increased (Table 2 and 4). Owing to its uniquely viral enzymatic activities, nsP1 represents an excellent target for antiviral compounds, while not affecting host cell mRNA capping that proceeds through a fundamentally different mechanism. The 3-aryl-[1,2,3]triazolo[4,5-d] pyrimidin-7(6H)-ones were first reported as a class of potent and selective inhibitors of CHIKV replication that target nsP1, with MADTP-314 as the prototype compound (53, 54). A resistance selection procedure with MADTP-314 and subsequent reverse genetics indicated that the single amino acid substitution P34S in the N-terminal part of nsP1 was responsible for resistance to MADTP-314 and several analogues of this compound (55). Recently, the 2-(4-(phenylsulfonyl)piperazine-1-yl)pyrimidine analogues known as the CHVB series, with CHVB-032 as the prototypical compound, were identified as potent and selective CHIKV inhibitors (56). Reverse genetics identified two mutations in the C-terminal region of nsP1, namely S454G and W456R, to be responsible for resistance to CHVB-032 and its analogues. Interestingly, the two families of compounds seem to target the same nsP1 functions, as the MADTP-resistant nsP1-P34S mutant is cross-resistant to CHVB-032 and its analogue CHVB-066 and, vice versa, the CHVB-resistant nsp1-S454G+W456R mutant is cross-resistant to a MADTP-314 analogue, MADTP-372 (57). Yet another phenotypic compound screen identified 6'-β-fluoro-homoaristeromycin (FHA) and 6'-fluoro-homoneplanocin A (FHNA) as potent CHIKV inhibitors with a very high therapeutic index (58, 59). The mutations G230R and K299E

in nsP1 were identified by resistance selection and reverse genetics to confer resistance to both FHA and FHNA (59). Difluoromethylornithine (DFMO), an inhibitor of ornithine decarboxylase 1, was shown to have a broad-spectrum antiviral effect on a variety of RNA viruses, including CHIKV (60). Interestingly, CHIKV can overcome polyamine depletion by acquiring mutations in nsP1. The combination of the G230R and V326M mutations in CHIKV nsP1 and *->opal524R in nsP3 was essential to confer resistance to DFMO (61). Despite its promising *in vitro* effects, there was little protection against CHIKV-induced disease in C57BL/6 mice that were fed DFMO in their drinking water prior to infection (60).

Mycophenolic acid (MPA) is a well-known immunosuppressive agent and ribavirin is a broad-spectrum guanosine analogue with immunomodulatory properties. Both compounds target the host enzyme inosine monophosphate dehydrogenase (IMPDH), which is important for the *de novo* synthesis of guanosine monophosphate (GMP) and the regulation of intracellular GTP levels. GTP is critical for at least two processes in alphavirus replication: it serves as a methyl acceptor molecule during mRNA capping and as a building block in nsP4-mediated RNA synthesis, as will be described below. The anti-CHIKV activity of MPA was shown to be associated with the depletion of the guanosine pool in cell culture (62). Similar to FHNA, treatment with MPA resulted in a release of virions with reduced specific infectivity (PFU per genome copy numbers). Earlier studies with SINV mapped the mutations responsible for the MPA-resistant phenotype to the region encoding nsP1. Viruses with the MPA-resistant phenotype were also resistant to ribavirin (63, 64). Later on, in-depth reverse genetics studies with a SINV cDNA clone demonstrated that only the mutations S23N and V302M in nsP1 were essential for MPA resistance (65). To date, CHIKV nsP1 crystal structure is not yet available, which makes it hard to appreciate the structural context of the various compound-resistant mutations and understand the molecular mechanisms underlying drug resistance. Taken together, the majority of CHIKV nsP1 inhibitors for which the molecular determinants of resistance were studied require a combination of two nsP1 mutations for compound-specific resistance. Since singular mutations did not cause resistance in most cases, the chance of the emergence of drug-resistant CHIKV variants during treatment appears to be low for these compounds.

Other CHIKV nsP1 inhibitors have been identified by using purified CHIKV nsP1 in enzymatic assays (Table 4). 5-iodotubercidin, an adenosine analogue, was recently discovered by screening with a novel capillary electrophoresis-based assay for MTase activity of CHIKV nsP1. The activity of the compound in this enzymatic assay was

validated in cell culture (66). This enzymatic assay uncouples the MTase and GTase activities and thus can be used to identify specific alphavirus nsP1 MTase inhibitors. An fluorescence polarization-based assay measuring competition for the GTP-binding site was used in a large HTS screen that identified lobaric acid as a potent CHIKV nsP1 inhibitor, which was also validated using live virus in cell-based assays (67). Since GTP binding is essential to perform the MTase step in mRNA capping, the assay identifies competitive MTase inhibitors.

Nonstructural protein 2 (nsP2)

Alphavirus nsP2 (798 aa) is a multifunctional protein which possesses several enzymatic activities, including nucleoside triphosphatase (NTPase) (68, 69), helicase (70) and RNA 5′ triphosphatase (RTPase) activity (48) in the N-terminal part of the protein and protease activity (71, 72) and a SAM-dependent RNA methyltransferase-like (SAM MTase-like) domain in the C-terminal part of nsP2. The NTPase and helicase functions are important for unwinding double-stranded RNA during CHIKV replication and the RTPase activity removes the γ-phosphate from the 5′ end of the RNA before the transfer of the cap-0 structure. The nsP2 protease activity is responsible for nsp123 and nsp1234 polyprotein processing (72). In the case of Old World alphaviruses, nsP2 can also induce host transcriptional shut-off and cytophathic effects (73). During host shut-off, nsP2 translocates to the nuclei of vertebrate cells to induce polyubiquitination of the catalytic subunit of the DNA-dependent RNA polymerase II, RPB1, and in this way subverts the cellular antiviral response (74, 75). The C-terminal SAM MTase-like domain plays a critical role in the nuclear function of alphavirus nsP2 (76) and inhibits the interferon response (77).

The crystal structure of the nsP2 protease domain has been solved and the protein is now used as an important target for antiviral development using computer-aided drug design (Table 3). A virtual screening campaign of a library of commercially available compounds using a homology model of CHIKV nsP2 protease identified compound 1 as an initial hit. The compound displayed anti-CHIKV activity in cell-based assays and SAR studies on 25 structural analogues yielded compound 25 which showed improved efficacy and lower cytotoxicity compared to lead compound 1 (78). Another study reported on five arylalkylidene derivates of 1,3-thiazolidin-4-one with anti-CHIKV activity in the low micromolar range, with compound 7 being the most potent. Using molecular docking, the compounds were shown to partially interact with the crystal structure of the nsP2 protease (79). Although the above-mentioned

studies identified novel nsP2-targeting molecules, they did not provide experimental evidence, e.g. using enzymatic assays, to demonstrate that nsP2 was *de facto* the target of these compounds. Computer-aided drug design was combined with cell-free assays for target validation of a set of 12 compounds designed against the CHIKV nsP2 protease using target-based modelling. The most promising compound 8 potently inhibited CHIKV replication in cell culture and was moderately active in the protease assay with recombinant CHIKV nsP2 (80). This illustrates the importance of confirming *in silico* predictions in enzymatic assays with purified protein as virtual binding does not always correlate with inhibition of enzymatic activity *in vitro*. Other inhibitors targeting nsP2 include small peptidomimetics discovered using a unique approach of quantum mechanical-based ligand descriptors. Compounds with lower molecular weight displayed greater inhibitory activity, likely due to superior access to the target pocket (81).

Nonstructural protein 3 (nsP3)

The functional role of alphavirus nsP3 (530 aa) is the least defined of all CHIKV nsPs. Three domains can be distinguished in nsP3: an N-terminal macrodomain (13), a Zn-binding alphavirus unique domain (AUD) (82) and a C-terminal hypervariable domain (HVD) (83). While the N-terminal part of nsP3 is well-conserved, the C-terminal HVD has very low sequence similarity even between closely related alphaviruses. Alphaviruses use their HVDs to recruit RNA-binding proteins typically found in stress granules, such as the G3BP proteins used by CHIKV, for the formation of pre-RCs that promote viral replication (84). Other cellular proteins from different families, specific for virus species and cell types, have been found to interact with nsP3 HVD (85). They function as the major determinants of cell specificity during viral replication. The nsP3 macrodomain affects various critical processes in the alphavirus replication cycle including nsP3 phosphorylation, (-) strand RNA synthesis, host translational shut-off and virulence (86). Importantly, ADP ribosylation of cellular proteins, a post-translational modification involved in a variety of cellular processes, is regulated by nsP3 macrodomain. The nsP3 macrodomain possesses both ADP-ribosyl-binding and ADP-ribosylhydrolase activities, by which it binds ADP-ribose and hydrolyses ADP-ribosylated residues on cellular proteins. The nsP3 macrodomain-mediated ADP-ribosyl-binding is necessary for initiating nsP synthesis and establishing RCs, while the ADP-ribosylhydrolase activity is important for amplification of RCs. Thus, the interaction of nsP3 macrodomain with ADP-ribosylated proteins is required for

efficient alphavirus replication (86). Besides that, the ADP-ribosylhydrolase activity is a determinant of neurovirulence in mice (87). nsP3 AUD appears to be a multifunctional domain that plays a role in virus genome replication (88).

To date, only a handful of small-molecule inhibitors targeting CHIKV nsP3 have been reported, perhaps due to the enigmatic role of nsP3 in viral replication. However, in-depth characterization of the nsP3 functional domains in recent years has contributed to the exploitation of nsP3 as a potential drug target. Given its highly conserved nature and the available crystal structure, the macrodomain represents an ideal site for development of specific anti-CHIKV antivirals. Baicalin is one of the very few compounds shown to interact with nsP3 using computational approach (89) with a confirmed anti-CHIKV activity in cell culture (90) (Table 3). However, the latter study revealed that baicalin inhibited early stages of CHIKV replication and has strong virucidal activity. Moreover, baicalin was shown to interact with the CHIKV E glycoprotein using molecular docking, which led to discrepancy with the previous study suggesting that nsP3 is the viral target of this compound. This again illustrates that it should become the norm that antiviral activity and mode of action of small-molecule inhibitors discovered using computer-aided drug design are validated in cell-based assays.

Nonstructural protein 4 (nsP4)

The nsP4 (611 aa) is the most conserved protein in the alphavirus family that functions as an RNA-dependent RNA polymerase (RdRp) responsible for replication of 49S genomic (+) strand RNA and transcription of the 26S sgRNA. In the early phase of the replication cycle, nsP4 together with P123 is part of an early replication complex (RC) that is responsible for the synthesis of full-length (-) strand RNA that will serve as template for synthesis of genomic and sgRNA. Following polyprotein processing, the late RC consisting of fully cleaved nsP1-4, mediates the synthesis of genomic RNA and 26S sgRNA (91). NsP4 also possesses a terminal adenylyltransferase (TATase) activity that catalyses the addition of a poly-A tail to the 3' end of the genome (92). In addition, nsP4 contains the signature GDD motif of the RdRp's catalytic core and mutation of both aspartate residues to alanine results in a complete loss of TATase activity (92).

Many RdRp inhibitors are nucleoside analogues. Because RdRp activity is absent from host cells, it represents a suitable target for development of antiviral agents (Table 2). Sofosbuvir is a uridine analogue that is clinically approved for the treatment of hepatitis C virus infection. It is administered as a uridine monophosphate

(UMP) prodrug that needs to be metabolized to yield the pharmacologically active compound sofosbuvir triphosphate (93). nsP4 is the predicted target of sofosbuvir in CHIKV-infected cells, based on molecular docking of the compound on the putative CHIKV nsP4 model. Treatment of hepatoma cells with sofosbuvir decreased CHIKV replication *in vitro* and its administration to infected adult Swiss mice resulted in reduced arthralgia-related paw inflammation (94).

β-D-N^4-hydroxycytidine (NHC) is a nucleoside analogue that inhibits CHIKV replication after it is converted to its active form NHC triphosphate. However, a direct relationship between NHC and its mode of action in CHIKV-infected cells has not yet been established. It was proposed that NHC may interfere with CHIKV replication through chain termination or mutagenesis (95). Studies with Venezuelan equine encephalitis virus, a New World alphavirus, demonstrated that resistance to NHC develops very inefficiently and is determined by a synergistic effect of multiple mutations in nsP4. Especially three nsP4-specific mutations, namely P187S, A189V and I190T, located in the index finger domain of the predicted nsP4 structure, are thought to be responsible for resistance to NHC. Interestingly, the NHC-resistant phenotype can revert back to wild-type after incorporation of the A201V mutation in nsP4, which has a negative effect on viral resistance to NHC (96).

Initially developed as an anti-influenza inhibitor, favipiravir (T-705) is a broad-spectrum nucleoside analogue that has also shown inhibitory activity against CHIKV (97). All of the favipiravir-resistant variants acquired the unique K291R mutation in nsP4, which is a highly conserved residue in the F1 motif of the RdRps of (+) strand RNA viruses (97). In addition, treatment with favipiravir reduced viral loads in the brain of infected AG129 mice and protected them from severe neurological disease. Favipiravir was also tested in immunocompetent C57BL/6J mice during the acute and chronic phase of CHIKV infection. Treatment with favipiravir during the acute phase rendered viral RNA, viral antigens and infectious particles undetectable. However, such a reduction was not observed upon favipiravir treatment during the chronic phase (98). Given that full-length CHIKV RNA could not be recovered from chronically-infected mice, it suggests that the viral RNA can be defective and unable to form infectious particles, corroborating earlier findings from studies with patient material.

As discussed above, ribavirin can block CHIKV replication by at least two different mechanisms, one of which is through RdRp inhibition. CHIKV passaging in the presence of ribavirin yielded a high-fidelity mutant containing a C483Y mutation in nsP4 (99). Interestingly, this CHIKV mutant generated populations with restricted genetic

diversity, which appears to result from a novel mechanism that differs from those typical for nucleoside analogues, such as chain termination or lethal mutagenesis. The impact of resistance mutations on the 3-D structure of nsP4 was based on homology modelling, since a crystal structure of the CHIKV RdRp is not yet available.

Despite the majority of nsP4-targeting compounds belonging to well-known classes of nucleoside analogues, compound screens have identified other potential drug candidates. For example, an HTS of advanced clinical candidates identified digoxin, a cardiac glycoside that antagonizes the sodium-potassium ATPase, as a potent CHIKV inhibitor. The V209I mutation in nsP4, situated in a well-conserved region of nsP4, was found to play a pivotal role in the development of digoxin-mediated resistance (100). Cytoplasmic proteins involved in CHIKV replication could also be targeted due to their direct interaction with CHIKV proteins. Hsp90 proteins are host proteins that serve as molecular chaperones with a wide array of functions. The cytoplasmic subunit HsP90α was shown to be the predominant interacting partner of nsP4 in co-immunoprecipitation experiments. Hsp90 proteins seem to play a role in stabilizing RCs during alphaviral infections. Hsp90 inhibitors HS-10 and SNX-2112 inhibited CHIKV replication in cell culture and they reduced CHIKV-induced joint swelling and viral load in infected mice (101). Direct evidence leading to nsP4 being the viral target of these compounds is however still lacking.

Inhibitors of CHIKV replication with an undefined target

6-azauridine is a broad-spectrum nucleoside analogue that has been widely used in patients for other indications. Its metabolite 6-azauridine 5'monophosphate was reported to inhibit the replication of several DNA and RNA viruses via targeting of the host orotidylic acid decarboxylase (102). Others have proposed a different mechanism of action, based on the interference with cellular UTP metabolism, leading to the so-called 'error' catastrophe (103). Multiple studies have demonstrated that 6-azauridine potently inhibits CHIKV replication, but its viral target has not been determined (104). A chemical library has identified a novel potent broad-spectrum small-molecule inhibitor RYL-634 with antiviral activity against many pathogenic viruses, including CHIKV. Dihydroorotate dehydrogenase (DHODH) was validated as the target enzyme of RYL-634 using activity-based protein profiling (105).

Atovaquone is a ubiquinone analogue and a well-known antimalarial and antiparasitic drug. Previous studies indicated that it can function through the inhibition of mitochondrial function or DHODH, the latter being required for the *de novo*

pyrimidine synthesis. Recently, atovaquone was found to inhibit CHIKV replication, but the mechanism underlying its precise mode of action remains unstudied. For Zika virus it was shown that atovaquone blocks DHODH and thereby leads to the depletion of intracellular nucleotide pools (106).

Another HTS campaign identified berberine, ivermectin and abamectin as strong inhibitors of CHIKV replication. Ivermectin and abamectin are broad-spectrum anti-parasitic drugs used for the treatment of humans and agricultural crops, respectively. Berberine possess antimicrobial properties and it has been tested for antiviral activity against a range of viruses, including herpes simplex virus, influenza virus and cytomegalovirus (107). Further elucidation of its anti-CHIKV effect showed that berberine impairs mitogen-activated protein kinase signalling pathways, although the specific molecular target of berberine remains unknown. Another study found that berberine affects post-replications steps in the CHIKV replication cycle by targeting interactions between genomic RNA and C protein that are required for correct nucleocapsid assembly (108). Moreover, treatment of CHIKV-infected C57BL6/J mice with berberine alleviated the symptoms of CHIKV-induced inflammatory disease (109).

Harringtonine, a cephalotaxine alkaloid, was discovered by screening a natural product compound library and found to also potently inhibit CHIKV replication. This compound acts on the post-entry stage of the CHIKV replication cycle and strongly interferes with CHIKV protein synthesis. It was postulated that harringtonine inhibits the host cell translation machinery and thereby leads to the suppression of translation of CHIKV nsPs and structural proteins (110). Silymarin is a flavonoid with anti-CHIKV activity that was also found to exert its antiviral activity at the post-entry stage (111). Imipramine is an FDA-approved antidepressant that exerts its antiviral effects at two distinct stages in CHIKV replication, the fusion/entry step and a post-fusion replication step. Because optimal fusion reactions and intracellular replication are both dependent on cholesterol, these processes are highly susceptible to imipramine, a class II cationic amphiphilic drug targeting cholesterol trafficking pathway (112). Tomatidine is a natural steroidal alkaloid that interferes with post-entry steps in the CHIKV replication cycle (113). Silvestrol is a natural compound that belongs to the flavaglines and is a specific inhibitor of the host RNA helicase eIF4A, which is part of the translation initiation complex. Silvestrol treatment of CHIKV-infected cells delayed the translation of viral proteins and prevented the host transcriptional shut-off (114). Andrographolide, a bicyclic diterpenoid lactone (115), micafungin, an antifungal agent (116), and MBZM-N-IBT (117) all inhibit CHIKV replication but their mechanism of action remains unknown.

Are drug-resistant mutants attenuated in mosquitoes?

Compared to single-host RNA viruses, the alternating use of insect and mammalian hosts restricts arbovirus adaptation to environmental pressures like treatment with antiviral compounds. Selection and fitness of new variants is influenced by replication competence in both vertebrate and invertebrate hosts. To date, only a few studies have specifically assessed the fitness of drug-resistant mutants in mosquitoes. Such information would be valuable for selecting an antiviral agent with minimal risk of inducing and spreading drug resistance in the environment. For example, a high-fidelity ribavirin-resistant variant containing the C483Y mutation in nsP4 had lower fitness in *Ae. aegypti* mosquitoes (99). Likewise, the favipiravir-resistant mutant carrying the K291R mutation in nsP4 also disseminated poorly in the bodies of *Ae. aegypti* mosquitoes and showed decreased transmission potential, while the MATDP-resistant mutant with the P34S mutation in nsP1 showed the same transmission efficiency as wild-type virus (118). Furthermore, a DFMO-resistant triple mutant carrying the G230R and V326M mutations in nsP1 and the nsP3-opal524R mutation replicated to higher titers in *Ae. albopictus* mosquitoes compared to wild-type virus (61). These studies indicate that drug-resistant mutants can have quite different phenotypes in mosquitoes and emphasize the need to determine their transmission potential for those antiviral drugs intended for clinical use.

How choice of cell line in CHIKV antiviral drug discovery can affect outcome

Vertebrate cells such as BHK-21 (baby hamster kidney) cells or Vero E6 (African green monkey kidney) cells are the most widely used cell lines for CHIKV antiviral drug screening. Fibroblast cell lines, such as MRC-5 (human lung fibroblast) or HFF-1 (human foreskin fibroblast) have also been used in multiple studies. Less frequently used cell lines include immortalized cells such as HeLa (human cervical carcinoma), Huh-7 or HepG2 (human hepatocellular carcinoma) and U2OS (human osteosarcoma). Cell lines usually vary with respect to drug uptake and intracellular metabolism. Therefore, it is anticipated that compounds that first need to be metabolized into their active form, such as nucleoside analogues, might show cell line-dependent differences in their antiviral activity profile. A study evaluating the anti-CHIKV efficacy of ribavirin and favipiravir, which need to be converted to their active triphosphate forms by host cell kinases, revealed differences in antiviral efficacy depending on the cell line used

for evaluation (119). Similarly, for immunomodulatory agents (not discussed in this review) the correct choice of cell line is especially relevant.

Concluding remarks

The lack of effective control measures, spread of new vectors, increased human travel and urbanization have largely contributed to CHIKV re-emergence between 2004-2020. The origin and the scale of a future chikungunya outbreak is hard to predict, which underscores the importance of developing effective countermeasures. Identifying and developing direct-acting and host-targeting antiviral drug options against CHIKV infection offers a promising approach for limiting viral replication and spread.

The major complaint of patients suffering from CHIKF is debilitating joint and muscle pain, which results in lost productivity and reduced quality of life. Antiviral treatment would represent a suitable measure to prevent and treat CHIKV infections and significantly lower the burden of disease in affected areas. A combination therapy for CHIKF may prove useful to reduce the likelihood of developing drug resistance, given that compounds with different viral/host targets can produce synergistic effects. In addition, chronic CHIKF patients with exacerbated response of their immune system can also be treated with immunomodulatory agents to alleviate joint arthralgia and inflammation.

Validation of CHIKV small-molecule inhibitors is currently performed in a variety of *in vitro* and *in vivo* models. Ideally, *in vivo* antiviral testing is performed in animal models that replicate the clinical course of CHIKV infection in humans. While the use of an immunocompromised acute model, such as AG129 mice, may provide more stringent conditions for antiviral evaluation, the use of an immunocompetent arthralgia model is more clinically relevant. The maximum benefit of an antiviral compound for treatment of CHIKF patients would be achieved by early administration during the acute phase of infection, in order to reduce the viral load and decrease the likelihood of developing chronic manifestations. Clinical studies with patient material have already indicated that residual viral material (RNA/protein) in joint tissue, rather than replicating virus, likely contributes to the immunopathology that is associated with CHIKV infection (120). Consequently, late antiviral treatment, i.e. during the chronic phase of CHIKV infection, targeting specific CHIKV functions and host pathways involved in viral replication would be less effective given the absence or low quantities of full-length viral RNA. This stresses the importance of fully understanding

the fundamental aspects of CHIKV-host interactions in patients with both acute and chronic disease.

In summary, the development of CHIKV small-molecule inhibitors is justified for both prophylactic and therapeutic use. Given the current absence of a vaccine, a clinically approved CHIKV small-molecule inhibitor would be especially advantageous in outbreak containment. Alternatively, it could be prescribed as a form of prophylaxis to local citizens in affected areas or to travellers at-risk.

Acknowledgements

We would like to thank Prof Eric Snijder for carefully reading the manuscript and providing valuable feedback. K.K. was supported by the Marie Sklodowska-Curie ETN European Training Network “ANTIVIRALS” (EU grant agreement 642434).

Table 1: Compounds targeting CHIKV entry and egress[a]

			In vitro efficacy				*In vivo* efficacy			
Compound[b]	**Viral target**	**Resistance mutation(s)**	**CHIKV strain (genotype)[c]**	**EC_{50} (µM) or other readout[d]**	**CC_{50} (µM)**	**Cell line**	**CHIKV strain (genotype)**	**Efficacy**	**Mouse model**	**Reference**
obatoclax(R)	E1	L369I (SFV)	LR2006 OPY1 (ECSA)	0.03 ± 0.01	20.1 ± 4.8	BHK-21	-	-	-	(21)
arbidol	E2	G82R	LR2006 OPY1 (ECSA)	12.2 ± 2.2	376	MRC5	-	-	-	(22)
suramin(R)	E2	N5R, H18Q	CHIKV-LS3	79 ± 11.6	> 1,000	VeroE6	0611aTw, 0810bTw, 0706aTw (Asian)	reduced viral load, foot swelling and histopathologic lesions	C57BL/6	(25, 28, 29)
picolinic acid	C	-	DRDE-07 (ECSA)	60% inhibition with 2 mM dose	n.s.	Vero	-	-	-	(30)
amantadine	6k	-	S27 (ECSA)	29.5	>200	Vero	-	-	-	(32)
chloroquine(R)	-	-	DRDE-06 (ECSA)	7.0 ± 1.5	> 260	Vero	-	-	-	(38)
doxycycline(R)	-	-	n.s. (ECSA)	10.95 ± 2.12	>100	Vero	061573 (ECSA)	no significant reduction in viral titre or pathology	ICR	(39)

			In vitro efficacy				*In vivo* efficacy			
Compound[b]	**Viral target**	**Resistance mutation(s)**	**CHIKV strain (genotype)[c]**	**EC_{50} (μM) or other readout[d]**	**CC_{50} (μM)**	**Cell line**	**CHIKV strain (genotype)**	**Efficacy**	**Mouse model**	**Reference**
curcumin	-	-	LR06-049 (ECSA)	3.89	11.6	HeLa	-	-	-	(41)
niclosamide	-	-	S27 (ECSA)	0.95 ± 0.22	> 20	BHK-21	-	-	-	(42)
nitazoxanide	-	-	S27 (ECSA)	2.96 ± 0.18	> 25	BHK-21	-	-	-	(42)
apigenin	-	-	LR2006 OPY1 (ECSA)	70.8	> 200	BHK-21	-	-	-	(43)
FL3	-	-	clinical isolate (ECSA)	0.0224	0.119	HEK-293T	-	-	-	(44)

[a]CC_{50}, 50% cytotoxic concentration; EC_{50}, 50% effective concentration; n.s. – not specified;- not determined/not done (*in vivo* studies); R – repurposed compound. The numbering of mutations that provide resistance is based on the CHIKV genome sequence of the strain indicated in the table, unless indicated otherwise.
[b]If the study described a family/class of compounds with antiviral activity, only the antiviral activity of the most potent and/or the most representative compound is reported.
[c]Only compounds for which the antiviral activity was tested using infectious CHIKV are included; compounds identified using only replicon/surrogate systems for which confirmatory experiments with infectious CHIKV were lacking are excluded.
[d]Where a compound showed activity in multiple cell lines and against multiple CHIKV strains, the best value (with corresponding cell line) is reported.

Table 2: Compounds targeting CHIKV replication[a]

			In vitro efficacy				*In vivo* efficacy			
Compound[b]	**Viral target**	**Resistance mutation(s)**	**CHIKVstrain (genotype)[c]**	**EC_{50} (µM) or other readout[d]**	**CC_{50} (µM)**	**Cell line**	**CHIKV strain (genotype)**	**Efficacy**	**Mouse model**	**Reference**
MADTP-314 (N) (DA)	nsP1	P34S	IO 899 (ECSA)	26 ± 11	> 743	Vero	-	-	-	(53-55)
CHVB-032 (N) (DA)	nsP1	S454G, W456R	IO 899 (ECSA)	2.7	> 75	Vero	-	-	-	(56, 57)
6′-β-fluoro-homoaristeromycin (N, NA) (DA)	nsP1	G230R, K299E	CHIKV-LS3	0.12 ± 0.04	> 250	VeroE6	-	-	-	(58, 59)
6′-fluoro-homoneplanocin A (N, NA) (DA)	nsP1	G230R, K299E	CHIKV-LS3	0.18 ± 0.11	> 250	VeroE6	-	-	-	(59)
difluoromethylornithine (R) (HT)	nsP1	G230R, V326M (nsP1) & *524R (nsP3)	LR06-049 (ECSA)	3 log_{10} reduction in titre with 500 µM dose	> 500	BHK-21	LR06-049 (ECSA)	modest reduction in CHIKV titres	C57BL/6	(60, 61, 121)
mycophenolic acid (R) (HT)	nsP1	S23N, V302M (SINV)	DRDE-06 (ECSA)	0.21 ±0.06	30 ± 3.1	Vero	-	-	-	(62, 63, 65)

			In vitro efficacy				*In vivo* efficacy			
Compound[b]	**Viral target**	**Resistance mutation(s)**	**CHIKVstrain (genotype)[c]**	**EC_{50} (µM) or other readout[d]**	**CC_{50} (µM)**	**Cell line**	**CHIKV strain (genotype)**	**Efficacy**	**Mouse model**	**Reference**
ribaviri (NA) (HT/DA)	nsP1/ nsP4	(Q21K), S23N, V302M (SINV)/ C483Y (CHIKV)	Ross C347 (ECSA)	341.1	> 30,000	Vero	-	-	-	(63, 99, 104)
sofosbuvir (NA) (DA)	nsP4	-	n.s. (Asian)	2.7 ± 0.5	402 ± 32	Huh-7	n.s.	reduced CHIKV-i nduced oedema and viral replication	Swiss Webster mice arthralgia model	(94)
β-D-N^4-hydroxycytidine (NA) (DA)	nsP4	P187S, A189V, I190T (VEEV)	LR2006 OPY1 (ECSA)	0.2 ± 0.1	7.7	Vero	-	-	-	(95, 96)
favipiravir (NA) (DA)	nsP4	K291R	IO 899 (ECSA)	25 ± 3	> 636	Vero-A	S27 (ECSA)	reduced mortality by >50% and improved disease outcome	AG129 lethal model	(97)

			In vitro efficacy				*In vivo* efficacy			
Compound[b]	**Viral target**	**Resistance mutation(s)**	**CHIKVstrain (genotype)[c]**	**EC_{50} (µM) or other readout[d]**	**CC_{50} (µM)**	**Cell line**	**CHIKV strain (genotype)**	**Efficacy**	**Mouse model**	**Reference**
							IO 899 (ECSA)	reduced viral replication in joints and extremities during acute phase	C57BL/6J	(98)
digoxin (R) (HT)	nsP4	V209I	SL15649 (ECSA)	0.048	> 10	U2OS	-	-	-	(100)
HS-10 (HT)	nsP4	-	Ross (ECSA)	> 2 log_{10} reduction in titre with 6.25 µM dose	> 100	HEK-293T	DMERI09/08 (ECSA)	reduced inflammation and viremia	SvA129	(101)
SNX-2112 (HT)	nsP4	-	Ross (ECSA)	> 2 log_{10} reduction in titre with 6.25 µM dose	> 100	HEK-293T	DMERI09/08 (ECSA)	reduced inflammation and viremia	SvA129	(101)

			In vitro efficacy				*In vivo* efficacy			
Compound[b]	**Viral target**	**Resistance mutation(s)**	**CHIKVstrain (genotype)[c]**	**EC_{50} (µM) or other readout[d]**	**CC_{50} (µM)**	**Cell line**	**CHIKV strain (genotype)**	**Efficacy**	**Mouse model**	**Reference**
6-azauridine (R)(NA) (HT/DA)	-	-	Ross C347 (ECSA)	0.8	208	Vero	-	-	-	(104)
RYL-634	-	-	n.s.	0.26	> 2.5	Vero	-	-	-	(105)
atovaquone (R)	-	-	LR06-049 (ECSA)	< 0.75	> 11.25	Vero	-	-	-	(106)
berberine	-	-	LR2006 OPY1 (ECSA)	> 5 log_{10} reduction in titre with 3 µM dose	> 100	BHK-21	LR2006 OPY1 (ECSA)	reduced inflammation and joint swelling	C57BL/6J	(107, 109)
ivermectin (R)	-	-	LR2006 OPY1 (ECSA)	> 4 log_{10} reduction in titre with 3 µM dose	37.9 ± 7.6	BHK-21	-	-	-	(107)
abamectin (R)	-	-	LR2006 OPY1 (ECSA)	> 4 log_{10} reduction in titre with 3 µM dose	28.2 ± 1.1	BHK-21	-	-	-	(107)
harringtonine	-	-	0708 (ECSA)	0.24	> 100	BHK-21	-	-	-	(110)
silymarin	-	-	MY/065/08/ FN295485 (ECSA)	35	881	Vero	-	-	-	(111)

			In vitro efficacy				*In vivo* efficacy			
Compound[b]	**Viral target**	**Resistance mutation(s)**	**CHIKVstrain (genotype)[c]**	**EC_{50} (μM) or other readout[d]**	**CC_{50} (μM)**	**Cell line**	**CHIKV strain (genotype)**	**Efficacy**	**Mouse model**	**Reference**
andrographolide	-	-	0708 (ECSA)	77.39	1,098	HepG2	-	-	-	(115)
micafungin (R)	-	-	S27 (ECSA)	20.6 ± 1.7	> 100	U2OS	-	-	-	(116)
MBZM-N-IBT	-	-	S27 (ECSA)	38.7	> 800	Vero	-	-	-	(117)
imipramine (R)	-	-	LR2006 OPY1 (ECSA)	3 log_{10} reduction in titre with 75 μM dose	> 100	HFF1	-	-	-	(112)
tomatidine	-	-	LR2006 OPY1 (ECSA)	1.3	156	Huh-7	-	-	-	(113)
silvestrol (HT)	-	-	IO 899 (ECSA)	0.00189	> 0.03	HEK-293T	-	-	-	(114)

[a]n.s. – not specified;- not determined/not done (*in vivo* studies); N, novel; NA, nucleoside analogue; R, repurposed compound; VEEV, Venezuelan equine encephalitis virus. The numbering of mutations that provide resistance is based on the CHIKV genome of the strain indicated in the table, unless indicated otherwise. DA, direct-acting compounds; HT, host-targeting compounds; HT/DA, both host-targeting and direct-acting compounds.

[b]If the study described a family/class of compounds with antiviral activity, only the antiviral activity of the most potent and or the most representative compound is reported.

[c]Only compounds for which the antiviral activity was tested using infectious CHIKV are included; compounds identified using only replicon/surrogate systems for which confirmatory experiments with infectious CHIKV were lacking were excluded.

[d]Where a compound showed activity in multiple cell lines and against multiple CHIKV strains, the best value (with corresponding cell line) is reported.

Table 3: CHIKV inhibitors identified by in silico approaches (molecular docking, homology modelling, pharmacophore modelling)

					In vitro efficacy			*In vivo* efficacy				
Compound	**Viral target**	**Resistance mutation(s)**	**Confirmed in enzymatic assays?**	**Confirmed in infected cells?**	**CHIKV strain (genotype)**	**EC50 (µM) or other readout[b]**	**CC_{50} (µM)**	**Cell line**	**CHIKV strain (genotype)**	**Efficacy**	**Mouse model**	**Reference**
25	nsP2	-[a]	no	yes	IO 899 (ECSA)	3.2 ± 1.8	101 ± 50	Vero	-	-	-	(78)
7	nsP2	-	no	yes	LR2006 OPY1 (ECSA)	0.42	> 100	Vero	-	-	-	(79)
8	nsP2	-	yes	yes	LR2006 OPY1 (ECSA)	~1.5	> 200	BHK-21	-	-	-	(80)
3a	nsP2	-	no	yes	n.s.	8.76 µg/ml	n.s.	Vero	-	-	-	(81)
4b	nsP2	-	no	yes	n.s.	8.94 µg/ml	n.s.	Vero	-	-	-	(81)
baicalin	nsP3	-	no	yes	MY/065/08/ FN295485 (ECSA)	5	> 600	Vero	-	-	-	(90)

[a]-, not determined/not done (*in vivo* studies)
[b]Data represent µM unless otherwise indicated.

Table 4: CHIKV inhibitors identified in in vitro biochemical assay/ assays with purified protein[a]

				In vitro efficacy				*In vivo* efficacy			
Compound	**Viral target**	**Resistance mutation(s)**	**Confirmed in infected cells?**	**CHIKV strain (genotype)**	**EC_{50} (µM)**	**CC_{50} (µM)**	**Cell line**	**CHIKV strain (genotype)**	**Efficacy**	**Mouse model**	**Reference**
5-iodotubercidin (NA)	nsP1	-	Yes	clinical isolate 119067	0.409	> 50	Vero	-	-	-	(66)
lobaric acid	nsP1	-	Yes	LR2006 OPY1 (ECSA)	9.9 ± 2.6	76.3 ± 2.1	BHK	-	-	-	(67)
sinefungin	nsP1	-	Yes	CHIKV LS3	184.9 ± 38.4	> 1,000	VeroE6	-	-	-	(66, 122) Kovacikova et al., unpublished

[a]For compounds identified using *in silico* approaches, only those compounds for which the antiviral activity was demonstrated in cell culture using infectious CHIKV are reported; all other compounds for which activity was claimed against CHIKV from in silico screens, but for which no activity in cell-based assays was reported, are excluded from this table.-, not determined/not done (*in vivo* studies)

References

1. Robinson MC. 1955. An epidemic of virus disease in Southern Province, Tanganyika Territory, in 1952-53. I. Clinical features. Trans R Soc Trop Med Hyg 49:28-32.
2. Chretien JP, Anyamba A, Bedno SA, Breiman RF, Sang R, Sergon K, Powers AM, Onyango CO, Small J, Tucker CJ, Linthicum KJ. 2007. Drought-associated chikungunya emergence along coastal East Africa. Am J Trop Med Hyg 76:405-7.
3. Vazeille M, Moutailler S, Coudrier D, Rousseaux C, Khun H, Huerre M, Thiria J, Dehecq JS, Fontenille D, Schuffenecker I, Despres P, Failloux AB. 2007. Two Chikungunya isolates from the outbreak of La Reunion (Indian Ocean) exhibit different patterns of infection in the mosquito, Aedes albopictus. PLoS One 2:e1168.
4. Cassadou S, Boucau S, Petit-Sinturel M, Huc P, Leparc-Goffart I, Ledrans M. 2014. Emergence of chikungunya fever on the French side of Saint Martin island, October to December 2013. Euro Surveill 19.
5. Rezza G, Nicoletti L, Angelini R, Romi R, Finarelli AC, Panning M, Cordioli P, Fortuna C, Boros S, Magurano F, Silvi G, Angelini P, Dottori M, Ciufolini MG, Majori GC, Cassone A. 2007. Infection with chikungunya virus in Italy: an outbreak in a temperate region. Lancet 370:1840-6.
6. Venturi G, Di Luca M, Fortuna C, Remoli ME, Riccardo F, Severini F, Toma L, Del Manso M, Benedetti E, Caporali MG, Amendola A, Fiorentini C, De Liberato C, Giammattei R, Romi R, Pezzotti P, Rezza G, Rizzo C. 2017. Detection of a chikungunya outbreak in Central Italy, August to September 2017. Euro Surveill 22.
7. Grandadam M, Caro V, Plumet S, Thiberge JM, Souares Y, Failloux AB, Tolou HJ, Budelot M, Cosserat D, Leparc-Goffart I, Despres P. 2011. Chikungunya virus, southeastern France. Emerg Infect Dis 17:910-3.
8. Delisle E, Rousseau C, Broche B, Leparc-Goffart I, L'Ambert G, Cochet A, Prat C, Foulongne V, Ferre JB, Catelinois O, Flusin O, Tchernonog E, Moussion IE, Wiegandt A, Septfons A, Mendy A, Moyano MB, Laporte L, Maurel J, Jourdain F, Reynes J, Paty MC, Golliot F. 2015. Chikungunya outbreak in Montpellier, France, September to October 2014. Euro Surveill 20.
9. Calba C, Guerbois-Galla M, Franke F, Jeannin C, Auzet-Caillaud M, Grard G, Pigaglio L, Decoppet A, Weicherding J, Savaill MC, Munoz-Riviero M, Chaud P, Cadiou B, Ramalli L, Fournier P, Noel H, De Lamballerie X, Paty MC, Leparc-Goffart I. 2017. Preliminary report of an autochthonous chikungunya outbreak in France, July to September 2017. Euro Surveill 22.
10. Suhrbier A. 2019. Rheumatic manifestations of chikungunya: emerging concepts and interventions. Nat Rev Rheumatol doi:10.1038/s41584-019-0276-9.
11. Law YS, Utt A, Tan YB, Zheng J, Wang S, Chen MW, Griffin PR, Merits A, Luo D. 2019. Structural insights into RNA recognition by the Chikungunya virus nsP2 helicase. Proc Natl Acad Sci U S A 116:9558-9567.
12. Narwal M, Singh H, Pratap S, Malik A, Kuhn RJ, Kumar P, Tomar S. 2018. Crystal structure of chikungunya virus nsP2 cysteine protease reveals a putative flexible loop blocking its active site. Int J Biol Macromol 116:451-462.

13. Malet H, Coutard B, Jamal S, Dutartre H, Papageorgiou N, Neuvonen M, Ahola T, Forrester N, Gould EA, Lafitte D, Ferron F, Lescar J, Gorbalenya AE, de Lamballerie X, Canard B. 2009. The crystal structures of Chikungunya and Venezuelan equine encephalitis virus nsP3 macro domains define a conserved adenosine binding pocket. J Virol 83:6534-45.
14. Vogel RH, Provencher SW, von Bonsdorff CH, Adrian M, Dubochet J. 1986. Envelope structure of Semliki Forest virus reconstructed from cryo-electron micrographs. Nature 320:533-5.
15. Paredes AM, Brown DT, Rothnagel R, Chiu W, Schoepp RJ, Johnston RE, Prasad BV. 1993. Three-dimensional structure of a membrane-containing virus. Proc Natl Acad Sci U S A 90:9095-9.
16. von Bonsdorff CH, Harrison SC. 1975. Sindbis virus glycoproteins form a regular icosahedral surface lattice. J Virol 16:141-5.
17. Smith TJ, Cheng RH, Olson NH, Peterson P, Chase E, Kuhn RJ, Baker TS. 1995. Putative receptor binding sites on alphaviruses as visualized by cryoelectron microscopy. Proc Natl Acad Sci U S A 92:10648-52.
18. Helenius A, Kartenbeck J, Simons K, Fries E. 1980. On the entry of Semliki forest virus into BHK-21 cells. J Cell Biol 84:404-20.
19. Wahlberg JM, Bron R, Wilschut J, Garoff H. 1992. Membrane fusion of Semliki Forest virus involves homotrimers of the fusion protein. J Virol 66:7309-18.
20. Gibbons DL, Ahn A, Chatterjee PK, Kielian M. 2000. Formation and characterization of the trimeric form of the fusion protein of Semliki Forest Virus. J Virol 74:7772-80.
21. Varghese FS, Rausalu K, Hakanen M, Saul S, Kummerer BM, Susi P, Merits A, Ahola T. 2017. Obatoclax Inhibits Alphavirus Membrane Fusion by Neutralizing the Acidic Environment of Endocytic Compartments. Antimicrob Agents Chemother 61.
22. Delogu I, Pastorino B, Baronti C, Nougairede A, Bonnet E, de Lamballerie X. 2011. In vitro antiviral activity of arbidol against Chikungunya virus and characteristics of a selected resistant mutant. Antiviral Res 90:99-107.
23. Silva LA, Khomandiak S, Ashbrook AW, Weller R, Heise MT, Morrison TE, Dermody TS. 2014. A single-amino-Acid polymorphism in chikungunya virus e2 glycoprotein influences glycosaminoglycan utilization. J Virol 88:2385-97.
24. Di Mola A, Peduto A, La Gatta A, Delang L, Pastorino B, Neyts J, Leyssen P, de Rosa M, Filosa R. 2014. Structure-activity relationship study of arbidol derivatives as inhibitors of chikungunya virus replication. Bioorg Med Chem 22:6014-25.
25. Albulescu IC, van Hoolwerff M, Wolters LA, Bottaro E, Nastruzzi C, Yang SC, Tsay SC, Hwu JR, Snijder EJ, van Hemert MJ. 2015. Suramin inhibits chikungunya virus replication through multiple mechanisms. Antiviral Res 121:39-46.
26. Ho YJ, Wang YM, Lu JW, Wu TY, Lin LI, Kuo SC, Lin CC. 2015. Suramin Inhibits Chikungunya Virus Entry and Transmission. PLoS One 10:e0133511.
27. Henss L, Beck S, Weidner T, Biedenkopf N, Sliva K, Weber C, Becker S, Schnierle BS. 2016. Suramin is a potent inhibitor of Chikungunya and Ebola virus cell entry. Virol J 13:149.
28. Albulescu IC, White-Scholten L, Tas A, Hoornweg TE, Ferla S, Kovacikova K, Smit JM, Brancale A, Snijder EJ, van Hemert MJ. 2020. Suramin Inhibits Chikungunya Virus Replication by Interacting with Virions and Blocking the Early Steps of Infection. Viruses 12.

29. Kuo SC, Wang YM, Ho YJ, Chang TY, Lai ZZ, Tsui PY, Wu TY, Lin CC. 2016. Suramin treatment reduces chikungunya pathogenesis in mice. Antiviral Res 134:89-96.
30. Sharma R, Fatma B, Saha A, Bajpai S, Sistla S, Dash PK, Parida M, Kumar P, Tomar S. 2016. Inhibition of chikungunya virus by picolinate that targets viral capsid protein. Virology 498:265-276.
31. Jing X, Ma C, Ohigashi Y, Oliveira FA, Jardetzky TS, Pinto LH, Lamb RA. 2008. Functional studies indicate amantadine binds to the pore of the influenza A virus M2 proton-selective ion channel. Proc Natl Acad Sci U S A 105:10967-72.
32. Dey D, Siddiqui SI, Mamidi P, Ghosh S, Kumar CS, Chattopadhyay S, Ghosh S, Banerjee M. 2019. The effect of amantadine on an ion channel protein from Chikungunya virus. PLoS Negl Trop Dis 13:e0007548.
33. Freedman A, Steinberg VL. 1960. Chloroquine in rheumatoid arthritis; a double blindfold trial of treatment for one year. Ann Rheum Dis 19:243-50.
34. Brighton SW. 1984. Chloroquine phosphate treatment of chronic Chikungunya arthritis. An open pilot study. S Afr Med J 66:217-8.
35. De Lamballerie X, Boisson V, Reynier JC, Enault S, Charrel RN, Flahault A, Roques P, Le Grand R. 2008. On chikungunya acute infection and chloroquine treatment. Vector Borne Zoonotic Dis 8:837-9.
36. Chopra A, Saluja M, Venugopalan A. 2014. Effectiveness of chloroquine and inflammatory cytokine response in patients with early persistent musculoskeletal pain and arthritis following chikungunya virus infection. Arthritis Rheumatol 66:319-26.
37. Maheshwari RK, Srikantan V, Bhartiya D. 1991. Chloroquine enhances replication of Semliki Forest virus and encephalomyocarditis virus in mice. J Virol 65:992-5.
38. Khan M, Santhosh SR, Tiwari M, Lakshmana Rao PV, Parida M. 2010. Assessment of in vitro prophylactic and therapeutic efficacy of chloroquine against Chikungunya virus in vero cells. J Med Virol 82:817-24.
39. Rothan HA, Bahrani H, Mohamed Z, Teoh TC, Shankar EM, Rahman NA, Yusof R. 2015. A combination of doxycycline and ribavirin alleviated chikungunya infection. PLoS One 10:e0126360.
40. von Rhein C, Weidner T, Henß L, Martin J, Weber C, Sliva K, Schnierle BS. 2016. Curcumin and Boswellia serrata gum resin extract inhibit chikungunya and vesicular stomatitis virus infections in vitro. Antiviral Res 125:51-7.
41. Mounce BC, Cesaro T, Carrau L, Vallet T, Vignuzzi M. 2017. Curcumin inhibits Zika and chikungunya virus infection by inhibiting cell binding. Antiviral Res 142:148-157.
42. Wang YM, Lu JW, Lin CC, Chin YF, Wu TY, Lin LI, Lai ZZ, Kuo SC, Ho YJ. 2016. Antiviral activities of niclosamide and nitazoxanide against chikungunya virus entry and transmission. Antiviral Res 135:81-90.
43. Pohjala L, Utt A, Varjak M, Lulla A, Merits A, Ahola T, Tammela P. 2011. Inhibitors of alphavirus entry and replication identified with a stable Chikungunya replicon cell line and virus-based assays. PLoS One 6:e28923.
44. Wintachai P, Thuaud F, Basmadjian C, Roytrakul S, Ubol S, Desaubry L, Smith DR. 2015. Assessment of flavaglines as potential chikungunya virus entry inhibitors. Microbiol Immunol doi:10.1111/1348-0421.12230.

45. Khan AH, Morita K, Parquet Md Mdel C, Hasebe F, Mathenge EG, Igarashi A. 2002. Complete nucleotide sequence of chikungunya virus and evidence for an internal polyadenylation site. J Gen Virol 83:3075-84.
46. Cross RK. 1983. Identification of a unique guanine-7-methyltransferase in Semliki Forest virus (SFV) infected cell extracts. Virology 130:452-63.
47. Ahola T, Kaariainen L. 1995. Reaction in alphavirus mRNA capping: formation of a covalent complex of nonstructural protein nsP1 with 7-methyl-GMP. Proc Natl Acad Sci U S A 92:507-11.
48. Vasiljeva L, Merits A, Auvinen P, Kaariainen L. 2000. Identification of a novel function of the alphavirus capping apparatus. RNA 5'-triphosphatase activity of Nsp2. J Biol Chem 275:17281-7.
49. Spuul P, Salonen A, Merits A, Jokitalo E, Kaariainen L, Ahola T. 2007. Role of the amphipathic peptide of Semliki forest virus replicase protein nsP1 in membrane association and virus replication. J Virol 81:872-83.
50. Laakkonen P, Ahola T, Kaariainen L. 1996. The effects of palmitoylation on membrane association of Semliki forest virus RNA capping enzyme. J Biol Chem 271:28567-71.
51. Bakhache W, Neyret A, Bernard E, Merits A, Briant L. 2020. Palmitoylated cysteines in Chikungunya virus nsP1 are critical for targeting to cholesterol-rich plasma membrane microdomains with functional consequences for viral genome replication. J Virol doi:10.1128/jvi.02183-19.
52. Wang HL, O'Rear J, Stollar V. 1996. Mutagenesis of the Sindbis virus nsP1 protein: effects on methyltransferase activity and viral infectivity. Virology 217:527-31.
53. Gigante A, Canela MD, Delang L, Priego EM, Camarasa MJ, Querat G, Neyts J, Leyssen P, Perez-Perez MJ. 2014. Identification of [1,2,3]Triazolo[4,5-d]pyrimidin-7(6H)-ones as Novel Inhibitors of Chikungunya Virus Replication. J Med Chem 57:4000-8.
54. Gigante A, Gomez-SanJuan A, Delang L, Li C, Bueno O, Gamo AM, Priego EM, Camarasa MJ, Jochmans D, Leyssen P, Decroly E, Coutard B, Querat G, Neyts J, Perez-Perez MJ. 2017. Antiviral activity of [1,2,3]triazolo[4,5-d]pyrimidin-7(6H)-ones against chikungunya virus targeting the viral capping nsP1. Antiviral Res 144:216-222.
55. Delang L, Li C, Tas A, Querat G, Albulescu IC, De Burghgraeve T, Guerrero NA, Gigante A, Piorkowski G, Decroly E, Jochmans D, Canard B, Snijder EJ, Perez-Perez MJ, van Hemert MJ, Coutard B, Leyssen P, Neyts J. 2016. The viral capping enzyme nsP1: a novel target for the inhibition of chikungunya virus infection. Sci Rep 6:31819.
56. Moesslacher J, Battisti V, Delang L, Neyts J, Abdelnabi R, Pürstinger G, Urban E, Langer T. 2020. Identification of 2-(4-(Phenylsulfonyl)piperazine-1-yl)pyrimidine Analogues as Novel Inhibitors of Chikungunya Virus. ACS Med Chem Lett 11:906-912.
57. Abdelnabi R, Kovacikova K, Moesslacher J, Donckers K, Battisti V, Leyssen P, Langer T, Puerstinger G, Quérat G, Li C, Decroly E, Tas A, Marchand A, Chaltin P, Coutard B, van Hemert M, Neyts J, Delang L. 2020. Novel Class of Chikungunya Virus Small Molecule Inhibitors That Targets the Viral Capping Machinery. Antimicrob Agents Chemother 64.
58. Shin YS, Jarhad DB, Jang MH, Kovacikova K, Kim G, Yoon JS, Kim HR, Hyun YE, Tipnis AS, Chang TS, van Hemert MJ, Jeong LS. 2020. Identification of 6'-beta-fluoro-homoaristeromycin as a potent inhibitor of chikungunya virus replication. Eur J Med Chem 187:111956.

59. Kovacikova K, Morren BM, Tas A, Albulescu IC, van Rijswijk R, Jarhad DB, Shin YS, Jang MH, Kim G, Lee HW, Jeong LS, Snijder EJ, van Hemert MJ. 2020. 6'-beta-Fluoro-Homoaristeromycin and 6'-Fluoro-Homoneplanocin A Are Potent Inhibitors of Chikungunya Virus Replication through Their Direct Effect on Viral Nonstructural Protein 1. Antimicrob Agents Chemother 64.
60. Mounce BC, Cesaro T, Moratorio G, Hooikaas PJ, Yakovleva A, Werneke SW, Smith EC, Poirier EZ, Simon-Loriere E, Prot M, Tamietti C, Vitry S, Volle R, Khou C, Frenkiel MP, Sakuntabhai A, Delpeyroux F, Pardigon N, Flamand M, Barba-Spaeth G, Lafon M, Denison MR, Albert ML, Vignuzzi M. 2016. Inhibition of Polyamine Biosynthesis Is a Broad-Spectrum Strategy against RNA Viruses. J Virol 90:9683-9692.
61. Mounce BC, Cesaro T, Vlajnić L, Vidiņa A, Vallet T, Weger-Lucarelli J, Passoni G, Stapleford KA, Levraud JP, Vignuzzi M. 2017. Chikungunya Virus Overcomes Polyamine Depletion by Mutation of nsP1 and the Opal Stop Codon To Confer Enhanced Replication and Fitness. J Virol 91.
62. Khan M, Dhanwani R, Patro IK, Rao PV, Parida MM. 2011. Cellular IMPDH enzyme activity is a potential target for the inhibition of Chikungunya virus replication and virus induced apoptosis in cultured mammalian cells. Antiviral Res 89:1-8.
63. Scheidel LM, Stollar V. 1991. Mutations that confer resistance to mycophenolic acid and ribavirin on Sindbis virus map to the nonstructural protein nsP1. Virology 181:490-9.
64. Scheidel LM, Durbin RK, Stollar V. 1987. Sindbis virus mutants resistant to mycophenolic acid and ribavirin. Virology 158:1-7.
65. Rosenblum CI, Scheidel LM, Stollar V. 1994. Mutations in the nsP1 coding sequence of Sindbis virus which restrict viral replication in secondary cultures of chick embryo fibroblasts prepared from aged primary cultures. Virology 198:100-8.
66. Mudgal R, Mahajan S, Tomar S. 2020. Inhibition of Chikungunya virus by an adenosine analog targeting the SAM-dependent nsP1 methyltransferase. FEBS Lett 594:678-694.
67. Feibelman KM, Fuller BP, Li L, LaBarbera DV, Geiss BJ. 2018. Identification of small molecule inhibitors of the Chikungunya virus nsP1 RNA capping enzyme. Antiviral Res 154:124-131.
68. Karpe YA, Aher PP, Lole KS. 2011. NTPase and 5'-RNA Triphosphatase Activities of Chikungunya Virus nsP2 Protein. PLoS One 6:e22336.
69. Rikkonen M, Peranen J, Kaariainen L. 1994. ATPase and GTPase activities associated with Semliki Forest virus nonstructural protein nsP2. J Virol 68:5804-10.
70. Gomez de Cedron M, Ehsani N, Mikkola ML, Garcia JA, Kaariainen L. 1999. RNA helicase activity of Semliki Forest virus replicase protein NSP2. FEBS Lett 448:19-22.
71. Hardy WR, Strauss JH. 1989. Processing the nonstructural polyproteins of sindbis virus: nonstructural proteinase is in the C-terminal half of nsP2 and functions both in cis and in trans. J Virol 63:4653-64.
72. Vasiljeva L, Valmu L, Kääriäinen L, Merits A. 2001. Site-specific protease activity of the carboxyl-terminal domain of Semliki Forest virus replicase protein nsP2. J Biol Chem 276:30786-93.
73. Utt A, Das PK, Varjak M, Lulla V, Lulla A, Merits A. 2015. Mutations conferring a noncytotoxic phenotype on chikungunya virus replicons compromise enzymatic properties of nonstructural protein 2. J Virol 89:3145-62.

74. Akhrymuk I, Kulemzin SV, Frolova EI. 2012. Evasion of the Innate Immune Response: the Old World Alphavirus nsP2 Protein Induces Rapid Degradation of Rpb1, a Catalytic Subunit of RNA Polymerase II. J Virol 86:7180-91.

75. Treffers EE, Tas A, Scholte FE, Van MN, Heemskerk MT, de Ru AH, Snijder EJ, van Hemert MJ, van Veelen PA. 2015. Temporal SILAC-based quantitative proteomics identifies host factors involved in chikungunya virus replication. Proteomics doi:10.1002/pmic.201400581.

76. Akhrymuk I, Lukash T, Frolov I, Frolova EI. 2019. Novel Mutations in nsP2 Abolish Chikungunya Virus-Induced Transcriptional Shutoff and Make the Virus Less Cytopathic without Affecting Its Replication Rates. J Virol 93.

77. Göertz GP, McNally KL, Robertson SJ, Best SM, Pijlman GP, Fros JJ. 2018. The Methyltransferase-Like Domain of Chikungunya Virus nsP2 Inhibits the Interferon Response by Promoting the Nuclear Export of STAT1. J Virol 92.

78. Bassetto M, De Burghgraeve T, Delang L, Massarotti A, Coluccia A, Zonta N, Gatti V, Colombano G, Sorba G, Silvestri R, Tron GC, Neyts J, Leyssen P, Brancale A. 2013. Computer-aided identification, design and synthesis of a novel series of compounds with selective antiviral activity against chikungunya virus. Antiviral Res 98:12-8.

79. Jadav SS, Sinha BN, Hilgenfeld R, Pastorino B, de Lamballerie X, Jayaprakash V. 2015. Thiazolidone derivatives as inhibitors of chikungunya virus. Eur J Med Chem 89:172-8.

80. Das PK, Puusepp L, Varghese FS, Utt A, Ahola T, Kananovich DG, Lopp M, Merits A, Karelson M. 2016. Design and validation of novel chikungunya virus protease inhibitors. Antimicrob Agents Chemother doi:10.1128/aac.01421-16.

81. El-Labbad EM, Ismail MA, Abou Ei Ella DA, Ahmed M, Wang F, Barakat KH, Abouzid KA. 2015. Discovery of Novel Peptidomimetics as Irreversible CHIKV NsP2 Protease Inhibitors Using Quantum Mechanical-Based Ligand Descriptors. Chem Biol Drug Des doi:10.1111/cbdd.12621.

82. Shin G, Yost SA, Miller MT, Elrod EJ, Grakoui A, Marcotrigiano J. 2012. Structural and functional insights into alphavirus polyprotein processing and pathogenesis. Proc Natl Acad Sci U S A 109:16534-9.

83. Foy NJ, Akhrymuk M, Akhrymuk I, Atasheva S, Bopda-Waffo A, Frolov I, Frolova EI. 2013. Hypervariable domains of nsP3 proteins of New World and Old World alphaviruses mediate formation of distinct, virus-specific protein complexes. J Virol 87:1997-2010.

84. Kim DY, Reynaud JM, Rasalouskaya A, Akhrymuk I, Mobley JA, Frolov I, Frolova EI. 2016. New World and Old World Alphaviruses Have Evolved to Exploit Different Components of Stress Granules, FXR and G3BP Proteins, for Assembly of Viral Replication Complexes. PLoS Pathog 12:e1005810.

85. Meshram CD, Agback P, Shiliaev N, Urakova N, Mobley JA, Agback T, Frolova EI, Frolov I. 2018. Multiple Host Factors Interact with the Hypervariable Domain of Chikungunya Virus nsP3 and Determine Viral Replication in Cell-Specific Mode. J Virol 92.

86. Abraham R, Hauer D, McPherson RL, Utt A, Kirby IT, Cohen MS, Merits A, Leung AKL, Griffin DE. 2018. ADP-ribosyl-binding and hydrolase activities of the alphavirus nsP3 macrodomain are critical for initiation of virus replication. Proc Natl Acad Sci U S A 115:E10457-e10466.

87. McPherson RL, Abraham R, Sreekumar E, Ong SE, Cheng SJ, Baxter VK, Kistemaker HA, Filippov DV, Griffin DE, Leung AK. 2017. ADP-ribosylhydrolase activity of Chikungunya virus macrodomain is critical for virus replication and virulence. Proc Natl Acad Sci U S A 114:1666-1671.

88. Gao Y, Goonawardane N, Ward J, Tuplin A, Harris M. 2019. Multiple roles of the non-structural protein 3 (nsP3) alphavirus unique domain (AUD) during Chikungunya virus genome replication and transcription. PLoS Pathog 15:e1007239.

89. Seyedi SS, Shukri M, Hassandarvish P, Oo A, Muthu SE, Abubakar S, Zandi K. 2016. Computational Approach Towards Exploring Potential Anti-Chikungunya Activity of Selected Flavonoids. Sci Rep 6:24027.

90. Oo A, Rausalu K, Merits A, Higgs S, Vanlandingham D, Bakar SA, Zandi K. 2018. Deciphering the potential of baicalin as an antiviral agent for Chikungunya virus infection. Antiviral Res 150:101-111.

91. Pietila MK, Hellstrom K, Ahola T. 2017. Alphavirus polymerase and RNA replication. Virus Res doi:10.1016/j.virusres.2017.01.007.

92. Tomar S, Hardy RW, Smith JL, Kuhn RJ. 2006. Catalytic core of alphavirus nonstructural protein nsP4 possesses terminal adenylyltransferase activity. J Virol 80:9962-9.

93. Bhatia HK, Singh H, Grewal N, Natt NK. 2014. Sofosbuvir: A novel treatment option for chronic hepatitis C infection. J Pharmacol Pharmacother 5:278-84.

94. Ferreira AC, Reis PA, de Freitas CS, Sacramento CQ, Villas Boas Hoelz L, Bastos MM, Mattos M, Rocha N, Gomes de Azevedo Quintanilha I, da Silva Gouveia Pedrosa C, Rocha Quintino Souza L, Correia Loiola E, Trindade P, Rangel Vieira Y, Barbosa-Lima G, de Castro Faria Neto HC, Boechat N, Rehen SK, Bruning K, Bozza FA, Bozza PT, Souza TML. 2019. Beyond Members of the Flaviviridae Family, Sofosbuvir Also Inhibits Chikungunya Virus Replication. Antimicrob Agents Chemother 63.

95. Ehteshami M, Tao S, Zandi K, Hsiao HM, Jiang Y, Hammond E, Amblard F, Russell OO, Merits A, Schinazi RF. 2017. Characterization of beta-D-N4-hydroxycytidine as a Novel Inhibitor of Chikungunya Virus. Antimicrob Agents Chemother doi:10.1128/aac.02395-16.

96. Urakova N, Kuznetsova V, Crossman DK, Sokratian A, Guthrie DB, Kolykhalov AA, Lockwood MA, Natchus MG, Crowley MR, Painter GR, Frolova EI, Frolov I. 2018. β-d-N (4)-Hydroxycytidine Is a Potent Anti-alphavirus Compound That Induces a High Level of Mutations in the Viral Genome. J Virol 92.

97. Delang L, Segura Guerrero N, Tas A, Querat G, Pastorino B, Froeyen M, Dallmeier K, Jochmans D, Herdewijn P, Bello F, Snijder EJ, de Lamballerie X, Martina B, Neyts J, van Hemert MJ, Leyssen P. 2014. Mutations in the chikungunya virus non-structural proteins cause resistance to favipiravir (T-705), a broad-spectrum antiviral. J Antimicrob Chemother 69:2770-84.

98. Abdelnabi R, Jochmans D, Verbeken E, Neyts J, Delang L. 2017. Antiviral treatment efficiently inhibits chikungunya virus infection in the joints of mice during the acute but not during the chronic phase of the infection. Antiviral Res doi:10.1016/j.antiviral.2017.09.016.

99. Coffey LL, Beeharry Y, Borderia AV, Blanc H, Vignuzzi M. 2011. Arbovirus high fidelity variant loses fitness in mosquitoes and mice. Proc Natl Acad Sci U S A 108:16038-43.

100. Ashbrook AW, Lentscher AJ, Zamora PF, Silva LA, May NA, Bauer JA, Morrison TE, Dermody TS. 2016. Antagonism of the Sodium-Potassium ATPase Impairs Chikungunya Virus Infection. MBio 7.

101. Rathore AP, Haystead T, Das PK, Merits A, Ng ML, Vasudevan SG. 2014. Chikungunya virus nsP3 & nsP4 interacts with HSP-90 to promote virus replication: HSP-90 inhibitors reduce CHIKV infection and inflammation in vivo. Antiviral Res 103:7-16.

102. Rada B, Dragun M. 1977. Antiviral action and selectivity of 6-azauridine. Ann N Y Acad Sci 284:410-7.

103. Scholte FE, Tas A, Martina BE, Cordioli P, Narayanan K, Makino S, Snijder EJ, van Hemert MJ. 2013. Characterization of synthetic Chikungunya viruses based on the consensus sequence of recent E1-226V isolates. PLoS One 8:e71047.

104. Briolant S, Garin D, Scaramozzino N, Jouan A, Crance JM. 2004. In vitro inhibition of Chikungunya and Semliki Forest viruses replication by antiviral compounds: synergistic effect of interferon-alpha and ribavirin combination. Antiviral Res 61:111-7.

105. Yang Y, Cao L, Gao H, Wu Y, Wang Y, Fang F, Lan T, Lou Z, Rao Y. 2019. Discovery, Optimization, and Target Identification of Novel Potent Broad-Spectrum Antiviral Inhibitors. J Med Chem 62:4056-4073.

106. Cifuentes Kottkamp A, De Jesus E, Grande R, Brown JA, Jacobs AR, Lim JK, Stapleford KA. 2019. Atovaquone Inhibits Arbovirus Replication through the Depletion of Intracellular Nucleotides. J Virol 93.

107. Varghese FS, Kaukinen P, Glasker S, Bespalov M, Hanski L, Wennerberg K, Kummerer BM, Ahola T. 2016. Discovery of berberine, abamectin and ivermectin as antivirals against chikungunya and other alphaviruses. Antiviral Res 126:117-24.

108. Wan JJ, Brown RS, Kielian M. 2020. Berberine Chloride is an Alphavirus Inhibitor That Targets Nucleocapsid Assembly. mBio 11.

109. Varghese FS, Thaa B, Amrun SN, Simarmata D, Rausalu K, Nyman TA, Merits A, McInerney GM, Ng LFP, Ahola T. 2016. The Antiviral Alkaloid Berberine Reduces Chikungunya Virus-Induced Mitogen-Activated Protein Kinase Signaling. J Virol 90:9743-9757.

110. Kaur P, Thiruchelvan M, Lee RC, Chen H, Chen KC, Ng ML, Chu JJ. 2013. Inhibition of chikungunya virus replication by harringtonine, a novel antiviral that suppresses viral protein expression. Antimicrob Agents Chemother 57:155-67.

111. Lani R, Hassandarvish P, Chiam CW, Moghaddam E, Chu JJ, Rausalu K, Merits A, Higgs S, Vanlandingham D, Abu Bakar S, Zandi K. 2015. Antiviral activity of silymarin against chikungunya virus. Sci Rep 5:11421.

112. Wichit S, Hamel R, Bernard E, Talignani L, Diop F, Ferraris P, Liegeois F, Ekchariyawat P, Luplertlop N, Surasombatpattana P, Thomas F, Merits A, Choumet V, Roques P, Yssel H, Briant L, Missé D. 2017. Imipramine Inhibits Chikungunya Virus Replication in Human Skin Fibroblasts through Interference with Intracellular Cholesterol Trafficking. Sci Rep 7:3145.

113. Troost B, Mulder LM, Diosa-Toro M, van de Pol D, Rodenhuis-Zybert IA, Smit JM. 2020. Tomatidine, a natural steroidal alkaloid shows antiviral activity towards chikungunya virus in vitro. Sci Rep 10:6364.

114. Henss L, Scholz T, Grünweller A, Schnierle BS. 2018. Silvestrol Inhibits Chikungunya Virus Replication. Viruses 10.

115. Wintachai P, Kaur P, Lee RC, Ramphan S, Kuadkitkan A, Wikan N, Ubol S, Roytrakul S, Chu JJ, Smith DR. 2015. Activity of andrographolide against chikungunya virus infection. Sci Rep 5:14179.

116. Ho YJ, Liu FC, Yeh CT, Yang CM, Lin CC, Lin TY, Hsieh PS, Hu MK, Gong Z, Lu JW. 2018. Micafungin is a novel anti-viral agent of chikungunya virus through multiple mechanisms. Antiviral Res 159:134-142.

117. Mishra P, Kumar A, Mamidi P, Kumar S, Basantray I, Saswat T, Das I, Nayak TK, Chattopadhyay S, Subudhi BB, Chattopadhyay S. 2016. Inhibition of Chikungunya Virus Replication by 1-[(2-Methylbenzimidazol-1-yl) Methyl]-2-Oxo-Indolin-3-ylidene] Amino] Thiourea(MBZM-N-IBT). Sci Rep 6:20122.

118. Delang L, Yen PS, Vallet T, Vazeille M, Vignuzzi M, Failloux AB. 2018. Differential Transmission of Antiviral Drug-Resistant Chikungunya Viruses by Aedes Mosquitoes. mSphere 3.

119. Franco EJ, Rodriquez JL, Pomeroy JJ, Hanrahan KC, Brown AN. 2018. The effectiveness of antiviral agents with broad-spectrum activity against chikungunya virus varies between host cell lines. Antivir Chem Chemother 26:2040206618807580.

120. Poo YS, Rudd PA, Gardner J, Wilson JA, Larcher T, Colle MA, Le TT, Nakaya HI, Warrilow D, Allcock R, Bielefeldt-Ohmann H, Schroder WA, Khromykh AA, Lopez JA, Suhrbier A. 2014. Multiple immune factors are involved in controlling acute and chronic chikungunya virus infection. PLoS Negl Trop Dis 8:e3354.

121. Mounce BC, Poirier EZ, Passoni G, Simon-Loriere E, Cesaro T, Prot M, Stapleford KA, Moratorio G, Sakuntabhai A, Levraud JP, Vignuzzi M. 2016. Interferon-Induced Spermidine-Spermine Acetyltransferase and Polyamine Depletion Restrict Zika and Chikungunya Viruses. Cell Host Microbe 20:167-77.

122. Kaur R, Mudgal R, Narwal M, Tomar S. 2018. Development of an ELISA assay for screening inhibitors against divalent metal ion dependent alphavirus capping enzyme. Virus Res 256:209-218.

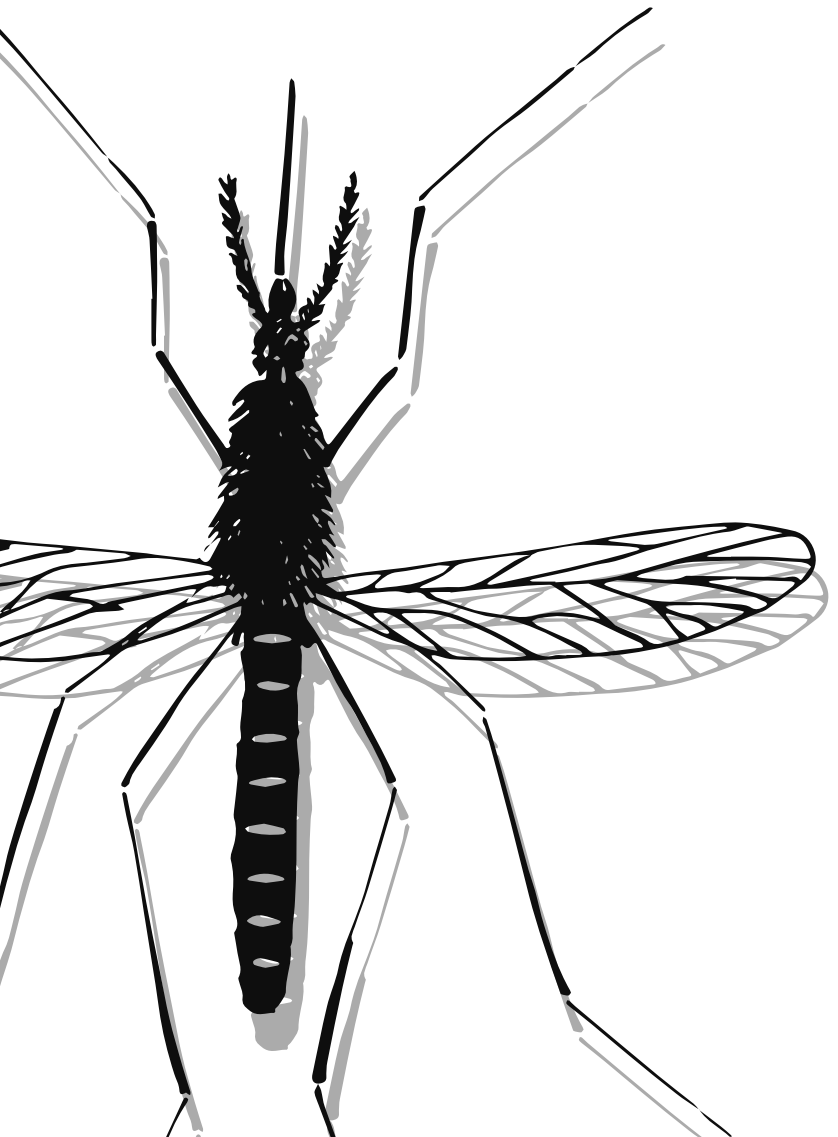

CHAPTER 3

Identification of 6'-fluorinated-aristeromycin and 6'-fluorinated-homoaristeromycin analogues as Chikungunya virus inhibitors

Kristina Kovacikova[a], Dnyandev B. Jarhad[b], Su Bin Wang[b], Yun Jeong Kong[b], Tong-Shin Chang[b], Eric J Snijder[a],Martijn J van Hemert[a] and Lak Shin Jeong[b]

[a] Department of Medical Microbiology, Leiden University Medical Center, Albinusdreef 2, 2333ZA Leiden, The Netherlands

[b] Research Institute of Pharmaceutical Sciences, College of Pharmacy, Seoul National University, Seoul 08826, South Korea

The work described in this chapter has been published in:

Yoon JS, Kim G, Jarhad DB, Kim HR, Shin YS, Qu S, Sahu PK, Kim HO, Lee HW, Wang SB, Kong YJ, Chang TS, Ogando NS, Kovacikova K, Snijder EJ, Posthuma CC, van Hemert MJ, Jeong LS. Design, Synthesis and Anti-RNA Virus Activity of 6'-Fluorinated-Aristeromycin Analogues. *J Med Chem*. 2019; 62(13): 6346-6362.

Shin YS, Jarhad DB, Jang MH, Kovacikova K, Kim G, Yoon JS, Kim HR, Hyun YE, Tipnis AS, Chang TS, van Hemert MJ, Jeong LS. Identification of 6'-β-fluoro-homoaristeromycin as a potent inhibitor of chikungunya virus replication. *Eur J Med Chem.* 2020; 187: 111956.

Abstract

6'-fluorinated-aristeromycin analogues were designed as dual-target antiviral compounds aimed at inhibiting both Chikungunya virus (CHIKV) RNA-dependent RNA polymerase and the host cell S-adenosyl-L-homocysteine (SAH) hydrolase. Our results demonstrated that the introduction of a fluorine at the 6'-position of aristeromycin to yield 6'-fluorinated-aristeromycin analogues enhanced the inhibition of SAH hydrolase as well as the antiviral activity of these compounds. Aristeromycin and the *N6*-mehyltaristeromycin analogues **2a-e** showed potent inhibition of SAH hydrolase, while only the aristeromycin derivatives **2b-c** exhibited antiviral activity against CHIKV. 6',6'-Difluoro-aristeromycin **(2c)** showed the strongest anti-CHIKV effect among the 6'-fluorinated-aristeromycin analogues, with more than 2 $\log_{10}$ reduction of the infectious progeny titer. Due to their substantial cytotoxicity, likely attributable to 5'-phosphorylation, one-carbon homologated 6'-fluorinated-aristeromycin analogues were designed. This approach was intended to prevent 5'-phosphorylation by cellular kinases while retaining the inhibitory activity against SAH hydrolase. Four out of five synthesized 6'-fluorinated-homoaristeromycin analogues **4a-e** exhibited potent inhibitory activity towards SAH hydrolase, among which 6'-β-fluoro-homoaristeromycin **(4a)** was the most potent (IC_{50} = 0.36 μM). 6'-β-Fluoro-homoaristeromycin **(4a)** also potently inhibited CHIKV replication (EC_{50} = 0.12 μM) in cytopathic effect (CPE)-reduction assays without inducing noticeable cytotoxicity. Remarkably, only **4a** displayed anti-CHIKV activity, whereas both **4a** and **4b** inhibited SAH hydrolase with similar IC_{50} values (0.36 μM and 0.37 μM, respectively), suggesting that **4a**'s antiviral activity did not merely depend on the inhibition of SAH hydrolase. This was supported by the fact that the antiviral effect was specific for CHIKV and the related alphavirus Semliki Forest virus, while none of the homologated analogues inhibited other plus-stranded RNA viruses, such as Severe acute respiratory syndrome coronavirus, Middle East respiratory syndrome coronavirus or Zika virus. The chemical synthesis of these compounds has been published elsewhere.

Introduction

Chikungunya virus (CHIKV) is an alphavirus belonging to the *Togaviridae* family that is transmitted by mosquitoes and causes a painful arthritis that can persist for months to years (1-3). CHIKV belongs to the + sense single stranded (ss) RNA virus group (Baltimore class IV) (4, 5), which means that their genomic RNA has the same polarity as mRNA and can be directly translated by host ribosomes in the infected cell. The CHIKV genome is translated into a polyprotein that is subsequently cleaved into individual nonstructural proteins 1-4 (nsPs) by a protease domain in nsP2. The nsPs 1-4 harbour a variety of enzymatic activities that are required for the replication of the viral RNA and invariably include an RNA-dependent RNA polymerase (RdRp) encoded by CHIKV nsP4 (6), an enzyme which is not present in uninfected cells. The alphavirus nsP4 transcribes the genomic RNA into a complementary- strand RNA that subsequently serves as the template for the synthesis of new + strand genomic and subgenomic RNA (7).

Many + strand RNA viruses, including CHIKV, encode methyltransferases (MTases) that are required for methylation of viral RNA to produce a cap structure at the 5' terminus. Because this capping process is crucial for the stability and translation of the viral RNA and evasion of the host innate immune response, viral MTases are considered promising targets for the development of antiviral therapy (8-10). Inhibition of MTases, such as the CHIKV MTase encoded by nsP1, can also be achieved indirectly, by the inhibition of S-adenosyl-L-homocysteine (SAH) hydrolase (11, 12). Under normal physiological conditions, this cellular enzyme catalyses the conversion of SAH into adenosine and L-homocysteine. Inhibition of SAH hydrolase leads to the accumulation of SAH in cells, which in turn inhibits S-adenosyl-L-methionine (SAM)-dependent transmethylase reactions by feedback inhibition (13, 14). The CHIKV nsP1-catalysed methylation of viral RNA is dependent on SAM. More specifically, CHIKV nsP1 uses SAM as a methyl donor to transfer a methyl group onto an acceptor molecule of guanosine-5'-triphosphate (GTP) to produce methylated GTP (m^7GTP). In the alphavirus RNA capping process, the GTP molecule is methylated before it is transferred onto the 5' end of viral RNA, which differs from the mechanism used by the host cell (8).

Compounds targeting cellular proteins might exhibit a broader spectrum of antiviral activity and less likelihood of developing drug resistance, although they are more likely to be toxic to the host cell. Thus, the approach of targeting cellular proteins such as SAH hydrolase can be considered as a promising strategy for the development

of broad-spectrum antiviral agents (13, 14). A number of compounds have been reported to act as SAH hydrolase inhibitors. Type I inhibitors act through inactivation of the NAD^+ cofactor of the enzyme, and their inhibitory effect on its catalytic activity can be reversed by the addition of an excess of NAD^+. Type II inhibitors are irreversible inhibitors of the SAH hydrolase that form covalent bonds with amino acid residues in the active site of the enzyme, a process which cannot be reversed by the addition of NAD^+ or adenosine, or by dialysis (13).

Because both CHIKV nsP1 and nsP4 are critical for virus replication, broad-spectrum nucleoside analogue inhibitors that could directly target nsP4 activity and/or indirectly inhibit the methylation of viral RNA through their effect on the host SAH hydrolase were designed (15). Modified nucleosides are usually taken up by cells via nucleoside transporters and can be successively converted into mono-, di-, and triphosphates by cellular kinases. Then, these modified nucleoside triphosphates (NTPs) can compete with natural NTPs during RNA synthesis or can be incorporated into the nascent viral RNA, leading to chain termination or detrimental mutations (16).

(-)-Aristeromycin **(1)** is a naturally occurring carbocyclic nucleoside that was originally identified as a metabolite of *Streptomyces citricolor* in 1967 (17). It is a type I SAH hydrolase inhibitor and exhibits potent antiviral activity against many viruses (13). However, it could not be further advanced into clinical development because of its cytotoxicity, which is likely linked to its conversion into a triphosphate form (18, 19). Therefore, **1** was used as a prototype for the design and synthesis of 6'-fluorinated-aristeromycin analogues as dual-target compounds (15). 6',6'-difluoro-aristeromycin, designated as compound **2c**, exhibited potent antiviral activities against CHIKV (EC_{50} 0.13 μM, CC_{50} >1.25 μM) (Table 1) and also against other emerging + strand RNA viruses such as Middle East Respiratory Syndrome coronavirus (MERS-CoV), Severe acute respiratory syndrome coronavirus (SARS-CoV) or Zika virus (ZIKV) (15). However, because compound **2c** still exhibited substantial cytotoxicity, presumably due to its 5'-phosphorylation, 6'-fluorinated-homoaristeromycin analogues **4a-e** were synthesized (20). These compounds were expected to retain their inhibitory activity towards SAH hydrolase without being 5'-phosphorylated by cellular kinases. The prevention of 5'-phosphorylation would be achieved by a one-carbon homologation step at the 5' position that is expected to displace the susceptible 5'-hydroxyl from the phosphate-transfer zone in the kinases (Fig. 1) (20). The chemical synthesis of both 6'-fluorinated-aristeromycin and 6'-fluorinated-homoaristeromycin analogues is described in (15) and (20). It is based on stereoselective electrophilic fluorination of silyl enol ether with Selectfluor as the fluorine source.

Lastly, to test the hypothesis whether 6'-fluorinated-aristeromycin analogues act as dual-target compounds and inhibit CHIKV RdRp, a phosphoramidate prodrug **3** of nucleoside **2**, was synthesized using the McGuigan ProTides approach (21-28). This method is designed to overcome the limitations associated with the parental nucleosides such as inefficient conversion to their corresponding 5'-monophosphate form and poor cellular uptake. In this chapter, the ability of all nucleosides to inhibit recombinant human SAH hydrolase is reported. Furthermore, the antiviral effect of 6'-fluorinated-aristeromycin and 6'-fluorinated-homoaristeromycin analogues on CHIKV is reported from cytophathic effect (CPE)-based assays and viral load reduction assays. These data were essential for providing more insight into the structure-activity relationships (SAR) of these CHIKV inhibitors.

Materials and Methods

SAH hydrolase assay

SAH hydrolase assays were performed as described previously in (29-32). The gene encoding human placental SAH hydrolase was cloned into expression plasmid pPROKcd20. Recombinant SAH hydrolase proteins was produced in *E. coli* JM109 in 50 mM Tris-HCl (pH 7.5) containing 2 mM ethylenediaminetetraacetic acid and was purified by DEAE-cellulose column (2.8 cm x 6 cm), ammonium sulphate fractionation and precipitation (35 – 60%), Sephacryl S-300HR (1.0 cm x 105 cm), and DEAE cellulose (2.8 cm x 24 cm). The protein purity was confirmed by 10 % sodium dodecyl sulphate polyacrylamide gel electrophoresis and Coomassie staining. The protein concentration was determined by using the Bradford method using a standard curve with different concentrations of bovine serum albumin. Enzyme activity was determined in reaction mixtures (250 µl) that contained 50 mM sodium phosphate (pH 8.0), 2 µM SAH hydrolase (0.5 µM tetrameric form), and varying concentrations of compounds. The reaction mixtures were pre-incubated with the compound for 10 min at 37 °C, after which the reaction was initiated by adding 100 µM SAH. The reaction was allowed to proceed for 20 min, followed by the addition of 5,5'-dithiobis-2-nitrobenzoate (DNTB) to a final concentration of 200 µM. The absorbance of the reaction product 5-thio-2-nitrobenzoic acid (TNB) was measured at 412 nm using a spectrophotometer (Varian, Cary 100). The molar extinction coefficient for TNB (ε_{412} = 13 700 M^{-1} cm^{-1}) was used in calculations to quantify TNB formation.

Cells, viruses and compounds

VeroE6 cells were maintained in Dulbecco's modified Eagle's medium (DMEM) supplemented with 8% foetal calf serum (FCS), 2 mM L-glutamine, 100 IU/ml of penicillin and 100 µg/ml of streptomycin, and were grown at 37 °C in a humidified incubator with 5% CO_2. Infections were performed in Eagle's minimal essential medium (EMEM) with 25 mM HEPES supplemented with 2% FCS, L-glutamine and antibiotics. Infectious clone-derived CHIKV (CHIKV-LS3) was generated as described by Scholte at al. (33). The compounds were dissolved in dimethylsulfoxide (DMSO) to obtain 20 mM stock solutions. All work with infectious CHIKV was performed inside biosafety cabinets in the BSL-3 facilities of the Leiden University Medical Center.

Antiviral CPE-reduction assay

VeroE6 cells were seeded at a density of 5000 cells/well in a total volume of 100 µl/well in 96-well plates. The following day, compound dilutions with concentrations of 150 µM, 50 µM, 16.7 µM and 5.6 µM were prepared in the infection medium by 3-fold serial dilution of the 150 µM solution. After replacing the culture medium with the respective dilutions of the compound, the cells were infected with CHIKV at a MOI of 0.005. Viability assays were conducted in parallel. Each compound was tested at each concentration in quadruplicate (4 biological replicates per concentration). The CellTiter 96 AQueous One Solution Cell Proliferation Assay was conducted at 96 hours post-infection (hpi) for CHIKV by adding 20 µl/well of the MTS/PMS reagent (Promega). The assay was stopped after 2 h by fixing the cells with 37% formaldehyde. The absorbance was measured at 495 nm in a Berthold Mithras LB 940 plate reader, and the values were expressed relative to uninfected (infection) or untreated (viability) controls. The results represent the average of quadruplicate samples expressed as the mean ± SD. Compounds that were found to be protective were further evaluated in CPE reduction assays by testing 8 different concentrations to determine the EC_{50} as previously described (33). The cytotoxicity (CC_{50}) of the compounds was determined in parallel, and all experiments were performed in quadruplicate. GraphPad Prism v8.0.1 was used for EC_{50} and CC_{50} determination by nonlinear regression.

Viral load reduction assay

VeroE6 cells were seeded at a density of 7.5 x 10^4 cells/well in 0.5 ml DMEM/8% FCS in 24-well cell culture plates and allowed to adhere overnight. The next day, compound

dilutions (0 – 1.5 μM) were prepared in EMEM/2% FCS to which CHIKV was added at a MOI of 0.1 to yield inoculum for infecting the cells. Cells were incubated at 37 °C with 250 μl/well of the inoculum for 1 h. After the infection, the cells were washed twice with 1 ml/well of warm phosphate-buffered saline (PBS) and 0.5 ml/well of fresh EMEM/2% FCS with different concentration of compound **2c** (0 – 1.5 μM) was added. The cells were incubated for 30 h at 37 °C, after which supernatants were harvested and stored at-80 °C to determine the infectious virus titer by plaque assay. Viability assays were conducted in parallel as described in the previous paragraph. Plaque assays with CHIKV were performed on VeroE6 cells as described previously (33). Compound **2c** was tested at each concentration in duplicate in two independent experiments (n = 4). GraphPad Prism v8.0.1 was used for statistical analysis with a one-way ANOVA multiple comparison test.

Results and Discussion

Inhibition of SAH hydrolase

The synthesized 6'-fluorinated-aristeromycin and 6'-fluorinated-homoaristeromycin analogues were assayed for their inhibitory activity against SAH hydrolase using enzymatic assays with recombinant SAH hydrolase (Table 1 and 2). All adenosine derivatives **2a-e** potently inhibited SAH hydrolase, but none of the pyrimidine analogues **2f-j** showed any inhibitory activity at concentrations up to 100 μM. In addition, none of the prodrugs **3a-c** exhibited inhibitory activity at concentrations up to 100 μM (Table 1). This result was expected because adenosine, and not the prodrug, is the substrate for SAH hydrolase. The 6'-fluorinated-homoaristeromycin analogues **4a** and **4b** also exhibited potent inhibitory activity against SAH hydrolase while 6,6'-difluoro-homoaristeromycin analogues **4d** and **4e** inhibited the SAH hydrolase to a lesser extent (Table 2). Among the aristeromycin analogues, 6'-β-fluoroaristeromycin **(2a)** was the most potent inhibitor (IC_{50} = 0.37 μM), which was 3.6-fold more potent than the control **1** (IC_{50} = 1.32 μM) (Table 1). However, 6'-α-fluoroaristeromycin (**2b**, IC_{50} = 9.70 μM) was 26-fold less potent than the corresponding 6'-β-fluoro analogue **2a** and 7.4-fold less active than the 6'-unsubstituted compound **1**. This indicates that the stereochemistry at the 6'-position is important for inhibitory activity. Interestingly, the introduction of two fluorines at the 6'-position resulting in 6',6'-difluoro-aristeromycin (**2c**, IC_{50} = 1.06 μM), yielded an analogue that was slightly more potent than the

control **1**. The inhibitory activity of the 6'-fluoroaristeromycin series can be ranked in the following order: 6'-β-F > 6',6'-F, F > 6' H > 6'-α-F. The introduction of a methyl group at the *N6*-amino group of **2a**, resulting in 6'-β-fluoro-*N6*-methyl-aristeromycin **2d**, decreased the inhibitory activity (IC_{50} = 4.39 μM) 11.9-fold, while the addition of a methyl group to the *N6*-amino group of **2c**, resulting in 6',6'-difluoro- *N6*-methyl-aristeromycin **2e**, increased the inhibitory activity (IC_{50} = 0.76 μM) 1.7-fold.

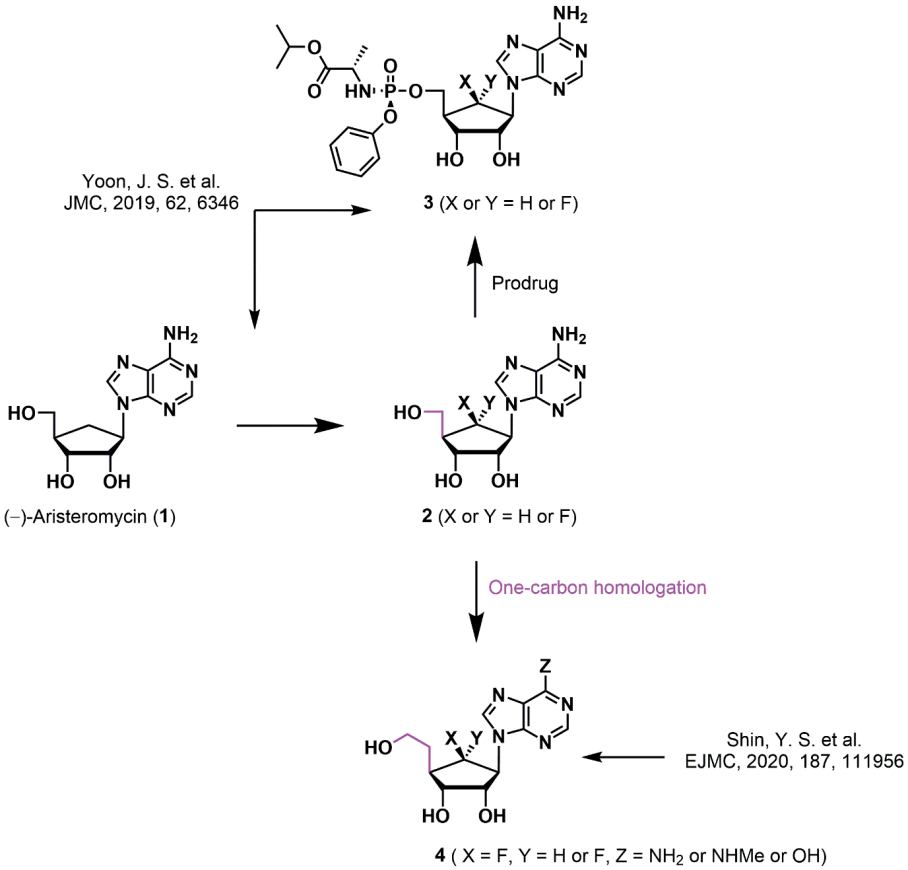

Figure 1. Rationale for the design of the target nucleosides **2**, **3** and **4.** The numbering of compounds **4** corresponds to **3** in (20). Adapted from (15) and (20).

These results demonstrate that the *N6*-methyladenine and adenine moieties do not lead to a decrease in inhibitory activity. The inhibitory activity for 6'-β-fluoro-homoaristeromycin **(4a)** and 6'-β-fluoro-*N6*-methyl-homoaristeromycin **(4b)** were comparable to that of **2a** (IC_{50}s of 0.36 μM and 0.37 μM, respectively). Nevertheless, the SAH hydrolase inhibition by 6,6'-difluoro-homoaristeromycin **(4d)**

and 6,6'-difluoro- *N6*-methyl-homoaristeromycin **(4e)** was 5.6-fold and 8.5-fold lower, respectively, compared to the most potent compounds. The inosine analogue **4c** did not inhibit SAH hydrolase, as no inhibitory activity was observed at the highest dose tested of 100 µM (Table 2).

Anti-CHIKV activity

The novel 6'-fluoro-aristeromycin analogues **2a-j** and **3a-c** as well as 6'-fluoro-homoaristeromycin analogues **4a-e** were screened for antiviral activity against CHIKV. The compounds were tested in CPE-reduction assays at 4 concentrations, that is, 150 µM, 50 µM, 16.7 µM and 5.6 µM by preparing 3-fold serial dilutions. Compounds that

Table 1. Inhibition of SAH hydrolase and CHIKV replication by aristeromycin analogues **2a-j** and **3a-c** [a, b, c]. Adapted from (15).

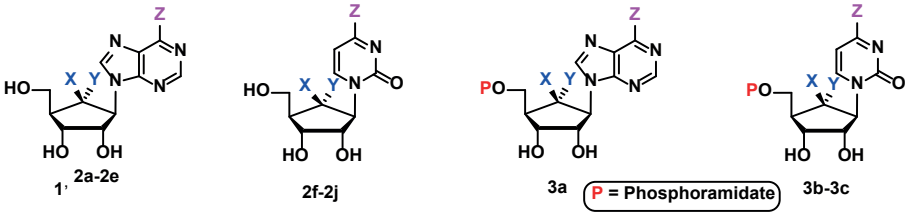

Compound no.	X	Y	Z	SAH hydrolase IC_{50} (µM)	CHIKV EC_{50} (µM)[a]	CHIKV CC_{50} (µM)[b]	CHIKV SI
1	H	H	NH_2	1.32	0.8	6.3	7.9
2a	F	H	NH_2	0.37	>100	>100	
2b	H	F	NH_2	9.70	0.53	1.32	2.49
2c	F	F	NH_2	1.06	0.13	>1.25	>9.6
2d	F	H	NHMe	4.39	>100	>100	
2e	F	F	NHMe	0.76	>100	>100	
2f	F	H	OH	>100	>100	>100	
2g	H	F	OH	>100	>100	>100	
2h	F	F	OH	>100	>100	>100	
2i	F	H	NH_2	>100	>100	>100	
2j	F	F	NH_2	>100	>100	>100	
3a	F	F	NH_2	>100	1.95	>12.5	>6.4
3b	F	H	OH	>100	>100	>100	
3c	F	F	OH	>100	>100	>100	

[a]EC_{50}: effective concentration to inhibit CHIKV replication in VeroE6 cells by 50%. [b]CC_{50}: cytotoxic concentration that reduces cell viability by 50%. EC_{50} >100 indicates that no antiviral activity was observed at the highest concentration tested because there was no protection. SI = CC_{50}/EC_{50}.

demonstrated antiviral activity in this primary screen were tested more extensively in dose-response experiments at 8 different concentrations to determine the half maximal effective concentration (EC_{50}). The half maximal cytotoxic concentration (CC_{50}) was determined in parallel in uninfected cell cultures (Table 1 and 2).

As shown in Table 1, aristeromycin derivatives **2b-c** demonstrated potent anti-CHIKV activity (EC_{50} = 0.13-0.53 μM), while aristeromycin derivative **2a**, other purine *N6*-methylaristeromycin derivatives **2d** and **2e** and pyrimidine derivatives **2f-j** did not show significant antiviral activities, not even at a dose of 100 μM. This result suggests that the antiviral activity might be due to an (indirect) effect on the CHIKV nsP1 through the inhibition of host SAH hydrolase. 6',6'-difluoro-aristeromycin **(2c)** was the most active aristeromycin analogue against CHIKV with an EC_{50} of 0.13 μM. 6'-α-fluoroaristeromycin **(2b)** also showed some inhibitory effects on CHIKV replication, but this was likely due to pleiotropic effects, as the selectivity index (SI) was <3. Among the phosphoramidate prodrugs **3a-c**, only the prodrug **3a** exhibited anti-CHIKV activity (Table 1). It may inhibit CHIKV nsP4 after conversion into the triphosphate form, although it remains to be determined in biochemical assays

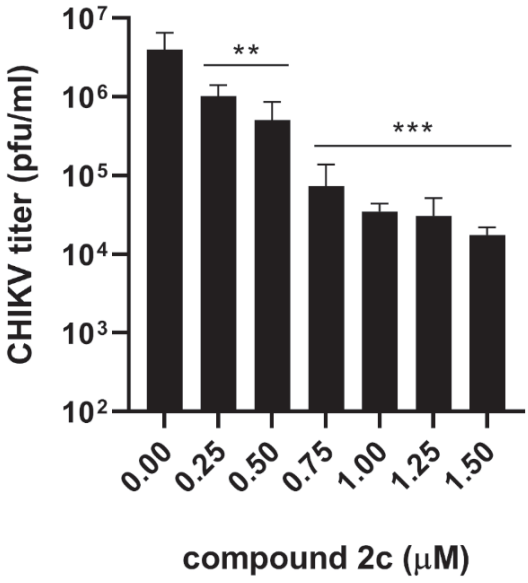

Figure 2. Effect of compound **2c** on the release of infectious progeny from CHIKV-infected VeroE6 cells. Cells were infected with CHIKV in medium with various concentrations of compound **2c** (x-axis). Infectious progeny titers were determined by plaque assay (n = 4). Significant differences are indicated by *: *, $p < 0.05$; **, $p < 0.01$; ***, $p < 0.001$; ****, $p < 0.0001$.

whether the triphosphate form affects the RdRp activity. Interestingly, the prodrug **3a** was less potent, but also much less cytotoxic than the parent compound **2c**, which is unusual as phosphoramidates are typically more potent than their parental drug (21-28). The phosphoramidate **3a** might be slowly hydrolysed to its 5'-monophosphate by metabolic enzymes, or to the parent drug **2c** by a phosphatase, which could inhibit SAH hydrolase, explaining the observed antiviral effect. A viral load reduction assay was performed with compound **2c** by infecting cells with CHIKV followed by treatment with different concentrations of **2c**. At 30 hpi, infectious progeny titers in the medium were determined by plaque assay. Treatment with concentrations higher than 1 μM of **2c** reduced infectious CHIKV titers by more than 2 $\log_{10}$ (Fig. 2).

Among the 6'-fluoro-homoaristeromycin analogues tested (Table 2), 6'-β-fluoro-homoaristeromycin **(4a)** showed potent anti-CHIKV activity (EC_{50} = 0.12 μM) without noticeable cytotoxicity up to 250 μM. This antiviral activity did not

Table 2. Inhibition of SAH hydrolase and CHIKV replication by 6'-fluorinated-5'-homoaristeromycin analogues **4a-e** [a, b, c]. The numbering of compounds **4a-e** corresponds to **3a-e** in (20). Adapted from (20).

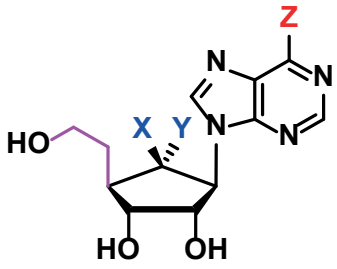

4

Compound no.	X	Y	Z	SAH hydrolase IC_{50} (μM)	CHIKV EC_{50} (μM)[a]	CHIKV CC_{50} (μM)[b]	CHIKV SI
4a	F	H	NH_2	0.36	0.12	>250	>1000
4b	F	H	NHMe	0.37	>100	>100	
4c	F	H	OH	>100	>100	>100	
4d	F	F	NH_2	2.03	ND[c]	>25	
4e	F	F	NHMe	3.05	>100	>100	

[a]EC_{50}: effective concentration to inhibit CHIKV replication in VeroE6 cells by 50%. [b]CC_{50}: cytotoxic concentration that reduces cell viability by 50%. [c]ND: not determined due to cytotoxicity of the compound. EC_{50} >100 indicates that no antiviral activity was observed at the highest concentration tested because there was no protection. SI = CC_{50}/EC_{50}.

merely seem to depend on the inhibition of SAH hydrolase, as **4a** and **4b** inhibited the enzyme with similar IC_{50} values (0.36 μM and 0.37 μM, respectively), although only **4a** displayed anti-CHIKV activity. In addition, although 6',6'-difluoro-aristeromycin **(2c)** displayed antiviral activity against CHIKV and several other + strand RNA viruses, including SARS-CoV, MERS-CoV, and ZIKV (15), the corresponding homologated analogue **4d** did not exhibit anti-CHIKV activity (Table 2). These results demonstrated that besides SAH hydrolase inhibition other effects may be involved in the antiviral activity of the homologated **4a-e** series.

Conclusions

6'-fluorinated-aristeromycin analogues **2a-j** were designed as dual-target antiviral compounds aimed at inhibiting both CHIKV nsP4 and the host SAH hydrolase. Phosphoramidate prodrugs **3a-c** were synthesized to determine whether these would inhibit CHIKV replication through an effect on CHIKV nsP4. The introduction of fluorine at the 6'-position was found to increase the inhibition of both SAH hydrolase activity and the replication of CHIKV and several other + strand RNA viruses (15). The 6'-fluorinated aristeromycin analogue **2c** inhibited SAH hydrolase activity and CHIKV replication more potently compared to the 6'-unsubstituted compound **1** (Table 1). Considering the results for all viruses tested, there was a correlation between the inhibition of SAH hydrolase and the antiviral activity of the compounds, suggesting that the latter was mainly due to the indirect inhibition of viral methylation reactions. The SAR studies and the lack of antiviral effects of several purine and pyrimidine analogues suggest that the antiviral effect of **1**, **2a** and **2c** is unlikely due to targeting of the viral RdRp (15). Compound **2c** appears to be interesting for further development and evaluation as a broad-spectrum antiviral agent, as it inhibited SARS-CoV, MERS-CoV and ZIKV in addition to CHIKV.

To reduce the cytotoxicity of 6'-fluorinated-aristeromycin analogues **2a** and **2c**, which is likely due to their 5'-phosphorylation by cellular kinases, 6'-fluorinated-homoaristeromycin analogues **4a-e** were designed. Among the compounds tested, 6'-β-fluoro-homoaristeromycin **(4a)** showed potent anti-CHIKV activity (EC_{50} 0.12 μM) without noticeable cytotoxicity at concentrations up to 250 μM, which resulted in a high selectivity index (Table 2). This indicates that one-carbon homologation may prevent 5'-phosphorylation and consequently cytotoxicity. This homologation had no effect on the inhibitory activity towards SAH hydrolase, as compounds **2a**

and **4a** inhibited this enzyme with very similar IC_{50} values (0.37 μM and 0.36 μM, respectively) (Table 1 and 2). The antiviral activity of **4a** was specific for CHIKV and to a lesser extent for some other alphaviruses (34), whereas other viruses have been shown to be sensitive to the SAH hydrolase inhibitors **2a** and **2c** (15). As mentioned earlier, it suggests that the potent anti-CHIKV activity of **4a** is based on more than the mere inhibition of SAH hydrolase. A detailed molecular study of the antiviral activity of 6'-β-fluoro-homoaristeromycin **(4a)** is discussed in Chapter 4 of this thesis.

Acknowledgments

K.K. was supported by the Marie Skłodowska-Curie ETN European Training Network "ANTIVIRALS" (EU grant agreement 642434).

References

1. Schwartz O, Albert ML. 2010. Biology and pathogenesis of chikungunya virus. Nat Rev Microbiol 8:491-500.
2. Lo Presti A, Lai A, Cella E, Zehender G, Ciccozzi M. 2014. Chikungunya virus, epidemiology, clinics and phylogenesis: A review. Asian Pac J Trop Med 7:925-32.
3. Ng LFP. 2017. Immunopathology of Chikungunya Virus Infection: Lessons Learned from Patients and Animal Models. Annu Rev Virol 4:413-427.
4. Baltimore D. 1971. Expression of animal virus genomes. Bacteriol Rev 35:235-41.
5. Modrow S, Falke D, Truyen U, Schätzl H. 2013. Viruses with Single-Stranded, Positive-Sense RNA Genomes, p 185-349, Molecular Virology doi:10.1007/978-3-642-20718-1_14. Springer Berlin Heidelberg, Berlin, Heidelberg.
6. Ahlquist P. 2002. RNA-dependent RNA polymerases, viruses, and RNA silencing. Science 296:1270-3.
7. Pietila MK, Hellstrom K, Ahola T. 2017. Alphavirus polymerase and RNA replication. Virus Res doi:10.1016/j.virusres.2017.01.007.
8. Decroly E, Ferron F, Lescar J, Canard B. 2011. Conventional and unconventional mechanisms for capping viral mRNA. Nat Rev Microbiol 10:51-65.
9. Cougot N, van Dijk E, Babajko S, Séraphin B. 2004. 'Cap-tabolism'. Trends Biochem Sci 29:436-44.
10. Ferron F, Decroly E, Selisko B, Canard B. 2012. The viral RNA capping machinery as a target for antiviral drugs. Antiviral Res 96:21-31.
11. Turner MA, Yang X, Yin D, Kuczera K, Borchardt RT, Howell PL. 2000. Structure and function of S-adenosylhomocysteine hydrolase. Cell Biochem Biophys 33:101-25.
12. Cantoni GL. 1986. The Centrality of S-Adenosylhomocysteinase in the Regulation of the Biological Utilization of S-Adenosylmethionine, p 227-238. *In* Borchardt RT, Creveling CR, Ueland PM (ed), Biological Methylation and Drug Design: Experimental and Clinical Role of S-Adenosylmethionine doi:10.1007/978-1-4612-5012-8_19. Humana Press, Totowa, NJ.
13. Wolfe MS, Borchardt RT. 1991. S-adenosyl-L-homocysteine hydrolase as a target for antiviral chemotherapy. J Med Chem 34:1521-30.
14. De Clercq E. 2002. Strategies in the design of antiviral drugs. Nat Rev Drug Discov 1:13-25.
15. Yoon J-s, Kim G, Jarhad DB, Kim H-R, Shin Y-S, Qu S, Sahu PK, Kim HO, Lee HW, Wang SB, Kong YJ, Chang T-S, Ogando NS, Kovacikova K, Snijder EJ, Posthuma CC, van Hemert MJ, Jeong LS. 2019. Design, Synthesis, and Anti-RNA Virus Activity of 6'-Fluorinated-Aristeromycin Analogues. Journal of Medicinal Chemistry 62:6346-6362.
16. Jordheim LP, Durantel D, Zoulim F, Dumontet C. 2013. Advances in the development of nucleoside and nucleotide analogues for cancer and viral diseases. Nat Rev Drug Discov 12:447-64.
17. Kusaka T, Yamamoto H, Shibata M, Muroi M, Kishi T. 1968. Streptomyces citricolor nov. sp. and a new antibiotic, aristeromycin. J Antibiot (Tokyo) 21:255-63.
18. Bennett LL, Jr., Allan PW, Rose LM, Comber RN, Secrist JA, 3rd. 1986. Differences in the metabolism and metabolic effects of the carbocyclic adenosine analogs, neplanocin A and aristeromycin. Mol Pharmacol 29:383-90.

19. Bennett LL, Jr., Bowdon BJ, Allan PW, Rose LM. 1986. Evidence that the carbocyclic analog of adenosine has different mechanisms of cytotoxicity to cells with adenosine kinase activity and to cells lacking this enzyme. Biochem Pharmacol 35:4106-9.
20. Shin YS, Jarhad DB, Jang MH, Kovacikova K, Kim G, Yoon JS, Kim HR, Hyun YE, Tipnis AS, Chang TS, van Hemert MJ, Jeong LS. 2020. Identification of 6'-beta-fluoro-homoaristeromycin as a potent inhibitor of chikungunya virus replication. Eur J Med Chem 187:111956.
21. Siddiqui AQ, Ballatore C, McGuigan C, De Clercq E, Balzarini J. 1999. The presence of substituents on the aryl moiety of the aryl phosphoramidate derivative of d4T enhances anti-HIV efficacy in cell culture: A structure-activity relationship. J Med Chem 42:393-9.
22. Mehellou Y, Rattan HS, Balzarini J. 2018. The ProTide Prodrug Technology: From the Concept to the Clinic. J Med Chem 61:2211-2226.
23. Mehellou Y, Balzarini J, McGuigan C. 2009. Aryloxy phosphoramidate triesters: a technology for delivering monophosphorylated nucleosides and sugars into cells. ChemMedChem 4:1779-91.
24. McGuigan C, Pathirana RN, Balzarini J, De Clercq E. 1993. Intracellular delivery of bioactive AZT nucleotides by aryl phosphate derivatives of AZT. J Med Chem 36:1048-52.
25. McGuigan C, Harris SA, Daluge SM, Gudmundsson KS, McLean EW, Burnette TC, Marr H, Hazen R, Condreay LD, Johnson L, De Clercq E, Balzarini J. 2005. Application of phosphoramidate pronucleotide technology to abacavir leads to a significant enhancement of antiviral potency. J Med Chem 48:3504-15.
26. McGuigan C, Hassan-Abdallah A, Srinivasan S, Wang Y, Siddiqui A, Daluge SM, Gudmundsson KS, Zhou H, McLean EW, Peckham JP, Burnette TC, Marr H, Hazen R, Condreay LD, Johnson L, Balzarini J. 2006. Application of phosphoramidate ProTide technology significantly improves antiviral potency of carbocyclic adenosine derivatives. J Med Chem 49:7215-26.
27. Sofia MJ, Bao D, Chang W, Du J, Nagarathnam D, Rachakonda S, Reddy PG, Ross BS, Wang P, Zhang HR, Bansal S, Espiritu C, Keilman M, Lam AM, Steuer HM, Niu C, Otto MJ, Furman PA. 2010. Discovery of a β-d-2'-deoxy-2'-α-fluoro-2'-β-C-methyluridine nucleotide prodrug (PSI-7977) for the treatment of hepatitis C virus. J Med Chem 53:7202-18.
28. Slusarczyk M, Lopez MH, Balzarini J, Mason M, Jiang WG, Blagden S, Thompson E, Ghazaly E, McGuigan C. 2014. Application of ProTide technology to gemcitabine: a successful approach to overcome the key cancer resistance mechanisms leads to a new agent (NUC-1031) in clinical development. J Med Chem 57:1531-42.
29. Jeong LS, Yoo SJ, Lee KM, Koo MJ, Choi WJ, Kim HO, Moon HR, Lee MY, Park JG, Lee SK, Chun MW. 2003. Design, synthesis, and biological evaluation of fluoroneplanocin A as the novel mechanism-based inhibitor of S-adenosylhomocysteine hydrolase. J Med Chem 46:201-3.
30. Lee KM, Choi WJ, Lee Y, Lee HJ, Zhao LX, Lee HW, Park JG, Kim HO, Hwang KY, Heo YS, Choi S, Jeong LS. 2011. X-ray crystal structure and binding mode analysis of human S-adenosylhomocysteine hydrolase complexed with novel mechanism-based inhibitors, haloneplanocin A analogues. J Med Chem 54:930-8.
31. Chandra G, Moon YW, Lee Y, Jang JY, Song J, Nayak A, Oh K, Mulamoottil VA, Sahu PK, Kim G, Chang TS, Noh M, Lee SK, Choi S, Jeong LS. 2015. Structure-Activity Relationships of Neplanocin A Analogues as S-Adenosylhomocysteine Hydrolase Inhibitors and Their Antiviral and Antitumor Activities. J Med Chem 58:5108-20.

32. Lozada-Ramírez JD, Martínez-Martínez I, Sánchez-Ferrer A, García-Carmona F. 2006. A colorimetric assay for S-adenosylhomocysteine hydrolase. J Biochem Biophys Methods 67:131-40.

33. Scholte FE, Tas A, Martina BE, Cordioli P, Narayanan K, Makino S, Snijder EJ, van Hemert MJ. 2013. Characterization of synthetic Chikungunya viruses based on the consensus sequence of recent E1-226V isolates. PLoS One 8:e71047.

34. Kovacikova K, Morren BM, Tas A, Albulescu IC, van Rijswijk R, Jarhad DB, Shin YS, Jang MH, Kim G, Lee HW, Jeong LS, Snijder EJ, van Hemert MJ. 2020. 6'-beta-Fluoro-Homoaristeromycin and 6'-Fluoro-Homoneplanocin A Are Potent Inhibitors of Chikungunya Virus Replication through Their Direct Effect on Viral Nonstructural Protein 1. Antimicrob Agents Chemother 64.

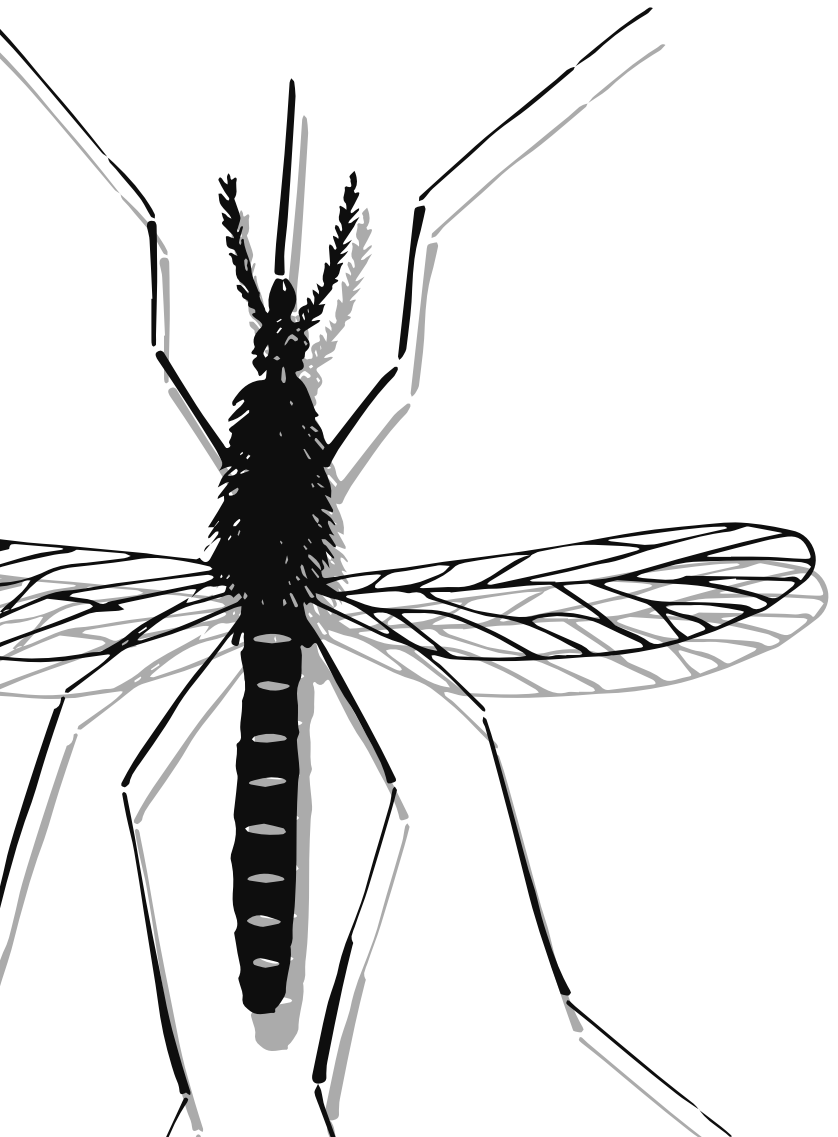

CHAPTER 4

6’-β-Fluoro-homoaristeromycin and 6’-fluoro-homoneplanocin A are potent inhibitors of Chikungunya virus replication through their direct effect on the viral nonstructural protein 1

Kristina Kovacikova[a], Bas M. Morren[a #], Ali Tas[a], Irina C. Albulescu[a&], Robin van Rijswijk[a ¥], Dnyandev B. Jarhad[b], Young Sup Shin[b], Min Hwan Jang[b], Guadong Kim[b], Hyuk Woo Lee[c], Lak Shin Jeong[b], Eric J. Snijder[a], and Martijn J. van Hemert[a]

[a] Department of Medical Microbiology, Leiden University Medical Center, Leiden,the Netherlands

[b] College of Pharmacy, Seoul National University, Seoul, South Korea

[c] Future Medicine Co., Ltd, Seoul, South Korea

[#] Current address: Department of Medical Biochemistry, Leiden Institute of Chemistry, Leiden University, Leiden, the Netherlands

[&] Current address: Department of Infectious Diseases and Immunology, Faculty of Veterinary Medicine, Utrecht University, Utrecht, the Netherlands

[¥] Current address: Franciscus gasthuis, Rotterdam, the Netherlands

Antimicrob Agents Chemother. 2020 Mar 24;64(4):e02532-19.

Abstract

Alphaviruses are arthropod-borne, positive-stranded RNA viruses capable of causing severe disease with high morbidity. Chikungunya virus (CHIKV) is an alphavirus that causes a febrile illness which can progress into chronic arthralgia. The current lack of vaccines and specific treatment for CHIKV infection underscores the need to develop new therapeutic interventions. To discover new antiviral agents, we performed a compound screen in cell culture-based infection models and identified two carbocyclic adenosine analogues, 6'-β-fluoro-homoaristeromycin (FHA) and 6'-fluoro-homoneplanocin A (FHNA), that displayed potent activity against CHIKV and Semliki Forest virus (SFV) with 50% effective concentrations in the nanomolar range at nontoxic concentrations. The compounds, designed as inhibitors of the host enzyme S-adenosylhomocysteine (SAH) hydrolase, impeded postentry steps in CHIKV and SFV replication. Selection of FHNA-resistant mutants and reverse genetics studies demonstrated that the combination of mutations G230R and K299E in CHIKV nonstructural protein 1 (nsP1) conferred resistance to the compounds. Enzymatic assays with purified wild-type (wt) SFV nsP1 suggested that an oxidized (3'-keto) form, rather than FHNA itself, directly inhibited the methyltransferase (MTase) activity, while a mutant protein with the K231R and K299E substitutions was insensitive to the compound. Both wt nsP1 and the resistant mutant were equally sensitive to the inhibitory effect of SAH. Our combined data suggest that FHA and FHNA inhibit CHIKV and SFV replication by directly targeting the MTase activity of nsP1, rather than through an indirect effect on host SAH hydrolase. The high potency and selectivity of these novel alphavirus mRNA capping inhibitors warrant further preclinical investigation of these compounds.

Introduction

Alphaviruses comprise a group of enveloped, positive-stranded (+) RNA viruses, which includes important human pathogens such as Chikungunya virus (CHIKV) and model viruses Semliki Forest virus (SFV) and Sindbis virus (SINV). CHIKV is an arthritogenic alphavirus that is primarily transmitted by the *Aedes aegypti* and *Aedes albopictus* mosquitoes and causes a debilitating illness known as chikungunya fever. Since its isolation in the present-day Tanzania in 1952/1953 (1), sporadic CHIKV outbreaks were reported throughout the African and Asian continents (2, 3). In 2004, the virus reemerged in Kenya and then spread eastward in the form of strains belonging to the East/Central/South African lineage that were better adapted to replication in *Aedes albopictus* due to an A226V substitution in the E1 protein. This resulted in large outbreaks in the South West Indian ocean islands in early 2005, in India in 2005/2006, and in Asia in the following years (4, 5). A small CHIKV outbreak in the Caribbean at the end of 2013 marked its arrival in the Americas, from which over 1.5 million infections have been reported since 2014. Following its introduction in Italy (2007, 2017) and France (2010, 2017) on several occasions via infected travellers, CHIKV has caused limited locally transmitted outbreaks in Europe (6-9). The geographical expansion of the *Aedes albopictus* vector and increased human travel pose the risk that CHIKV may become endemic in new territories.

Symptomatic CHIKV infection often manifests itself by short-lived fever and recurrent joint pain, which can last for months to years (10). Despite its widespread emergence and high morbidity, antiviral medication is not available and the current treatment consists of administration of nonsteroidal anti-inflammatory drugs to alleviate pain. Over the past years, there have been efforts to develop both direct-acting and host-targeting small-molecule inhibitors into antiviral drugs to treat CHIKV infection (11). Several potent CHIKV inhibitors that interfere with the functions of individual viral nonstructural proteins or the polymerase complex have been reported, including ribavirin, 6-azauridine, mycophenolic acid, and favipiravir (T-705) (12-14). Nevertheless, the current lack of antiviral therapy for human CHIKV infections and the generally low success rate of drug development programs underscore the need to search for compounds with improved efficacy.

Alphaviruses replicate in the cytoplasm of infected cells. Following entry, the viral genome is translated into a nonstructural polyprotein, which is subsequently processed into nonstructural protein 1 (nsP1) to nsP4 (reviewed in reference (15))

The 5’ end of the viral genomic and subgenomic RNAs is modified by viral enzymes to give rise to a cap-0 (m^7GpppA) structure. This cap structure is important for the alphavirus replication cycle since it protects the viral mRNAs from degradation by host 5’-to-3’ exonucleases, enables efficient translation of viral mRNAs, and plays a role in innate immune evasion. Alphavirus capping proceeds in an unconventional reaction sequence that differs from that used by the host cell, which is confined to the nucleus. In the case of the cytoplasmic alphavirus capping reaction, a GTP molecule undergoes methylation before it is transferred onto the 5’ end of the viral RNA, making the viral mRNA capping reaction an attractive target for antiviral drug development (16).

Like cellular methylation reactions, many viral methylation reactions use S-adenosylmethionine (SAM) as a methyl donor to produce the cap structure at the 5’ end of viral RNAs. A by-product and feedback inhibitor of this process is S-adenosylhomocysteine (SAH), which is subsequently hydrolyzed by the host enzyme SAH hydrolase. Inhibition of SAH hydrolase leads to accumulation of SAH, which indirectly interferes with mRNA capping (17). SAH hydrolase was first identified as a target for antiviral compounds in 1982, and since then several inhibitors of this enzyme have been reported (17, 18). These are known to possess antitumor and antimicrobial activities and have shown potent antiviral activity against a range of negative-stranded RNA viruses, double-stranded RNA viruses, and DNA viruses; examples include pox-, paramyxo- , rhabdo-, filo-, bunya-, arena-, and reoviruses (reviewed in reference (19). Recently, we have also described SAH hydrolase inhibitors that target a broad spectrum of (+) RNA viruses, such as some coronaviruses, Zika virus, and CHIKV (20).

Both alphavirus nsP1 and nsP2 contribute to the formation of the cap-0 structure at the 5’ end of the mRNA: nsP1 harbors the methyltransferase (MTase; GTP + SAM → m^7GTP + SAH) and guanylyltransferase (GTase; m^7GTP + nsP1 → m^7GMP-nsP1 + pyrophosphate) activities while nsP2 possesses the RNA triphosphatase (RTPase) activity that removes the 5’ γ-phosphate from the nascent RNA (21-23). So far, 3-aryl-[1,2,3]triazolo[4,5-*d*]pyrimidin-7(6*H*)-ones were identified as selective inhibitors of CHIKV nsP1 activity, both in cell culture infection models and in *in vitro* assays with purified Venezuelan Equine Encephalitis virus (VEEV) nsP1 (24, 25). More recently, the CHVB series of compounds has been described, which displays a similar activity profile (26). Enzyme-based screening assays have also identified compounds that target nsP1, such as lobaric acid, a natural compound that was a hit in a CHIKV nsP1 GTP displacement assay-based screen (27). In addition, an ELISA-based screening campaign of more than 1,200 compounds using VEEV nsP1 has led to

the identification of at least 18 potential nsP1 inhibitors (28). Recently, a similar assay with CHIKV nsP1 has been used to screen for CHIKV nsP1 inhibitors (29). Targeting the alphavirus capping pathway thus provides a new avenue for developing specific inhibitors of this sensitive point in the alphavirus replication cycle.

Here we report our findings from screening a library of 80 carbocyclic adenosine and selenoadenosine analogues designed to inhibit the cellular enzyme SAH hydrolase. We identified 6'-β-fluoro-homoaristeromycin (FHA) and 6'-fluoro-homoneplanocin A (FHNA) as potent CHIKV and SFV inhibitors. By selection of escape mutants and reverse engineering we identified CHIKV nsP1 as the viral target for these compounds. Biochemical assays monitoring the formation of the ^{32}P-labelled m^{7}GMP-nsP1 covalent intermediate indicated that nsP1 was directly inhibited by the compounds. More specifically, an oxidized form of FHNA directly inhibited the MTase activity (but not the GTase activity) of purified SFV nsP1. Taken together, we demonstrated that the mode of action of FHA and FHNA is based on a direct inhibitory effect on nsP1 rather than inhibition of host SAH hydrolase.

Materials and Methods

Cells and virus strains

VeroE6 cells were maintained in Dulbecco modified Eagle medium (DMEM; Lonza) supplemented with 8% fetal calf serum (FCS; Bodinco), 100 IU/ml penicillin (Sigma) and 100 µg/ml streptomycin (Sigma) at 37˚C in 5% CO_2 atmosphere (DMEM-8% FCS). Infections were performed in Eagle minimal essential medium (EMEM; Lonza) with 25 mM HEPES (Lonza) supplemented with 2% FCS, 2 mM L-glutamine (Sigma), and antibiotics (EMEM-2% FCS). Baby hamster kidney (BHK-21) cells were cultured in Glasgow modified Eagle medium (Gibco) supplemented with 7.5% FCS, 10 mM HEPES, 8% tryptose phosphate broth (Gibco), and antibiotics.

CHIKV LS3 (CHIKV; GenBank accession no. KC149888) is an infectious clone-derived virus, described in Scholte et al. (30). The SFV4 strain and Sindbis virus HR small plaque strain were used in cytopathic effect reduction assays to determine the antiviral spectrum of compounds.

Compounds

FHA, FHNA and their related analogues were synthesized as described elsewhere (31). The compounds were dissolved in dimethyl sulfoxide (DMSO) to obtain 20 mM stocks and were stored at 4˚C until further use. MADTP-372 was dissolved as 10 mM stock in DMSO and used as described previously (24). Mycophenolic acid (MPA), 6-azauridine (6-au), S-adenosylhomocysteine (SAH) and guanylyl-imido-diphosphate (GIDP) were purchased from Sigma. S-Adenosylmethionine (SAM) and nicotinamide adenine dinucleotide (NAD^+) were obtained from New England Biolabs. S-Adenosyl-[methyl-^{3}H] methionine, [γ-^{32}P]ATP and [α-^{32}P]GTP are products of Perkin-Elmer.

Cytopathic effect (CPE) reduction assay

VeroE6 cells were seeded in 96-well clusters at a density of 5 x 10^3 cells/well in 100 µl/well of DMEM-8% FCS and were allowed to adhere overnight. Next day, the medium was replaced with serial dilutions of the compounds to be tested, made in EMEM-2% FCS. Subsequently, the cells were infected with 50 µl/well of CHIKV inoculum (MOI of 0.005), or were left uninfected by adding 50 µl/well EMEM-2% FCS. Alternatively, 1 x 10^4 VeroE6 cells/well were seeded in 80 µl/well of DMEM-8% FCS, followed by compound treatment and infection with 20 µl/well SINV or SFV inoculum (MOI of 0.025). The uninfected cells served as a control to assess potential cytotoxic/cytostatic effects of compound treatment. Each assay was performed in quadruplicate in the same plate. Cell viability was measured using the MTS/PMS [3-(4,5-dimethylthiazol-2-yl)-5-(3-carboxymethoxyphenyl)-2-(4-sulfophenyl)-2H-tetrazolium/phenazine methosulfate] method (Promega, The Netherlands) by adding 20 µl/well of MTS reagent. Depending on the virus used, this was done at 40, 76, or 96 hpi for SFV, SINV, and CHIKV, respectively. The cells were incubated for 2 h, followed by fixation with 30 µl/well of 37% formaldehyde. The optical density at 490 nm (OD_{490}) was measured using an Envision plate reader (Perkin-Elmer). The 50% effective concentration (EC_{50}), defined as the concentration of compound required to inhibit virus-induced cell death by 50%, and the 50% cytotoxic concentration (CC_{50}), defined as the concentration of compound that reduced the OD_{490} value of uninfected cells to 50% of that of untreated control cells, were both determined using nonlinear regression with GraphPad Prism v8.0.

Viral load reduction assay

VeroE6 cells were seeded in 12-well clusters at a density of 1.5 x 10^5 cells/well in 1 ml/well of DMEM-8% FCS, and were incubated overnight. The cells were pretreated with 0 to 10 µM FHNA for CHIKV and 0 to 50 µM FHNA for SFV for 2 h and infected with CHIKV at an MOI of 1 or SFV at an MOI of 5 by adding 250 µl/well of inoculum in EMEM-2% FCS with corresponding FHNA dilutions. After incubation for 1 h at 37˚C on a rocker, the cells were washed three times with warm phosphate-buffered saline (PBS) and further incubated with EMEM-2% FCS in the presence of increasing concentrations of FHNA. At 8 hpi for SFV and 20 hpi for CHIKV, 500 µl of the culture medium was harvested for viral titer determination. The cells were harvested in 500 µl of TriPure to isolate RNA for intracellular CHIKV genome copy number determination, or in 250 µl 4x Laemmli sample buffer (4x LSB) for Western blot analysis.

Determination of viral titers

VeroE6 cells were seeded in 6-well clusters at a density of 3.5 x 10^5 cells/well in 2 ml/well of DMEM-8%FCS, followed by overnight incubation at 37°C. Samples were 10-fold serially diluted in EMEM-2%FCS and 500 µl/well of each dilution was used to infect confluent monolayers of VeroE6 cells for 1 h at 37˚C on a rocker. The inoculum was removed and replaced with 2 ml/well of an overlay containing DMEM, 1.2% Avicel (FMC BioPolymer), 2% FCS, 50 mM HEPES, and antibiotics. After a 3-day incubation, monolayers were fixed with 3.7% formaldehyde in PBS and plaques were visualized with crystal violet staining.

Denaturing agarose gel electrophoresis and in-gel hybridization

TriPure-isolated RNA samples were mixed with 1.33x formaldehyde denaturation mix (67% formamide, 23% formaldehyde, 6.7% glycerol, 10 mM morpholinepropanesulfonic acid [MOPS; pH 7.2], 6.7 mM NaAc, 2.7 mM EDTA, 0.07% sodium dodecyl sulfate [SDS] and 0.03% bromophenol blue). After denaturation for 15 min at 75˚C, RNAs were separated in 1.5% denaturing formaldehyde-agarose gels using the MOPS buffer system. Genomic, subgenomic, and negative-strand CHIKV RNA were detected by direct hybridization of the dried agarose gel with ^{32}P-labelled strand-specific oligonucleotide probes as described by Scholte et al (30). The probes were labelled with [γ-^{32}P]ATP in a 1h reaction at 37˚C containing 1 µl of T4 polynucleotide kinase (Invitrogen) and 2 µl of T4 forward reaction buffer (Invitrogen). The dried gels were

first pre-hybridized in 5x SSPE buffer (0.9 M NaCl, 50 mM NaH_2PO_4, 5 mM EDTA, pH 7.4), 5 x Denhardt's solution, 0.05% SDS and 0.1 mg/ml Homomix I at 55˚C for 3 h, after which the ^{32}P-labelled strand-specific probes were added to the buffer, followed by overnight incubation. Hybridized gels were washed twice for 15 min with 5x SSPE with 0.05% SDS. Gels were analyzed using Phosphorimager screens and a Typhoon-9410 scanner (GE Healthcare). An image of one representative experiment is shown.

Quantitative RT-PCR (qRT-PCR)

Intracellular RNA was isolated from cells using TriPure isolation reagent (Life Technologies) according to the manufacturer's instructions. Extracellular RNA was isolated from 150 µl of the medium of infected cells using the QIAamp viral RNA minikit (Macherey-Nagel). Both intracellular and extracellular RNA were used to determine the copy numbers of CHIKV genomic RNA (probe in nsP1-coding region, CHIKV assay 1) and total CHIKV RNA (probe in E1-coding region, CHIKV assay 2b) using internally controlled multiplex quantitative TaqMan real-time PCR. During cell lysis, the samples were spiked with a fixed amount of equine arteritis virus (EAV) to control for variations in RNA isolation or qRT-PCR efficiency. For intracellular RNA samples, PGK1 mRNA expression levels were also monitored to correct for variations in isolation or qRT-PCR efficiency. A 10-µl reaction mixture was composed of 1.25 µl of template RNA, 2.5 µl of TaqMan Fast Virus one-step master mix (Thermo Fisher Scientific), 0.5 µl CHIKV assay 1 (forward primer: AAGCTCCGCGTCCTTTACCAAG, reverse primer: CCAAATTGTCCTGGTCTTCCT, probe: 5'FAM-CCAATGTCTTCAGCCTGGACACCTT-3'black hole quencher (BHQ)1), 0.5 µl CHIKV assay 2b (forward primer: CTAGCTATAAAACTAAUAGAGCAGGAAATTG, reverse primer: GACTTTTCCTGCGGCAGATGC, probe: 5'TexasRed-CGCCAGCAAGGAG GATGATGTCGGA-3'BHQ2),0.5 µl EAV assay (forward primer: CATCTCTTGCTTTGCTC CTTAG, reverse primer: AGCCGCACCTTCACATTG, probe: 5'CY5-CGCTGTCAGAAC AACATTATTGCCCAC3'-BHQ2) or PGK1 assays and 4.75 µl of nuclease-free water (Sigma). All reactions were performed in triplicate in a 384-well plate using the CFX384 Touch real-time PCR detection system and the following program: 5 min at 50˚C, 20 s at 95˚C, followed by 46 cycles of 5 s at 95˚C and 30 s at 60˚C. Data were analyzed with CFX manager 3.1 software (Bio-Rad). For absolute quantification, standard curves were generated using 10-fold serial dilutions of known quantities of *in vitro*-transcribed RNA.

Time-of-drug-addition assay

VeroE6 cells were seeded in 12-well clusters at a density of 1.5 x 10^5 cells/well in 1 ml/well of DMEM-8% FCS, and were incubated overnight. The cells were pretreated with FHNA for 12 h, before they were infected with 250 µl/well CHIKV inoculum (MOI of 1) in EMEM-2% FCS containing 10 µM FHNA or SFV inoculum (MOI of 5) in EMEM-2% FCS containing 50 µM FHNA. After incubation for 1 h at 37˚C on a rocker, the cells were washed three times with warm PBS to remove the unbound virus. The cells were then incubated with EMEM-2% FCS and FHNA was added at various time points post infection at 2-h intervals. At 16 hpi for CHIKV and 10 hpi for SFV, 500 µl of the medium was harvested for virus titration by plaque assay and RNA isolation as described above. The intracellular RNA was isolated from the cells with the TriPure method to determine CHIKV genome copy numbers by qRT-PCR as described above.

Selection of compound-resistant virus mutants

A previously described five-step protocol (14) was used to select for FHNA-resistant virus variants. In the first step, VeroE6 cells were seeded in 96-well clusters at a density of 5 x 10^3 cells/well in 100 µl/well of DMEM-8% FCS and were allowed to adhere overnight. The next day, the lowest concentration of FHNA and the highest input of CHIKV which resulted in complete block of virus-induced CPE was determined by performing antiviral assays with 500 to 1,000 PFU of CHIKV per well and 0 to 10 µM FHNA. In the second step, four 96-well clusters containing VeroE6 cells were set up per dose (5 and 10 µM) and infected with the previously determined optimal viral input (500 PFU/well). At 4 days postinfection, supernatants were collected from the five wells with the most pronounced signs of CHIKV-induced CPE. In the third step, these supernatants (potentially) containing compound-resistant variants were purified by titration in presence of the 10 µM inhibitory dose of the compound. Following a 4-day incubation, seven supernatants from wells which produced CPE at the highest viral dilution were collected from the 96-well clusters (for some original samples, 2 supernatants were collected). In the fourth step, reference stocks of the seven supernatants containing FHNA-resistant variants were grown in T-25 flasks, which were harvested after 3 to 4 days, when full CPE was observed. After determination of the viral titers by plaque assay, the reference stocks were used for resistance phenotyping as described below. At the same time, the resistance genotype was determined by full-genome Sanger sequencing as described below. The virus variants obtained after the five selection rounds are referred to as ‘P5 variants’.

Reverse genetics

Mutations were reverse-engineered into the CHIKV LS3 full-length cDNA clone using the QuikChange site-directed mutagenesis kit (Agilent) according to the manufacturer's instructions (primer sequences available upon request). The constructs were verified by sequencing using 18 primers covering the whole CHIKV genome sequence (Leiden Genome Technology Center).

Sequencing of virus genomes

Four overlapping PCR amplicons were generated from CHIKV RNA via cDNA synthesis using RevertAid H Minus Reverse Transcriptase (Thermo Fisher Scientific), RiboLock RNase inhibitor (Thermo Fisher Scientific), 5x reaction buffer, 10 mM deoxynucleoside triphosphate mix, and primers (sequences available upon request). In the second step, combinations of primers (sequences available upon request) were used to generate five PCR products with the following program: 5 min at 95˚C followed by 30 cycles of 30 s at 95˚C, 30 s at 55˚C and 3 min at 72˚ and terminated by 10 min at 72˚C. Amplicons were gel purified and sequenced using 18 primers (sequences available upon request). The nucleotide sequences were assembled in Geneious software 9.1.5 and the complete genomes of the resistant variants were compared to the CHIKV-LS3 genome.

Resistance and cross-resistance phenotypic assay

Essentially the same protocol was used as described above for the CPE reduction assays, with the modification that 10-fold higher MOIs were used (MOI of 0.05, meaning 500 PFU/well). MPA and 6-au were included for cross-resistance evaluation of reverse-engineered viruses.

Growth kinetics determination

VeroE6 cells were seeded in 24-well clusters at a density of 7.5 x 10^4 cells/well in 0.5 ml/well of DMEM-8% FCS and incubated overnight. Half of the clusters were pretreated with 10 µM FHNA for 12 h, and half were left untreated. The infections with recombinant CHIKV were performed with 250 µl/well inoculum (MOI of 1) in EMEM-2% FCS in the presence or absence of 10 µM FHNA. After incubation for 1 h at 37˚C on a rocker, the cells were washed three times with warm PBS and further incubated with 500 µl/well EMEM-2% FCS with or without 10 µM FHNA. At 1, 4, 8, 12,

16, 20 and 24 hpi, the supernatants were harvested for determination of the viral titer by plaque assay (see above).

Cloning, expression, and purification of wild-type and mutant SFV nsP1

The DNA sequence encoding SFV nsP1 (amino acid 1 to 537 of the SFV replicase polyprotein) carrying a C-terminal hexahistidine (6xHis) tag was cloned between the NcoI and XmaI restriction sites of the pET34 vector, downstream of the T7 RNA polymerase promotor. To generate mutants, site-directed mutagenesis was performed using a QuikChange site-directed mutagenesis kit (Agilent) according to the manufacturer's instructions (primers available on request). All mutations were confirmed by Sanger sequencing. Proteins were expressed in *E. coli* Rosetta cells (Novagen) by induction with 0.5 mM isopropyl-β-D-thiogalactopyranoside (IPTG) in yeast extract-tryptone (2xYT) medium (16 g of Bacto tryptone, 10 g of yeast extract, and 5 g of NaCl in 1 liter), after the OD_{600} of the culture grown at 37˚C had reached 0.6 to 0.7. After 16 h incubation at 19 ˚C, bacterial cells were harvested by centrifugation at 5,000 rpm for 15 min at 4˚C. The cell pellets were then resuspended in 10 ml of resuspension buffer (20 mM HEPES [pH 7.5], 300 mM NaCl, 5% glycerol) supplemented with one tablet EDTA-free protease inhibitor cocktail (Roche), 10 mg of freshly dissolved lysozyme (Merck), 300 U of DNAse I, and 3 mM $MgCl_2$. After incubation on a rotor for 30 min at 4 ˚C, cells were disrupted by sonication. Soluble protein fractions containing wt or mutant SFV nsP1 were obtained by centrifugation of the lysate at 10,000 x *g* for 30 min at 4˚C. This soluble fraction was used for batch protein purification under native conditions with 500 µl of Talon beads (TaKaRa). Talon beads were equilibrated in 10 ml of resuspension buffer. Next, 10 ml of soluble fraction was incubated with the beads on a horizontal shaker for 1 h at 4 ˚C. The beads were washed three times with 10 ml of wash buffer (20 mM HEPES [pH 7.5], 300 mM NaCl, 5% glycerol, 30 mM imidazole) by centrifugation for 5 min at 2,000 x *g* and 4 ˚C. The protein was eluted from the beads in 1 ml of elution buffer (20 mM HEPES [pH 7.5], 300 mM NaCl, 5% glycerol, 300 mM imidazole) by first incubating the beads in elution buffer at room temperature for 15 min and then pelleting the beads at 2,000 x *g* for 5 min at 4˚C. This step was repeated once more to remove any residual protein from the beads. The eluted protein was concentrated, and buffer was exchanged using Amicon Ultra-15 ultrafiltration units (Merck) and storage buffer containing 25 mM HEPES (pH 7.5) and 100 mM NaCl. Proteins were stored at -80°C. The concentration of purified

proteins was determined by Bradford protein assay (Bio-Rad), and their purity was assessed by SDS-PAGE and Coomassie blue staining with GelCode blue stain reagent (Thermo Fisher).

nsP1 enzymatic activity assay (monitoring formation of m^7GMP-nsP1 reaction intermediate)

The covalent m^7GMP-nsP1 intermediate formation assay protocol was adapted from (22, 32). The activity of SFV nsP1 was measured in 30 µl mixture containing 25 mM HEPES (pH 7.5), 5 mM DTT, 10 mM KCl, 2 mM $MgCl_2$, 100 µM SAM, 0.75 mCi of [α^{32}P] GTP (3000 Ci/mmol), and 500 nM wt or mutant SFV nsP1. The reaction mixture was incubated at 30˚C for 30 min, and the reaction was stopped by adding 3 µl of 10% SDS. Alternatively, assays were performed under nonreducing conditions by omitting DTT from the reaction as described above, and in some samples 1 mM NAD^+ was added. Next, reactions were mixed with 4xLSB, and then 10 µl samples were resolved on a 10% SDS-PAGE gel. The gel was stained using the Coomassie method with GelCode blue stain reagent to check for equal protein loading. Subsequently, the gel was dried and a Phosphorimager screen was placed on top. After overnight or a 7-day (reactions without DTT) exposure, the ^{32}P-labelled covalent m^7GMP-nsP1 intermediate products were visualized with a Typhoon Imager (Amersham).

Results

FHA and FHNA inhibit alphavirus replication

We performed a cytophathic effect (CPE) reduction assay-based screen of 80 adenosine and selenoadenosine analogues for their ability to inhibit CHIKV, SFV, and SINV replication. VeroE6 cells were incubated with compound doses in the range of 0 to 150 µM and then infected with CHIKV, SFV and SINV at a low multiplicity of infection (MOI). Following initial hit validation, we identified two compounds, FHA and FHNA, that inhibited CHIKV replication in the nanomolar range with an EC_{50} of 0.12 and 0.18 µM, respectively, without apparent cytotoxicity (50% cytotoxic concentration (CC_{50}) > 250 µM). This resulted in selectivity indexes (SI) of > 1,000 for both compounds. FHA and FHNA also inhibited SFV replication, although less potently, with 50% effective concentration (EC_{50}) values of 3.9 µM and 5.2 µM, respectively. The compounds did not confer protection to infection with SINV, a more distantly related alphavirus (Table 1).

Table 1. The antiviral effect of FHA and FHNA on CHIKV, SFV and SINV replication in CPE reduction assays

Virus	CHIKV			SFV			SINV	
Compound	**EC_{50}[a] (μM)**	**CC_{50}[b] (μM)**	**SI[c]**	**EC_{50} (μM)**	**CC_{50} (μM)**	**SI**	**EC_{50} (μM)**	**CC_{50} (μM)**
FHA	0.12 ± 0.04	> 250	> 1,000	3.9 ± 3.5	> 250	> 64	-	> 250
FHNA	0.18 ± 0.11	> 250	> 1,000	5.2 ± 3.2	> 250	> 48	-	> 250

[a]EC_{50}, concentration of compound that reduces virus-induced CPE by 50%. The EC_{50} is expressed as the mean ± the standard deviation.
[b]CC_{50}, a concentration of compound that reduces cell viability by 50%.
[c]SI, selectivity index, calculated as CC_{50}/EC_{50}.

The antiviral activity of FHNA was tested in a single-cycle dose response assay by infecting VeroE6 cells with CHIKV and SFV at a high MOI, followed by treatment with 2-fold serial dilutions of the compound ranging from 0.1 to 10 μM for CHIKV and 3.1 to 50 μM for SFV. Cells were pretreated for 2 h and the compound remained present throughout the infection until samples were harvested. At 8 h postinfection (hpi), the levels of both genomic and subgenomic, as well as negative-strand, CHIKV RNA were reduced in a dose-dependent manner, while the levels of host 18S rRNA remained unchanged (Fig. 1A). FHNA also inhibited the release of CHIKV infectious progeny in a dose-dependent manner with 5 and 10 μM doses of the compound reducing viral titers by 2.5 $\log_{10}$ and 3 to 4 $\log_{10}$, respectively, compared to infected untreated cells (Fig. 1B). The inhibition of the production of SFV infectious progeny was less pronounced, nevertheless, > 1 $\log_{10}$ reduction was observed already with 12.5 μM FHNA (Fig. 1C). For practical reasons, further experiments were done with FHNA because larger quantities of this compound were available at the time.

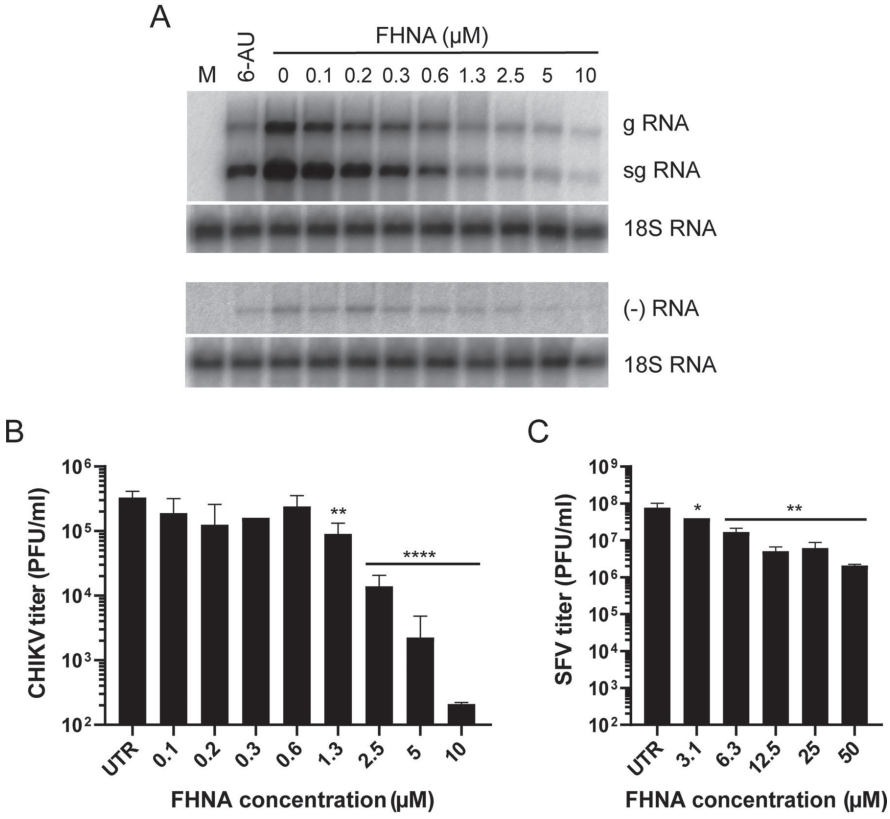

Figure 1. FHNA inhibits CHIKV replication in a dose-dependent manner. (A) VeroE6 cells were infected with CHIKV at an MOI of 1 and treated with 0 to 10 μM FHNA. A 20 μM dose of 6-azauridine was included as a positive control. At 8 hpi intracellular RNA was isolated with TRIzol reagent and subjected to denaturing agarose gel electrophoresis and in-gel hybridization with ^{32}P-labelled probes specific for positive- and negative-strand CHIKV RNA. 18S rRNA was used as a loading control. (B) VeroE6 cells were pretreated with 0 to 10 μM FHNA for 2 h and then infected with CHIKV at an MOI of 1. After 1 h of incubation, the inoculum was replaced with medium containing 0 to 10 μM FHNA. At 20 hpi, the supernatants were harvested for virus titration by plaque assay. (C) VeroE6 cells were pretreated with 0 to 50 μM FHNA for 2 h and then infected with SFV at an MOI of 5. After 1 h of incubation, the inoculum was replaced with medium containing 0 to 50 μM FHNA. At 8 hpi, the supernatants were harvested for virus titration by plaque assay. UTR, untreated. The data for panels B and C represent the mean ± the standard deviations (SD) of two independent experiments performed in duplicate. Statistical analysis was performed using a one-way ANOVA multiple comparison test. Statistically significant differences are indicated by asterisks (*. *, $P < 0.05$; **, $P < 0.01$; ***, $P < 0.001$; ****, $P < 0.0001$).

FHNA inhibits an early step in the CHIKV and SFV replication cycle

To investigate the inhibitory effect of FHNA on CHIKV and SFV replication in more detail, time-of-addition experiments were performed to determine the time frame during which viral infection could be inhibited. In this assay, VeroE6 cells were either pretreated with 10 µM (CHIKV) or 50 µM (SFV) of FHNA for 12 h, treated at the time of infection, or with 2-h intervals postinfection with CHIKV and SFV at a high MOI. The greatest reduction in the release of CHIKV infectious progeny occurred when the cells were pretreated, but inhibition of replication could be observed until 8 hpi (Fig. 2A). For SFV, treatment with FHNA led to a significant reduction in infectious progeny release upon pretreatment and when treatment was started before 1 hpi. When the start of treatment was postponed until 2 hpi or later, only negligible effects on SFV progeny titers were observed compared to untreated controls (Fig. 2B). In summary, maximal impairment of CHIKV and SFV replication by FHNA was observed when it was present prior to infection or during the early stages of virus replication, suggesting that uptake or metabolic conversion of the compound is slow and/or that FHNA interferes with an early step in the CHIKV and SFV replication cycle.

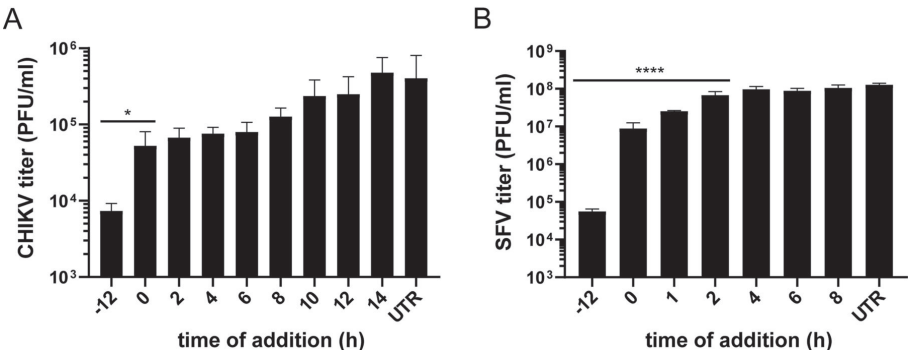

Figure 2. FHNA inhibits early steps in the CHIKV and SFV replication cycle. (A) VeroE6 cells were pretreated with 10 µM FHNA for 12 h, treated at the time of infection or with 2-h intervals postinfection until the time samples were harvested. The cells were infected with CHIKV at an MOI of 1, and the supernatants were harvested at 16 hpi for virus titration by plaque assay. (B) VeroE6 cells were pretreated with 50 µM FHNA for 12 h, treated at the time of infection or with 1 or 2-h intervals postinfection until the samples were harvested. The cells were infected with SFV at an MOI of 5, and the supernatants were harvested at 8 hpi for virus titration by plaque assay. UTR, untreated. The data for panels A and B represent the mean ± the standard deviations (SD) of two independent experiments performed in duplicate. Statistical analysis was performed using a one-way ANOVA multiple comparison test. Statistically significant differences are indicated by asterisks (*. *, $P < 0.05$; **, $P < 0.01$; ***, $P < 0.001$; ****, $P < 0.0001$).

Treatment with FHNA decreases CHIKV specific infectivity

We isolated total intracellular and extracellular RNA from FHNA-treated and untreated CHIKV-infected cells at 12 and 16 hpi, respectively. CHIKV genomic and subgenomic RNA copy numbers in these samples were determined by internally controlled multiplex Taqman quantitative reverse transcription-PCR (qRT-PCR). Treatment with 10 µM FHNA only had a limited effect on the copy numbers of intracellular genomic and subgenomic CHIKV RNA when cells were pretreated, and hardly reduced copy numbers when the compound was added at the time of infection or later (Fig. 3A). Interestingly, also minimal changes in the extracellular CHIKV RNA copy numbers were observed upon FHNA treatment (Fig. 3B). This was in contrast to the clear reduction in infectious progeny titers (Fig. 2A), which led us to determine the CHIKV specific

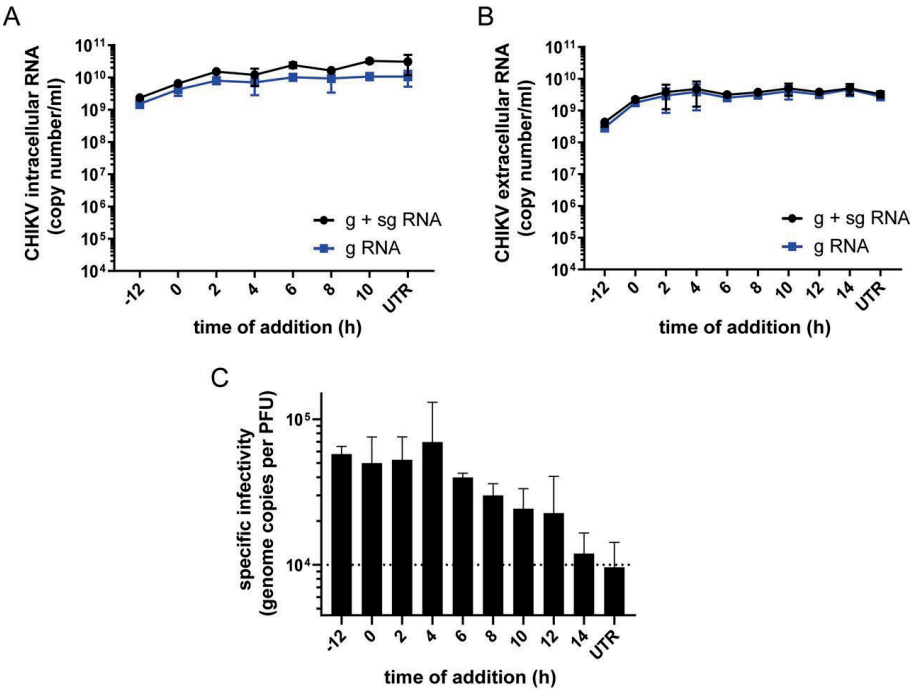

Figure 3. Treatment with FHNA decreases CHIKV specific infectivity. (A) VeroE6 cells were pretreated with 10 µM FHNA for 12 h, treated at the time of infection or with 2-h intervals postinfection. The cells were infected with CHIKV at an MOI of 1, the intracellular CHIKV RNA was isolated at 12 hpi and the extracellular CHIKV RNA was isolated at 16 hpi. (B) Genome copy numbers were determined by an internally controlled multiplex Taqman qRT-PCR with probes specific for the nsP1 (gRNA) and E1 (g + sgRNA) coding regions. The data for panels A and B represent the mean ± the standard deviations (SD) of two independent experiments performed in duplicate. (C) The CHIKV specific infectivity at each treatment interval was determined by dividing the number of genome copies by the infectious virus yield (PFU/ml). UTR, untreated.

infectivity by calculating the ratio between genome copy number and infectious virus yield for the different treatment intervals. As evident from Fig. 3C, there was a decrease in specific infectivity when infected cells were pretreated or treated early in infection (-12 to 4 h). This suggests that FHNA causes a relative increase in noninfectious CHIKV particles, perhaps containing genomes unable to start an infection, e.g. because they are not capped. When 10 µM FHNA was added later during the infection (> 6 h) the specific infectivity of CHIKV particles improved and gradually reached the levels of an untreated control (Fig. 3C).

Mutations in CHIKV nsP1 confer resistance to FHNA

In order to identify the viral target of the compound, we selected escape mutants by passaging CHIKV in the presence of FHNA. We used a previously described five-step resistance selection protocol (14), which can identify compound-resistant variants within a heterogeneous virus mixture exhibiting differing degrees of drug resistance. Mutations that are overrepresented within the resulting compound-resistant heterogeneous viral population are subsequently identified by sequencing. With this experimental set-up, we selected CHIKV escape mutants using a 10 µM dose of the compound, which resulted in the isolation of seven variants (Fig. 4). The seven compound-resistant variants were substantially less sensitive to the antiviral effect of FHNA to various extents, with EC_{50} values ranging from 1.3 to 14.1 µM, compared to

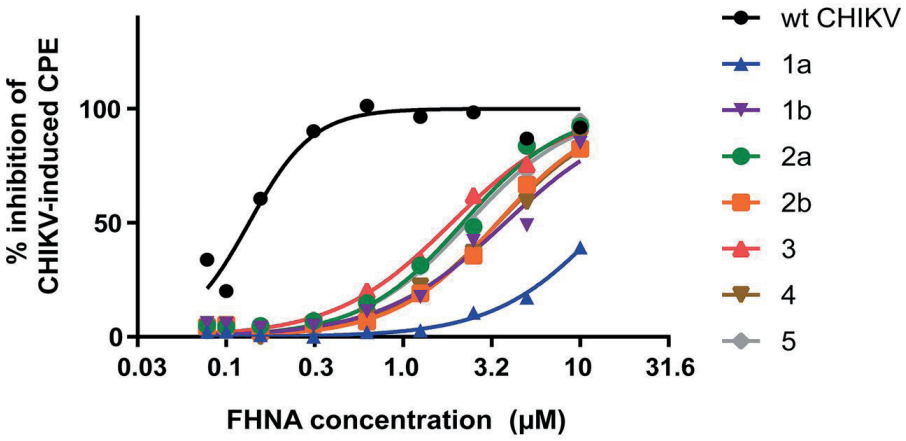

Figure 4. Selection of FHNA-resistant variants. Dose-response curve of the seven FHNA-resistant variants in comparison with wt CHIKV. Variants originating from the same biological replicate (progenitor) are distinguished by a letter a or b next to numbers 1-5.

0.14 µM for wild-type (wt) CHIKV (Table 2). Variant 1a showed by far the largest shift in the EC_{50} value (Fig. 4) and a > 100-fold resistance compared to wt CHIKV (Table 2). To identify mutations that confer FHNA resistance, we determined the genotype of all seven compound-resistant variants by whole genome sequencing, which revealed ten nonsilent mutations in the CHIKV open reading frame encoding the nonstructural polyprotein. We found four mutations in the nsP1-coding region, two mutations in the nsP2-coding region, and four mutations in the nsP3-coding region, some of which occurred in multiple of the seven variants, while others were unique to a particular variant (Table 3). No mutations were found in the CHIKV nsP4-coding region, the RNA-dependent RNA polymerase, suggesting that FHNA does not inhibit CHIKV by targeting viral RNA synthesis. To determine which mutation or combination of mutations was responsible for resistance, we reverse-engineered all mutations into the CHIKV-LS3 cDNA clone, either singularly or in the combinations detected in the original variants. In total, we generated ten single recombinant CHIKV (rCHIKV) mutants, five double rCHIKV mutants and three triple rCHIKV mutants (Fig. 5). The relative resistance level of these rCHIKV mutants varied between 1 and 122-fold higher compared to wt CHIKV (Table 4). All single rCHIKV mutants, except $rCHIKV^{*524R}$ (* denotates the opal stop codon UGA at the end of the nsP3-coding region) and the nonviable $rCHIKV^{A137V}$, exhibited a 2- to 9-fold increased resistance (Table 4), indicating that a single mutation

Table 2. Phenotypes of putative FHNA-resistant variants.

Variant	EC_{50} (µM)[a]	Fold resistance[b]
CHIKV wt	0.14 ± 0.01	1
1a	14.10 ± 0.01	>100
1b	3.4 ± 0.6	24
2a	1.7 ± 0.7	12
2b	3.0 ± 0.6	21
3	1.3 ± 0.8	9
4	3.8 ± 0.3	27
5	1.8 ± 0.8	13

[a]The EC_{50} is expressed as the mean ± the standard deviation.
[b]The fold resistance = (EC_{50} variant/EC_{50} wt).

Table 3. FHNA resistant variants carry mutations in CHIKV nsP1-3.

Amino acid change	Protein	Variants
R171Q	nsP1	4, 2[a], 2[b]
G230R	nsP1	1[a]
K299E	nsP1	1[a]
L455P	nsP1	3
A511S	nsP2	2[a], 2[b]
T675A	nsP2	1[b]
G117R	nsP3	5
A137V	nsP3	4
H342Q	nsP3	1[b], 2[b]
*524R	nsP3	1[a], 1[b]

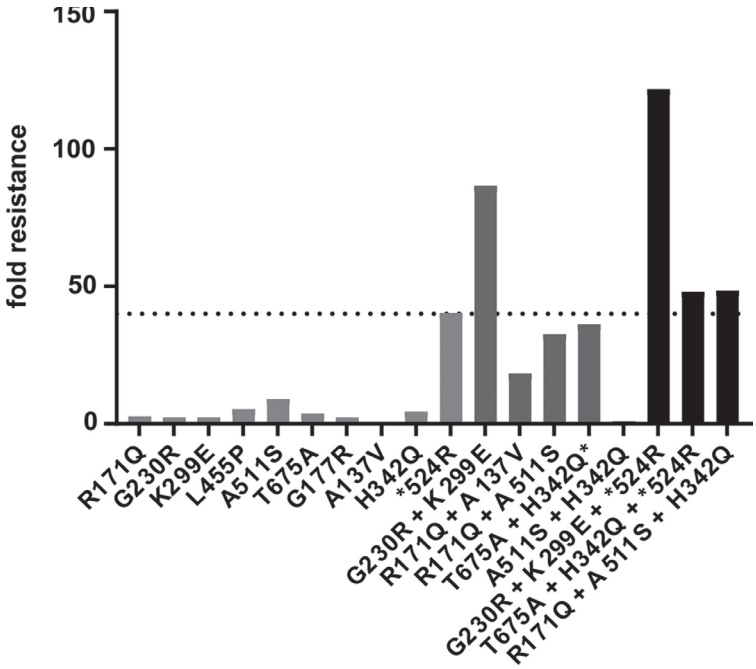

Figure 5. Resistance level of reverse-engineered CHIKV containing mutations selected by passaging CHIKV in the presence of FHNA in the five-step protocol. The graph shows the fold resistance to FHNA (compared to wt CHIKV) of the ten single rCHIKV mutants, five double rCHIKV mutants, and three triple rCHIKV mutants that were reverse engineered. The dashed line represents the cutoff value of 40 (level of resistance caused by the nonspecific *524R mutation) that was used to exclude mutants with a nonspecific resistance to FHNA.

in the CHIKV genome was not sufficient to reproduce the resistance phenotypes observed for the original variants. Mutant rCHIKV^{*524R} was found to be 40-fold more resistant compared to wt CHIKV; however, the loss of the opal stop codon (*524R) is not specifically related to FHNA treatment, since it was also found in natural isolates and has been previously observed when CHIKV was passaged in the presence of the unrelated compound suramin (Albulescu et al., unpublished). Therefore, we chose a 40-fold increase in EC_{50} as a cutoff value (dashed line in Fig 5), and for further analysis only considered mutants with resistance levels exceeding that of the wt virus by > 40-fold (Fig. 5). Among these, variants with two mutations in nsP1, rCHIKV$^{G230R+K299E}$ and rCHIKV$^{G230R+K299E+*524R}$, were the most resistant, displaying a 87- and 122-fold increases in resistance, respectively, compared to wt CHIKV (Table 4, indicated in boldface). We conclude that the combination of the G230R and K299E mutations in nsP1 is

Table 4. Phenotypic resistance and characteristics of all rCHIKV mutants generated by reverse engineering and compared to wt CHIKV.

Recombinant CHIKV	EC_{50} (μM)[a]	Fold resistance[b]
wt	0.21 ± 0.07	1
nsP1-R171Q	0.58 ± 0.37	3
nsP1-G230R	**0.50 ± 0.33**	**2**
nsP1-K299E	**0.50 ± 0.08**	**2**
nsP1-L455P	1.1 ± 1.1	5
nsP2-A511S	1.9 ± 0.6	9
nsP2-T675A	0.80 ± 0.08	4
nsP3-G177R	0.51 ± 0.02	2
nsP3-A137V[c]	ND[d]	-
nsP3-H342Q	0.94 ± 0.01	5
nsP3-*524R	8.5 ± 2.3	40
nsP1-G230R + nsP1-K299E	**18.2 ± 4.2**	**87**
nsP1-R171Q + nsP3-A137V	3.9 ± 1.3	18
nsP1-R171Q + nsP2-A511S	6.9 ± 2.6	33
nsP2-T675A + nsP3-H342Q[e]	7.6 ± 0.2	36
nsP2-A511S + nsP3-H342Q	0.18 ± 0.09	1
nsP1-G230R + nsP1-K299E + nsP3-*524R	**25.6 ± 0.1**	**122**
nsP2-T675A + nsP3-H342Q + nsP3-*524R	10.1 ± 6.8	48
nsP1-R171Q + nsP2-A511S + nsP3-H342Q	10.2 ± 2.6	49

[a]The EC_{50} is expressed as the mean ± the standard deviation .
[b]The fold resistance = (EC_{50} recombinant mutant/EC_{50} wt). Explanation for boldfacing can be found in text.
[c]Not viable.
[d]ND, not determined.
[e]The mutation H342Q reverted back to wt.

sufficient and required for phenotypic resistance, while the individual mutations hardly provide any resistance (Table 4, indicated in boldface). Importantly, the FHNA-resistant rCHIKV$^{G230R+K299E}$ was also resistant to FHA, suggesting that both compounds have a similar mode of action. We reasoned that the higher level of resistance of (rCHIKV$^{G230R+K299E+*524R}$ compared to rCHIKV$^{G230R+K299E}$ was due to the nonspecific effects of the *524R mutation.

The G230R and K299E mutations in nsP1 confer specific resistance to FHNA

In order to assess whether the G230R and K299E mutations confer specific resistance to FHNA, we tested the sensitivity of rCHIKV$^{G230R+K299E}$ and several other mutants to the unrelated CHIKV inhibitors mycophenolic acid (MPA) and 6-azauridine. MPA targets inosine monophosphate dehydrogenase and 6-azauridine is an inhibitor of orotidylic acid decarboxylase, leading to depletion of intracellular GTP and UTP pools, respectively (33). Both rCHIKV$^{G230R+K299E}$ and rCHIKV$^{G230R+K299E+*524R}$ exhibited minimal cross-resistance to either MPA or 6-azauridine, with a 1- to 4-fold increase in resistance compared to wt CHIKV (Table 5). Mutant rCHIKV^{*524R} displayed a 16- to 30-fold increased resistance toward both inhibitors, which are mechanistically unrelated to FHNA, once more emphasizing that this mutation causes an increase in cytopathogenicity or replication kinetics that is unrelated to specific drug resistance. Another CHIKV nsP1 mutant, rCHIKV^{R171Q}, which displayed a 3-fold increased resistance to FHNA, also displayed cross-resistance to MPA (Table 5). The R171Q mutation in nsP1 was also identified independently during resistance selection for the unrelated compound suramin (Albulescu et al., unpublished), and therefore is considered nonspecific.

Table 5. Cross-resistance of FHNA-resistant and other mutants against mycophenolic acid and 6-azauridine.

Recombinant CHIKV	Mycophenolic acid		6-azauridine	
	EC_{50} (μM)[a]	Fold resistance[b]	EC_{50} (μM)	Fold resistance
wt	0.4 ± 0.01	1	0.3 ± 0.01	1
nsP1-R171Q	4.2 ± 2.8	11	0.8 ± 0.1	3
nsP3-*524R	6.3 ± 11.4	16	8.9 ± 3.4	30
nsP1-G230R + nsP1-K299E	1.1 ± 0.5	3	1.1 ± 0.1	4
nsP1-G230R + nsP1-K299E + nsP3-*524R	0.5 ± 0.03	1	0.9 ± 0.1	4

[a]The EC_{50} is expressed as the mean ± the standard deviation.
[b]The fold resistance = (EC_{50} recombinant mutant/EC_{50} wt).

To assess whether the observed increased FHNA resistance is due to a nonspecific increase in replication kinetics, we performed growth curves with rCHIKV wt, rCHIKV$^{G230R+K299E}$ and rCHIKV$^{G230R+K299E+*524R}$ in the presence or absence of 10 µM FHNA. Compared to rCHIKV wt, both rCHIKV$^{G230R+K299E}$ and rCHIKV$^{G230R+K299E+*524R}$ replicated only slightly faster in the absence of compound (Fig. 6A) and produced larger plaques (Fig. 6C). In the presence of 10 µM FHNA, both mutant viruses evidently replicated better than rCHIKV wt (Fig. 6B). Nevertheless, both mutant viruses were still inhibited by the

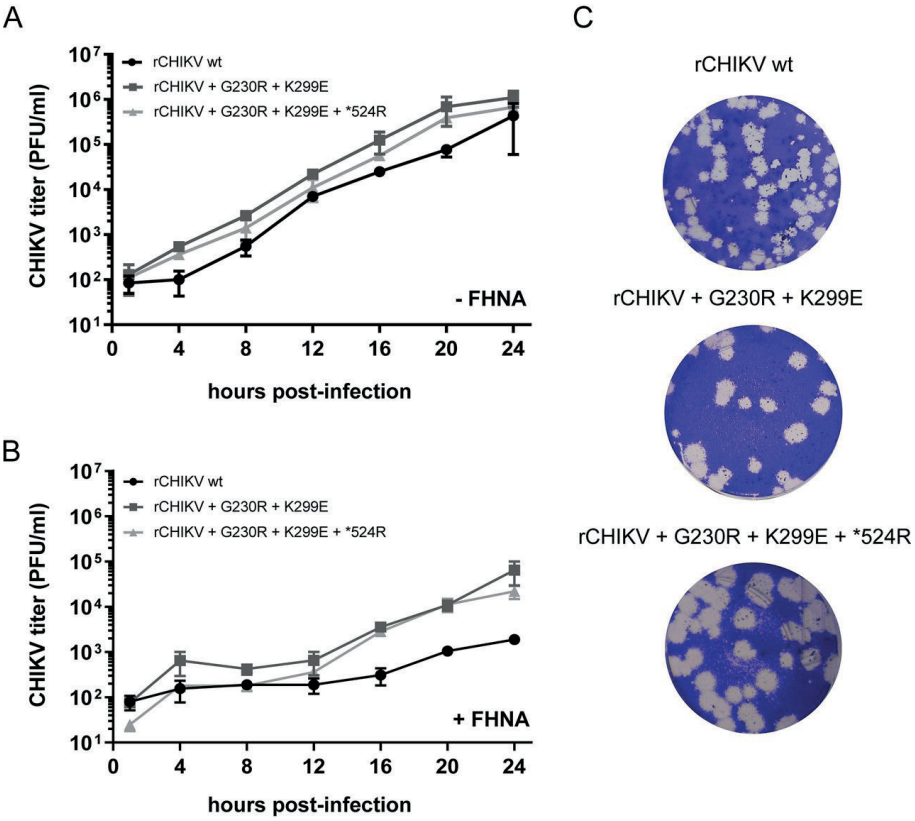

Figure 6. Characterization of rCHIKV with mutations in CHIKV nsp1 and opal stop codon. (A) Growth curve for selected double or triple rCHIKV mutants was performed in the absence of FHNA. VeroE6 cells were infected with CHIKV at an MOI of 1, and supernatants were harvested at 4-h intervals until 24 hpi to determine infectious progeny titers by plaque assay. (B) Growth curve for selected double or triple rCHIKV mutants was performed in the presence of 10 µM FHNA. VeroE6 cells were pretreated with 10 µM FHNA for 12 h prior to infection and infected with CHIKV at an MOI of 1. The compound remained present on the cells throughout the course of the infection. The supernatants were harvested at 4-h intervals until 24 hpi for titration by plaque assay. The data for panels A and B represent the mean ± the standard deviations (SD) of two independent experiments performed in duplicate. (C) Plaque phenotype of rCHIKV$^{G230R+K299}$ and rCHIKV$^{G230R+K299E+*524R}$ in comparison with recombinant wt CHIKV.

compound, as infectious progeny titers were still at least 1.5 $\log_{10}$ lower at 12 hpi and 1.2 $\log_{10}$ lower at 24 hpi in comparison to untreated controls. Taken together, the cross-resistance analysis indicated that the G230R and K299E mutations cause a FHNA-specific resistance.

Purified SFV nsP1 with the K231R and K300E mutations is enzymatically less active *in vitro*

In order to study the effect of FHNA on the enzymatic activity of alphavirus nsP1 and to better understand how the CHIKV nsP1 mutations G230R and K299E may contribute to resistance, we performed *in vitro* enzymatic assays with purified nsP1. Since we were unable to obtain enzymatically active CHIKV nsP1, these assays were performed using purified wt SFV nsP1, SFV nsP1 containing either the K231R or the K300E mutation, and SFV nsP1 containing both mutations. As shown in the sequence alignment in Fig. 7A, SFV residues K231 and K300 correspond to G230 and K299 in the CHIKV nsP1 sequence. As controls, we included two previously described catalytic site mutants: SFV nsP1 ^{H38A}, which is deficient in GTase activity but has retained MTase activity, and SFV nsP1 ^{D64A}, which is devoid of both MTase and GTase activities (32). The enzymatic activity of these proteins was evaluated in an *in vitro* assay monitoring the formation of the covalent m^7GMP-nsP1 complex, an important intermediate in the alphavirus capping reaction. This reaction uses [α^{32P}]GTP and SAM as substrates and requires both the MTase and GTase activities of nsP1. In the presence of both substrates, a radiolabeled reaction product of ~64 kDa (^{32}P-m^7GMP-nsP1) was indeed observed upon analysis by SDS-PAGE and autoradiography (Fig. 7B). This product was not observed when SAM was not included in the reaction, confirming the specificity of the biochemical assay (Fig. 7B). Next, we compared the activities of the various nsP1 mutants and wt nsP1, by assessing the kinetics of ^{32}P-m^7GMP-nsP1 formation (Fig. 7C, right panel) in reactions with the same amount of enzyme (Fig. 7C, left panel). The formation of ^{32}P-m^7GMP-nsP1 was clearly visible when using wt SFV nsP1, as early as 10 min after the start of the reaction, and it steadily increased over time. The active site mutants SFV nsP1^{H38A} and SFV nsP1^{D64A} were hardly active, as only trace amounts of the ^{32}P-m^7GMP-nsP1 intermediate were detected after a 30- or 60-min reaction. Interestingly, the mutant proteins with the single K231R or K300E mutation and the double mutant combining these two mutations displayed very little activity compared to wt SFV nsP1. In fact, the signal observed for these mutants was comparable to that

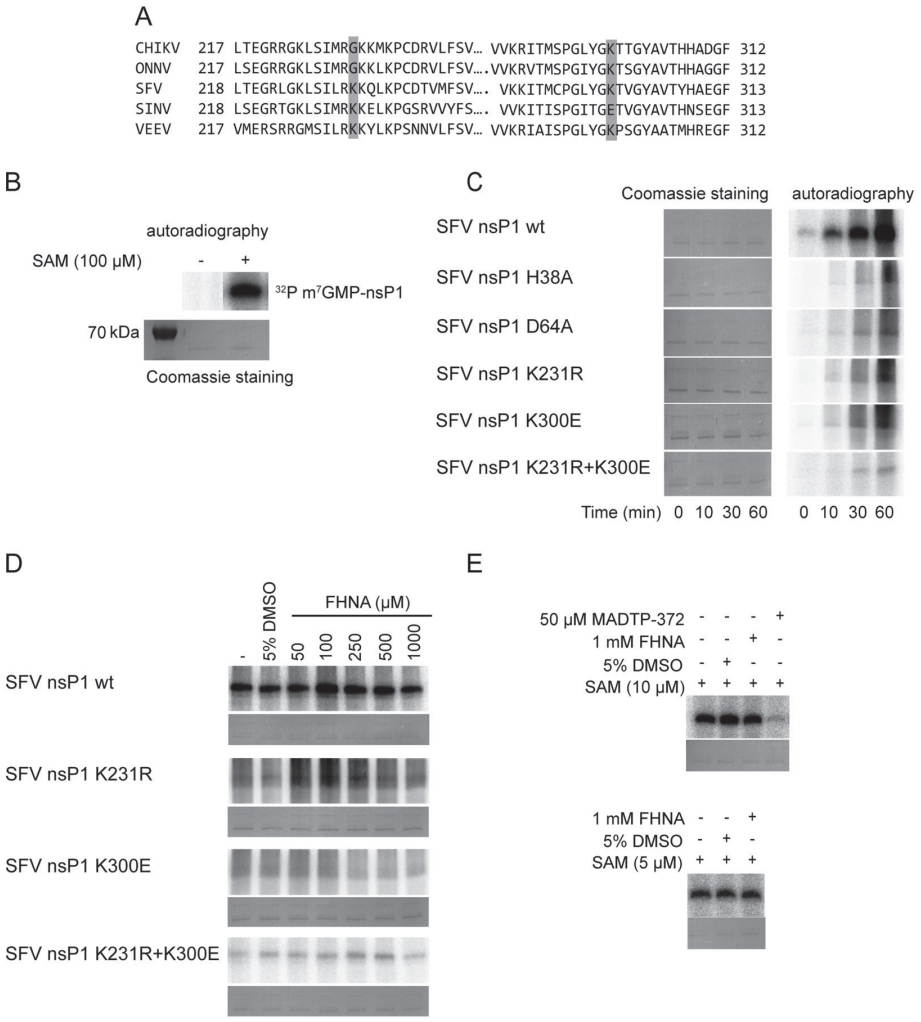

Figure 7. (A) Multiple sequence alignment of nsP1 of selected alphaviruses. Only specific parts of the protein near the region of interest are shown. The mutations G230R and K299E are highlighted in grey. (B) Formation of the α^{32}P-m^{7}GMP-nsP1 intermediate after incubation of the purified recombinant wt SFV nsP1 with [α^{32}P]GTP in the presence or absence of 100 µM SAM in a 30-min reaction. Coomassie blue staining with GelCode blue reagent was used to demonstrate the loading of equal protein quantities. (C) Kinetics of the α^{32}P-m^{7}GMP-nsP1 covalent intermediate formation of wt SFV nsP1 and mutants. The reaction mixture containing [α^{32}P]GTP and 100 µM SAM was stopped with 10 % SDS either at *t* = 0 min (negative control) or left to proceed for *t* = 10, 30 or 60 min. (D) A dose-response assay to assess the effect of FHNA on the formation of the α^{32}P-m^{7}GMP-nsP1 reaction intermediate by wt SFV nsP1 and mutant proteins after treatment with 50 µM to 1 mM FHNA. (E) Effect of 1 mM FHNA and 50 µM control compound MADTP-372 on the formation of the α^{32}P-m^{7}GMP-nsP1 covalent intermediate in the presence of 5 or 10 µM SAM. The reaction was performed at 30°C for 30 min and stopped with 10 % SDS. In all cases, the α^{32}P-m^{7}GMP-nsP1 covalent intermediate was visualized after overnight exposure of the Phosphorimager screen.

of the active site mutants in this assay. The K231R and K300E mutations appear to specifically affect the MTase activity, as the GTase activity of the respective proteins was unchanged in an assay (22) with m^7GTP and SAH (data not shown).

FHNA does not directly inhibit the enzymatic activities of SFV nsP1

First, we investigated whether FHNA directly inhibits wt SFV nsP1 and whether SFV nsP1 $^{K231R+K300E}$ displays a differential sensitivity to the compound. To this end, *in vitro* assays were performed with wt SFV nsP1 and mutants in the presence of 50 µM to 1 mM FHNA. We did not observe any inhibitory effect of FHNA, while control compound MADTP-372 clearly inhibited the reaction (Fig. 7D and E), and we observed no difference between wt and mutant SFV nsP1 proteins in response to FHNA treatment, suggesting that the compound has no direct inhibitory effect on SFV nsP1. Since FHNA might act as a competitive inhibitor by binding to the SAM/SAH-binding site of SFV nsP1, we performed an assay with 5 or 10 µM of SAM (instead of the standard 100 µM) and 1 mM compound. Our results indicated that even a 200-fold molar excess of the compound had no direct inhibitory effect on the protein's enzymatic activity (Fig. 7E).

The K231R and K300E mutations do not increase nsP1's affinity for SAM or resistance to inhibition by SAH

Given that FHNA did not directly inhibit the formation of the covalent m^7GMP-nsP1 intermediate, we tested whether its inhibitory effect is related to the inhibition of SAH hydrolase. Inhibition of this host cell enzyme in cell-based assays would increase intracellular SAH concentrations while decreasing SAM levels. In the *in vitro* assay, SAH clearly inhibited the enzymatic activity of wt nsP1, as the formation of the m^7GMP-nsP1 reaction intermediate was inhibited in a dose-dependent manner by the addition of SAH (Fig. 8A). In the presence of 1 mM SAH, a 100-fold molar excess over SAM, the reaction was fully inhibited. Importantly, normalization of the activity in the presence of different concentrations of SAH to the activity of untreated control protein revealed that both wt SFV nsP1 and SFV nsP1 $^{K231R+K300E}$ were inhibited by SAH to a similar extent. Next, we assessed whether the mutations responsible for FHNA resistance lowered the affinity of SFV nsP1 for SAM, allowing the protein to be active in the presence of reduced SAM levels. There was a clear dose-dependent increase in the activity of wt SFV nsP1 when the SAM concentrations in the reaction were gradually increased

from 1 to 10 µM (Fig. 8B). SFV nsP1 $^{K231R+K300E}$ behaved in a similar manner and did not appear to be more active at low SAM levels (Fig. 8B). Taken together, these results demonstrate that the K231R and K300E mutations do not increase the affinity of SFV nsP1 for SAM nor do they affect its sensitivity to inhibition by SAH.

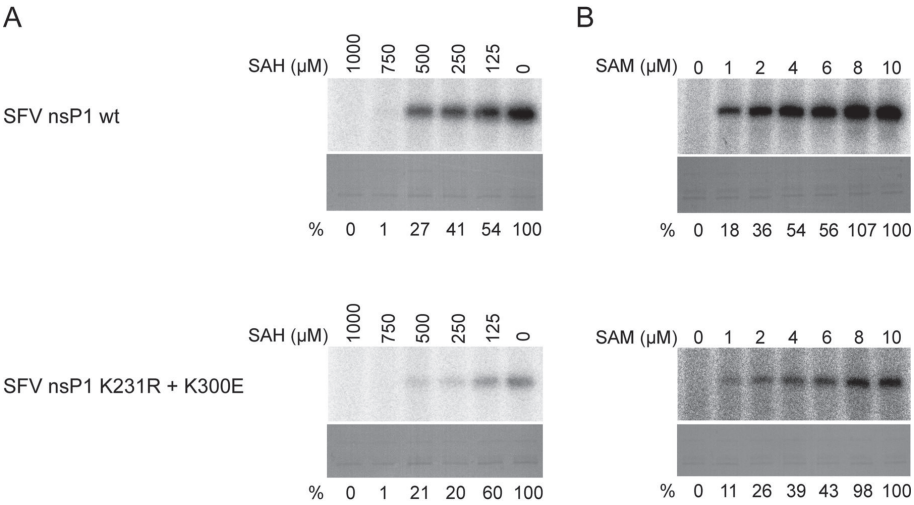

Figure 8. Sensitivity of wt SFV nsP1 and SFV nsP1 K231R + K300E to inhibition by SAH and dependence on SAM. (A) wt SFV nsP1 and the double mutant were incubated with [α^{32}P]GTP and 10 µM SAM in the presence of 0 to 1 mM SAH at 30°C for 30 min, and then the reaction was stopped with 10 % SDS. (B) wt SFV nsP1 and double mutant were incubated with [α^{32}P]GTP and 0 to 10 µM SAM at 30°C for 30 min, and then the reaction was stopped with 10 % SDS. In both panels A and B the α^{32}P-m^{7}GMP-nsP1 covalent intermediate was visualized after overnight exposure of the Phosphorimager screen. Coomassie blue staining was used to demonstrate loading of equal protein quantities. The relative inhibition by SAH (indicated as the percentage of untreated control below the lanes in panel A) of both wt SFV nsP1 and SFV nsP1 double mutant were calculated using QuantityOne software by dividing the volume of the bands of interest by the untreated control. The relative activities at various concentrations of SAM expressed as percentages of the activity at 10 µM SAM is indicated below each lane in panel B.

A metabolite of FHNA directly interferes with the enzymatic activities of SFV nsP1

Since we also identified FHNA analogues that efficiently inhibit host SAH hydrolase *in vitro* without being active against CHIKV in cell-based assays (31), we re-considered the possibility of a direct effect of the compound on nsP1 activity. It has been previously shown that inhibition of host SAH hydrolase by halo-neplanocin A analogues is based on a mechanism that involves the oxidation of the compound to its 3'-keto form by NAD^+ (34). Therefore, we investigated whether an oxidized (3'-keto) form of FHNA

directly inhibits SFV nsP1 activity by performing enzymatic assays under nonreducing conditions and in the presence or absence of NAD^+. Omission of dithiothreitol (DTT) from the reaction is important to allow oxidation of FHNA. Interestingly, 1 mM FHNA inhibited wt SFV nsP1 by > 40% under nonreducing conditions, i.e. in the absence of DTT. The level of inhibition increased by > 50% when 1 mM NAD^+ was added into the reaction mixture containing 1 mM compound (Fig. 9A). In contrast, the SFV nsP1 mutant protein with K231R and K300E substitutions was much less sensitive to FHNA under nonreducing conditions with about 20% reduction in signal. In the presence of NAD^+, the signal further reduced by only about 6 %, suggesting that the mutant was resistant to FHNA (Fig. 9B). Therefore, we concluded that an oxidized (3'-keto) form of FHNA that can be formed under nonreducing conditions, enhanced by NAD^+, directly inhibited SFV nsP1. We also demonstrated that the K231R and K300E mutations render the nsP1 protein less sensitive to the inhibitory effect of oxidized FHNA.

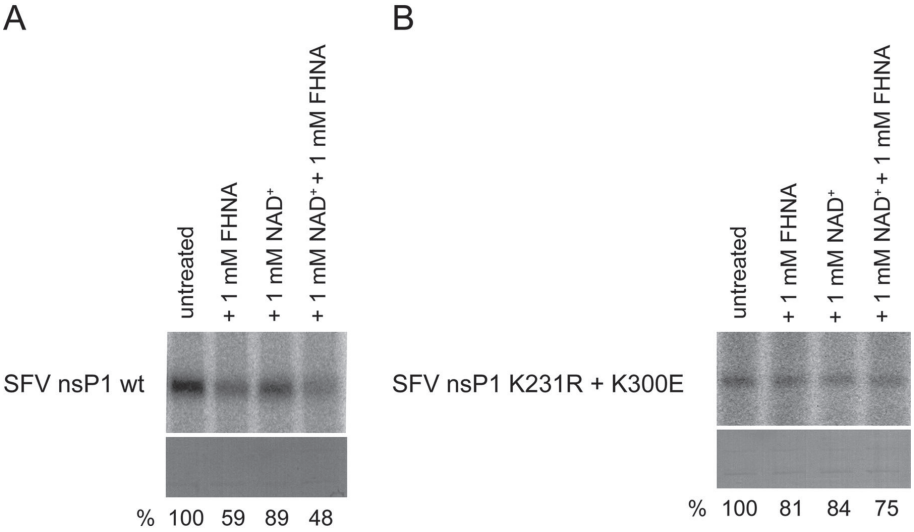

Figure 9. Effect of oxidized FHNA on the activity of wt and mutant SFV nsP1 under nonreducing conditions. (A) wt SFV nsP1 was incubated with [α^{32}P]GTP and 10 µM SAM and was left untreated, incubated with 1 mM FHNA, with 1 mM NAD^+, or a combination of 1 mM FHNA and 1 mM NAD+ at 30°C for 30 min. The reaction was performed in the absence of DTT and was stopped with 10 % SDS. (B) The reactions as described in panel A were performed with the SFV nsP1 K231R + K300E mutant. In both panels A and B the α^{32}P-m^{7}GMP-nsP1 covalent intermediate was visualized following 7-day exposure of the Phosphorimager screen. The relative activity (expressed as the percentage of untreated control) is indicated below the lanes in panels A and B. It was calculated using QuantityOne software by dividing the volume of the bands of interest by that of the untreated control. Coomassie blue staining was used to demonstrate equal protein loading.

Discussion

The burden of mosquito-transmitted diseases such as chikungunya fever is expected to rise in the future due to increased global travel, climate change, and other factors. The search for antiviral drugs to treat CHIKV infections in the clinic has so far proven unsuccessful. In the present study, we identified two carbocyclic adenosine analogues, FHA and FHNA, as inhibitors of CHIKV and SFV replication. These compounds were originally designed as substrate analogue inhibitors of the host enzyme SAH hydrolase and were shown to inhibit this enzyme *in vitro* with 50% inhibitory concentration values of 0.37 and 0.91 μM, respectively (31). In CPE reduction assays, FHA and FHNA strongly inhibited CHIKV with EC_{50} values of 0.12 and 0.18 μM, respectively. They also inhibited SFV, although less potently, with EC_{50} values of 3.9 and 5.2 μM, respectively. Time-of-addition assays indicated that FHNA inhibited CHIKV and SFV rather early in their replication cycle, with, in particular, pretreatment of cells resulting in a strong reduction of CHIKV and SFV infectious progeny (Fig. 2). Pretreatment with SAH hydrolase inhibitors increases intracellular concentrations of SAH, which could indirectly interfere with SAM-dependent methylation reactions such as those involved in mRNA capping (35, 36). The inhibition of the host enzyme SAH hydrolase was shown to be responsible for inhibition of influenza virus replication, which was caused by the accumulation of intracellular SAH and reduced viral mRNA capping (37). Alternatively, pretreatment with SAH hydrolase inhibitors could be necessary to allow sufficient uptake or metabolic conversion of the compounds to their active form. We observed a reduction in CHIKV specific infectivity upon FHNA treatment (virtually unchanged genome copy numbers, but lower infectious progeny titers in the medium), suggesting a relative increase in the production of noninfectious particles. These might contain genomes that lack a functional cap structure, since this is known to be a major determinant of alphavirus infectivity (38).

To identify the viral target of FHNA, we have selected compound-resistant CHIKV variants by repeated virus passaging in the presence of FHNA (Fig. 4). Subsequent genotyping and reverse genetics studies demonstrated that the combination of the G230R and K299E mutations in nsP1 was responsible for the specific resistance to FHA and FHNA. An additional mutation of the opal stop codon to an arginine codon (*524R) at the end of the nsP3-coding sequence further increased resistance, but this appeared to be a nonspecific effect (cell culture adaptation). In an independent study with the polyamine inhibitor difluoromethylornithine (DFMO), Mounce et al. found that the G230R mutation in CHIKV nsP1 contributes to resistance to polyamine

depletion (39). This might reflect the interconnectedness of pathways linked to methionine metabolism and polyamine biosynthesis (17, 40). In contrast to our finding of the nonspecific effect of the mutation, Mounce et al. reported that the *524R mutation in combination with nsP1 mutations was important for DFMO resistance.

Alignment of alphavirus nsP1 sequences (Fig. 7A) revealed that CHIKV and O'nyong-nyong virus contain a glycine at position 230, while the corresponding position is occupied by a basic lysine residue in several other alphaviruses, including SFV. In the FHNA-resistant CHIKV variant, this residue was mutated into an arginine, another basic amino acid, which might explain why wt SFV is intrinsically less sensitive to the compound than CHIKV. At position 299/300, all aligned alphavirus nsP1 sequences except SINV contain a lysine, which was mutated to a glutamic acid in the resistant CHIKV variant. SINV already contains a glutamic acid at this position, which might explain why this virus is not sensitive to FHNA (Fig. 7A). In order to study the mode of action of FHNA in more detail and to investigate the mechanism by which the G230R and K299E mutations in CHIKV nsP1 confer drug resistance, we performed enzymatic assays with purified SFV nsP1. SFV nsP1 MTase activity (41) and GTase activity (21) were previously demonstrated using soluble fractions from *Escherichia coli* cells expressing nsP1. The previously described experimental conditions formed the basis for purification of enzymatically active SFV nsP1. We found that the SFV nsP1 K231R, K300E and K231R+K300E mutants were much less active than the wt protein in an assay that measures both MTase and GTase activity using the formation of a ^{32}P-labelled m^{7}GMP-nsP1 as a read-out. The activities of the SFV nsP1 K231R, K300E and K231R+K300E mutants were comparable to those of the active site mutants H38A and D64A (Fig. 7C). This suggests that FHNA resistance of the K231R+K300E mutant is not simply due to higher enzymatic activity of nsP1. Furthermore, FHNA itself did not serve as a methyl donor as no reaction products were formed when SAM was substituted with FHNA (data not shown). We then explored whether the mode of action of FHNA was associated with the inhibition of the host SAH hydrolase, which leads to increased intracellular SAH levels. The enzymatic activities of purified wt SFV nsP1 and the SFV nsP1 K231R+K300E mutant were inhibited by SAH to the same extent (Fig. 8A). Moreover, both proteins exhibited a similar affinity for SAM (Fig. 8B). This is relevant for the mode of action of FHNA, since increased SAH levels in the host cell would lead to a decrease in SAM levels and interfere with SAM-dependent methylation reactions, including alphavirus nsP1-mediated mRNA capping. Our results demonstrate that FHNA resistance was not associated with increased resistance to

the inhibitory effect of SAH or due to increased activity at low SAM concentrations. We then set out to investigate whether FHNA had a direct inhibitory effect on SFV nsP1, since we have also identified an FHNA analogue with a similar inhibitory activity against the host SAH hydrolase *in vitro* that is completely devoid of anti-CHIKV activity in cell-based assays (31). Previously it was shown that halo-neplanocin A analogues inhibit SAH hydrolase via a mechanism that requires the NAD^+ and the oxidation of the compound to a 3'-keto form (34). Therefore, we investigated the effect of FHNA on the enzymatic activity of nsP1 under nonreducing conditions and in the presence of NAD^+. Under these conditions, wt SFV nsP1 was clearly inhibited in the presence of 1 mM FHNA and 1 mM NAD^+ by > 50% (Fig. 9A), suggesting that an oxidized form of the compound, likely the 3'-keto form, directly inhibits the MTase activity of nsP1. In contrast, the mutant protein containing the K231R and K300E mutations was much less affected by the same treatment, resulting in 25% reduction of the signal (Fig. 9B). Our results show that these mutations render the protein less sensitive to the inhibitory effect of the oxidized compound and suggest this is the basis for FHNA resistance. Of note, the overall activity of nsP1 appeared to be lower when DTT was omitted from the reaction, since the amount of ^{32}P-labelled m^7GMP-nsP1 reaction intermediate was lower compared to the standard assay that includes 5 mM DTT.

Taken together, our enzymatic assays provided important insight into the molecular mechanism of FHNA-mediated inhibition of CHIKV and SFV in infected cells. Based on our findings, we argue that FHNA is predominantly a direct-acting inhibitor of alphavirus mRNA capping due to the direct effect of an oxidized form of FHNA on the SFV nsP1 MTase activity, rather than an indirect effect via the inhibition of host SAH hydrolase. We are aware that we cannot directly extrapolate the findings of the *in vitro* studies with purified SFV nsP1 to the situation in CHIKV-infected cells. Unfortunately, obtaining enzymatically active CHIKV nsP1 was not technically possible.

Alphavirus nsP1 harbors the enzymatic activities required for viral RNA capping in an N-terminal MTase-GTase domain, whereas the enzyme is also palmitoylated and associates with membranes (42, 43). In addition, it contains a membrane-binding amphipathic helix that is essential for the assembly of viral replication organelles (44). The region around position 231 of the SFV nsP1 sequence is rich in lysines and arginines, which are important for membrane binding (45). Therefore, it would also be interesting to investigate whether the FHNA-resistant nsP1 proteins, which have an additional positive charge in this region, would exhibit increased affinity for the negatively charged phospholipids found in membranes. Since it has been proposed

that the membrane association of alphavirus nsP1 is required for its enzymatic activities (45, 46), the amino acid residues involved in membrane binding, such as the K231 residue in SFV, might also be important for the MTase and GTase activities. Earlier studies indicated that mutation of these basic residues (in a triple mutant of SFV nsP1 with R230A, K231A, K232A mutations) reduced MTase activity (45). However, there are currently no alphavirus nsP1 structures available and therefore it is not yet possible to understand how our mutations map to the protein's three-dimensional structure, how they are positioned with respect to the SAM binding pocket and how an oxidized form of FHNA could bind to nsP1. Whether SAM and SAH use the same binding pocket or bind to different sites in the proximity of the GTP binding site also remains to be elucidated. The structures of CHIKV and SFV nsP1 might show differences which could influence their sensitivity to the compound and the effect of the mutations. The elucidation of the CHIKV nsP1 crystal structure is essential to perform compound docking studies that could explain the direct inhibitory activity of FHNA.

In summary, FHA and FHNA have been identified as potent inhibitors of CHIKV and SFV replication in cell culture. The barrier to resistance is expected to be high as two point mutations in nsP1 are required to confer resistance. Their potent antiviral activity, coupled with the fact that they target unique virus-specific enzymatic activities, warrants the further evaluation of FHA and FHNA as potential antiviral drugs to prevent or treat CHIKV infections.

Acknowledgements

KK was supported by the Marie Skłodowska-Curie ETN European Training Network "ANTIVIRALS" (EU Grant Agreement no. 642434).

References

1. Ross RW. 1956. The Newala epidemic. III. The virus: isolation, pathogenic properties and relationship to the epidemic. J Hyg (Lond) 54:177-91.
2. Moore DL, Reddy S, Akinkugbe FM, Lee VH, David-West TS, Causey OR, Carey DE. 1974. An epidemic of chikungunya fever at Ibadan, Nigeria, 1969. Ann Trop Med Parasitol 68:59-68.
3. Chhabra M, Mittal V, Bhattacharya D, Rana U, Lal S. 2008. Chikungunya fever: a re-emerging viral infection. Indian J Med Microbiol 26:5-12.
4. Charrel RN, de Lamballerie X, Raoult D. 2007. Chikungunya outbreaks--the globalization of vectorborne diseases. N Engl J Med 356:769-71.
5. Zeller H, Van Bortel W, Sudre B. 2016. Chikungunya: Its History in Africa and Asia and Its Spread to New Regions in 2013-2014. J Infect Dis 214:S436-s440.
6. Manica M, Guzzetta G, Poletti P, Filipponi F, Solimini A, Caputo B, Della Torre A, Rosa R, Merler S. 2017. Transmission dynamics of the ongoing chikungunya outbreak in Central Italy: from coastal areas to the metropolitan city of Rome, summer 2017. Euro Surveill 22.
7. Calba C, Guerbois-Galla M, Franke F, Jeannin C, Auzet-Caillaud M, Grard G, Pigaglio L, Decoppet A, Weicherding J, Savaill MC, Munoz-Riviero M, Chaud P, Cadiou B, Ramalli L, Fournier P, Noel H, De Lamballerie X, Paty MC, Leparc-Goffart I. 2017. Preliminary report of an autochthonous chikungunya outbreak in France, July to September 2017. Euro Surveill 22.
8. Rezza G, Nicoletti L, Angelini R, Romi R, Finarelli AC, Panning M, Cordioli P, Fortuna C, Boros S, Magurano F, Silvi G, Angelini P, Dottori M, Ciufolini MG, Majori GC, Cassone A. 2007. Infection with chikungunya virus in Italy: an outbreak in a temperate region. Lancet 370:1840-6.
9. Grandadam M, Caro V, Plumet S, Thiberge JM, Souares Y, Failloux AB, Tolou HJ, Budelot M, Cosserat D, Leparc-Goffart I, Despres P. 2011. Chikungunya virus, southeastern France. Emerg Infect Dis 17:910-3.
10. Schwartz O, Albert ML. 2010. Biology and pathogenesis of chikungunya virus. Nat Rev Microbiol 8:491-500.
11. Ching KC, L FPN, Chai CLL. 2017. A compendium of small molecule direct-acting and host-targeting inhibitors as therapies against alphaviruses. J Antimicrob Chemother doi:10.1093/jac/dkx224.
12. Briolant S, Garin D, Scaramozzino N, Jouan A, Crance JM. 2004. In vitro inhibition of Chikungunya and Semliki Forest viruses replication by antiviral compounds: synergistic effect of interferon-alpha and ribavirin combination. Antiviral Res 61:111-7.
13. Khan M, Dhanwani R, Patro IK, Rao PV, Parida MM. 2011. Cellular IMPDH enzyme activity is a potential target for the inhibition of Chikungunya virus replication and virus induced apoptosis in cultured mammalian cells. Antiviral Res 89:1-8.
14. Delang L, Segura Guerrero N, Tas A, Querat G, Pastorino B, Froeyen M, Dallmeier K, Jochmans D, Herdewijn P, Bello F, Snijder EJ, de Lamballerie X, Martina B, Neyts J, van Hemert MJ, Leyssen P. 2014. Mutations in the chikungunya virus non-structural proteins cause resistance to favipiravir (T-705), a broad-spectrum antiviral. J Antimicrob Chemother doi:10.1093/jac/dku209.

15. Pietila MK, Hellstrom K, Ahola T. 2017. Alphavirus polymerase and RNA replication. Virus Res doi:10.1016/j.virusres.2017.01.007.
16. Decroly E, Ferron F, Lescar J, Canard B. 2011. Conventional and unconventional mechanisms for capping viral mRNA. Nat Rev Microbiol 10:51-65.
17. Wolfe MS, Borchardt RT. 1991. S-adenosyl-L-homocysteine hydrolase as a target for antiviral chemotherapy. J Med Chem 34:1521-30.
18. De Clercq E. 1987. S-adenosylhomocysteine hydrolase inhibitors as broad-spectrum antiviral agents. Biochem Pharmacol 36:2567-75.
19. De Clercq E. 1998. Carbocyclic adenosine analogues as S-adenosylhomocysteine hydrolase inhibitors and antiviral agents: recent advances. Nucleosides Nucleotides 17:625-34.
20. Yoon JS, Kim G, Jarhad DB, Kim HR, Shin YS, Qu S, Sahu PK, Kim HO, Lee HW, Wang SB, Kong YJ, Chang TS, Ogando NS, Kovacikova K, Snijder EJ, Posthuma CC, van Hemert MJ, Jeong LS. 2019. Design, Synthesis, and Anti-RNA Virus Activity of 6'-Fluorinated-Aristeromycin Analogues. J Med Chem 62:6346-6362.
21. Ahola T, Kaariainen L. 1995. Reaction in alphavirus mRNA capping: formation of a covalent complex of nonstructural protein nsP1 with 7-methyl-GMP. Proc Natl Acad Sci U S A 92:507-11.
22. Li C, Guillen J, Rabah N, Blanjoie A, Debart F, Vasseur JJ, Canard B, Decroly E, Coutard B. 2015. mRNA Capping by Venezuelan Equine Encephalitis Virus nsP1: Functional Characterization and Implications for Antiviral Research. J Virol 89:8292-303.
23. Vasiljeva L, Merits A, Auvinen P, Kaariainen L. 2000. Identification of a novel function of the alphavirus capping apparatus. RNA 5'-triphosphatase activity of Nsp2. J Biol Chem 275:17281-7.
24. Delang L, Li C, Tas A, Querat G, Albulescu IC, De Burghgraeve T, Guerrero NA, Gigante A, Piorkowski G, Decroly E, Jochmans D, Canard B, Snijder EJ, Perez-Perez MJ, van Hemert MJ, Coutard B, Leyssen P, Neyts J. 2016. The viral capping enzyme nsP1: a novel target for the inhibition of chikungunya virus infection. Sci Rep 6:31819.
25. Gigante A, Gomez-SanJuan A, Delang L, Li C, Bueno O, Gamo AM, Priego EM, Camarasa MJ, Jochmans D, Leyssen P, Decroly E, Coutard B, Querat G, Neyts J, Perez-Perez MJ. 2017. Antiviral activity of [1,2,3]triazolo[4,5-d]pyrimidin-7(6H)-ones against chikungunya virus targeting the viral capping nsP1. Antiviral Res 144:216-222.
26. Abdelnabi R, Kovacikova K, Moesslacher J, Donckers K, Battisti V, Leyssen P, Langer T, Puerstinger G, Quérat G, Li C, Decroly E, Tas A, Marchand A, Chaltin P, Coutard B, van Hemert M, Neyts J, Delang L. 2020. Novel Class of Chikungunya Virus Small Molecule Inhibitors That Targets the Viral Capping Machinery. Antimicrob Agents Chemother 64.
27. Feibelman KM, Fuller BP, Li L, LaBarbera DV, Geiss BJ. 2018. Identification of small molecule inhibitors of the Chikungunya virus nsP1 RNA capping enzyme. Antiviral Res 154:124-131.
28. Ferreira-Ramos AS, Li C, Eydoux C, Contreras JM, Morice C, Querat G, Gigante A, Perez Perez MJ, Jung ML, Canard B, Guillemot JC, Decroly E, Coutard B. 2019. Approved drugs screening against the nsP1 capping enzyme of Venezuelan equine encephalitis virus using an immuno-based assay. Antiviral Res 163:59-69.

29. Kaur R, Mudgal R, Narwal M, Tomar S. 2018. Development of an ELISA assay for screening inhibitors against divalent metal ion dependent alphavirus capping enzyme. Virus Res 256:209-218.
30. Scholte FE, Tas A, Martina BE, Cordioli P, Narayanan K, Makino S, Snijder EJ, van Hemert MJ. 2013. Characterization of synthetic Chikungunya viruses based on the consensus sequence of recent E1-226V isolates. PLoS One 8:e71047.
31. Chandra G, Moon YW, Lee Y, Jang JY, Song J, Nayak A, Oh K, Mulamoottil VA, Sahu PK, Kim G, Chang TS, Noh M, Lee SK, Choi S, Jeong LS. 2015. Structure-Activity Relationships of Neplanocin A Analogues as S-Adenosylhomocysteine Hydrolase Inhibitors and Their Antiviral and Antitumor Activities. J Med Chem 58:5108-20.
32. Ahola T, Laakkonen P, Vihinen H, Kääriäinen L. 1997. Critical residues of Semliki Forest virus RNA capping enzyme involved in methyltransferase and guanylyltransferase-like activities. J Virol 71:392-7.
33. Subudhi BB, Chattopadhyay S, Mishra P, Kumar A. 2018. Current Strategies for Inhibition of Chikungunya Infection. Viruses 10.
34. Lee KM, Choi WJ, Lee Y, Lee HJ, Zhao LX, Lee HW, Park JG, Kim HO, Hwang KY, Heo YS, Choi S, Jeong LS. 2011. X-ray crystal structure and binding mode analysis of human S-adenosylhomocysteine hydrolase complexed with novel mechanism-based inhibitors, haloneplanocin A analogues. J Med Chem 54:930-8.
35. Ault-Riche DB, Lee Y, Yuan CS, Hasobe M, Wolfe MS, Borcherding DR, Borchardt RT. 1993. Effects of 4'-modified analogs of aristeromycin on the metabolism of S-adenosyl-L-homocysteine in murine L929 cells. Mol Pharmacol 43:989-97.
36. Cools M, de Clercq E. 1989. Correlation between the antiviral activity of acyclic and carbocyclic adenosine analogues in murine L929 cells and their inhibitory effect on L929 cells S-adenosylhomocysteine hydrolase. Biochem Pharmacol 38:1061-7.
37. Ransohoff RM, Narayan P, Ayers DF, Rottman FM, Nilsen TW. 1987. Priming of influenza mRNA transcription is inhibited in CHO cells treated with the methylation inhibitor, neplanocin A. Antiviral Res 7:317-27.
38. Sokoloski KJ, Haist KC, Morrison TE, Mukhopadhyay S, Hardy RW. 2015. Noncapped Alphavirus Genomic RNAs and Their Role during Infection. J Virol 89:6080-92.
39. Mounce BC, Cesaro T, Vlajnic L, Vidina A, Vallet T, Weger-Lucarelli J, Pasoni G, Stapleford KA, Levraud JP, Vignuzzi M. 2017. Chikungunya virus overcomes polyamine depletion by mutation of nsP1 and the opal stop codon to confer enhanced replication and fitness. J Virol doi:10.1128/jvi.00344-17.
40. van Brummelen AC, Olszewski KL, Wilinski D, Llinas M, Louw AI, Birkholtz LM. 2009. Co-inhibition of Plasmodium falciparum S-adenosylmethionine decarboxylase/ornithine decarboxylase reveals perturbation-specific compensatory mechanisms by transcriptome, proteome, and metabolome analyses. J Biol Chem 284:4635-46.
41. Laakkonen P, Hyvonen M, Peranen J, Kaariainen L. 1994. Expression of Semliki Forest virus nsP1-specific methyltransferase in insect cells and in Escherichia coli. J Virol 68:7418-25.
42. Peranen J, Laakkonen P, Hyvonen M, Kaariainen L. 1995. The alphavirus replicase protein nsP1 is membrane-associated and has affinity to endocytic organelles. Virology 208:610-20.
43. Laakkonen P, Ahola T, Kaariainen L. 1996. The effects of palmitoylation on membrane association of Semliki forest virus RNA capping enzyme. J Biol Chem 271:28567-71.

44. Ahola T, Karlin DG. 2015. Sequence analysis reveals a conserved extension in the capping enzyme of the alphavirus supergroup, and a homologous domain in nodaviruses. Biol Direct 10:16.
45. Ahola T, Lampio A, Auvinen P, Kaariainen L. 1999. Semliki Forest virus mRNA capping enzyme requires association with anionic membrane phospholipids for activity. EMBO J 18:3164-72.
46. Lampio A, Kilpelainen I, Pesonen S, Karhi K, Auvinen P, Somerharju P, Kaariainen L. 2000. Membrane binding mechanism of an RNA virus-capping enzyme. J Biol Chem 275:37853-9.

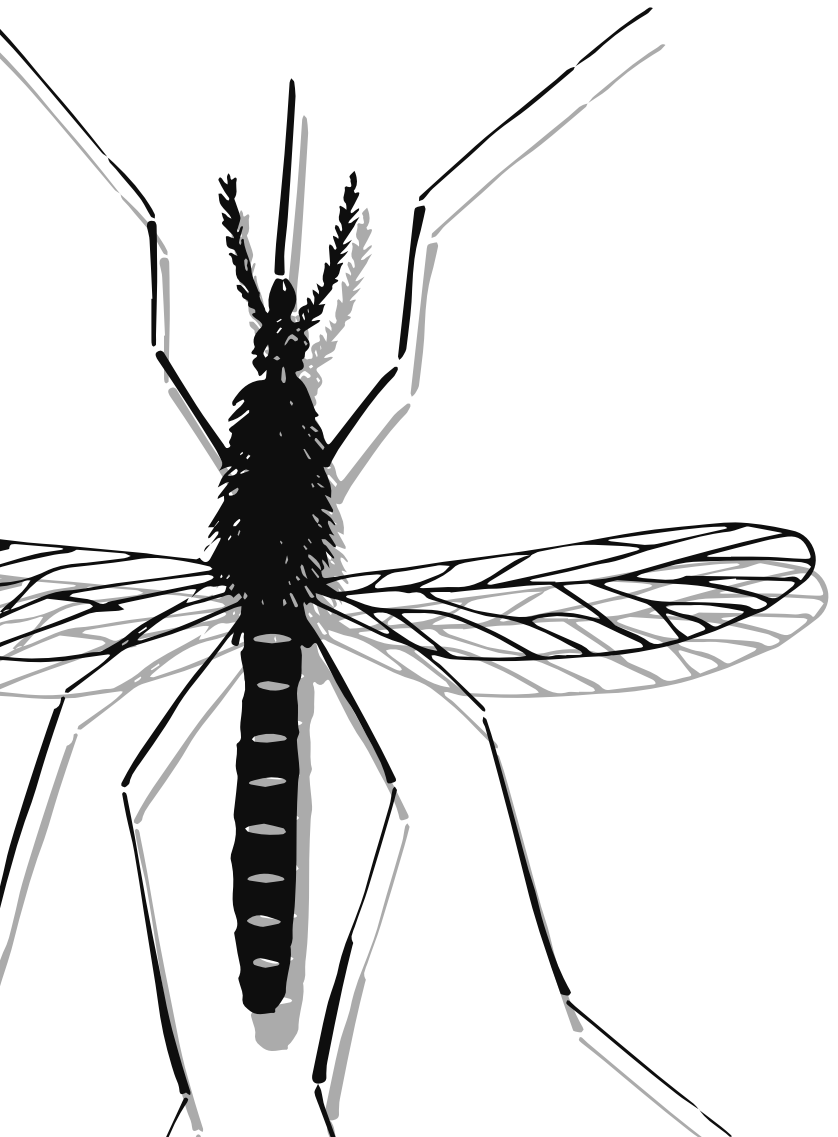

CHAPTER 5

Novel class of Chikungunya virus small molecule inhibitors that targets the viral capping machinery

Kristina Kovacikova[1#], Rana Abdelnabi[2#], Julia Moesslacher[3], Kim Donckers[2], Verena Battisti[4], Pieter Leyssen[2], Thierry Langer[4], Gerhard Puerstinger[3], Gilles Quérat[5], Changqing Li[6], Etienne Decroly[6], Ali Tas[1], Arnaud Marchand[7], Patrick Chaltin[7], Bruno Coutard[5], Martijn van Hemert[1], Johan Neyts[2#], Leen Delang[2#]

[#]Contributed equally

[1]Molecular Virology Laboratory, Department of Medical Microbiology, Leiden University Medical Center, Albinusdreef 2, 2333 ZA Leiden, the Netherlands.

[2]KU Leuven, Department of Microbiology, Immunology and Transplantation, Rega Institute for Medical Research, Laboratory of Virology and Chemotherapy, 3000 Leuven, Belgium.

[3]Department of Pharmaceutical Chemistry, University of Innsbruck, Innsbruck, Austria.

[4]University of Vienna, Department of Pharmaceutical Chemistry, Vienna, Austria.

[5]Unité des Virus Emergents (UVE: Aix-Marseille Univ - IRD 190 - Inserm 1207 - IHU Méditerranée Infection), Marseille, France

[6]Aix Marseille Univ, CNRS, AFMB UMR7257, Marseille, France

[7]Centre for Drug Design and Discovery, KU Leuven, B-3001 Leuven, Belgium.

Antimicrob Agents Chemother. 2020 Jun 23;64(7):e00649-20.

Abstract

Despite the worldwide reemergence of the chikungunya virus (CHIKV) and the high morbidity associated with CHIKV infections, there is no approved vaccine or antiviral treatment available. Here, we aimed to identify the target of a novel class of CHIKV inhibitors i.e. CHVB series. CHVB compounds inhibit the *in vitro* replication of CHIKV isolates with 50% effective concentrations in the low-micromolar range. A CHVB-resistant variant ($CHVB^{res}$) was selected that carried two mutations in the gene encoding nonstructural protein 1 (nsP1) (responsible for viral RNA capping), one mutation in nsP2 and one mutation in nsP3. Reverse genetics studies demonstrated that both nsP1 mutations were necessary and sufficient to achieve ~18-fold resistance, suggesting that CHVB targets viral mRNA capping. Interestingly, $CHVB^{res}$ was cross-resistant to the previously described CHIKV capping inhibitors from the MADTP series, suggesting they share a similar mechanism of action. In enzymatic assays, CHVB inhibited the methyltransferase and guanylyltransferase activities of alphavirus nsP1 proteins. To conclude, we identified a class of CHIKV inhibitors that targets the viral capping machinery. The potent anti-CHIKV activity makes this chemical scaffold a potential candidate for CHIKV drug development.

Introduction

Chikungunya virus (CHIKV) is an arthropod-borne virus that belongs to the genus *Alphavirus* of the *Togaviridae* family (1, 2). After two decades of sporadic outbreaks in Africa and Asia, CHIKV reemerged in Kenya in 2004, after which large epidemics of CHIKV infections were reported in several Indian Ocean islands and Southeast Asian countries (3). At the end of 2013, the first local transmission of CHIKV occurred in the Americas. Since then, millions of CHIKV cases have been reported in the Caribbean region as well as in several countries of Central and South America (4). Most recently, in 2018, CHIKV caused outbreaks in Brazil, India, Sudan and Thailand (5). Due to the high socioeconomic impact of CHIKV infections, the virus is now considered an imminent health threat to tropical and temperate areas colonized by *Aedes* mosquitoes.

Acute CHIKV infections are characterized by fever, arthralgia, and, in many cases, maculopapular rash (6). Although a CHIKV infection is rarely fatal, 15 to 60% of patients suffer from chronic debilitating polyarthritis that can last for weeks up to years after the acute infection (1, 6). Recently, severe neurological complications such as Guillain-Barré syndrome and meningoencephalitis, have also been reported during CHIKV infections (1, 7). Other complications associated with CHIKV infections include myocarditis, pancreatitis, and kidney failure (8).

Despite the worldwide spread and the high morbidity rate of CHIKV infections, there is no licensed vaccine or antiviral treatment available. The current treatment is only symptomatic (2). A number of classes of antiviral compounds targeting either a viral or a host factor have been reported to inhibit CHIKV replication in cell-based assays (9, 10), but none have progressed to clinical trials. We previously reported on the first class of inhibitors ([1,2,3]triazolo[4,5-d]pyrimidin-7(6H)-ones, the MADTP series, that block the capping of CHIKV RNA genomes. The MADTP compounds mainly target the guanylyltransferase (GTase) activity of Venezuelan Equine Encephalitis virus (VEEV) nsP1 (11). This class of compounds has a low barrier to resistance, since only a single mutation in CHIKV nsP1 (proline-34-serine) resulted in high resistance to the compounds (11). Ideally, antiviral drugs should have a high barrier to resistance to avoid rapid emergence of drug-resistant variants.

In a large-scale cytopathic effect (CPE)-based anti-CHIKV screening campaign (33,000 molecules), we identified CHVB-00 (N-ethyl-2-(4-((4-fluorophenyl) sulfonyl) piperazin-1-yl)-6-methylpyrimidin-4-amine) as a molecule that was able to completely inhibit CHIKV replication at nontoxic concentrations (50% effective concentration [EC_{50}] value of 8.7 ± 0.5 μM, 50% cytotoxic concentration [CC_{50}] of 122 ± 24 μM) (Fig. 1).

Initial hit optimization resulted in the synthesis and biological evaluation of 67 analogs. Of these analogs, 24 molecules were more potent than the original hit compound. The synthesis of this class of molecules and the structure-activity relationship will be published elsewhere (12). Here, we report on the particular characteristics of the anti-CHIKV activity of this class of compounds and the molecular mechanism underlying the antiviral activity.

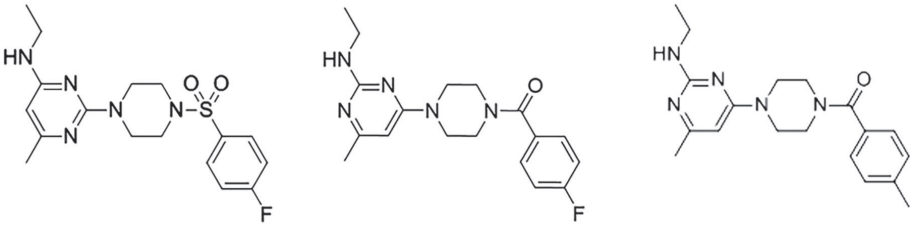

Figure 1. Chemical structures of the initial hit and selected analogs of the CHVB series.

Materials and Methods

Cells, viruses and compounds

African green monkey kidney cells (Vero cells [ATCC CCL-81], VeroE6 cells [ATCC CRL-1586]), Baby hamster kidney [BHK-21] cells were maintained as described before (11). CHIKV and other alphaviruses strains are as mentioned before (11). CHIKV LS3 (GenBank accession no. KC149888), which was used for reverse genetics studies, is derived from a full-length cDNA clone belonging to the collection of the Leiden University Medical Center, The Netherlands (13).

CHVB-032 and CHVB-066 (Fig. 1) were synthesized in the laboratory of G. Pürstinger (University of Innsbruck, Austria) and T. Langer (University of Vienna, Austria). MADTP-0372 was synthesized by M.J. Pérez-Pérez (Spanish National Research Council, CSIC) (11). T-705 (favipiravir) was purchased as a custom synthesis product from BOC Sciences. Chloroquine was purchased from Sigma.

CPE reduction assay

Vero cells were seeded at a density of 2.5×10^4 in 96-well plates (BD Falcon) and were allowed to adhere overnight. The next day, cells were treated with a dilution series of the compounds, after which the cultures were infected with CHIKV-899 (multiplicity of infection [MOI] of 0.01). On day 5 postinfection, the inhibition of CPE was quantified using MTS/PMS as described by the manufacturer (Promega). The cells were checked by microscope for minor signs of virus-induced CPE or compound-induced adverse effects on the cell monolayer morphology. The 50% effective concentration (EC_{50}), which is defined as the concentration of compound that is required to inhibit virus-induced cell death by 50%, was determined using logarithmic interpolation.

Virus yield assay

Vero cells were seeded in 96-well plates at a density of 5×10^4 cells/well. The next day, cells were treated with serial dilutions of the compound and then infected with CHIKV-899 (MOI of 0.01). Two hours postinfection, the cells were washed to remove nonadsorbed virus, followed by incubation with the same serial dilutions of compounds. After 48 h of incubation, supernatants were collected and viral RNA was quantified by real-time quantitative RT-PCR (qRT-PCR), while the amount of infectious progeny virus was determined by titration assay (50% cell culture infectious dose [$CCID_{50}$]/ml) as described before (14).

Delay of treatment assay

Vero cells were seeded in 96-well plates at a density of 5×10^4 cells/well. The following day, cells were infected with CHIKV 899 (MOI of 1) for 1 h at 37°C, after which the viral inoculum was removed, and cells were washed 3 times with the assay medium. The selected compounds (20 µM CHVB-032, 5 µM CHVB-066, 50 µM MADTP-0372, 200 µM T-705 or 50 µM of chloroquine) were added to cells at 0, 2, 4, 6, 8 and 10 h after infection. At 12 h postincubation (i.e. one viral replication cycle), culture supernatants were collected for quantification of extracellular viral RNA load (by qRT-PCR) and infectious virus progeny (by endpoint titration).

Selection of compound-resistant virus isolates

A 5-step clonal resistance selection protocol was used to isolate CHVB-resistant virus variants as previously described (15). In the first step, Vero cells were seeded in 96-well plates at a density of 2.5×10^4 cells/well and were allowed to adhere overnight. Subsequently, antiviral assays were performed in a checkerboard format using serial dilutions of CHVB-032 and different amounts of CHIKV-899 (ranging from 10 to 1,000 $CCID_{50}$). After 5 days of incubation, all assay wells were checked microscopically. Based on these data, the lowest concentration of compound and the highest virus input at which complete and reproducible inhibition of virus-induced CPE was observed were selected. In the second step, three 96-well plates containing adherent Vero cells were treated with the selected CHVB-032 concentration of 29 μM and then were infected with the optimal amount of virus (50 $CCID_{50}$). After 5 days, 7 assay wells (out of 162) showed signs of virus-induced CPE, with only 4 of them showing full CPE. The supernatants of these 4 wells were collected and semipurified 6-fold by titration (1:5 dilution series) in the presence of 29 μM of CHVB-032. Four virus isolates (one from each original sample) were selected that produced the most pronounced signs of CPE in the presence of CHVB-032 at the lowest virus input possible. Subsequently, the resistant phenotype of the selected virus isolates was determined in comparison with the wild-type virus in CPE reduction assays. In parallel, the genotype was determined by full genome sequencing.

Assays for alphavirus nsP1 enzymatic activity

The DNA sequence encoding SFV nsP1 (amino acid 1 to 537) with C-terminal hexahistidine (6xHis) tag was cloned into the pET34 vector. Recombinant wild-type and active site mutant D64A were expressed in *E. coli* Rosetta cells (Novagen) following overnight induction with 0.5 mM isopropyl-β-D-thiogalactopyranoside (IPTG) at 19˚C. The recombinant proteins were batch purified by immobilized metal affinity chromatography (IMAC) using Talon (Cobalt) beads (TaKaRa), and the eluted protein was concentrated and used in the covalent m^7GMP-nsP1 complex formation assay (16). This assay was performed in a 30-μl mixture containing 25 mM HEPES pH 7.5, 5 mM dithiothreitol, 10 mM KCl, 2 mM $MgCl_2$, 10 μM S-adenosylmethionine (SAM), 0.75 mCi of [α^{32}P] GTP (3,000 Ci/mmol) and 0.5 μM SFV nsP1 wt or D64A mutant. The reaction mixture was incubated at 30˚C for 30 min and stopped by adding 3 μl of 10% SDS. The inactivated reaction mixture was mixed with 4xLSB (Laemmli Sample Buffer)

and 10 µl samples were resolved on a 10% SDS-PAGE gel. The gel was dried, and a PhosphorImager screen was placed on top. After overnight exposure, the ^{32}P-labelled covalent m^{7}GMP-nsP1 intermediate products were visualized with a Typhoon Imager (Amersham). The protocols for VEEV nsP1 enzymatic activity assays were previously described (11).

Statistical analysis

Graphing and statistical analysis were performed using Prism8 software (GraphPad).

Results

Molecules of the CHVB series inhibit the replication of various CHIKV isolates in cell culture

The antiviral efficacy of CHVB-032 and CHVB-066 against the CHIKV-899 strain was assessed in a CPE reduction assay on Vero cells. Both molecules exerted potent inhibition of virus-induced CPE, with EC_{50} values of 2.7 µM and 0.45 µM, respectively (Fig. 2A). When assessing the potential adverse effects of the compounds on Vero cells (by colorimetric readout using MTS/PMS), CHVB-032 was less cytotoxic than CHVB-066 (CC_{50} values of >75 µM and 15 µM, respectively) (Fig. 2A). The anti-CHIKV

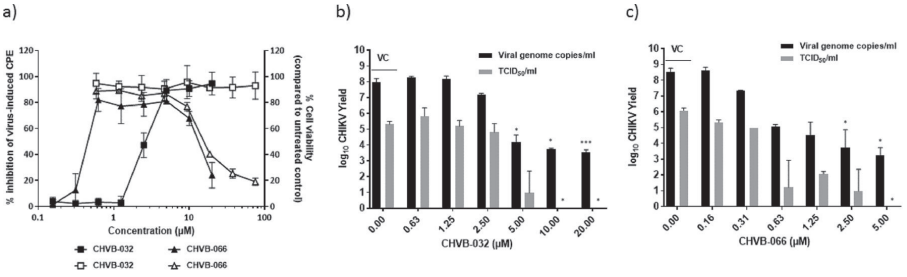

Figure 2. CHVB compounds are selective inhibitors of CHIKV replication. (A) Dose-response effect of CHVB-032 and CHVB-066 on CHIKV899-induced cytopathic effect (CPE) [filled squares and filled triangles, respectively] (MOI 0.01) and cell viability (open squares and open triangles, respectively) as quantified in Vero cells by the MTS/PMS method. Data are mean values ± the standard deviations (SD) from at least three independent experiments. The effect of different concentrations of CHVB-032 (B) and CHVB-066 (C) on the release of CHIKV particles by CHIV899-infected Vero cells (MOI 0.01) was quantified by real-time qRT-PCR (for viral RNA; black columns) and endpoint titration assay (for infectious progeny virus particles; grey columns) at 48h p.i. Data shown are mean values ± SD from at least two independent experiments. Significant differences from untreated virus control were analyzed by two-tailed Student's *t* test (*, $P < 0.05$; ***, $P < 0.005$). TCID, tissue culture infectious dose; VC, virus control (untreated).

activity was further confirmed in a virus yield assay in which treatment with both CHVB compounds resulted in a marked dose-dependent reduction of viral RNA replication and production of infectious virus progeny, with a pronounced > 4 $\log_{10}$ reduction at the highest tested concentrations (Fig. 2B and C). The antiviral activity of CHVB-032 was further evaluated against various CHIKV isolates (Venturini [Italy 2008], St Martin 20235 P2, St Martin 20236 P3, EFS-1 P3 Martinique and Congo 95 [2011]). CHVB-032 reduced the viral RNA yield of all the tested CHIKV isolates, with EC_{50} values in the range of 1.2 to 7.3 µM (Table 1). However, the compound was devoid of antiviral activity against other alphaviruses, i.e. O'Nyong Nyong virus, Mayaro virus strain TC625, Barmah Forest virus strain BH2193 and Ross River virus 5281v (data not shown).

Table 1. Antiviral activity of CHVB-032 compound against different chikungunya virus isolates.

	CHVB-032	
CHIKV strain	**EC_{50} (µM)**	**EC_{90} (µM)**
899 (lab)	2.7 ± 0.4[a]	5.5 ± 0.2[a]
OPY1 (La Reunion)	1.24 ± 0.3[b]	6.7 ± 0.5[b]
Venturi (Italy)	2.1 ± 0.4[b]	2.6 ± 0.4[b]
Congo (Congo)	1 ± 0.15[b]	1.2 ± 0.1[b]
St Martin 20235 P2	1.7 ± 0.4[b]	5 ± 0.3[b]
St Martin 20236 P3	4.1 ± 0.6[b]	17 ± 8[b]
EFS-1 P3 Martinique	7.3 ± 2.3[b]	13 ± 3[b]

[a] CPE reduction
[b] Viral RNA reduction

CHVB compounds inhibit a postentry step in the CHIKV replication cycle

A delay-of-treatment assay was performed to estimate the stage of CHIKV replication cycle inhibited by the CHVB series. Chloroquine was used in this assay as a reference compound for early-stage inhibition, as this molecule is known to interfere with virus entry (17). MADTP-0372 (inhibits viral RNA capping) and T-705 (inhibits viral RNA synthesis) were used as reference molecules for replication stage inhibition (11, 15). Similar to the inhibition profile of the MADTP-0372 compound, CHVB-032 and CHVB-066 reduced viral RNA (Fig. 3A) and infectious virus loads (Fig. 3B) when added to the infected cells up to 4h postinfection (p.i.), suggesting that compounds

in the CHVB series target a postentry step in the CHIKV replication cycle. To confirm the absence of an effect on virus entry, a CHIKV entry assay was performed using CHIKV pseudoparticles (CHIKVpp) as described before (18). In contrast to chloroquine, the CHVB compounds did not inhibit the entry of CHIKVpp in BGM cells (Fig. 3C), demonstrating that CHVB compounds act at a postentry stage of the CHIKV replication cycle.

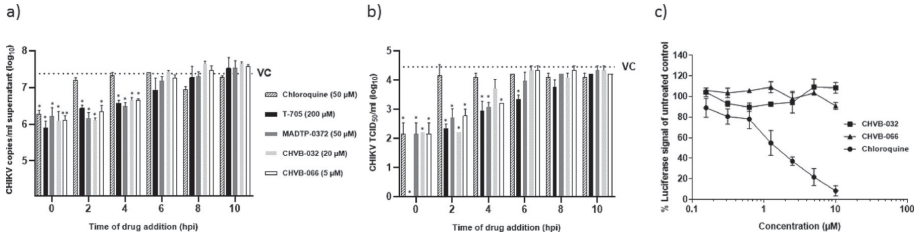

Figure 3. CHVB compounds inhibit a postentry step in the CHIKV replication cycle. The delay of treatment effect of CHVB-032 (20 µM; light grey columns) and CHVB-066 (5 µM; white columns) on viral replication in CHIKV899-infected Vero cells (MOI of 1) was determined at 12h p.i. by real-time qRT-PCR (A) and end-point titration assay (B). Chloroquine (50 µM; dashed columns) served as a reference compound for early-stage inhibition, whereas MADTP-0372 (50 µM; dark grey columns) and T-705 (200 µM; black columns) served as references for postentry-stage inhibition. Data are mean values ± SD from at least two independent experiments. Significant differences from untreated virus control were analyzed by two-tailed Student's *t* test (*, $P < 0.05$; **, $P < 0.01$). (C) The effect of CHVB-032 (filled squares) and CHVB-066 (filled triangles) on CHIKV entry using CHIKV pseudoparticles (CHIKVpp). Chloroquine (filled circles) served as a reference compound for early-stage inhibition. BGM cells were treated with serial dilutions of each compound and then were infected with CHIKVpp. On day 3 p.i., cells were washed and then lysed to determine the luciferase activity. Data presented as percentage relative light units (RLU) of the untreated control, and the values plotted are mean values ± SD from at least three independent experiments. TCID, tissue culture infectious dose; VC, virus control (untreated).

CHVB-resistant variants carry mutations in CHIKV nsP1, nsP2 and nsP3 proteins

To identify the viral target of the CHVB series, a resistance selection procedure (11) was performed using CHVB-032 to generate compound-resistant virus variants. In total, four independent, putative CHVB-resistant virus variants were obtained. CPE reduction assays showed that only resistant virus strain 4 was markedly less susceptible to CHVB compounds, displaying a 19-fold resistance to CHVB-066 (Table 2). Resistant virus 4 was also resistant to other CHVB analogs (Table 3). Whole-genome sequencing of the resistant viruses revealed that all the variants carried an S454G mutation in nsP1 and an M703T mutation in the methyltransferase-like (MTase-like) domain of nsP2 (Table 4). Resistant virus 4 acquired two additional mutations, W456R in nsP1

and L494P in the highly variable domain of nsP3, whereas resistant virus 3 had an additional mutation, H280Q, in the alphavirus unique domain (AUD) of nsP3 (Table 4). Deep sequencing of the original virus stock used for resistance selection revealed that only the nsP3-L494P mutation was preexisting in the virus population with a frequency of 23.5%.

Table 2. Phenotype of putative CHVB-resistant clones

CHIKV strain	CHVB-066	
	EC_{50} (μM)	Fold resistance[a]
Wt	0.55 ± 0.01	1
Resistant virus 1	1.6 ± 0.3	2.9
Resistant virus 2	0.94 ± 0.05	1.7
Resistant virus 3	0.63 ± 0.4	1.1
Resistant virus 4	13 ± 0.4	19

[a] Fold resistance is EC_{50} variant/EC_{50} wt.

Table 3. Phenotype of resistant virus 4 against different CHVB analogs

Compound	EC_{50} (μM)		Fold resistance[a]
	wt	Resistant virus 4	
CHVB-023	1.2	7.5	6.5
CHVB-057	0.86	17.3	20
CHVB-032	2.7	> 100	> 37

[a] Fold resistance is EC_{50} variant/EC_{50} wt.

Table 4. CHVB-resistant variants carry mutations in CHIKV nsP1 to nsP3 genes

Protein	wt	Resistant virus 1	Resistant virus 2	Resistant virus 3	Resistant virus 4	Conserved in CHIKV
nsP1	**S454**	S454G	S454G	S454G	S454G	82%
	W456				W456R	97.9%
nsP2	**M703**	M703T	M703T	M703T	M703T	99.3%
nsP3	**H280**			H280Q		99.8%
	L494				L494P	99.3%

To determine which of the identified mutations contributed to phenotypic resistance against the compound, these mutations were introduced into the CHIKV LS3 cDNA clone using site-directed mutagenesis as described before (11). The

susceptibility of the recombinant CHIKV variants to the antiviral activity of the CHVB compounds was determined in a CPE reduction assay (Fig 4). Despite the presence of S454G and M703T mutations in all resistant clones, the single mutants rCHIKV+S454G and rCHIKV+M703T were not resistant to CHVB-032 or CHVB-066 (Fig. 4).With EC_{50} values of 0.38 µM and 0.31 µM, respectively, these variants were even more sensitive to the antiviral effect of CHVB-066 than wt virus (Table 5). A more sensitive phenotype was also found for CHVB-032. The combination of the S454G and M703T mutations in rCHIKV+S454G+M703T also did not yield a compound-resistant phenotype but rather one with increased susceptibility, as an EC_{50} value of 0.32 µM was determined (Table 5). The other mutations present in resistant virus 4 were then introduced into the CHIKV infectious clone in various combinations. Recombinant rCHIKV+W456R was as

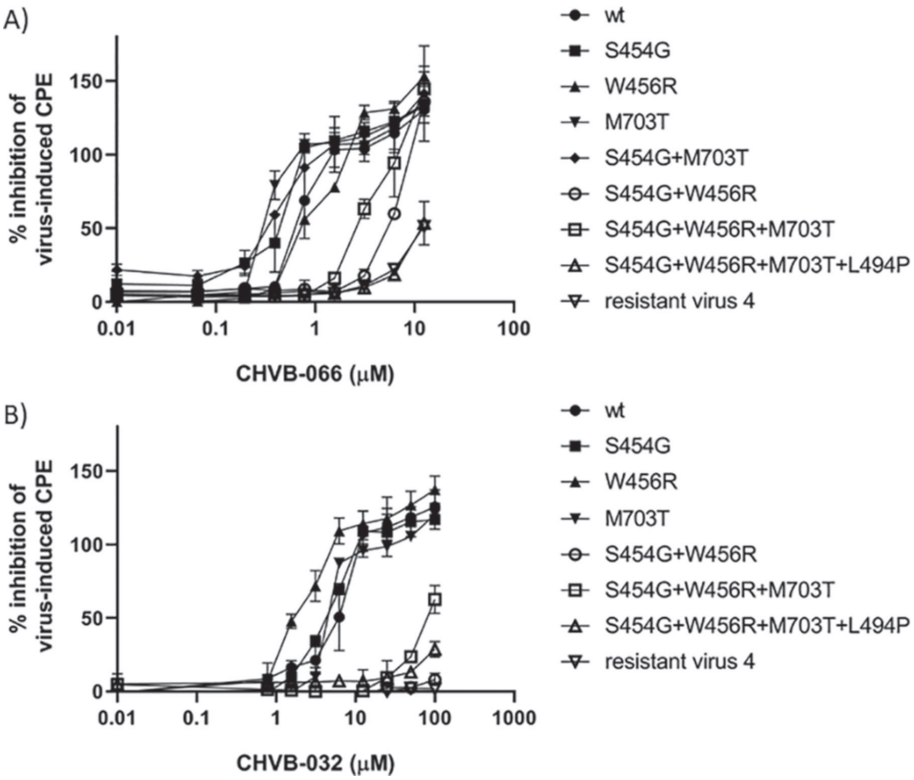

Figure 4. Phenotypic resistance of reverse-engineered CHVB-resistant mutants compared to resistant virus 4 and rCHIKV wt**.** Wild-type (filled circles) and recombinant CHIKV strains with individual or combined mutations that were identified in the CHVB-resistant isolate 4 (open down triangles) were assessed in a CPE reduction assay with increasing doses of CHVB-066 (A) and CHVB-032 (B). VeroE6 cells were treated with 0 to 12.5 µM CHVB-066 or 0 to 100 µM CHVB-032 and infected with rCHIKV LS3 wt or the recombinant CHIKV mutants at an MOI of 0.05. Four days postinfection, the cell viability was determined by the MTS/PMS method. Data represent

the means ± SD from at least two independent experiments performed in quadruplicate (*n*=8). CPE, cytopathic effect; wt, wild-type.

susceptible to CHVB-066 (EC_{50} of 0.76 μM) as wt virus, and it was even more susceptible to CHVB-032 (EC_{50} of 1.76 μM) compared to wt virus. Interestingly, it was specifically the combination of the two nsP1 mutations S454G and W456R that increased the resistance to CHVB-066 8-fold (EC_{50} of 5.4 μM) and to CHVB-032 more than 18-fold (EC_{50} of > 100 μM) (Table 5). The S454G and W456R mutations in nsP1 provided the virus the same level of resistance against CHVB-032 as the originally isolated resistant variant 4, and, thus, were sufficient to result in the CHVB-032-resistant phenotype. Introduction of the nsP2-M703T mutation in the variant with the nsP1-S454G and -W456R mutations (rCHIKV+S454G+W456R+M703T) did not further increase the resistance to both compounds (EC_{50} of 2.6 μM for CHVB-066 and EC_{50} of 81 μM for CHVB-032) (Table 5). This amino acid at position 703 is located in the MTase-like domain of nsP2, suggesting an interaction of this domain with nsP1 during the viral RNA capping. Importantly, the presence of all four mutations that were identified in resistant virus 4 in the reverse-engineered virus resulted in a CHVB-066-resistant phenotype comparable to that of the originally isolated virus 4 (EC_{50} of 12 μM) (Fig. 4). This reverse-engineered virus, rCHIKV+S454G+W456+M703T+L494P, was also

Table 5. Phenotypic resistance of CHVB-resistant mutants compared to those of original resistant virus 4 and rCHIKV wt

	CHVB-066		CHVB-032	
CHIKV strain	**EC_{50} (μM)**	**Fold resistance[a]**	**EC_{50} (μM)**	**Fold resistance**
wt	0.65 ± 0.002	1	5.45 ± 1.64	1
nsP1-S454G	0.38 ± 0.09	< 1	4.10 ± 0.16	< 1
nsP1-W456R	0.76 ± 0.1	1.2	1.76 ± 0.27	< 1
nsP2-M703T	0.31 ± 0.01	< 1	4.53 ± 0.02	< 1
nsP1-S454G + nsP2-M703T	0.32 ± 0.01	< 1	ND[b]	ND
nsP1-S454G + nsP1-W456R	5.4 ± 0.2	8.3	> 100	> 18
nsP1-S454G + nsP1-W456R + nsP2-M703T	2.6 ± 0.3	4.1	81 ± 10	15
nsP1-S454G + nsP1-W456R + nsP2-M703T + nsP3-L494P	12 ± 3.7	18.5	> 100	> 18
Resistant virus 4	13 ± 04	20	> 100	> 18

[a] Fold resistance is EC_{50} variant/EC_{50} wt.
[b] ND, not determined.

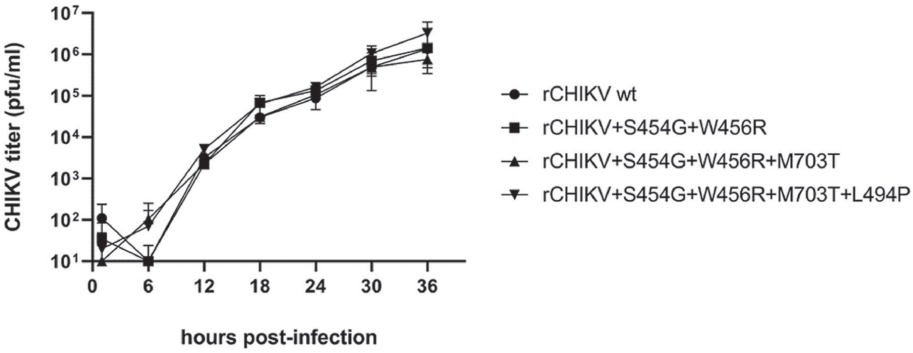

Figure 5. Growth kinetics of CHVB-066-resistant mutants in comparison with rCHIKV wt. VeroE6 cells were infected with CHIKV LS3 wt (filled circles) and the reverse-engineered double (filled squares), triple (filled up triangles) and quadruple (filled down triangles) mutants at an MOI of 0.1 for 1h at 37 °C. Following infection, the cells were washed twice with warm phosphate-buffered saline (PBS) and the medium was replaced with Eagle's minimal essential medium-2% fetal calf serum. At 6-h intervals, samples from the medium were harvested and stored at -80 °C. At 1 h postinfection, a sample was taken to determine how much virus of the inoculum remained after washing. The virus titers in the samples were determined by plaque assay. The experiment represents means ± SD from two independent infections titrated in duplicate (*n*=4). PFU, plaque-forming units; wt, wild-type; rCHIKV, recombinant CHIKV.

fully resistant to CHVB-032 (EC_{50} of > 100 µM). In summary, the S454G and W456R mutations in CHIKV nsP1 are sufficient and required for CHVB-032 resistance and a high level of resistance to CHVB-066. Maximum resistance to CHVB-066 required two additional mutations in nsP2 and nsP3, suggesting CHVB-066 has a higher barrier to resistance than CHVB-032. To exclude that the observed resistance is due to increased replication, the growth kinetics of the three variants with the highest fold resistance values were investigated. All the recombinant variants replicated with kinetics very similar to those of rCHIKV wt. Noticeably, at 6h postinfection, the reverse-engineered viruses with the M703T substitution in nsP2 produced higher titers than the other viruses, but at later time points there were no differences (Fig. 5).

The CHVB-resistant variants are cross-resistant to other CHIKV nsP1 inhibitors

Cross-resistance studies were performed with favipiravir and MADTP-0372. Favipiravir was able to protect cells against CHIKV-induced CPE for all the recombinant viruses tested, with EC_{50} values in the range of 90 to 142 µM, comparable to the wt (Table 6) Interestingly, the CHVB-resistant mutant with two mutations in nsP1 and the CHVB-resistant mutant with four mutations proved fully cross-resistant to MADTP-0372 (EC_{50}

of > 25 µM). Likewise, the MADTP-resistant mutant (carrying the nsP1-P34S mutation) was fully cross-resistant to CHVB-066 (EC_{50} of > 12.5 µM), suggesting that the modes of action of the CHVB and MADTP series are similar (Table 6).

Table 6. Cross-resistance of CHVB-resistant mutants against favipiravir and MADTP-0372

CHIKV strain	Favipiravir		MADTP-0372	
	EC_{50} (µM)	Fold resistance[a]	EC_{50} (µM)	Fold resistance
wt	115 ± 5.4	1	1.2 ± 0.06	1
nsP1-S454G + nsP1-W456R	136 ± 7.5	1.2	> 25	20
nsP1-S454G + nsP1-W456R + nsP2-M703T	90 ± 8.6	< 1	ND	ND
nsP1-S454G + nsP1-W456R + nsP2-M703T + nsP3-L494P	142 ± 25	1.2	> 25	20

[a] Fold resistance is EC_{50} variant/EC_{50} wt.

CHVB compounds inhibit the enzymatic functions of VEEV and SFV nsP1

The alphavirus nsP1 possesses both MTase and GTase activities, which are required for the capping of viral RNA (19). Because CHVB-resistant mutants displayed clear cross-resistance to the MADTP series, we assessed the effect of CHVB-032 and CHVB-066 on the enzymatic activities of purified recombinant nsP1. Since attempts to purify recombinant CHIKV nsP1 from *Escherichia coli* failed to obtain enzymatically active protein, *in vitro* assays with purified nsP1 of VEEV (19) and Semliki Forest virus (SFV) (16) were used. The *in vitro* GTase activity of VEEV nsP1 was quantified by measuring the formation of the m^7GMP-nsP1 complex by Western blotting, using m^7GTP as a substrate and an anti-m^3G/m^7Gp antibody for detection. The MTase activity of VEEV nsP1 was quantified by a filter-based assay using ^{3}H-*S*-adenosylmethionine (SAM). CHVB-066 inhibited the GTase activity of VEEV nsP1 in a concentration-dependent manner with a 50% inhibitory concentration (IC_{50}) of < 0.5 µM, more potently than the known inhibitor sinefungin (Fig. 6A). The MTase activity of VEEV nsP1 was also inhibited, but the effect was less pronounced (IC_{50} of 1.9 µM) (Fig. 6B). Since VEEV belongs to a different serocomplex than CHIKV, we wanted to confirm the inhibition of the m^7GMP-nsP1 complex formation using the nsP1 protein of SFV, which is

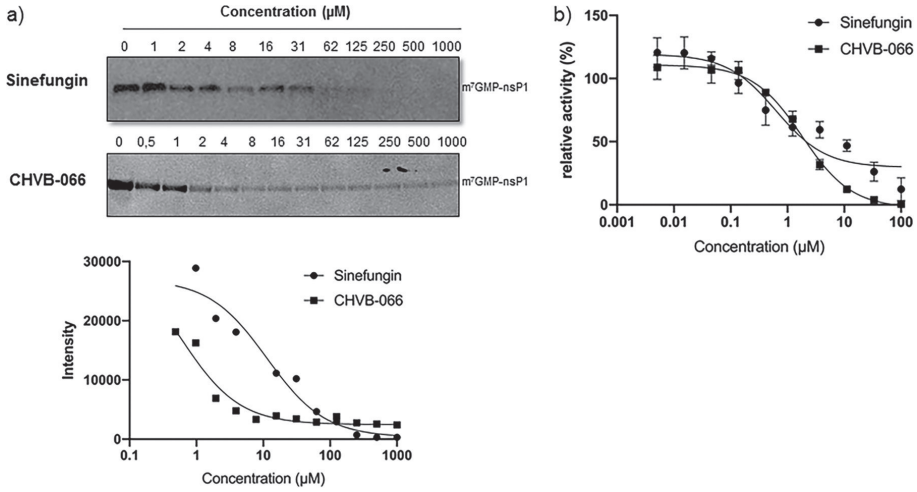

Figure 6. Effect of CHVB-066 on the enzymatic activities of VEEV nsP1. (A) Dose-response effect of CHVB-066 (filled squares) on the *in vitro* guanylylation of VEEV nsP1. Sinefungin (filled circles) was included in the assay as a reference compound. The formation of m^7GMP-nsP1 complex was detected by Western blotting using an anti-methyl^3/^{7}Gp antibody. (B) Dose-response effect of CHVB-066 (filled squares) on the MTase activity of VEEV nsP1. The nsP1-MTase product (^{3}H-methyl) GIDP was measured by a scintillation counter. Data presented are the average values ± SD from two independent experiments.

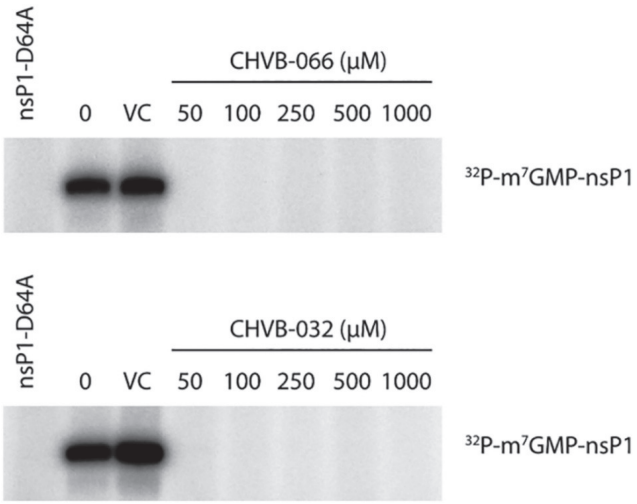

Figure 7. The effect of CHVB-032 and CHVB-066 on the enzymatic activities of SFV nsP1. Purified wt SFV nsP1 was incubated for 30 min at 30°C with increasing doses (50 μM to 1 mM) of CHVB-032 or CHVB-066, the concentration of solvent present at the highest dose of compound, i.e. 5% of dimethyl sulfoxide (DMSO) (VC) or left untreated (0). The D64A mutant was used as a negative control (left lane). The samples were resolved on a 10% SDS-PAGE gel, and the covalent ^{32}P-labelled m^7GMP-nsP1 reaction product was detected by autoradiography after overnight exposure. VC, virus control (untreated).

genetically more closely related to CHIKV (20). The readout of the SFV nsP1 assay is the formation of the covalent ^{32}P-labelled m^{7}GMP-nsP1 complex by using [α^{32}P]GTP and SAM as reaction substrates, thereby measuring the combined activities of the MTase and GTase. An active-site mutant with the D64A substitution was included as a negative control, since this mutant lacks MTase and GTase activity (21). CHVB-066 and CHVB-032 completely inhibited the activity of the wt SFV nsP1 protein at all tested doses (50 µM to 1 mM) (Fig. 7). These data demonstrate that the CHVB compounds directly inhibit the enzymatic activity of nsP1, particularly the MTase activity.

Discussion

Capping of viral mRNA is an essential posttranscriptional modification that influences subsequent downstream processing, translation, nuclear export, and stability of mRNA. Viruses have developed different strategies to cap their genomes and thereby mimic the cap structure of the host cell. Viral RNA caps can be acquired by a cap-snatching mechanism (orthomyxoviruses), or viruses can covalently attach a peptide (picornaviruses) or a cap moiety to their 5' ends (such as alphaviruses) (22, 23). The alphavirus nsP1 and nsP2 proteins contain the MTase, GTase and RNA triphosphatase (RTPase) functions that are needed for the viral RNA capping pathway. This alphavirus capping mechanism is unique and proceeds in a sequence that differs from the capping mechanism in the host cell. First, a GTP molecule is methylated using SAM as a methyl donor and producing SAH as a by-product of the reaction. In the second step, the methylated GTP (m^{7}GTP) is transferred onto nsP1, releasing pyrophosphate and forming the m^{7}GMP-nsP1 covalent intermediate (24). In the third step, the m^{7}GMP is attached to the first nucleotide of the viral RNA, which had been modified by the RTPase activity of nsP2 to remove the γ-phosphate (25). Inhibitors targeting this unique capping pathway may have a limited effect on cellular capping and host MTases (26).

We previously demonstrated, for the first time, that small molecule inhibitors of the alphavirus capping machinery could efficiently and completely inhibit CHIKV replication in cell culture (11). This compound series with a triazolopyrimidinone scaffold, known as the MADTP series, inhibits the GTase activity of VEEV nsP1 in an *in vitro* assay. Recently, 6'-β-fluoro-homoaristeromycin and 6'-fluoro-homoneplanocin A also have been shown to potently inhibit CHIKV replication by targeting nsP1 (16). These compounds affected the MTase activity of SFV nsP1 in enzymatic assays.

Other reports on CHIKV nsP1 as an antiviral target have followed, using target-based screening methods. A nsP1-GTP competition screen resulted in the identification of several small molecules able to compete with GTP for the CHIKV nsP1-GTP binding site (27). In contrast, an enzyme-linked immunosorbent assay to identify inhibitors of CHIKV nsP1 by measuring the formation of the m^7GMP-nsP1 complex did not result in the identification of new inhibitors (28). A similar assay using VEEV nsP1, on the other hand, resulted in the identification of a number of molecules that inhibited the GTase activity (by >80%), and cross-resistance studies indicated that their mechanism differed from that of the MADTP series (26). We now describe a third series of CHIKV nsP1-targeting compounds with yet another chemical scaffold, but the same target as the MADTP series, since CHVB-resistant viruses were cross-resistant to MADTP-0372 and vice versa. The described MADTP-resistant virus carried the P34S mutation in nsP1, whereas the CHVB-resistant viruses described here require at least two mutations, S454G and W456R, in nsP1 to confer resistance. Interestingly, during our initial attempts to produce virus stocks of recombinant CHIKV mutants, we noticed the emergence of the P34S mutation in viruses with the W456R mutation. Because several mutants, in particular the ones containing the W456R mutation, exhibited the tendency to revert back to wt, we started culturing our virus stocks in the presence of compound to retain mutations. Under this selection pressure, the P34S mutation was no longer identified by Sanger sequencing. This might explain why the mutation did not appear during the resistance selection procedure for the CHVB compounds, as these conditions might have favored the presence of the W456R mutation over the P34S mutation. Although a crystal structure of CHIKV nsP1 is currently not available to support our hypothesis, we suggest that the P34 residue in the N-terminal region of the protein might be in close proximity to the W456 in the C-terminal region of the protein.

Similar to the MADTP series, the CHVB series is also CHIKV specific, with no or modest antiviral activity against other alphaviruses in cell-based assays. Because the enzymatically active region of the alphavirus nsP1 is well conserved, it is puzzling that neither series is inactive against other alphaviruses. It was recently shown that the Sindbis virus generates a high amount of noncapped viral genomes, more specifically during the early stage of the replication cycle (29). It is not known whether the same holds true for CHIKV. A possible explanation for the differential susceptibility of alphaviruses to the two series of compounds is that CHIKV is very susceptible to capping inhibitors because it generates more capped viral genomes than other

alphaviruses. The crystal structures of nsP1 proteins of CHIKV and other alphaviruses could provide answers, but such structures have not yet been resolved.

In contrast to the MADTP series, which required only one amino acid substitution at position 34 (P34S) in nsP1 to develop full resistance, resistance to CHVB-032 required the presence of two mutations in nsP1, and full resistance to CHVB-066 even required two additional mutations in nsP2 and nsP3. Moreover, in the second step of the resistance selection protocol, 17% of culture wells showed full CHIKV-induced CPE for the MADTP series (24 wells out of 144) versus only 2.5% (4 wells out of 162) in case of the CHVB series. These data suggest that the barrier to resistance is higher for the CHVB series and that the development of resistance in the clinical settings is less likely to occur, as two mutations are needed. Furthermore, in the reverse-engineered variants mutations causing resistance to CHVB compounds tended to revert back to wt in the absence of selective pressure.

In conclusion, we report on a novel class of small molecule inhibitors of the CHIKV capping machinery. Several other CHIKV inhibitors that target the capping have been reported, indicating that the capping machinery of the virus is an interesting target for antiviral drug development.

Acknowledgments

We thank Caroline Collard, Tom Bellon and Nick Verstraeten for their excellent technical assistance in the acquisition of the antiviral data.

Funding

This work has been supported by the European Union FP7 Program under SILVER grant agreement No. 260644, the Marie Curie ITN “EUVIRNA” grant agreement No. 264286 and the Marie Curie ITN “ANTIVIRALS” grant agreement No. 642434. RA was funded by a PDM postdoc scholarship of KU Leuven. The funding source had no role in the design, implementation, analysis, interpretation, or decision to publish this study.

References

1. Morrison CR, Plante KS, Heise MT. 2016. Chikungunya Virus: Current Perspectives on a Reemerging Virus. Microbiol Spectr 4.
2. Lahariya C, Pradhan SK. 2006. Emergence of chikungunya virus in Indian subcontinent after 32 years: A review. J Vector Borne Dis 43:151-60.
3. Burt FJ, Rolph MS, Rulli NE, Mahalingam S, Heise MT. 2012. Chikungunya: a re-emerging virus. Lancet 379:662-71.
4. Weaver SC, Forrester NL. 2015. Chikungunya: Evolutionary history and recent epidemic spread. Antiviral Res 120:32-9.
5. European Centre for Disease Prevention and Control. 2019, January 25. Communicable Disease Threats Report Week 4, 20-26 January 2019. https://ecdc.europa.eu/sites/portal/files/documents/communicable-disease-threats-report-26-january-2019.pdf. Accessed
6. Gasque P, Couderc T, Lecuit M, Roques P, Ng LF. 2015. Chikungunya virus pathogenesis and immunity. Vector Borne Zoonotic Dis 15:241-9.
7. Gerardin P, Couderc T, Bintner M, Tournebize P, Renouil M, Lemant J, Boisson V, Borgherini G, Staikowsky F, Schramm F, Lecuit M, Michault A. 2016. Chikungunya virus-associated encephalitis: A cohort study on La Reunion Island, 2005-2009. Neurology 86:94-102.
8. Thiberville SD, Moyen N, Dupuis-Maguiraga L, Nougairede A, Gould EA, Roques P, de Lamballerie X. 2013. Chikungunya fever: Epidemiology, clinical syndrome, pathogenesis and therapy. Antiviral Res 99:345-70.
9. Abdelnabi R, Neyts J, Delang L. 2015. Towards antivirals against chikungunya virus. Antiviral Res 121:59-68.
10. Abdelnabi R, Neyts J, Delang L. 2017. Chikungunya virus infections: time to act, time to treat. Curr Opin Virol 24:25-30.
11. Delang L, Li C, Tas A, Querat G, Albulescu IC, De Burghgraeve T, Guerrero NA, Gigante A, Piorkowski G, Decroly E, Jochmans D, Canard B, Snijder EJ, Perez-Perez MJ, van Hemert MJ, Coutard B, Leyssen P, Neyts J. 2016. The viral capping enzyme nsP1: a novel target for the inhibition of chikungunya virus infection. Sci Rep 6:31819.
12. Moesslacher J, Battisti V, Delang L, Neyts J, Abdelnabi R, Pürstinger G, Urban E, Langer T. 2020. Identification of 2-(4-(Phenylsulfonyl)piperazine-1-yl)pyrimidine Analogues as Novel Inhibitors of Chikungunya Virus. ACS Med Chem Lett 11:906-912.
13. Scholte FE, Tas A, Martina BE, Cordioli P, Narayanan K, Makino S, Snijder EJ, van Hemert MJ. 2013. Characterization of synthetic Chikungunya viruses based on the consensus sequence of recent E1-226V isolates. PLoS One 8:e71047.
14. Abdelnabi R, Amrun SN, Ng LF, Leyssen P, Neyts J, Delang L. 2017. Protein kinases C as potential host targets for the inhibition of chikungunya virus replication. Antiviral Res 139:79-87.
15. Delang L, Segura Guerrero N, Tas A, Querat G, Pastorino B, Froeyen M, Dallmeier K, Jochmans D, Herdewijn P, Bello F, Snijder EJ, de Lamballerie X, Martina B, Neyts J, van Hemert MJ, Leyssen P. 2014. Mutations in the chikungunya virus non-structural proteins cause resistance to favipiravir (T-705), a broad-spectrum antiviral. J Antimicrob Chemother 69:2770-84.

16. Kovacikova K, Morren BM, Tas A, Albulescu IC, van Rijswijk R, Jarhad DB, Shin YS, Jang MH, Kim G, Lee HW, Jeong LS, Snijder EJ, van Hemert MJ. 2020. 6'-beta-Fluoro-homoaristeromycin and 6'-fluoro-homoneplanocin A are potent inhibitors of chikungunya virus replication through their direct effect on the viral non-structural protein 1. Antimicrob Agents Chemother in press.
17. Khan M, Santhosh SR, Tiwari M, Lakshmana Rao PV, Parida M. 2010. Assessment of in vitro prophylactic and therapeutic efficacy of chloroquine against Chikungunya virus in vero cells. J Med Virol 82:817-24.
18. Salvador B, Zhou Y, Michault A, Muench MO, Simmons G. 2009. Characterization of Chikungunya pseudotyped viruses: Identification of refractory cell lines and demonstration of cellular tropism differences mediated by mutations in E1 glycoprotein. Virology 393:33-41.
19. Li C, Guillen J, Rabah N, Blanjoie A, Debart F, Vasseur JJ, Canard B, Decroly E, Coutard B. 2015. mRNA Capping by Venezuelan Equine Encephalitis Virus nsP1: Functional Characterization and Implications for Antiviral Research. J Virol 89:8292-303.
20. Powers AM, Brault AC, Shirako Y, Strauss EG, Kang W, Strauss JH, Weaver SC. 2001. Evolutionary relationships and systematics of the alphaviruses. J Virol 75:10118-31.
21. Ahola T, Laakkonen P, Vihinen H, Kaariainen L. 1997. Critical residues of Semliki Forest virus RNA capping enzyme involved in methyltransferase and guanylyltransferase-like activities. J Virol 71:392-7.
22. Decroly E, Ferron F, Lescar J, Canard B. 2011. Conventional and unconventional mechanisms for capping viral mRNA. Nat Rev Microbiol 10:51-65.
23. Strauss JH, Strauss EG. 1994. The alphaviruses: gene expression, replication, and evolution. Microbiol Rev 58:491-562.
24. Ahola T, Kaariainen L. 1995. Reaction in alphavirus mRNA capping: formation of a covalent complex of nonstructural protein nsP1 with 7-methyl-GMP. Proc Natl Acad Sci U S A 92:507-11.
25. Vasiljeva L, Merits A, Auvinen P, Kaariainen L. 2000. Identification of a novel function of the alphavirus capping apparatus. RNA 5'-triphosphatase activity of Nsp2. J Biol Chem 275:17281-7.
26. Ferreira-Ramos AS, Li C, Eydoux C, Contreras JM, Morice C, Querat G, Gigante A, Perez Perez MJ, Jung ML, Canard B, Guillemot JC, Decroly E, Coutard B. 2019. Approved drugs screening against the nsP1 capping enzyme of Venezuelan equine encephalitis virus using an immuno-based assay. Antiviral Res 163:59-69.
27. Feibelman KM, Fuller BP, Li L, LaBarbera DV, Geiss BJ. 2018. Identification of small molecule inhibitors of the Chikungunya virus nsP1 RNA capping enzyme. Antiviral Res 154:124-131.
28. Kaur R, Mudgal R, Narwal M, Tomar S. 2018. Development of an ELISA assay for screening inhibitors against divalent metal ion dependent alphavirus capping enzyme. Virus Res 256:209-218.
29. LaPointe AT, Moreno-Contreras J, Sokoloski KJ. 2018. Increasing the Capping Efficiency of the Sindbis Virus nsP1 Protein Negatively Affects Viral Infection. mBio 9.

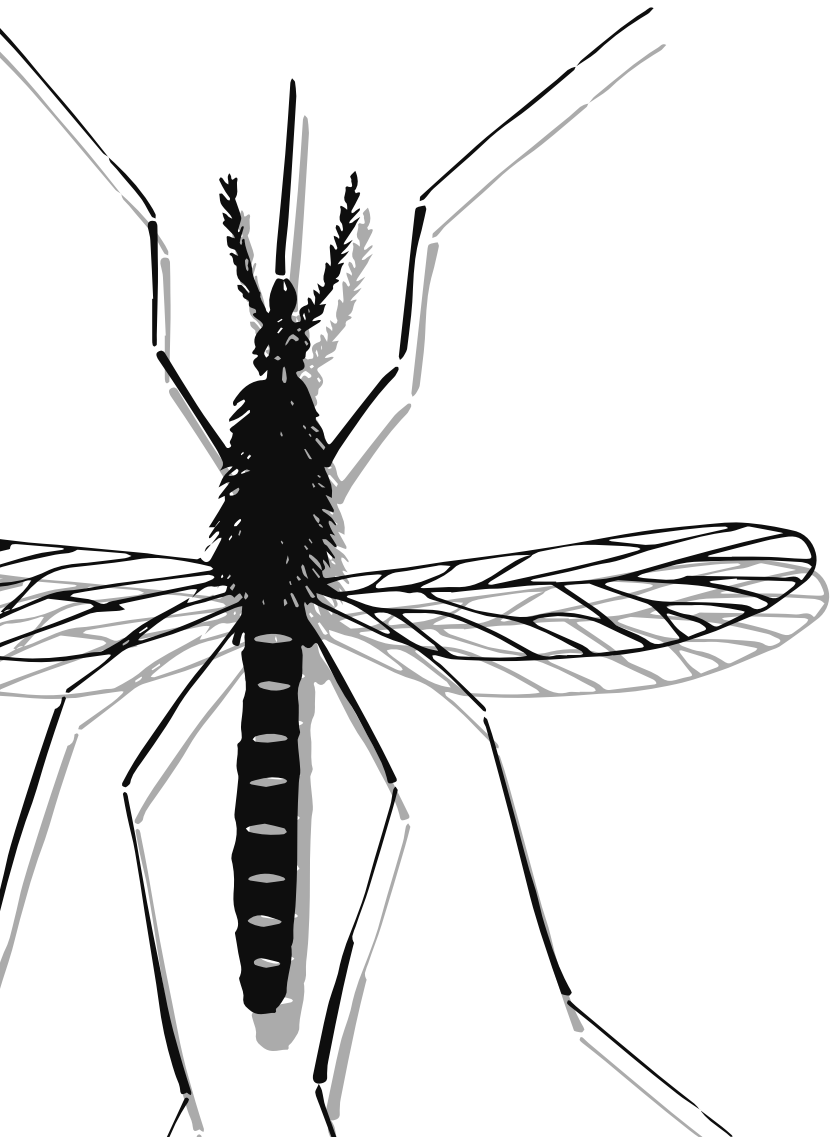

CHAPTER 6

Structural insights into the mechanisms of action of functionally distinct classes of Chikungunya virus nonstructural protein 1 inhibitors

Kristina Kovacikova[a], Marina Gorostiola González[b, c], Rhian Jones[d], Juan Reguera[d], Alba Gigante[e], María-Jesús Pérez-Pérez[e], Gerhard Pürstinger[f], Julia Moesslacher[g], Thierry Langer[h], Lak Shin Jeong[i], Leen Delang[j], Johan Neyts[j], Eric J Snijder[a], Gerard J P van Westen[b] and Martijn J van Hemert[a]

[a] Department of Medical Microbiology, Leiden University Medical Center, Leiden, the Netherlands

[b] Division of Drug Discovery and Safety, Leiden Academic Centre for Drug Research, Leiden University, Leiden, the Netherlands

[c] Oncode Institute, Leiden, the Netherlands

[d] Aix-Marseille Université, INSERM, CNRS, AFMB UMR 7257, Marseille, France

[e] Instituto de Química Médica (IQM-CSIC), Juan de la Cierva 3, E-28006, Madrid, Spain

[f] Department of Pharmaceutical Chemistry, University of Innsbruck, Innsbruck, Austria

[g] Department of Pharmacy, University of Innsbruck, 6020 Innsbruck, Austria

[h] Department of Pharmaceutical Chemistry, University of Vienna, Vienna, Austria

[i] College of Pharmacy, Seoul National University, Seoul, South Korea

[j] KU Leuven, Department of Microbiology, Immunology and Transplantation, Rega Institute for Medical Research, Laboratory of Virology and hemotherapy, Leuven, Belgium

Submitted to AAC

Abstract

Chikungunya virus (CHIKV) nonstructural protein 1 (nsP1) harbours the methyltransferase (MTase) and guanylyltransferase (GTase) activities needed for viral RNA capping and represents a promising antiviral drug target. We compared the antiviral efficacy of nsP1 inhibitors belonging to the MADTP, CHVB and FHNA series [6'-fluoro-homoneplanocin A (FHNA), its 3'-keto form and 6'-β-Fluoro-homoaristeromycin]. Cell-based phenotypic cross-resistance assays revealed that the CHVB and MADTP series shared a similar mode of action that differed from that of the FHNA series. In biochemical assays with purified Semliki Forest virus nsP1, CHVB compounds strongly inhibited MTase and GTase activities, while MADTP-372 and the 3'-keto form of FHNA had only a moderate inhibitory effect. The first of its kind molecular docking studies with the cryo-EM structure of CHIKV nsP1, which is assembled into a dodecameric ring, revealed that the MADTP and CHVB series bind at the SAM-binding site in the capping domain, where they would function as (non) competitive inhibitors. The FHNA series was predicted to bind at the secondary binding pocket in the Ring-Aperture Membrane-Binding and Oligomerization domain, potentially interfering with membrane binding and oligomerization of nsP1. Our cell-based and enzymatic assays, in combination with molecular docking and mapping of compound-resistance mutations to the nsP1 structure allowed us to group nsP1 inhibitors into functionally distinct classes. This study identified druggable pockets in the nsP1 dodecameric structure and provides a basis for rational design, optimization and combination of inhibitors of this unique antiviral drug target.

Introduction

Chikungunya virus (CHIKV) and Semliki Forest virus (SFV) are Old World alphaviruses belonging to the *Togaviridae* family. This group includes mosquito-borne enveloped viruses with single-stranded, positive-sense RNA genomes of approximately 12 kb. CHIKV is an arthritogenic alphavirus transmitted by the *Aedes aegypti* and *Aedes albopictus* mosquitoes. Infections with Old World alphaviruses such as CHIKV typically result in symptoms like fever, rash and polyarthritis/polyarthralgia. In roughly two thirds of the cases, a CHIKV infection progresses into a severe form of persistent debilitating joint paint with long-term sequelae (1). Since its re-emergence in Kenya in 2004, CHIKV has infected millions of people worldwide following its introduction into new territories in Asia, the Caribbean, the Americas and southern Europe (2). Despite recent advances in CHIKV vaccine development (3), prophylactic and/or therapeutic treatment for CHIKV infection is still lacking.

Alphavirus nonstructural proteins (nsPs) are released from a polyprotein precursor by proteolytic cleavage and are indispensable in the alphaviral life cycle (4). The viral replication complex, formed by nsP1-4, assembles in intracellular compartments, termed spherules, which are derived from the host plasma membrane (5, 6). NsP1 is responsible for membrane association of the replication complex (7, 8). In addition, nsP1 catalyses the viral RNA capping, whereby the 5' end of the nascent RNA is modified by attachment of a cap-0 (m^7GpppA) structure. Capping of alphavirus RNA is an essential step in the replication cycle as the cap structure protects viral mRNA from cellular exonucleases, enables its efficient translation and prevents recognition by the host innate immune system. Alphaviruses use a mechanism of mRNA capping that is distinct from that of the host cell. While cellular capping enzymes methylate GTP after it has been transferred to the 5' end of the RNA, alphavirus nsP1 first methylates GTP, after which the methylated GTP (m^7GTP) is covalently attached onto nsP1 and subsequently transferred to RNA (9). In the first step of the alphaviral capping reaction sequence, S-adenosylmethionine (SAM)-dependent N7-methyltransferase (MTase) methylates a GTP molecule while releasing S-adenosylhomocysteine (SAH) as a by-product (10, 11). In the second step, the guanylyltransferase (GTase) activity of nsP1 mediates the attachment of m^7GTP to nsP1 to form the covalent intermediate m^7GMP-nsP1 with release of pyrophosphate (PPi) (12). In the final reaction step, m^7GMP is transferred onto the modified 5' end of the viral mRNAs. Preceding this event, the RNA 5' triphosphatase activity of nsP2

removes the 5'-terminal γ-phosphate from triphosphorylated viral RNAs to yield 5' diphosphate RNAs that can serve as substrate for the m^7GMP transfer from m^7GMP-nsP1, resulting in the formation of a cap-0 structure (13). Early sequence analyses predicted that the N-terminal domain of alphavirus nsP1 [approximately 200 amino acids (aa)] contains a Rossmann fold with conserved sequence motifs, referred to as the 'Core' region, and harbours the MTase activity (14). Later predictions suggested that the putative alphavirus MTase-GTase domain corresponds to the 'Core' region and a C-terminal extension from aa 250 to approximately aa 406, termed the 'Iceberg' region (15). Enzymatic assays with truncated SFV nsP1 indicated that the first 500 aa are required for full enzymatic activity (16). Despite knowledge obtained from mutagenesis studies with recombinant SFV nsP1, the binding sites for the endogenous ligands SAM and GTP are currently not known. A SINV nsP1 mutant resistant to low intracellular GTP levels harbours three mutations in nsP1, namely glutamine-21-lysine (Q21K), serine-23-asparagine (S23N) and valine-302-methionine (V302M) (17), indicating that a potential GTP-binding site might include residues from both the N-terminal and the 'Iceberg' regions of the protein. Furthermore, it is known that specific mutations and deletions within the MTase-GTase domain of alphavirus nsP1 abolish enzymatic activity and yield non-viable viruses (16, 18). For example, the SFV nsP1 aspartic acid-64-alanine (D64A) mutant was unable to bind SAM in a UV cross-linking assay and this mutation interfered with its MTase activity. Furthermore, the SFV nsP1 histidine-38-alanine (H38A) mutation selectively destroyed the GTase activity, presumably by abolishing the covalent attachment of m^7GMP to nsP1 (16). Besides mutational analysis, little progress has been made with regard to understanding and characterizing alphavirus nsP1 functional domains due to the lack of a crystal structure that could provide insight into the spatial organization of various functional residues.

Several CHIKV nsP1 inhibitors have been discovered in recent years (reviewed in (19)), which indicates that alphavirus nsP1 is a promising antiviral drug target. MADTP-372 is a compound belonging to the 3-aryl-[1,2,3]triazolo[4,5-d]pyrimidin-7(6H)-ones or MADTP series (20). Resistance selection and genotyping showed that a proline-34-serine (P34S) substitution in the N-terminal part of CHIKV nsP1 results in resistance to MADTP compounds (21). A threonine-246-alanine (T246A) substitution was also identified as a MADTP resistance mutation (unpublished). 6'-β-Fluoro-homoaristeromycin (FHA) and 6'-fluoro-homoneplanocin A (FHNA) are carbocyclic adenosine analogues with potent anti-CHIKV activity, originally designed as S-adenosylhomocysteine (SAH) hydrolase inhibitors (22). CHIKV mutants carrying

the glycine-230-arginine (G230R) and lysine-299-glutamic acid (K299E) substitutions in nsP1 are resistant to these compounds (22). CHVB-032 and CHVB-066 belong to 2-(4(phenylsulfonyl)piperazine-1-yl)pyrimidine analogues, also known as the CHVB series (23). Selection of resistant variants and reverse genetics studies indicated that (primarily) the combined serine-454-glycine (S454G) and tryptophan-456-arginine (W456R) substitutions in the C-terminal part of CHIKV nsP1 are responsible for CHVB resistance (24). Sinefungin is a SAM analogue that inhibits Venezuelan Equine Encephalitis virus (VEEV) and CHIKV nsP1 in enzymatic assays measuring either MTase or GTase activity (25-27). Besides sinefungin, MADTP-372 and CHVB-066 have also been shown to inhibit the GTase activity of VEEV nsP1 in enzymatic assays (21, 24). We have previously shown that CHVB compounds completely block *in vitro* activity of SFV nsP1 in a covalent m^7GMP-nsP1 complex formation assay (24) and we now report a similar, although less potent, effect for the MADTP series.

Here, we set out to explore the cross-functional relationships between the various CHIKV nsP1 inhibitors (Fig. 1). We aimed to investigate whether these compounds share a similar mechanism of action, by, for example, sharing a binding pocket, and whether this could be linked to a function, e.g. interfering with SAM- or GTP-binding site. To this end, we compared the inhibitors in cell-based cross-resistance assays, enzymatic assays and performed molecular docking on the recently solved CHIKV nsP1 cryo-EM structure (28).

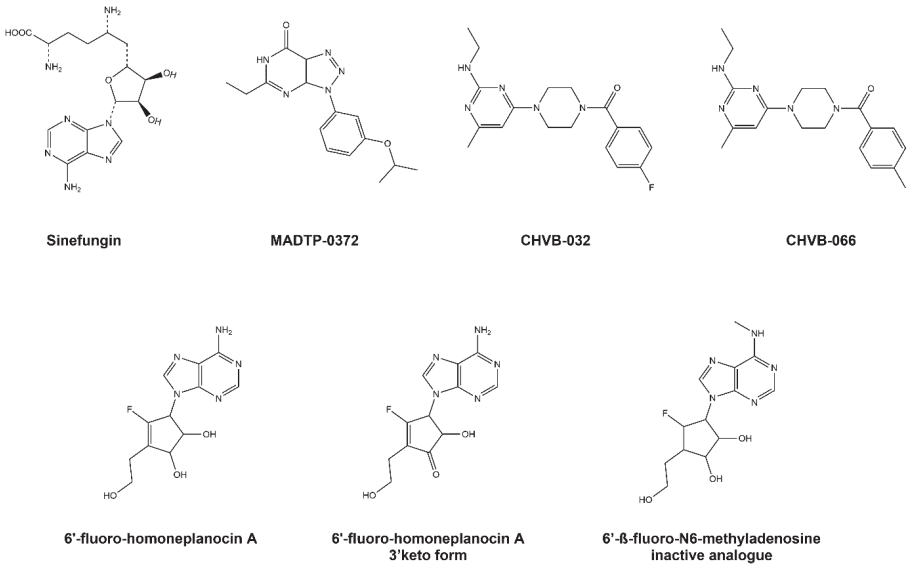

Figure 1: Chemical structures of the CHIKV nsP1-targeting compounds used in this study.

Materials and Methods

Cells and virus strains

VeroE6 cells were grown in Dulbecco's Modified Eagle Medium (DMEM) supplemented with 8% fetal calf serum (FCS) and penicillin/streptomycin. Infection assays were performed in Eagle's Minimum Essential Medium (EMEM) supplemented with 2% FCS, 2 mM L-glutamine and penicillin/streptomycin. CHIKV LS3 (CHIKV, GenBank KC149888) is an infectious clone-derived virus (29). CHIKV nsP1-P34S is a reverse-engineered LS3-derived mutant that is resistant to MADTP compounds (21). CHIKV nsP1-G230R+K299E is a reverse-engineered LS3-derived mutant resistant to FHA and FHNA (22). CHIKV nsP1-S454G+W456R is a reverse-engineered LS3-derived mutant resistant to CHVB-032 and CHVB-066 (24). Semliki Forest virus (SFV) strain SFV4 was used in cytopathic effect (CPE) reduction assays to assess the antiviral spectrum of nsP1 inhibitors.

Compounds

FHA, FHNA and 6'-β-fluoro-N^6-methyladenosine (FMA) were synthesized as described elsewhere (30). The compounds were maintained as 20 mM stock in DMSO at 4°C and used as described before (22). MADTP-372 was synthesized as described elsewhere (20) and 10 mM stock solutions in DMSO were prepared and used as described before (21). Sinefungin (Sanbio) was dissolved to 50 mM in MiliQ. Favipiravir (BOC Sciences) was dissolved to 100 mM in DMSO. CHVB-032 and CHVB-066 were synthesized as described elsewhere (23). CHVB-066 (25.4 mM) and CHVB-032 (29.1 mM) stock solutions in DMSO were prepared and used as described (24). All compounds except FHA, FHNA and FMA were stored at-20°C.

CPE reduction assay

CPE reduction assays were performed as described previously (22). In short, VeroE6 cells were seeded in 96-well clusters at a density of 5 x 10^3 cells/well in DMEM supplemented with 8% FCS. The next day, the cells were incubated with serial dilutions of compounds prepared in EMEM supplemented with 2% FCS and infected with 50 µl/well of CHIKV (MOI 0.005) or SFV (MOI 0.025) or left uninfected. For phenotypic cross-resistance assays, a 10 times higher MOI was used (0.05; 500 PFU/well). The SFV- and CHIKV-infected plates were incubated for 32 h and 96 h, respectively. Cell viability was measured using the MTS/PMS method (Promega, The Netherlands) by

adding 20 µl/well of MTS reagent. The cells were incubated for 2 h followed by fixation with 30 µl/well of 37% formaldehyde. Absorption was measured at 490 nm using an Envision Plate Reader (Perkin Elmer, US). The 50% effective concentration (EC_{50}), defined as the concentration of compound required to inhibit virus-induced cell death by 50%, and the 50% cytotoxic concentration (CC_{50}), defined as the concentration of compound that reduced the cell viability to 50% of that of untreated control cells, were determined using non-linear regression with GraphPad Prism v8.0.

m^7GMP-nsP1 covalent complex formation assay

The covalent m^7GMP-nsP1 complex formation assay was performed as described previously (22). Briefly, the activity of SFV nsP1 was measured in a standard 30 µl reaction containing 25 mM HEPES pH 7.5, 5 mM DTT, 10 mM KCl, 2 mM $MgCl_2$, 100 µM SAM, 0.75 mCi of [α^{32}P] GTP (3000 Ci/mmol) and 0.5 µM wild-type (wt) SFV nsP1 or active site mutant D64A. The reaction was incubated at 30˚C for 30 min and stopped by adding 3 µl of 10% SDS. The reaction mixtures were mixed with 4x Laemmli Sample Buffer (LSB) and then 10 µl samples were separated in a 10% SDS-PAGE gel. The dried gels were placed in a cassette with a PhosphoImager screen. After overnight exposure, the ^{32}P-labelled covalent m^7GMP-nsP1 intermediate products were visualized with a Typhoon Imager (Amersham).

System preparation and CHIKV nsP1 molecular docking

Docking was performed using ICM Pro software, version 3.9-1b (Molsoft LLC, San Diego) (31, 32). The apo CHIKV nsP1 cryo-EM structure representing a dodecameric ring (PDB 6Z0V) was prepared by adding and optimizing the position of hydrogen atoms, as well as the orientation and protonation states of histidine and cysteine residues, and the orientation of glutamine and asparagine residues. ‘Chain A’ in the cryo-EM structure was used as the main nsP1 monomeric structure (referred to as n), and chains n+1 and n-1, flanking chain n, were considered to acknowledge the complexed nature of active nsP1. The binding pockets of endogenous ligands, GTP and SAM, were defined using their corresponding binding pocket residues as proposed by Jones *et al* (28). Both ligands were docked separately using default settings without constraints. Potential small-molecule binding pockets were identified using the ICM Pocket Finder method (33, 34), using chains n and n-1 as a starting point. Two predicted pockets, surrounded by 33 and 18 residues, respectively, were selected based on mutagenesis data. The proposed inhibitors CHVB-066, CHVB-032, MADTP-372, sinefungin, FHNA, 3’-keto

form of FHNA, and FMA were docked into the defined binding pockets with default settings and 10 poses stored for each of them. All ligands were routinely prepared by adding hydrogen atoms and assigning atomic charges. The docking results were analysed in light of the available experimental data, and docking poses were selected accordingly between the top two poses based on docking score and interaction networks.

Results

Cross-resistance analysis of CHIKV nsP1 mutants resistant to different nsP1-targeting compounds

The anti-CHIKV activity of a variety of nsP1-targeting compounds, i.e. CHVB-032, CHVB-066, MADTP-372, FHA, FHNA and sinefungin, was compared in a multi-cycle CPE-reduction assay on VeroE6 cells (Table 1). FHA and CHVB-066 were the most potent compounds with EC_{50} values below 1 µM. FHNA, CHVB-032 and MADTP-372 inhibited CHIKV with EC_{50} in the low micromolar range (1.2 - 3.4 µM). Sinefungin was not a potent inhibitor of CHIKV replication in cell culture, as its EC_{50} was 184.9 µM. None of the compounds was cytotoxic at the effective concentrations. Furthermore, the same compounds were tested against SFV in the same type of multi-cycle infection assay. Interestingly, only FHA and FHNA inhibited SFV replication with EC_{50} values in the low micromolar range (3.9 - 5.2 µM), while the rest of the compounds did not exhibit any antiviral effect against SFV.

Table 1: The antiviral activity of nsP1 inhibitors on CHIKV and SFV replication in CPE reduction assays.

Virus	CHIKV		SFV	
Compound	EC_{50} (µM)[a]	CC_{50} (µM)[b]	EC_{50} (µM)	CC_{50} (µM)
FHA	0.7 ± 0.08	> 250	3.9 ± 3.5	> 250
FHNA	1.2 ± 0.03	> 250	5.2 ± 3.2	> 250
CHVB-066	0.6 ± 0.1	25	NA[c]	25
CHVB-032	3.4 ± 0.3	> 100	NA	> 100
MADTP-372	2.7 ± 0.2	> 100	NA	> 100
sinefungin	184.9 ± 38.4	> 1,000	NA	> 1,000

[a]EC_{50}, concentration of compound that reduces virus-induced CPE by 50%
[b]CC_{50}, concentration of compound that reduces cell viability by 50%
[c]Not active

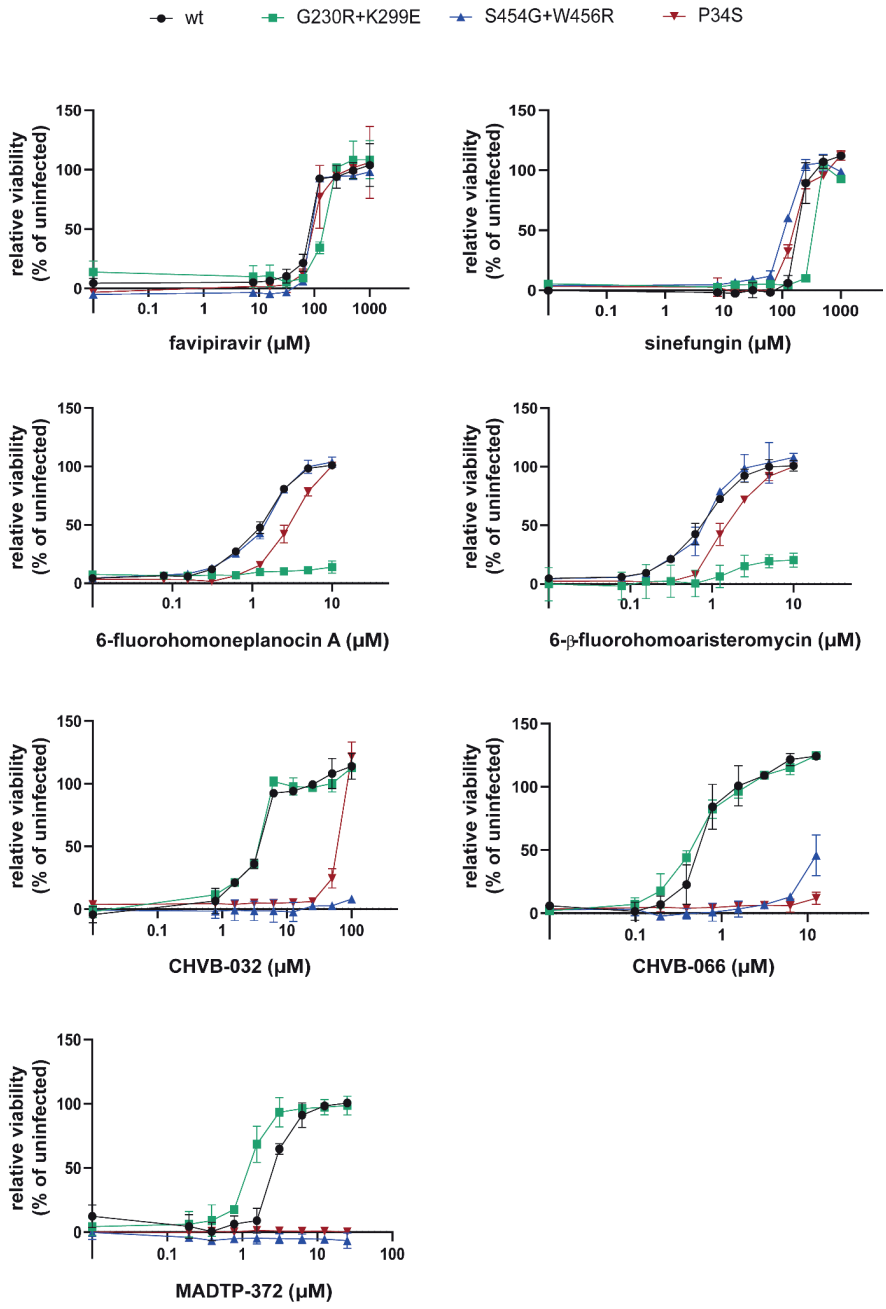

Figure 2: Cross-resistance analysis of compound-resistant CHIKV strains with mutations in nsP1. The sensitivity of wt CHIKV and mutants nsP1-G230R+K299E, nsP1-S454G+W456R and nsP1-P34S towards various nsP1-targeting inhibitors was assessed in CPE reduction assays in VeroE6 cells. The mechanistically unrelated compound favipiravir, which targets nsP4, was included as a control.

Table 2: Resistance and cross-resistance of CHIKV nsP1 compound-resistant mutants nsP1-G230R+K299E, nsP1-S454G+W456R and nsP1-P34S against CHIKV nsP1 inhibitors and against a mechanistically unrelated compound favipiravir.

		rCHIKV P34S		rCHIKV G230R + K299E		rCHIKV S454G + W456R	
Compound	**wt**	**EC_{50} (μM)**	**Fold resistance[a]**	**EC_{50} (μM)**	**Fold resistance**	**EC_{50} (μM)**	**Fold resistance**
FHA	0.7 ± 0.08	1.6 ± 0.2	2.3	> 10	14.3	0.7 ± 0.08	1
FHNA	1.2 ± 0.03	2.8 ± 0.3	2.4	> 10	8.6	1.2 ± 0.1	1
CHVB-066	0.6 ± 0.1	> 12.5	20.8	0.3 ± 0.04	< 1	> 12.5	20.8
CHVB-032	3.4 ± 0.3	52.4 ± 0.8	14.4	3.4 ± 0.2	1	> 100	29.4
MADTP-372	2.7 ± 0.2	> 25	9.3	1.2 ± 0.2	< 1	> 25	9.3
sinefungin	184.9 ± 38.4	150.8 ± 2.5	< 1	274.5 ± 0.2	1.5	109.8 ± 3.9	< 1
favipiravir	79.8 ±1.4	95.9 ± 12.8	1.2	135 ± 5	1.7	89.5 ± 0.2	1.1

[a]Fold resistance = EC_{50} variant/EC_{50} wt

Next, the CHIKV nsP1 mutant carrying the P34S substitution (resistant to MADTP-372) (21), the CHIKV nsP1 mutant carrying the G230R and K299E substitutions (resistant to FHA and FHNA) (22) and, the CHIKV nsP1 mutant carrying the S454G and W456R substitutions (resistant to CHVB-032 and CHVB-066) (24), were tested in cross-resistance phenotypic assays in all possible compound-virus combinations and against the unrelated compound favipiravir (Fig. 2). All resistant mutants were sensitive to favipiravir, a nucleoside analogue that inhibits the CHIKV nsP4 RNA-dependent RNA polymerase (35), and sinefungin, a SAM analogue. CHIKV nsP1-P34S, which was originally selected as a MADTP-resistant virus, was completely resistant to MADTP-372 and to CHVB-066 at the tested concentrations, and it was > 14-fold more resistant to CHVB-032 than wt virus (Fig. 2). Furthermore, CHIKV nsP1-S454G+W456R, originally identified as CHVB-resistant virus, was completely resistant to CHVB-032 and also cross-resistant to MADTP-372 at the tested doses, and to a lesser extent to CHVB-066 (Fig. 2). This suggested that the compounds of the CHVB and MADTP series share a similar mechanism of action. CHIKV nsP1-G230R+K299E was resistant to FHA and FHNA but was sensitive to the CHVB and MADTP series (Fig. 2), suggesting a different mechanism of action that is unrelated to that of the CHVB and MADTP series.

The comparison of fold resistance values, determined as the ratio of the EC_{50} values of the resistant and wt CHIKV, for each resistant mutant-compound combination is included in Table 2.

Inhibition of SFV nsP1 enzymatic activity by nsP1-targeting compounds

We next determined the inhibitory effect of sinefungin, MADTP-372, CHVB-032 and CHVB-066 in an enzymatic assay with purified wt SFV nsP1 that monitors the formation of the covalent m^7GMP-nsP1 complex. This assay measures both MTase and GTase activities and uses the formation of a radioactive ^{32}P-m^7GMP-nsP1 as a readout (22). The active site mutant D64A was used as a negative control as it is devoid of MTase activity (16). CHVB-032 and its analogue CHVB-066 completely blocked the formation of the ^{32}P-m^7GMP-nsP1 covalent complex, as published previously (24). MADTP-372 also inhibited the formation of the ^{32}P-m^7GMP-nsP1 covalent intermediate, but less effectively, as some radioactive signal was still detected even at a 1 mM dose of compound. Sinefungin, on the other hand, was a very inefficient inhibitor, given a slight and steady reduction of signal across the tested concentration range (50 µM to 1 mM) (Fig. 3A). Sinefungin appeared to stimulate GTase activity, as some product was formed in reactions lacking SAM, but containing 50 µM sinefungin (Fig. 3B). This might explain why sinefungin was inactive in a CPE-reduction assay with SFV and exhibited a high EC_{50} value in an assay with CHIKV (Table 1). FHNA (not shown) inhibited the formation of the ^{32}P-m^7GMP-nsP1 covalent intermediate to a lesser extent in a modified assay lacking DTT (22). The 3'-keto form of FHNA, which is suspected to be the active form of the molecule (22), could unfortunately not be tested because we were unable to synthesize this molecule. The combined data from the cell-based cross-resistance analysis and enzymatic assays with purified wt SFV nsP1 suggested that the various compounds can be divided into distinct classes based on their mode of actions. Therefore, we set out to perform molecular docking studies with the individual nsP1 inhibitors and the CHIKV nsP1 cryo-EM structure, in order to understand the structural basis of nsP1 inhibition and to obtain more insights into the potential mechanisms of action of these compounds at the molecular level.

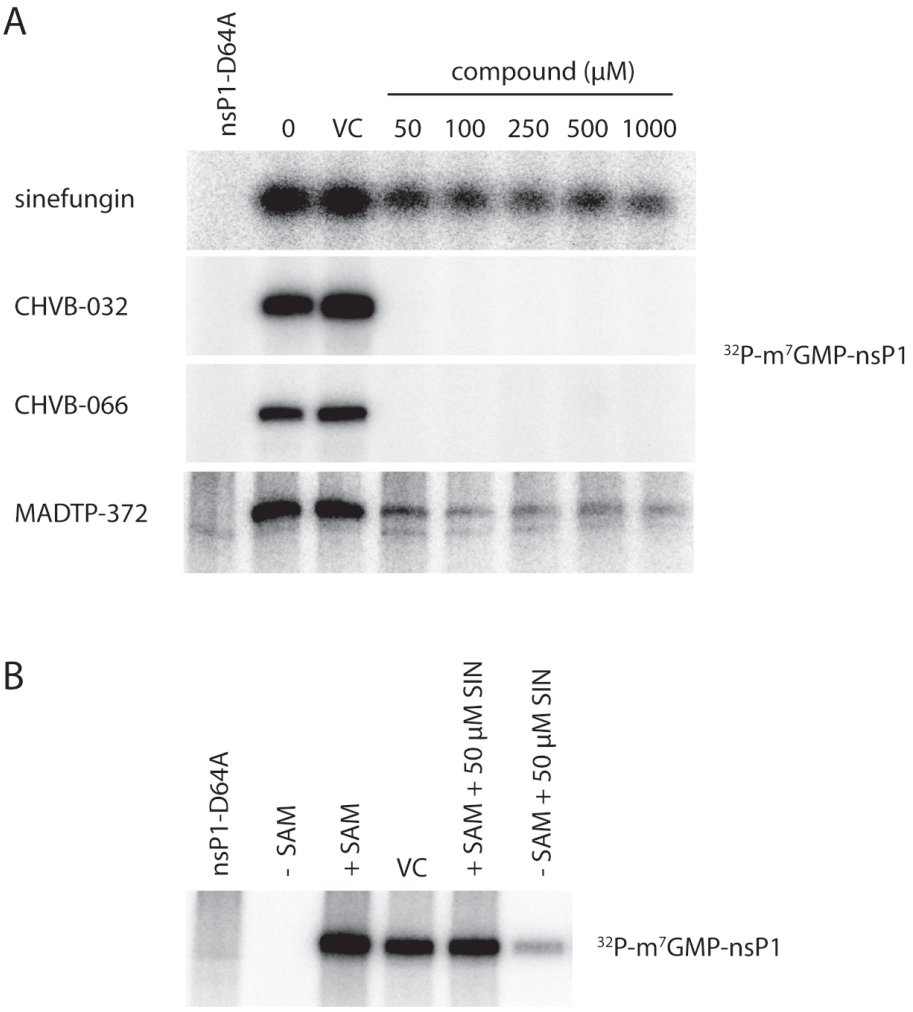

Figure 3: Inhibitory effect of selected compounds on the enzymatic activity of purified wt SFV nsP1 in a biochemical assay that measures the formation of the covalent ^{32}P-m^{7}GMP-nsP1 reaction intermediate. (A) wt SFV nsP1 was incubated with α ^{32}P-GTP and 100 μM SAM and treated with increasing doses (50 μM to 1 mM) of inhibitors. SFV nsP1 D64A was used as a negative control. VC – DMSO-treated control. (B) wt SFV nsP1 was incubated with α ^{32}P-GTP with or without 50 μM sinefungin (SIN) and in the presence or absence of 100 μM SAM. SFV nsP1 D64A was used as a negative control. VC- DMSO-treated control.

Predicted CHIKV nsP1 binding pockets and poses of endogenous ligands

Using the ICM Pocket Finder method (33, 34) and the available CHIKV nsP1 cryo-EM structure representing a dodecameric ring (Fig. 4A and 4B), we identified an elongated ligand binding site, referred to as pocket 1 or the main binding pocket, which is depicted in Fig. 4.

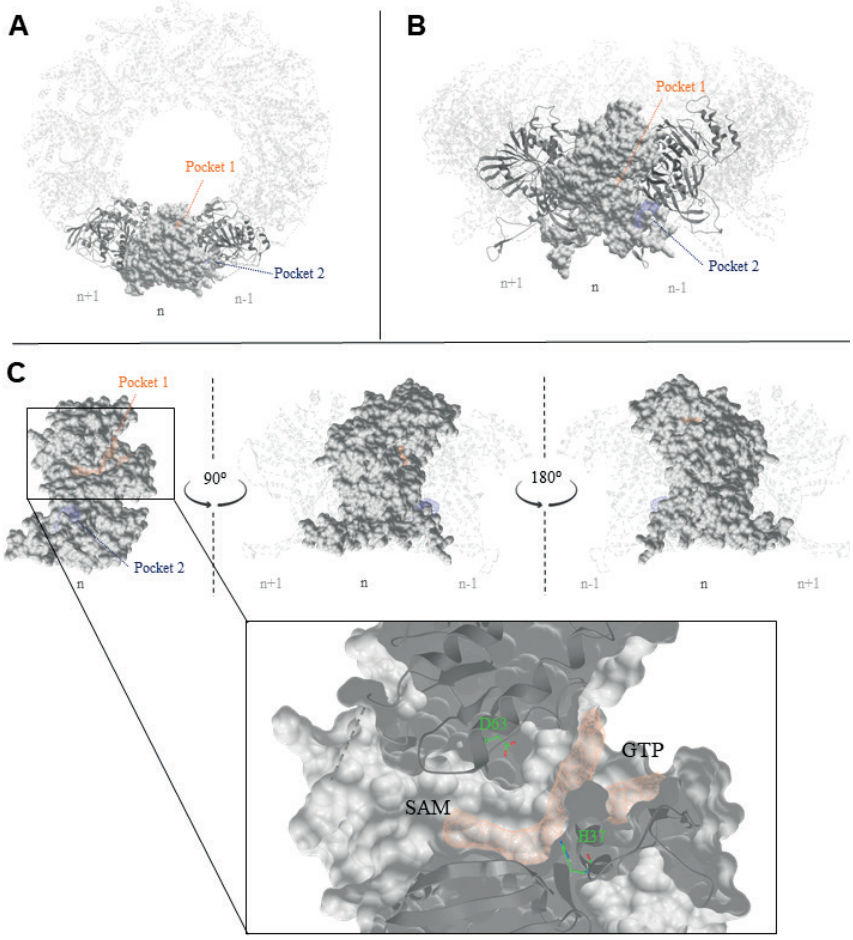

Figure 4: The predicted binding pockets in the CHIKV nsP1 oligomeric structure. (A) Top view of the nsP1 dodecameric ring. Predicted main binding pocket (pocket 1, in orange) and secondary binding pocket (pocket 2, in blue) by the ICM Pocket Finder method. (B) Front view of the nsP1 dodecameric ring. (C) The predicted main binding pocket is elongated and contains two binding sites virtually divided by the catalytic residues H37 and D63, that correspond to the SAM- and GTP-binding sites. Three consecutive nsP1 protomers with subscripts n, n+1 and n-1 were used to define these pockets within the nsP1 complex (PDB 6Z0V).

This pocket is part of the capping domain of nsP1 carrying out the MTase and GTase functions. We further recognized two binding sites in this predicted main binding pocket, which are virtually separated by H37 and D63, and correspond to the GTP- and SAM-binding sites, as defined previously (28). A secondary binding pocket, referred to as pocket 2 in Fig. 4, was identified in the Ring-Aperture Membrane-Binding and Oligomerization (RAMBO) domain of nsP1 involved in membrane binding and oligomerization of nsP1 protomers (28). Based on secondary structure predictions and cross-linking studies with recombinant SFV nsP1 (16), the catalytic site of CHIKV nsP1 is most likely flanked by H37 and D63. The endogenous ligands, GTP and SAM, are expected to bind in the proximity of these residues, as depicted in Fig. 5. However, in the available apo CHIKV nsP1 cryo-EM structure, the D63 residue, which is thought to be the anchor point for SAM (16), is too deeply buried in the protein structure to be accessible to endogenous ligands in docking simulations. Residue H37 is part of the catalytic loop in the active site, defined as a four aa region between residues P34 and H37. We hypothesize that a conformational change takes place during the capping reactions, which increases the solvent exposure of H37 and D63. The proposed GTP-SAM binding mode, depicted in Fig. 5, serves as a reference point in the docking analysis of the various inhibitors in the main binding pocket.

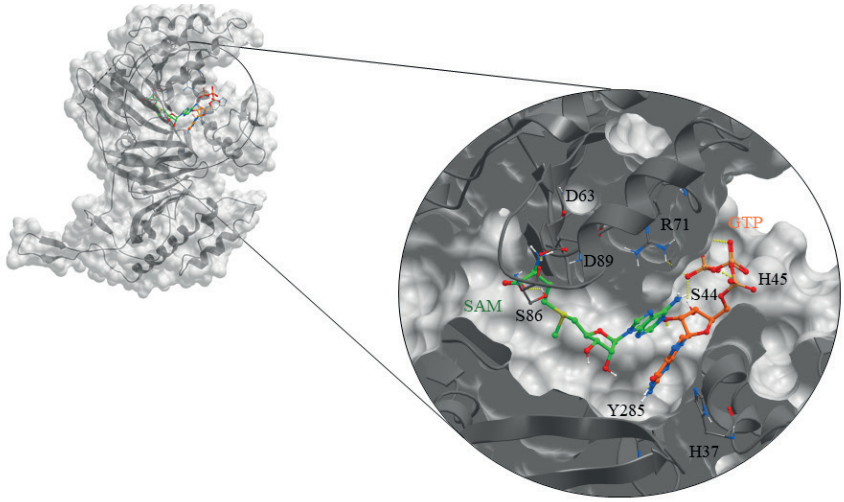

Figure 5: Suggested binding mode of the endogenous ligands, GTP (orange) and SAM (green), in the catalytic pocket of CHIKV nsP1 (grey) generated by molecular docking. Known catalytic residues H37 and D63 are not directly involved in binding, most likely due to the available conformation of the CHIKV nsP1 cryo-EM structure (PDB 6Z0V), where D63 is deeply buried in the protein structure.

Mapping of resistance mutations on the nsP1 structure

Our cross-resistance studies with CHIKV nsP1 mutants revealed a pattern for drug resistance to various CHIKV nsP1-targeting compounds. Namely, the MADTP and CHVB series appear to share a similar mode of action while FHNA and its 3'-keto form (further referred to as the FHNA series) appear to interfere with the CHIKV nsP1 function via a different mechanism. Fig. 6 shows the positions of the aa changes responsible for resistance to these inhibitors on a graphical representation of three consecutive nsP1 protomers as part of nsP1 dodecameric ring (28). The subscripts n+1, n and n-1 refer to the nsP1 protomer to which each aa residue belongs. Residue $P34_n$, the mutation of which causes resistance to the MADTP series, is part of the catalytic loop in the active site and delimits the GTP-binding site. Residues $G230_n$ and $K299_n$, which are mutated in FHNA-resistant virus, are found in different functional regions of nsP1. Residue $G230_n$ is located in the membrane binding and oligomerization (MBO) loop 1 that folds over the n-1 protomer. Residue $K299_n$ lines the entrance to the SAM-binding site of the n+1 protomer. Residues $G230_n$ and $K299_{n-1}$ flank a smaller predicted binding pocket (pocket 2 in Fig. 4) that could explain the mode of action of the FHNA

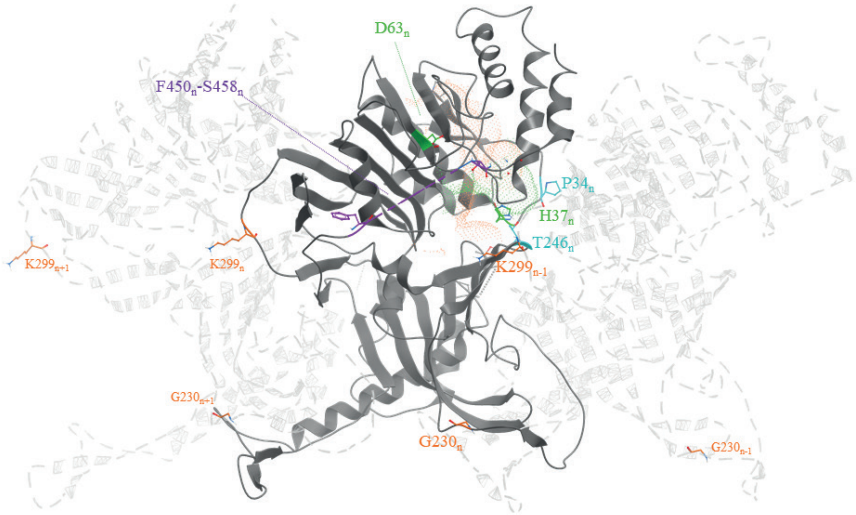

Figure 6: Key amino acid residues linked to drug resistance to CHIKV nsP1 inhibitors mapped to the CHIKV nsP1 cryo-EM structure (PDB 6Z0V) represented as three consecutive nsP1 protomers n, n+1 and n-1. In green, the catalytic residues H37 and D63. In blue, residues P34 and T246, involved in drug resistance to the MADTP series. In orange, residues G230 and K299, conferring drug resistance to the FHNA series. In purple, residues F450 to S458 flank the area where residues S454 and W456, involved in drug resistance to the CHVB series, would be located. Orange and green dotted volumes represent the proposed binding pockets of GTP and SAM, respectively, for reference.

series and the mechanism of drug resistance. Unfortunately, the CHIKV nsP1 cryo-EM structure includes a density gap between residues 450-458 and, therefore, the position of residues S454 and W456, which are mutated in the CHVB-resistant virus, could not be mapped. Presumably, both $S454_n$ and $W456_n$ are located in the proximity of the entrance to the SAM-binding site, based on the position of aa flanking this region.

Predicted binding mode of CHIKV nsP1-targeting compounds

Docking studies with the CHIKV nsP1 cryo-EM structure predicted that compounds of the CHVB and MADTP series bind at the SAM-binding site of `the main binding pocket (Fig. 7A and 7B). In this model, hydrogen bonds with the backbone of Y154 and A155 seem crucial for ligand binding of both series of compounds. Compounds of the CHVB series (CHVB-032 and CHVB-066) are predicted to bind more strongly compared to MADTP-372 (i.e. with lower docking scores) (Table 3). In mutagenesis experiments, it was observed that the mutations P34S and, to a lesser extent, T246A are involved in drug resistance to MADTP-372. Both residues form part of the catalytic site of nsP1 while only P34 is located in the catalytic loop (Fig. 6). Considering the predicted binding poses of MADTP-372 and CHVB compounds, they are unlikely to make direct interactions with P34 or T246, since the distance to these residues is too large. However, residues P34 and, to a lesser extent, T246 appear to be crucial for maintaining the conformation of the catalytic loop in the active site, and their mutations are likely to affect the activity of any small molecule binding at the main binding pocket. The S454G and W456R substitutions, which confer drug resistance to the compounds of the CHVB series, could not be directly mapped in the available cryo-EM structure, but they are likely positioned at the entrance of the SAM-binding site (Fig. 6). Mutations in this region of nsP1 could arise due to a compensatory effect increasing SAM binding or SAM access to the SAM-binding site. Consequently, compensatory mutations would counteract the inhibition by CHVB compounds. The SAM analogue sinefungin was also docked at the predicted main binding pocket, but its pose is not considered here, since it was expected to bind in a similar way as SAM. Based on the docking results presented in Table 3, it could be that sinefungin preferentially drifts to the GTP-binding site because it is more solvent-exposed compared to the SAM-binding site in the current CHIKV nsP1 conformation. The docking results for the FHNA series support the hypothesis that they target a different region and function of nsP1, as

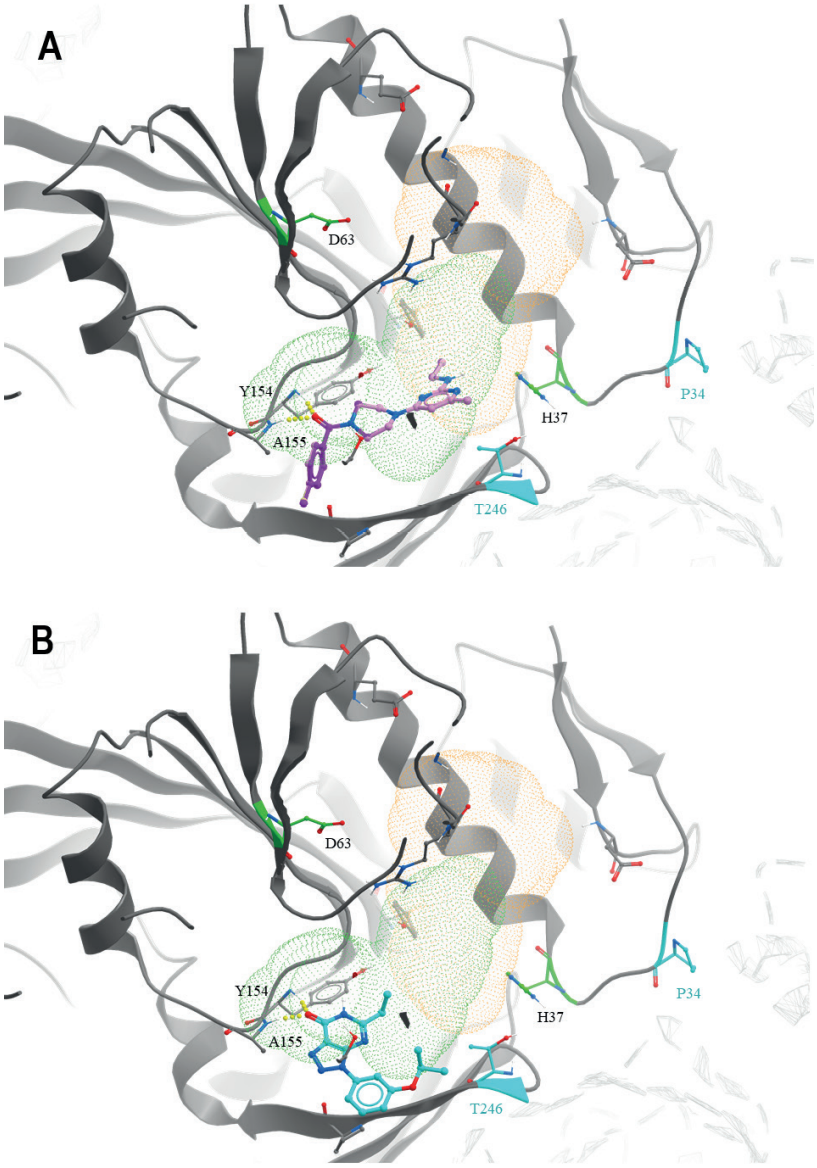

Figure 7: Predicted binding mode of the CHVB and MADTP series in the CHIKV nsP1 SAM-binding site of the main binding pocket (PDB 6Z0V). (A) CHVB-066 (purple) and CHVB-032 (pink) in complex with CHIKV nsP1, occupying the SAM-binding site (green dots). Both CHVB compounds form hydrogen bonds with Y154 and A155 (in yellow) and share a common binding mode. The strength of hydrogen bonds is represented by the diameter of the sphere. (B) MADTP-372 (blue) in complex with CHIKV nsP1, occupying the SAM-binding site (green dots). This compound forms hydrogen bonds with Y154 and A155 (in yellow). P34 (in blue) is the main residue responsible for MADTP compound resistance. T246 (in blue) is an additional residue that upon mutation causes some level of resistance to MADTP.

Table 3: Docking results for selected poses from the ICM small molecule docking method in the main binding pocket (pocket 1) for the endogenous ligands, GTP and SAM, and inhibitors belonging to the CHVB, MADTP, and FHNA series.

Compound	Pocket [a]	Pose	Score [b]	Hbond [c]	Hphob [c]	VwInt [c]
GTP	GTP	1	-33.68	-19.15	-3.27	-31.4
SAM	SAM	1	-2.65	-7.75	-5.30	-21.55
Sinefungin	1 (GTP)	1	-17.35	-11.13	-4.862	-22.55
CHVB-066	1 (SAM)	1	-21.76	-5.051	-7.936	-22.71
CHVB-032	1 (SAM)	1	-21.29	-5.124	-7.414	-21.72
MADTP-372	1 (SAM)	1	-17.54	-5.711	-6.509	-22.21
FHNA	1 (GTP)	2	-14.15	-6.059	-4.099	-21.66
3'-keto form of FHNA	1 (GTP)	1	-13.88	-7.497	-3.73	-18.34
FMA	1 (GTP)	1	-14.97	-6.949	-4.094	-21.27

[a] SAM and GTP in brackets refer to the SAM- and GTP-binding sites, respectively, within the main binding pocket (pocket 1).
[b] Not comparable between different binding pockets.
[c] Hbond, Hphob and VwInt, contribution of the hydrogen bond, hydrophobic, and van der Waals interaction networks to the docking score.

Table 4: Docking results for selected poses from the ICM small molecule docking method in the secondary binding pocket (pocket 2) for inhibitors belonging to the CHVB, MADTP, and FHNA series.

Compound	Pocket	Pose	Score [a]	Hbond [b]	Hphob [b]	VwInt [b]
Sinefungin	2	1	-8.302	-10.93	-4.45	-23.17
CHVB-066	2	1	-6.819	-0.685	-6.887	-24.27
CHVB-032	2	1	-16.51	-3.084	-5.966	-24.1
MADTP-372	2	1	-9.269	-2.374	-4.28	-22.88
FHNA	2	1	-10.26	-4.138	-3.471	-19.22
3'-keto form of FHNA	2	2	-11.25	-8.237	-3.701	-21.76
FMA	2	1	-10.36	-5.363	-3.548	-15.02

[a] Not comparable between different binding pockets.
[b] Hbond, Hphob and VwInt, contribution of the hydrogen bond, hydrophobic, and van der Waals interaction networks to the docking score.

they preferably bind to pocket 2 in the RAMBO domain of nsP1 (Fig. 8A). In pocket 2, the compounds of the FHNA series would form hydrogen bonds with residues close to residue G230, which is involved in drug resistance to this series (Fig. 8B). The inactive analogue FMA could also be docked in pocket 2, but it portrayed a different binding mode, providing a structural basis for the differences in antiviral activity between FHNA and the inactive analogue. In general, the CHVB and MADTP

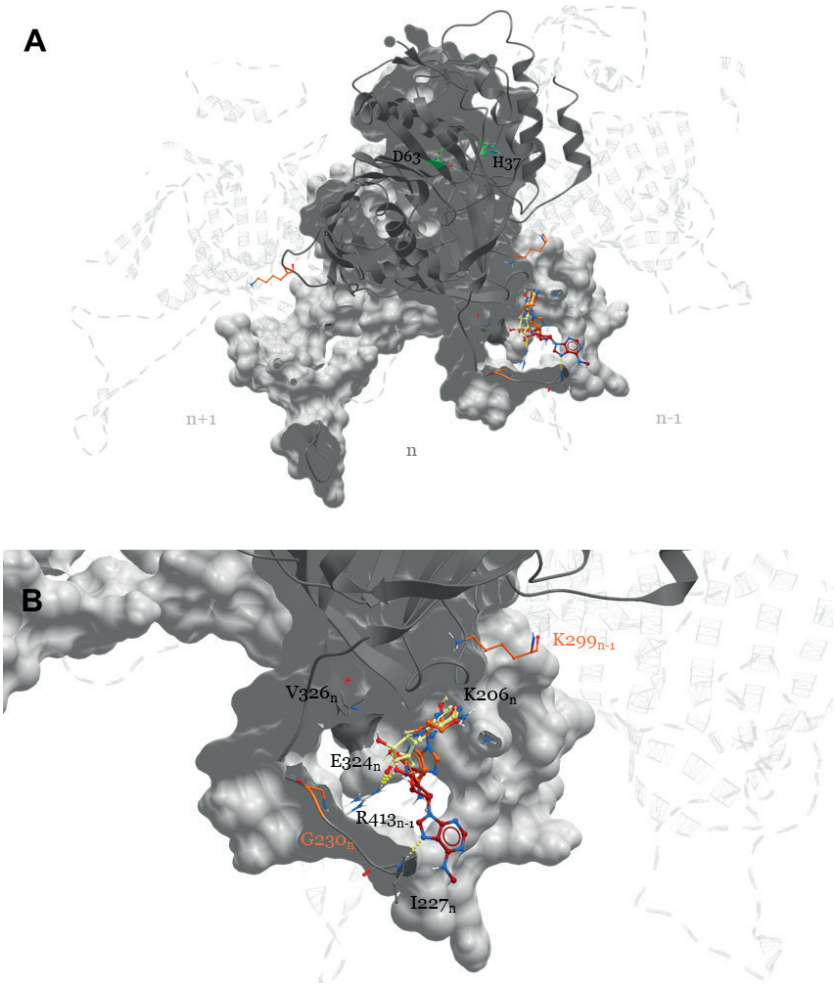

Figure 8: Binding mode of the FHNA series in the CHIKV nsP1 secondary binding pocket. (A) The FHNA series is suggested to bind to a secondary binding pocket (pocket 2) in the RAMBO domain of CHIKV nsP1 (PDB 6Z0V) outside of the main binding pocket. (B) The defined binding pocket is flanked by residues $G230_n$ and $K299_{n-1}$. FHNA and FHA share a similar binding mode that is not shared by the inactive analogue FMA.

series bind with lower affinity to pocket 2 (Table 4), with the exception of CHVB-032, which seems to be stabilized both by hydrogen bonds and hydrophobic interactions in this pocket. The difference between the docking scores of CHVB-066 and CHVB-032 could explain the higher potency of CHVB-066 in anti-CHIKV assays (Table 1), whereby CHVB-032 could be more easily sequestered in pocket 2 compared to its analogue CHVB-066.

Discussion

In this study we have explored the cross-functional relationships of a variety of chemically distinct CHIKV nsP1 inhibitors (Fig. 1). Here, we present a model that could explain the antiviral mechanisms of the inhibitors belonging to the MADTP, CHVB and FHNA series. Cell-based phenotypic cross-resistance assays revealed that the CHVB and MADTP series shared a similar mode of action that differs from that of the FHNA series. Interestingly, all of the CHIKV nsP1 mutants that were resistant to the different nsP1-targeting compounds were sensitive to sinefungin (Fig. 2). In enzymatic assays with wt SFV nsP1, CHVB-032 and CHVB-066 completely blocked the formation of the ^{32}P-m^{7}GMP-nsP1 covalent complex while MADTP-372 also inhibited enzymatic activity, although less potently (Fig. 3A). Sinefungin only weakly inhibited the enzymatic activity and, curiously, its addition to the assay in the absence of SAM led to the formation of a radioactive product, presumably the ^{32}P-m^{7}GMP-nsP1 covalent complex (Fig. 3A and 3B). Both the cell-based and enzymatic assays indicated that these CHIKV nsP1 inhibitors target different functions of the protein. To elucidate the mechanism of action of these compounds in more detail, we performed a molecular docking study with the recently solved CHIKV nsP1 cryo-EM structure. Importantly, the molecular docking experiments described here were performed on an enzymatically active form of CHIKV nsP1. Recently, Jones *et. al.* described that CHIKV nsP1 is active when assembled as oligomers into a ring-shaped membrane-associated complex (28). Using this structure, we identified two binding pockets within a single nsP1 protomer: the main binding pocket (pocket 1) in the capping domain, and the secondary binding pocket (pocket 2) in the RAMBO domain (Fig. 4). The main binding pocket, which forms the catalytic site of CHIKV nsP1, is further divided into two binding sites occupied by the endogenous ligands SAM and GTP (Fig. 5). The mutations responsible for drug resistance to the MADTP, CHVB and FHNA series mapped to different functional regions of CHIKV nsP1 (Fig. 6), supporting our observations from the cell-based and enzymatic assays. The molecular docking experiments predicted that the MADTP and CHVB series bind at the SAM-binding site in the main binding pocket (Fig. 7A and 7B). Here, the MADTP and CHVB compounds would likely exert their inhibitory effect by competing with SAM. The differences in potency of these compounds are supported by differences in docking scores. In contrast, the compounds of the FHNA series most probably bind to a different region of nsP1, seemingly not directly disrupting the catalytic activity (Fig. 8). Instead, the FHNA series appears to interfere with membrane

binding and oligomerization of nsP1 by binding to pocket 2 in the RAMBO domain, and thus indirectly affecting the nsP1 enzymatic function. Lastly, sinefungin does not seem to bind in a similar way to the inhibitors of the MADTP, CHVB and FHNA series. Despite the fact that sinefungin structurally resembles SAM, it preferentially docked at the GTP-binding site (Table 3). However, the docking results for sinefungin need to be interpreted with caution because the SAM's binding pose in itself is not very reliable in the current CHIKV nsP1 conformation. As mentioned in the Materials and Methods, SAM and sinefungin were docked differently (i.e. using different docking grids or reference residues). In addition, more experimental data would need to be obtained to explain why sinefungin stimulates GTase activity and does not serve as a competitive SAM inhibitor. In summary, we identified several classes of CHIKV nsP1 inhibitors with unique modes of action by our cell-based and biochemical assays as well as molecular docking studies.

Furthermore, the molecular docking experiments revealed interesting observations regarding the structural impact of the mutated residues in the MADTP-, CHVB- and FHNA-resistant viruses. The residues conferring resistance to the MADTP and CHVB series were found to gate the SAM-binding site in the main binding pocket (Fig. 6). Specifically, the residues that are mutated in the MADTP-resistant viruses (substitutions P34S and T246A) were located in close proximity to the catalytic residue H37. The residues that are mutated in the CHVB-resistant viruses (substitutions S454G and W456R) were predicted to be located in the proximity to the SAM-binding site despite a density gap in the CHIKV nsP1 structure, which precluded precise mapping of these residues (Fig. 6). Given the predicted position of these aa, both MADTP and CHVB compounds are unlikely to directly interact with these residues in the active site. The observed drug resistance could be achieved by compensatory mutations that destabilize the active site, e.g. the MADTP resistance mutation P34S could affect the position of the catalytic loop in the active site, including the position of the catalytic residue H37. The ensuing conformational change of the active site could thus negatively influence the binding mode of the MADTP series. The same negative effect would be expected to occur by mutating other residues in the catalytic loop, for example, by altering the charge of residue D36. The CHVB resistance mutations also appear to be compensatory as they are predicted to be located further away from the SAM-binding site. These mutations could facilitate SAM binding or increase SAM access to the SAM-binding site. On the contrary, residues $G230_{n}$ and $K299_{n-1}$, which are mutated in the FHNA-resistant virus, flank pocket 2 in the RAMBO domain (Fig. 6).

Residue G230 is located in the MBO loop 1 involved in the formation of membrane-binding spikes, facilitating membrane binding and assembly of oligomeric nsP1. More specifically, residue $G230_n$ promotes interactions with the RAMBO MBO loop 2 of the n-1 protomer. Residue $K299_n$ gates the entry to the SAM-binding site of the n+1 protomer. Interestingly, the V326M substitution, which together with G230R, was previously implicated in resistance to difluoromethylornithine (36), also mapped to pocket 2, suggesting that compounds linked to inhibition of methionine metabolism localize to a discrete binding site within the nsP1 structure (Fig. 8). Furthermore, nsP1 oligomerization allosterically activates the enzyme, therefore, mutations that disrupt this process are expected to lead to a loss of nsP1 enzymatic activity (28). Our enzymatic assays with wt SFV nsP1 revealed that the 3'-keto form of FHNA only partially inhibited the formation of the ^{32}P-m^{7}GMP-nsP1 covalent intermediate (22). The rather negligible inhibitory effect of the 3'-keto form of FHNA in the covalent complex formation assay in comparison with compounds belonging to the MADTP and CHVB series could be explained by its allosteric effect on the nsP1 enzymatic activity, affecting oligomerization of nsP1. Last but not least, FMA, which was inactive in CHIKV CPE-reduction assays, showed a different binding mode compared to active FHNA, which differ by the N-methylation at the N6 position of the purine ring and the double bond on the cyclohexyl ring.

The major limitation of this study and the current model is that the available CHIKV nsP1 cryo-EM structure has no ligands in the active site. In addition, the findings by Jones *et al.* suggest a complex mechanism of nsP1 oligomerization and activation (28), which would be very difficult to capture with the techniques used in this study, potentially leading to discrepancies between the modelled and experimental data. Importantly, the molecular docking experiments presented in this study were performed on the dodecameric form of CHIKV nsP1, which could lead to a potential bias when docking compounds on the monomeric nsP1. For example, MADTP-372 preferentially binds at the GTP-binding site when docked to the monomeric nsP1 as opposed to the oligomeric nsP1. Here, we reported on molecular docking of CHIKV nsP1 inhibitors considering the whole CHIKV nsP1 complex, as we aimed to approximate our results to the active form of CHIKV nsP1 likely found in CHIKV-infected cells, as suggested by Flock House virus tomographic reconstructions of infected cells (28). Furthermore, the resistance mutations described in this study were not located in the compound docking sites in the apo nsP1 structure. Their position might further change upon conformational reorganization of nsP1, which is predicted

to occur after m^7GTP relocates in the proximity of the catalytic residue H37 in the main binding pocket to form the covalent intermediate m^7GMP-nsP1 (28). Previous studies using recombinant SFV or VEEV nsP1 mutants expressed in *E. coli* defined residues important for the catalytic activity of alphavirus nsP1. For example, SFV nsP1 mutants carrying aa substitutions of conserved residues are either completely inactive in assays measuring both MTase and GTase activity (D64A, D90A and C142A) or had a very low level of activity (C135A and Y249A) (16), suggesting an important role of these residues in RNA capping. Using a similar assay, mutational studies with VEEV nsP1 showed that the mutant D63A was devoid of MTase activity while the mutant H37A had abrogated GTase activity (37). All of these residues are positioned at or near the active site in the current CHIKV nsP1 model. Residues H37 and Y248 line the GTP-binding site while residue D89 is exclusively involved in SAM binding. Residues C134 and C141 are found in the Zn binding site below the active site (28). Residue Q19 in VEEV nsP1 was identified as a key residue for the MTase activity, and it was shown that a Q19K mutation modulates SAM and GTP binding (38). This residue was shown to be important for the enzymatic activity of nsP1 and would be expected to lie in the proximity of the active site. Nevertheless, the recent findings by Jones *et al.* describing the process of CHIKV nsP1 oligomerization into structurally novel capping rings challenge the biochemical data from these assays (28). Confirmatory experiments with oligomeric wt and mutant CHIKV nsP1 would need to be performed to validate the results obtained with other forms of alphavirus nsP1. It still remains very puzzling why compounds docking at the active site of CHIKV nsP1, including the MADTP and CHVB series and sinefungin, are not active against a related alphavirus SFV (Table 1). Previously, it was shown that FHA and FHNA, which were active against both CHIKV and SFV, were inactive against SINV (22), and the MADTP and CHVB series were also found to be inactive against other alphaviruses (21, 24). The current opinion in the field holds that the ring-shaped membrane-associated nsP1 complex is conserved among alphaviruses. Besides its enzymatic functions important for RNA capping, the nsP1 complex plays a key role in anchoring the replication complex (nsP1-4) to membranes (4). The nsP1 capping ring appears to interacts with nsP4 on both inner and outer sides of the pore (28).

Taken altogether, this study predicts the mode of action of several CHIKV nsP1 inhibitors. We would like to emphasize that our conclusions are drawn based on a combined interpretation of docking poses and mutagenesis data. Nevertheless, other docking possibilities may exist, especially if different conformations of CHIKV

nsP1 (i.e. other atomic structures in complex with either endogenous or targeted ligands, or monomeric nsP1) would be considered. Our combined data suggest that compounds belonging to the MADTP and CHVB series likely interfere with CHIKV nsP1 functions directly via (non)competitive inhibition of SAM binding. FHNA and its 3'-keto form seem to bind outside of the catalytic site occupied by SAM and GTP and likely have an indirect effect on nsP1 function, possibly by disrupting nsP1 oligomerisation and membrane binding and/or through an allosteric effect on the catalytic site. Since nsP1 oligomerization stabilizes the capping domain, inhibiting this process would compromise the ability of CHIKV nsP1 to perform RNA capping. Our study demonstrates that CHIKV nsP1 is an interesting and relevant antiviral drug target that could be efficiently inhibited by compounds with different mechanisms of action. This would allow development of combination therapy directed at this unique viral activity by combining functionally distinct nsP1 inhibitors and thus lowering the risk of emergence of antiviral drug resistance.

Acknowledgements

K.K. was supported by the Marie Sklodowska-Curie ETN European Training Network "ANTIVIRALS" (EU grant agreement 642434). M.G.G. was supported by funding from the Oncode Institute, the Netherlands. R. J. and J.R. were supported by the ATIP-Avenir program and the Bettencourt Shueller Foundation. M.-J.P.-P. acknowledges the financial support of AEI (PID2019-105117RR-C22).

References

1. Suhrbier A. 2019. Rheumatic manifestations of chikungunya: emerging concepts and interventions. Nat Rev Rheumatol doi:10.1038/s41584-019-0276-9.
2. Burt FJ, Chen W, Miner JJ, Lenschow DJ, Merits A, Schnettler E, Kohl A, Rudd PA, Taylor A, Herrero LJ, Zaid A, Ng LFP, Mahalingam S. 2017. Chikungunya virus: an update on the biology and pathogenesis of this emerging pathogen. Lancet Infect Dis 17:e107-e117.
3. Schrauf S, Tschismarov R, Tauber E, Ramsauer K. 2020. Current Efforts in the Development of Vaccines for the Prevention of Zika and Chikungunya Virus Infections. Front Immunol 11:592.
4. Pietila MK, Hellstrom K, Ahola T. 2017. Alphavirus polymerase and RNA replication. Virus Res doi:10.1016/j.virusres.2017.01.007.
5. Froshauer S, Kartenbeck J, Helenius A. 1988. Alphavirus RNA replicase is located on the cytoplasmic surface of endosomes and lysosomes. J Cell Biol 107:2075-86.
6. Kujala P, Ikaheimonen A, Ehsani N, Vihinen H, Auvinen P, Kaariainen L. 2001. Biogenesis of the Semliki Forest virus RNA replication complex. J Virol 75:3873-84.
7. Lampio A, Kilpelainen I, Pesonen S, Karhi K, Auvinen P, Somerharju P, Kaariainen L. 2000. Membrane binding mechanism of an RNA virus-capping enzyme. J Biol Chem 275:37853-9.
8. Spuul P, Salonen A, Merits A, Jokitalo E, Kaariainen L, Ahola T. 2007. Role of the amphipathic peptide of Semliki forest virus replicase protein nsP1 in membrane association and virus replication. J Virol 81:872-83.
9. Decroly E, Ferron F, Lescar J, Canard B. 2011. Conventional and unconventional mechanisms for capping viral mRNA. Nat Rev Microbiol 10:51-65.
10. Mi S, Stollar V. 1991. Expression of Sindbis virus nsP1 and methyltransferase activity in Escherichia coli. Virology 184:423-7.
11. Laakkonen P, Hyvönen M, Peränen J, Kääriäinen L. 1994. Expression of Semliki Forest virus nsP1-specific methyltransferase in insect cells and in Escherichia coli. J Virol 68:7418-25.
12. Ahola T, Kaariainen L. 1995. Reaction in alphavirus mRNA capping: formation of a covalent complex of nonstructural protein nsP1 with 7-methyl-GMP. Proc Natl Acad Sci U S A 92:507-11.
13. Vasiljeva L, Merits A, Auvinen P, Kaariainen L. 2000. Identification of a novel function of the alphavirus capping apparatus. RNA 5'-triphosphatase activity of Nsp2. J Biol Chem 275:17281-7.
14. Rozanov MN, Koonin EV, Gorbalenya AE. 1992. Conservation of the putative methyltransferase domain: a hallmark of the 'Sindbis-like' supergroup of positive-strand RNA viruses. J Gen Virol 73 (Pt 8):2129-34.
15. Ahola T, Karlin DG. 2015. Sequence analysis reveals a conserved extension in the capping enzyme of the alphavirus supergroup, and a homologous domain in nodaviruses. Biol Direct 10:16.
16. Ahola T, Laakkonen P, Vihinen H, Kaariainen L. 1997. Critical residues of Semliki Forest virus RNA capping enzyme involved in methyltransferase and guanylyltransferase-like activities. J Virol 71:392-7.

17. Scheidel LM, Stollar V. 1991. Mutations that confer resistance to mycophenolic acid and ribavirin on Sindbis virus map to the nonstructural protein nsP1. Virology 181:490-9.
18. Wang HL, O'Rear J, Stollar V. 1996. Mutagenesis of the Sindbis virus nsP1 protein: effects on methyltransferase activity and viral infectivity. Virology 217:527-31.
19. Kovacikova K, van Hemert MJ. 2020. Small molecule inhibitors of Chikungunya virus: mechanisms of action and antiviral drug resistance. Antimicrob Agents Chemother doi:10.1128/aac.01788-20.
20. Gigante A, Canela MD, Delang L, Priego EM, Camarasa MJ, Querat G, Neyts J, Leyssen P, Perez-Perez MJ. 2014. Identification of [1,2,3]Triazolo[4,5-d]pyrimidin-7(6H)-ones as Novel Inhibitors of Chikungunya Virus Replication. J Med Chem 57:4000-8.
21. Delang L, Li C, Tas A, Querat G, Albulescu IC, De Burghgraeve T, Guerrero NA, Gigante A, Piorkowski G, Decroly E, Jochmans D, Canard B, Snijder EJ, Perez-Perez MJ, van Hemert MJ, Coutard B, Leyssen P, Neyts J. 2016. The viral capping enzyme nsP1: a novel target for the inhibition of chikungunya virus infection. Sci Rep 6:31819.
22. Kovacikova K, Morren BM, Tas A, Albulescu IC, van Rijswijk R, Jarhad DB, Shin YS, Jang MH, Kim G, Lee HW, Jeong LS, Snijder EJ, van Hemert MJ. 2020. 6'-beta-Fluoro-Homoaristeromycin and 6'-Fluoro-Homoneplanocin A Are Potent Inhibitors of Chikungunya Virus Replication through Their Direct Effect on Viral Nonstructural Protein 1. Antimicrob Agents Chemother 64.
23. Moesslacher J, Battisti V, Delang L, Neyts J, Abdelnabi R, Pürstinger G, Urban E, Langer T. 2020. Identification of 2-(4-(Phenylsulfonyl)piperazine-1-yl)pyrimidine Analogues as Novel Inhibitors of Chikungunya Virus. ACS Med Chem Lett 11:906-912.
24. Abdelnabi R, Kovacikova K, Moesslacher J, Donckers K, Battisti V, Leyssen P, Langer T, Puerstinger G, Quérat G, Li C, Decroly E, Tas A, Marchand A, Chaltin P, Coutard B, van Hemert M, Neyts J, Delang L. 2020. Novel Class of Chikungunya Virus Small Molecule Inhibitors That Targets the Viral Capping Machinery. Antimicrob Agents Chemother 64.
25. Mudgal R, Mahajan S, Tomar S. 2020. Inhibition of Chikungunya virus by an adenosine analog targeting the SAM-dependent nsP1 methyltransferase. FEBS Lett 594:678-694.
26. Kaur R, Mudgal R, Narwal M, Tomar S. 2018. Development of an ELISA assay for screening inhibitors against divalent metal ion dependent alphavirus capping enzyme. Virus Res 256:209-218.
27. Allison AB, Stallknecht DE, Holmes EC. 2015. Evolutionary genetics and vector adaptation of recombinant viruses of the western equine encephalitis antigenic complex provides new insights into alphavirus diversity and host switching. Virology 474:154-62.
28. Jones R, Bragagnolo G, Arranz R, Reguera J. 2020. Capping pores of alphavirus nsP1 gate membranous viral replication factories. Nature. Accepted for publication.
29. Scholte FE, Tas A, Martina BE, Cordioli P, Narayanan K, Makino S, Snijder EJ, van Hemert MJ. 2013. Characterization of synthetic Chikungunya viruses based on the consensus sequence of recent E1-226V isolates. PLoS One 8:e71047.
30. Chandra G, Moon YW, Lee Y, Jang JY, Song J, Nayak A, Oh K, Mulamoottil VA, Sahu PK, Kim G, Chang TS, Noh M, Lee SK, Choi S, Jeong LS. 2015. Structure-Activity Relationships of Neplanocin A Analogues as S-Adenosylhomocysteine Hydrolase Inhibitors and Their Antiviral and Antitumor Activities. J Med Chem 58:5108-20.

31. Abagyan R, Totrov M, Kuznetsov D. 1994. ICM—A new method for protein modeling and design: Applications to docking and structure prediction from the distorted native conformation. Journal of Computational Chemistry 15:488-506.
32. Neves MA, Totrov M, Abagyan R. 2012. Docking and scoring with ICM: the benchmarking results and strategies for improvement. J Comput Aided Mol Des 26:675-86.
33. An J, Totrov M, Abagyan R. 2004. Comprehensive identification of “druggable” protein ligand binding sites. Genome Inform 15:31-41.
34. An J, Totrov M, Abagyan R. 2005. Pocketome via comprehensive identification and classification of ligand binding envelopes. Mol Cell Proteomics 4:752-61.
35. Delang L, Segura Guerrero N, Tas A, Querat G, Pastorino B, Froeyen M, Dallmeier K, Jochmans D, Herdewijn P, Bello F, Snijder EJ, de Lamballerie X, Martina B, Neyts J, van Hemert MJ, Leyssen P. 2014. Mutations in the chikungunya virus non-structural proteins cause resistance to favipiravir (T-705), a broad-spectrum antiviral. J Antimicrob Chemother 69:2770-84.
36. Mounce BC, Cesaro T, Vlajnic L, Vidina A, Vallet T, Weger-Lucarelli J, Pasoni G, Stapleford KA, Levraud JP, Vignuzzi M. 2017. Chikungunya virus overcomes polyamine depletion by mutation of nsP1 and the opal stop codon to confer enhanced replication and fitness. J Virol doi:10.1128/jvi.00344-17.
37. Heidari Z, Tinsley J, Bickerdike R, McLoughlin MF, Zou J, Martin SA. 2015. Antiviral and metabolic gene expression responses to viral infection in Atlantic salmon (Salmo salar). Fish Shellfish Immunol 42:297-305.
38. Nadia R, Oney OG, Gilles Q, Bruno C, Etienne D, Bruno C. 2020. Mutations on VEEV nsP1 relate RNA capping efficiency to ribavirin susceptibility. Antiviral Res doi:10.1016/j.antiviral.2020.104883:104883.

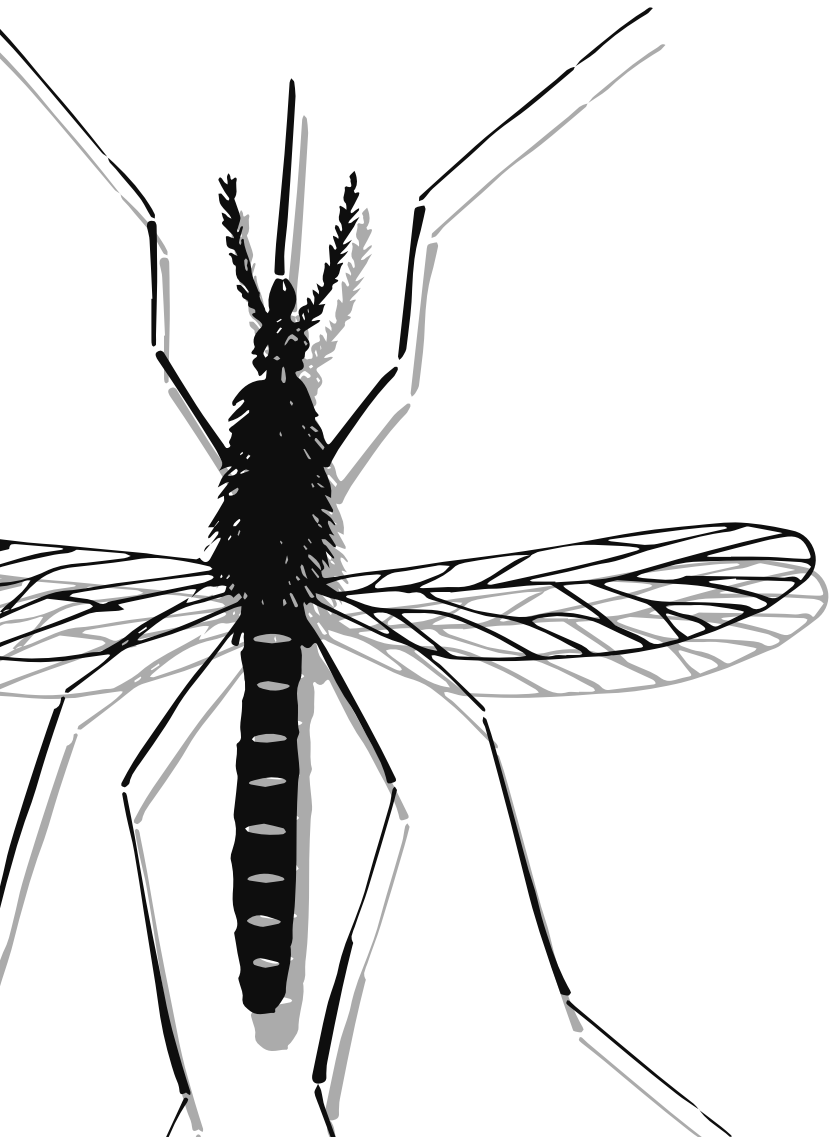

CHAPTER 7

General Discussion

The highly epidemic potential of CHIKV was only truly appreciated after the large epidemics occurred at the beginning of the 21st century. CHIKV remains a serious health problem, mostly in developing countries with poor healthcare infrastructure and high incidence of *Aedes* mosquito vectors. So far, registered antiviral therapies and vaccines are not available and CHIKF treatment is only symptomatic. The main objective of this thesis was to develop novel antiviral strategies against CHIKV. The research described in this thesis focused on identifying prospective CHIKV inhibitors and characterizing their modes of action using cell-based assays, enzymatic assays with purified protein and molecular docking. More specifically, **Chapters 3-6** describe studies ranging from the identification of small-molecule inhibitors in cell-based screens to in-depth elucidation of the mechanism of action of selected potent inhibitors, which were found to inhibit CHIKV nsP1. CHIKV nsP1 was first identified as an antiviral target in 2016, with a report describing the MADTP compound series as potent inhibitors of this protein (1). NsP1 performs unique virus-specific enzymatic functions responsible for viral RNA capping, thus representing a good target for antiviral therapy. This thesis has contributed to the CHIKV antiviral field by the identification of novel RNA capping inhibitors with specific yet distinct inhibitory effects on the nsP1 enzymatic functions. Furthermore, this thesis for the first time describes the use of a CHIKV nsP1 cryo-EM structure for molecular docking studies with small-molecule inhibitors. This final chapter places the results of this thesis in the context of the current literature and discusses some unexpected findings. The highlights and limitations of the antiviral studies with CHIKV nsP1 are summarized and discussed below.

Identification of CHIKV inhibitors and characterization of their mechanisms of action

Compounds identified as prospective CHIKV nsP1 inhibitors originate from screens of repurposed or natural compounds as well as newly synthesized molecules. The CHIKV nsP1 inhibitors described in this thesis have been chemically synthesized and contain novel chemical moieties, as described in **Chapters 2-3.** 6'-fluorinated-aristeromycin and 6'-fluorinated-homoaristeromycin analogues were designed as dual-target compounds against both a viral and a host target. Therefore, their inhibitory activity was first validated in an enzymatic assay with a recombinant S-adenosyl-L-homocysteine (SAH) hydrolase and subsequently in CHIKV CPE-reduction assays (**Chapter 3**). Two of the prototype compounds, namely 6'-β-fluoro-

homoaristeromycin (FHA) and 6′-fluoro-homoneplanocin A (FHNA), showed stronger inhibition in CHIKV CPE-reduction assays (EC_{50} 0.12 ± 0.04 μM and 0.18 ± 0.11 μM, respectively) compared to the enzymatic assays with SAH hydrolase, suggesting their antiviral effect could be direct rather than indirect via inhibition of the host SAH hydrolase (**Chapters 3-4**). The inhibition of the latter host enzyme indirectly interferes with the nsP1-mediated methylation reactions via a negative feedback mechanism due to SAH build-up. Despite the inhibition of SAH hydrolase having been studied with various SAH hydrolase inhibitors in cell culture in the past, a direct link between the inhibition of SAH hydrolase and FHA/FHNA has not been established in our study using cell-based assays. The opportunities for measuring metabolites such as SAM and SAH in infected treated and untreated cells have been explored but have proved to be complex, as many players feed into the cellular methylation pathway. It was also not possible to perform the SAH hydrolase knockdown by siRNA mediated gene silencing, for example, as the SAH hydrolase is considered an essential host factor in the cellular methylation pathway. Despite lack of direct evidence that FHA/ FHNA act via inhibition of the host SAH hydrolase, the viral target of these compounds was determined by resistance passaging and generation of resistant mutants by reverse genetics. The resistance passaging protocol used and described in **Chapters 4-5** differs from the conventional passaging approach performed in the presence of suboptimal compound concentrations. Instead, this method relies on using a high viral dose in the presence of compound concentrations that confer full protection in CPE-reduction assays. The wells containing 'viral breakthrough', i.e. viruses with mutations that increase fitness, are then further passaged, again in the presence of a compound dose conferring full protection against virus-induced CPE, as in the previous step. The objective is to obtain a viral population where the mutants conferring resistance to the compound represent the majority. While this selection procedure allows rapid identification of resistant mutants, it does not discriminate between mutations that originated due to resistance to the compound and those that arose as a consequence of cell culture adaptation. Mutations responsible for cell culture adaptation in VeroE6 cells, such as R171Q and T301K in CHIKV nsP1 and opal524R in CHIKV nsP3, have been detected previously (2). Therefore, the mutation of opal524R in CHIKV nsP3 identified in our study was considered as non-specific. Because the resistance passaging method described here does not allow for parallel passaging of wt virus to reveal such non-specific mutations, all identified mutations have to be reverse-engineered into an infectious cDNA clone, either singularly or in combinations. The inability to

exclude non-specific mutations is the major downside of this method, as opposed to conventional passaging where wt virus is passaged in parallel in untreated cells. Our mechanism of action studies described in **Chapters 4-5** identified CHIKV nsP1, the enzyme responsible for viral RNA capping, as the target of both FHA and FHNA, and the CHVB compounds. Reverse genetics confirmed that resistance against FHA/FHNA and CHVB compounds required two mutations in CHIKV nsP1. The equivalents of the mutations that confer resistance to FHNA in CHIKV, namely G230R and K299E, were introduced into an SFV infectious cDNA clone. The SFV nsP1 mutants with a single mutation K231R or K300E and the K231R/K300E double mutant were tested for resistance in SFV CPE-reduction assays. Unlike for CHIKV nsP1 mutants, none of these SFV nsP1 mutants proved to be resistant to FHNA (data not shown). However, it is important to mention that these mutations were not selected by resistance passaging, therefore the mutations responsible for SFV resistance to FHNA were either located elsewhere in the nsP1 sequence and/or more than two mutations were responsible for the resistance phenotype. Importantly, the enzymatic assays with wt SFV nsP1 were able to demonstrate at least a partial direct inhibitory effect of the metabolized form of FHNA, the 3'-keto form. Unfortunately, despite several efforts, the 3'-keto form of FHNA could not be chemically synthesized (unpublished). Assays with the purified SFV nsP1 carrying the K231R and K300E mutations showed that this protein was enzymatically less active and also partially resistant to the inhibitory effect of the 3'-keto form of FHNA (**Chapter 4**), in contrast to the same mutant in SFV CPE-reduction assays. This clearly demonstrates differences between the conformation of the protein in infected cells and its accessibility to inhibitors compared to *in vitro* assays. This topic is revisited in more detail below. Although the direct link between FHA/FHA and the inhibition of SAH hydrolase could not be established, the effect of both SAM and SAH on the activity of purified wt SFV nsP1 and mutant K231R/K300E nsP1 was tested in enzymatic assays. The results of these assays disproved an (inhibitory) effect of both SAH and SAM on the protein, indicating that the mechanism of action of FHA/FHNA is independent of the inhibition of SAH hydrolase.

Is RNA capping a good target for antiviral drug development?

The 5' cap structure is unique to eukaryotic cellular and viral mRNAs, as it is absent from other domains of life. Although the capping pathway is well conserved in all eukaryotes, the structure and genetic organization of the capping enzymes differ

between species (3). In the conventional RNA capping pathway of eukaryotic cells, the cap is formed by three enzymatic reactions at the 5' end of the nascent mRNA (Fig. 1). First, the 5' triphosphate end of pre-mRNA is hydrolysed to a diphosphate by an RNA 5' triphosphatase (RTPase). Second, a guanylyltransferase (GTase) adds guanosine 5' monophosphate (GMP) to the diphosphate RNA via a covalent enzyme-GMP intermediate. Finally, the GpppN cap is methylated at the N7 position by a guanine-N7 methyltransferase (MTase). This process generates the minimal cap-0 structure (m^7GpppN) found mainly in lower eukaryotes. In higher eukaryotes, further methylation by ribose 2'-O-methyltransferases (2'-O MTases) occurs at the 2' position of the first nucleotides in the RNA transcript, to generate cap-1 (m^7GpppNmN) and cap-2 (m^7GpppNmNmN) structures (4). S-adenosyl-L-methionine (SAM) serves as a methyl donor for both the N-7 and 2'-O methylation reactions. S-adenosyl-L-homocysteine (SAH) is a demethylated by-product that is released during the reaction and can inhibit SAM-dependent MTases.

In contrast to some viruses that require two methylation steps, alphaviruses need only one methylation event for production of a functional 5' cap. An alphavirus 5' cap is identical to the cellular 5' RNA cap, albeit its synthesis proceeds via a non-conventional mechanism. The alphavirus nsP1 MTase first methylates a GTP molecule to produce 7-methylguanosine (m^7GTP) (5). The nsP1 GTase is then responsible for the covalent attachment of m^7GTP onto nsP1, resulting in the formation of the covalent m^7GMP-nsP1 intermediate and releasing a pyrophosphate (PPi) (6, 7). The nsP2 RTPase removes the 5' γ-phosphate from nascent RNAs to produce 5' diphosphate-containing RNAs ready to receive the methylated m^7GMP cap (8). Finally, the nsP1 GTase transfers m^7GMP onto the diphosphate RNAs. Thus, both alphavirus nsP1 and nsP2 are involved in RNA capping. The cap structure protects the mRNA from degradation by host 5'-3' exoribonucleases as well as against a number of innate immune sensors that detect the presence of uncapped viral RNAs as 'non-self'. Lastly, the cap is required for translation by host ribosomes that recognize the N7-methylated cap structure

Alphavirus RNA capping is an interesting target for CHIKV antiviral drug development owing to the virus-specific enzymatic functions and mechanistic differences between cellular and viral 5' cap formation. While cellular MTase and GTase enzymes often contain canonical catalytic motifs (KDKE and KxDG, respectively), alphavirus nsP1 does not contain these signature sequences, opening the possibility of selective inhibition (9). Studies with an SINV infectious cDNA clone have also shown that point mutations of H39, D91, R94 and Y249 that abolish nsP1 enzymatic activity

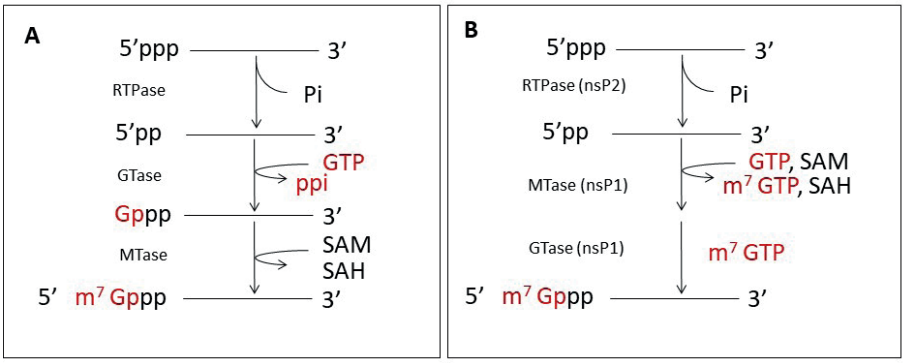

Figure 1: Comparison of the host (A) and alphavirus (B) RNA capping pathway.

render the virus non-viable (10). It is possible to achieve a complete block of replication by targeting the 5' cap, as illustrated by the CHVB compounds that fully blocked CHIKV replication at specific doses in the low micromolar range in a $TCID_{50}$-based assay (**Chapter 5**). As alphavirus RNA capping occurs exclusively in the cytoplasm drugs designed to specifically target this process are not expected to trigger adverse reactions. In the alphavirus replication cycle, two RNA molecules are co-transcriptionally capped – the genome and the sgRNA. Inhibition of this process should have a profound negative effect on alphavirus replication. Furthermore, the activation of innate immune pathways, including the type I IFN response, by the presence of uncapped RNA molecules, is expected to enhance the impact of drugs targeting RNA capping. Under such circumstances, RNAs with immature or incomplete cap structures would be targeted for degradation by the RNA decay machinery.

Nevertheless, some considerations need to be made when developing CHIKV nsP1 inhibitors. Antiviral drug resistance to CHIKV nsP1 inhibitors is known to develop, typically requiring the presence of two mutations, as discussed in **Chapter 2**. A virus can also develop alternative pathways to resist the effect of antiviral compounds. For example, DENV was reported to alternate between cap-dependent and cap-independent translation mechanisms (11), which could be problematic for the development of specific DENV capping inhibitors. Another potential downside of using nsP1 as a specific antiviral target is the limited level of conservation between different members of the *Togaviridae* family. It is known that alphavirus nsP1 displays approximately 60-65% sequence similarity despite the enzymatically active part being well-conserved. The unique structural features that increase the selectivity of this

antiviral target could come at the cost of a broad-spectrum antiviral effect. Despite the latest findings by Jones *et al.* that alphavirus nsP1 forms a conserved structure composed of 12 nsP1 protomers arranged into a ring-shaped membrane-associated complex (12), it is still not understood why some inhibitors are specific towards CHIKV nsP1 while others are not. This is exemplified by the CHVB compound series described in **Chapter 5**, which inhibited various CHIKV strains but was not active against related alphaviruses. Perhaps unsurprisingly, the MADTP compound series that is predicted to bind in the same pocket as the CHVB series based on docking studies described in **Chapter 6**, also had a limited antiviral spectrum. The MADTP-314 compound and its analogues potently inhibited several CHIKV strains, but were less active against VEEV and not active against closely related alphaviruses like ONNV (1).

Detection and role of uncapped RNAs produced during the alphavirus replication cycle

The absence of a 5' cap structure was identified as a primary molecular determinant of SINV particle infectivity (13). The viral RNAs produced during an infection are not universally 5' capped as previously thought. In fact, it has been shown that a significant amount of uncapped genomic RNAs, composed primarily of the 5' monophosphate RNAs, are packaged into particles during the course of a SINV infection (13). There appears to be no preferential packaging of either 5' capped or uncapped genomic RNA in mammalian or mosquito cells during a SINV infection. A more detailed mechanistic study in tissue culture models revealed that nsP1 mutations can modulate the production of uncapped RNAs. Specifically, alanine substitutions at positions Y286 and N376 of SINV nsP1 led to decreased RNA capping efficiencies and an alanine substitution at position D355 increased RNA capping efficiencies (14). Importantly, SINV appears to be much more sensitive to mutations that increase RNA capping efficiency compared to those that decrease RNA capping efficiency. In addition, increasing the viral capped-to-uncapped RNA ratio had a detrimental effect on overall viral particle production (14). These observations strongly indicate that there is a role for uncapped RNAs during the replication cycle, whereby decreased amount of uncapped RNAs negatively affects viral particle assembly. However, the precise underlying molecular mechanisms are unknown. It would be interesting to know whether uncapped RNAs play a similar role during CHIKV replication and whether any of the mutations responsible for resistance to CHIKV nsP1 inhibitors, such as FHA/

FHNA or CHVB compounds, are able to modulate capping efficiencies. Our data from **Chapter 4** have shown that treatment with the capping inhibitors FHA and FHNA led to an increased genomes-to-PFU ratio. The balance between the capped and uncapped RNAs might have been altered in favour of uncapped RNAs early during the replication cycle. To measure the ratio of capped-to-uncapped RNAs, an XRN1-based qRT-PCR assay was set up to discriminate the amounts of these molecules in a sample (data not shown). This assay was originally designed for SFV, a model alphavirus that has been extensively studied in our laboratory, based on the principle described by LaPointe et al. (14) and on the assumption that SFV and SINV have similar capping efficiencies. The assay uses the 5'-3' exoribonuclease XRN1 that digests 5' monophosphate RNAs, but leaves 5'di/triphosphate RNAs and 5' caps intact. After an enzymatic digestion by XRN1, only capped RNAs are expected to be left in the sample preparation. In addition, the samples are internally spiked with a yellow fever virus (YFV) *in vitro*-transcribed RNA fragment. Control reactions contain YFV RNA that is first treated with RNA 5' pyrophosphodydrolase (RppH) that removes 5' di/triphosphate RNAs and 5' caps, leaving only 5' monophosphate RNAs for degradation by XRN1. The net result of the combined RppH and XRN1 treatment is the absence of YFV RNA. The ratio of capped-to-uncapped RNAs is then compared between XRN1-treated and untreated samples by detection with qRT-PCR using specific SFV and YFV probes. Experimentally, we have determined that there is approximately 3% YFV RNA remaining after digestion with both RppH and XRN1, demonstrating the assay is sufficiently sensitive to show differences between samples. However, in our assay with FHNA-treated and untreated intracellular and extracellular SFV RNA, there was large variation between the sample replicates in the assay. Therefore, it was not possible to draw a conclusion about the effect of FHNA treatment on SFV RNA capping. This could be attributed to the instability of uncapped viral transcripts, especially outside of the cellular environment. Thus, RNA degradation could be the main reason for replicate variability. It must be stated that the effect of FHNA on CHIKV RNA capping is expected to be greater, because FHNA was a more potent inhibitor of CHIKV compared to SFV, as described in **Chapter 4**. Furthermore, the SFV nsP1 K231R/K300E double mutant was not resistant to FHNA treatment in cell culture, suggesting that these mutations unlikely play a role in altering the capped-to-uncapped ratio during the SFV replication cycle. Other systems for detecting capped and uncapped RNAs include immunoaffinity purification of m^7G-capped transcripts using the anti-m^3G/m^7G antibody (Ab)-coupled beads. This method was used for the characterization of

the 5' termini of the genomic and four sg RNAs of Berne torovirus (15), a member of the nidovirus order. Our protocol differed in using qRT-PCR for detection of CHIKV RNA instead of ^{32}P-labelled oligonucleotide probes for Northern blot hybridization analysis. This assay was used to determine the amount of capped CHIKV RNA bound to the Ab-coupled beads. However, despite our best efforts, we failed to ascertain the specificity of the anti-m^{3}G/m^{7}G Ab when using an uncapped CHIKV transcript, which impacted the overall reliability of this assay set-up. For these reasons and unresolved contamination problems, we decided not to quantify capped CHIKV RNA using this assay (data not shown). Another method uses qRT-PCR for detection of RNA-adapter-containing RNAs obtained by enzymatic treatment of intracellular or extracellular SINV RNAs. In this approach, 5' monophosphate-containing RNAs are generated by an initial treatment with a phosphatase followed by treatment with either a decapping enzyme or a kinase. The resulting capped and uncapped reaction mixtures serve as substrates for a ligation with an RNA adapter. In this way, the RNA-adapter-containing molecules can be compared to the total amount of viral genomic RNA in order to determine the ratio of capped-to-uncapped RNAs (13). However, the major disadvantages of the immunoprecipitation method with the anti-m^{3}G/m^{7}G Ab and the adapter ligation method are that both are labour-intensive and require multiple (enzymatic) steps to obtain capped and uncapped RNAs for quantification by qRT-PCR. The XRN1-based qRT-PCR assay is simpler, faster and less error-prone compared to the other methods, which is why it remains the best method for determining the ratio of capped-to-uncapped RNAs from virally-infected samples.

Deciphering the enzymatic functions of alphavirus nsP1: what we have learned from the past

In vitro assays with SFV-infected cell lysates were developed already in the early 1980s to understand the SFV-specific enzyme functions in more detail. The first *in vitro* assays used ^{3}H-labelled SAM to produce methylated caps at the 5' termini of genomic and sg RNAs by the so called 'methylating enzyme', found in the mitochondrial pellet fractions (P15) of SFV-infected cells (16). The discovery that the enzyme responsible for the 'mehylating' activity, termed MTase, originated from a virus-specific protein came soon after (17). MTase activity was associated with the SFV replication complex based on evidence demonstrating that MTase from SFV-infected P15 extracts differed in substrate specificity from the cellular enzyme because, unlike the host enzyme, it

could catalyse the methylation of GTP to m^7GTP. Furthermore, the MTase reaction could take place in the presence of EDTA, although the activity was reduced if divalent cations (Mg^{2+}) were absent from the reaction. Preparations of SFV-infected P15 fractions at different time points also revealed that the MTase activity appeared during the first 2 h post-infection, coinciding with the synthesis of a viral protein during the early stages of the SFV replication cycle (17). The direct link between MTase activity and nsP1 was revealed by expressing a SINV nsP1 mutant resistant to low methionine levels in *E. coli.* This mutant expressed an MTase with much higher affinity for SAM compared to wt nsP1 (18). Later on, SFV nsP1 was also successfully expressed in *E. coli* and recombinant baculovirus (AcNPV-nsP1)-infected cells, although finding a suitable purification method was not successful at the time due to heavy protein aggregation in these expression systems (5, 7). The MTase assays with the *E. coli* lysates confirmed that the reaction is specific for GTP and dGTP while the natural cap analogue of SFV RNAs, GpppA, could not serve as a methyl acceptor molecule. Furthermore, the enzyme could not methylate capped SFV transcripts, a feature in which alphavirus nsP1 MTase differs from other virus families (5). The ability of SFV nsP1 to form a covalently bound enzyme-guanylate complex typical for GTases was discovered using P15 fractions from recombinant baculovirus (AcNPV-nsP1)-infected cells. The GTase assays, which included α^{32}P-GTP and SAM in the reaction mixture of nsP1-containing cell lysates, used the formation of a 68 kDa ^{32}P-labelled m^7GMP-nsP1 covalent intermediate as a readout. As opposed to the MTase activity, the GTase activity was dependent on the presence of divalent cations (Mg^{2+} or Mn^{2+}) for the reaction to proceed. The covalent linkage between nsP1 and m^7GMP was found to occur via a phosphamide bond (6). Using crosslinking assays with *E. coli* lysate containing recombinant SFV nsP1, residues D64 and D90 were found to be critical for SAM binding whereas residue H38 was linked to covalent binding of m^7GMP (7). These residues are conserved across the alphavirus-like superfamily, which suggested that other members of this family use similar mechanisms for 5' cap formation. Altogether, these studies indicated that alphavirus nsP1 is a source of at least two unique virus-specific enzymatic functions, the MTase and the GTase, and that the GTase is dependent on MTase. Later studies focused on deciphering the functional details of these enzymatic activities using radiolabel- and fluorescence-based assays with purified wt and mutant proteins.

SINV nsP1 expressed in *E. coli* and purified to homogeneity was the first purified alphavirus nsP1 capping enzyme. The protein retained its MTase and GTase activities, which indicated that membrane association is not required for

the enzymatic activity (19). In a more recent study with VEEV nsP1 purified from *E. coli*, a non-radioactive Western blot assay using the anti-m^3G/m^7G Ab was set up to study the GTase independently from the MTase (20). This reaction used m^7GTP and SAH as substrates while, in the past, a chemically synthesized [^{14}C]m^7GTP was used. This non-radioactive GTase assay confirmed the results of the previous study, which showed that ^{14}C-labelled nsP1 could only be synthesized in the presence of both [^{14}C]m^7GTP and SAH and that addition of SAM had no effect (7). The Western blot assay relies on the detection of the m^7GMP-nsP1 covalent complex using immunoblotting with anti-m^3G/m^7G Ab. Mutational analyses of the MTase and GTase activities revealed that substitutions of residues H37 and D63 completely abolished the formation of the m^7GMP covalent complex, as discovered for SFV nsP1. It also revealed that replacement of other residues, namely D354 and R365, increased the complex formation and that substitutions of Y285, N369 and N375 decreased complex formation. Some of these residues were found to be involved in modulating RNA capping efficiencies, as discussed before. Lastly, the guanylyltransfer of m^7GMP onto a 5' diphosphate RNA oligonucleotide was demonstrated using an assay with purified VEEV nsP1 (20). Therefore, it is now possible to uncouple all steps of the alphavirus RNA capping pathway using enzymatic assays reflecting each of the successive steps.

On the basis of the above-mentioned literature, we have established a purification protocol for SFV nsP1. It should be noted that the SFV nsP1 that was used for the activity assays in **Chapters 4-6** was purified to about 70-80% homogeneity, based on the SDS-PAGE analysis and Coomassie Blue staining. An assay detecting the formation of the m^7GMP-nsP1 covalent intermediate, which studies both MTase and GTase activities, and uses $\alpha^{32}P$-GTP and SAM as substrates, was developed to assess the antiviral effect of compounds described in **Chapters 4-6** and as discussed below. The MTase assays for SFV nsP1 were developed based on enzymatic assays with SINV and VEEV nsP1, as described in (19, 20). In our experimental conditions, the MTase reaction was stopped with excess SAH and loaded directly on the DEAE membrane. The detection of radioactive signal in this assay relies on the fact that the positively charged membrane binds to the negatively-charged nucleic acids such as [^3H]GIDP while the rest is washed away. The radioactivity that is retained on the membrane is then absorbed by the scintillation liquid and measured in the scintillation counter. However, this approach failed to detect SFV nsP1 MTase activity despite several attempts (counts per minute at or below background level; data not shown), while the MTase activity was detected for the vaccinia virus (VV) capping enzyme used as

a positive control. To avoid detection of background due to [^{3}H]SAM and to avoid clogging on the membrane, [^{3}H]GIDP was extracted 3x with phenol buffered in 100 mM Tris-HCl pH 8.0 to yield a pure preparation, similar to a previously published protocol (19). The extraction is based on the separation of [^{3}H]SAM into the phenol phase and the methylated acceptor [^{3}H]GIDP into the aqueous phase. The radioactivity in the extracted aqueous phase was then mixed with the scintillation liquid and measured by scintillation counting. Nevertheless, this method also did not lead to detection of the MTase activity of SFV nsp1 (data not shown). It could be that the SFV nsP1 preparation that was used for these assays was contaminated with traces of SAH due to incomplete purification, which would have distorted the assay equilibrium and would have had a negative effect on the enzymatic activity. It is also very likely that this assay is not sensitive enough to detect the MTase activity compared to the radioactive assay with α^{32}P-GTP and SAM measuring both MTase and GTase activities.

Inhibitors of alphavirus nsP1 in enzymatic assays

The main purpose of developing the covalent complex formation assay with SFV nsP1 was to assess the antiviral effect of RNA capping inhibitors on this antiviral target, as described in **Chapters 4-6**. Obtaining purified CHIKV nsP1 has been notoriously difficult, which is why our enzymatic assays were developed using a close relative of CHIKV nsP1, SFV nsP1. The quest for alphavirus RNA capping inhibitors has started more than 20 years ago with the development of functional enzymatic assays that uncoupled the individual steps of the RNA capping pathway. One of the first antiviral enzymatic assays with SFV nsP1 used partially purified bacterial supernatant (S15) fractions to study the effect of GTP analogues. Although some of the cap analogues could effectively inhibit the MTase and GTase of SFV nsP1, they could also interfere with translation by competing for ribosomal binding (21). More recently, sinefungin and aurintricarboxylic acid (ATA), a known inhibitor of flavivirus RNA capping, were shown to inhibit MTase and GTase activities in antiviral assays with purified VEEV nsP1. In contrast, ribavirin triphosphate (RTP) was very poorly active in both assays (20). This demonstrates that alphavirus nsP1 behaves differently from other enzymes such as the VV capping enzyme, as RTP can act directly as a substrate for the VV capping enzyme and form a covalent RMP-enzyme intermediate (22). The above-mentioned assays were based on the use of substrates containing radioactive isotopes, the use of which has diminished over the last decade. Despite their sensitivity, radioactive assays

are often discontinued due to potential health risks, reduced production of radioactive isotopes by commercial suppliers, limited half-life and costly waste disposal. More recently, non-radioactive methods have been developed that obviate the need for radiolabelled substrates. For example, a high throughput (HT) ELISA-based GTase assay was used for screening of 1220 compounds and identified 18 compounds inhibiting guanylylated VEEV nsP1. The best compounds showed improved IC_{50} values compared to the reference compound sinefungin (IC_{50} 29.1 ± 2.6 μM) (23). A screen using a similar ELISA-based assay with CHIKV nsP1 confirmed the results with VEEV nsP1, with sinefungin and ATA having low IC_{50} values of 2.7 μM and 5.7 μM, respectively, while RTP was a poor inhibitor of CHIKV nsP1 with an IC_{50} in the millimolar range (24). Another method, a fluorescence polarization (FP)-based assay with CHIKV nsP1, was developed to monitor the displacement of fluorescently-labelled GTP analogues in real time using a pure monomeric CHIKV nsP1. This was the first report describing structural features of GTP that are important for GTP binding within CHIKV nsP1 (25). The same HT FP-based assay was used to screen 3051 compounds and identified lobaric acid as a potent competitive inhibitor of GTP binding (K_i 7.0 ± 0.6 μM) and anti-CHIKV activity (EC_{50} 5.9 ± 1.4 μM) (26). Our studies in Chapters **4-6** describing the *in vitro* antiviral effect of CHVB and MADTP compounds, sinefungin, FHNA and its modified 3'-keto form were performed with SFV nsP1. CHVB compounds completely blocked the formation of the ^{32}P-labelled m^7GMP-nsP1 covalent intermediate while MADTP-372, sinefungin and the 3'-keto form of FHNA reduced the signal to a lesser extent. Overall, these assays demonstrated the antiviral effect of CHIKV nsP1 inhibitors in an assay system with a purified alphavirus nsP1 protein.

Discovery of alphavirus nsP1 capping complex and implications for future antiviral research

Towards the end of 2020, a new discovery describing alphavirus nsP1 capping rings has challenged our interpretations of the biochemical data on alphavirus nsP1 that accumulated over the last decades. For the first time, it was demonstrated that CHIKV nsP1 is active in ring-like oligomeric complexes and that these complexes are conserved among alphaviruses and beyond (12). The CHIKV nsP1 complex assembles into a dodecameric ring with a central pore, that is composed of a crown, a waist and a membrane-binding skirt. The active sites of the capping MTase-GTase domain form positively-charged pockets at the top of the crown while the membrane-binding

spikes protrude from the bottom of the skirt. The oligomerization of the nsP1 complex is needed to allosterically activate the enzyme and stabilize the conformation of the capping domain. Therefore, the enzymatic activity of monomeric nsP1 seems to be only residual compared to the enzymatic activity of oligomeric nsP1, which is expected to several times exceed that of the monomeric nsP1. Furthermore, these enzymatically active rings are associated with the membrane within the spherule necks, controlling access to these cellular invaginations harbouring newly synthesized viral RNA, as suggested in the past (27).

In **Chapter 6**, we performed molecular docking studies with the CHIKV nsP1 cryo-EM structure. Our results revealed that CHVB and MADTP series dock at the SAM-binding site of the oligomeric nsP1 complex. Interestingly, they tend to dock at the GTP-binding site of the monomeric nsP1. Therefore, it's important to further elucidate whether the nsP1 complex is the predominant structural form in infected cells as well as the speed of nsP1 complex assembly. Besides the capping domain, CHIKV nsP1 also contains the RAMBO domain that makes up the waist and skirt regions of the complex. The FHNA series docks at a binding pocket in this domain, leading to disruption of membrane binding and oligomerization of nsP1. The identification of the predicted compound-docking sites in these functionally distinct regions of CHIKV nsP1 is supported by the resistance-inducing mutations that localize in the vicinity of these sites. The residues mutated in the MADTP- and CHVB-resistant viruses gate the active site and the residues involved in FHNA resistance line a pocket in the RAMBO domain, as further described in **Chapter 6**. Altogether, our molecular docking studies classified the CHIKV nsP1 inhibitors into functionally distinct groups. However, some of our earlier findings, including the specific antiviral activity of MADTP and CHVB series against CHIKV but not against related alphaviruses, could not be addressed with the available structural information. Therefore, the structural context for inhibition of MADTP or CHVB series still needs to be further investigated, given that their docking positions can change depending on the oligomeric state of nsP1. This is counterintuitive, as one would expect a defined binding pose for inhibitors specifically targeting CHIKV nsP1. Nevertheless, it must be re-emphasized that the current CHIKV nsP1 structure did not contain ligands in the active site, and that CHIKV nsP1 is predicted to undergo conformational reorganization affecting the active site. The characterization of the precise location of SAM- and GTP-binding sites within the alphavirus nsp1 structure, including the thus far elusive residues involved in MTase and GTase activities, would represent the first step towards identification of broad-spectrum small molecule

inhibitors of alphavirus nsP1. This information could also be harnessed for *in silico* screening and rational design of selective alphavirus nsP1 inhibitors. Another potential avenue for drug design would be the development of allosteric inhibitors of alphavirus nsp1, by targeting the druggable pocket in the RAMBO domain of nsP1.

Do arboviruses pose a global threat for the future?

Mosquitoes, like all other organisms, respond to selective pressures imposed by their changing environments. Climate change and urbanisation have been the major drivers of arbovirus spread to new territories with previously unexposed populations. The changing epidemiology in these new regions could be disruptive to healthcare systems and economies of the affected countries that have not had a history of arboviral diseases. For example, predictive models indicate that arboviruses will pose an increased threat to Africa due to their year-around circulation and the abundance of *Aedes* mosquitos on this continent. This shift can be explained by differences in thermal optima between the mosquito vectors for malaria and arboviruses, such as dengue and chikungunya. While malaria transmission by *Anopheles gambiae* peaks at 25°C, arbovirus transmission by *Ae. aegypti* peaks at 29°C (28, 29), which can lead to geographical shifts in *Ae. aegypti*-transmitted viruses with warmer temperatures, for example in sub-Saharan Africa. The shift from malaria to arboviral diseases has already occurred in much of Latin America, where malaria transmission has substantially declined in the past three decades and, at the same time, dengue, chikungunya and Zika incidence have increased (30). While malaria control programs have undoubtly played an indispensable role in controlling malaria transmission, the influence of temperature and human movement on vector-borne disease transmission has been largely unrecognized. In addition, CHIKV has expanded to cooler regions of the world due to adaptation to a new vector - *Ae. albopictus* -, which thrives at lower environmental temperatures compared to *Ae. aegypti*. This indicates that, besides ecological changes, alteration of the genetic make-up of viruses such as CHIKV can affect vector competence and their distribution in the environment. The latest statistics show that the most CHIKV-affected countries lie in Central and South America, with Brazil having the largest number of reported cases, and in South-East Asia, dominated by Malaysia and Thailand. There have been no autochthonous cases of CHIKV reported in continental Europe in 2019 or 2020 (https://www.ecdc.europa.eu/en/chikungunya-monthly).

Concluding remarks

In this thesis, several important topics related to inhibition of CHIKV nsP1 by small-molecule inhibitors have been discussed. Here, a few key points of importance to the field of (alpha)virology and antiviral drug development are highlighted. First, it was shown that potent and specific inhibitors of the CHIKV RNA capping can be developed by using novel synthetic approaches to fill the CHIKV antiviral drug discovery pipeline. Moreover, it was demonstrated that the resistance to CHIKV nsP1 inhibitors can develop, and that the barrier to resistance typically consists of two amino acid substitutions in the non-conserved regions of nsP1. Besides identifying the viral drug target in cell-based assays, it is important to validate the viral target of direct-acting CHIKV nsP1 inhibitors in different experimental systems, for example, in enzymatic assays with purified protein, to confirm target specificity. As shown with the use of the recently solved CHIKV nsP1 cryo-EM structure, which is assembled into a dodecameric ring, the oligomerization state of nsP1 can have an impact on the molecular docking of CHIKV nsP1 inhibitors and can influence the interpretation of our findings from cell-based and enzymatic assays. More importantly, our studies showed that the use of a CHIKV nsP1 structure is instrumental for identifying and validating druggable pockets or binding sites. In addition, such knowledge can contribute to rational design and improvement of CHIKV active molecules for development into a much-needed antiviral therapy. Given that antiviral drug resistance is known to develop for CHIKV inhibitors, it appears that combination therapy consisting of two or more direct-acting inhibitors or a direct-acting inhibitor together with a host-directed inhibitor or an immunomodulatory agent is the best approach for tackling CHIKF and that this strategy can increase the barrier to resistance. To conclude, this thesis stresses the importance of further research in the arbovirus field as arboviruses will undoubtly represent a global health threat in the future due to their unpredictable epidemiology.

References

1. Delang L, Li C, Tas A, Querat G, Albulescu IC, De Burghgraeve T, Guerrero NA, Gigante A, Piorkowski G, Decroly E, Jochmans D, Canard B, Snijder EJ, Perez-Perez MJ, van Hemert MJ, Coutard B, Leyssen P, Neyts J. 2016. The viral capping enzyme nsP1: a novel target for the inhibition of chikungunya virus infection. Sci Rep 6:31819.
2. Albulescu IC, White-Scholten L, Tas A, Hoornweg TE, Ferla S, Kovacikova K, Smit JM, Brancale A, Snijder EJ, van Hemert MJ. 2020. Suramin Inhibits Chikungunya Virus Replication by Interacting with Virions and Blocking the Early Steps of Infection. Viruses 12.
3. Shuman S. 2002. What messenger RNA capping tells us about eukaryotic evolution. Nat Rev Mol Cell Biol 3:619-25.
4. Ferron F, Decroly E, Selisko B, Canard B. 2012. The viral RNA capping machinery as a target for antiviral drugs. Antiviral Res 96:21-31.
5. Laakkonen P, Hyvönen M, Peränen J, Kääriäinen L. 1994. Expression of Semliki Forest virus nsP1-specific methyltransferase in insect cells and in Escherichia coli. J Virol 68:7418-25.
6. Ahola T, Kääriäinen L. 1995. Reaction in alphavirus mRNA capping: formation of a covalent complex of nonstructural protein nsP1 with 7-methyl-GMP. Proc Natl Acad Sci U S A 92:507-11.
7. Ahola T, Laakkonen P, Vihinen H, Kääriäinen L. 1997. Critical residues of Semliki Forest virus RNA capping enzyme involved in methyltransferase and guanylyltransferase-like activities. J Virol 71:392-7.
8. Vasiljeva L, Merits A, Auvinen P, Kaariainen L. 2000. Identification of a novel function of the alphavirus capping apparatus. RNA 5'-triphosphatase activity of Nsp2. J Biol Chem 275:17281-7.
9. Ghosh A, Lima CD. 2010. Enzymology of RNA cap synthesis. Wiley Interdiscip Rev RNA 1:152-72.
10. Wang HL, O'Rear J, Stollar V. 1996. Mutagenesis of the Sindbis virus nsP1 protein: effects on methyltransferase activity and viral infectivity. Virology 217:527-31.
11. Edgil D, Polacek C, Harris E. 2006. Dengue virus utilizes a novel strategy for translation initiation when cap-dependent translation is inhibited. J Virol 80:2976-86.
12. Jones R, Bragagnolo G, Arranz R, Reguera J. 2020. Capping pores of alphavirus nsP1 gate membranous viral replication factories. Nature. Accepted for publication.
13. Sokoloski KJ, Haist KC, Morrison TE, Mukhopadhyay S, Hardy RW. 2015. Noncapped Alphavirus genomic RNAs and their role during infection. J Virol doi:10.1016/j.antiviral.2015.03.013 10.1128/jvi.00553-15.
14. LaPointe AT, Moreno-Contreras J, Sokoloski KJ. 2018. Increasing the Capping Efficiency of the Sindbis Virus nsP1 Protein Negatively Affects Viral Infection. mBio 9.
15. van Vliet AL, Smits SL, Rottier PJ, de Groot RJ. 2002. Discontinuous and non-discontinuous subgenomic RNA transcription in a nidovirus. Embo j 21:6571-80.
16. Cross RK, Gomatos PJ. 1981. Concomitant methylation and synthesis in vitro of Semliki Forest virus (SFV) ss RNAs by a fraction from infected cells. Virology 114:542-54.
17. Cross RK. 1983. Identification of a unique guanine-7-methyltransferase in Semliki Forest virus (SFV) infected cell extracts. Virology 130:452-63.

18. Mi S, Stollar V. 1991. Expression of Sindbis virus nsP1 and methyltransferase activity in Escherichia coli. Virology 184:423-7.
19. Tomar S, Narwal M, Harms E, Smith JL, Kuhn RJ. 2011. Heterologous production, purification and characterization of enzymatically active Sindbis virus nonstructural protein nsP1. Protein Expr Purif 79:277-84.
20. Li C, Guillén J, Rabah N, Blanjoie A, Debart F, Vasseur JJ, Canard B, Decroly E, Coutard B. 2015. mRNA Capping by Venezuelan Equine Encephalitis Virus nsP1: Functional Characterization and Implications for Antiviral Research. J Virol 89:8292-303.
21. Lampio A, Ahola T, Darzynkiewicz E, Stepinski J, Jankowska-Anyszka M, Kaariainen L. 1999. Guanosine nucleotide analogs as inhibitors of alphavirus mRNA capping enzyme. Antiviral Res 42:35-46.
22. Bougie I, Bisaillon M. 2004. The broad spectrum antiviral nucleoside ribavirin as a substrate for a viral RNA capping enzyme. J Biol Chem 279:22124-30.
23. Ferreira-Ramos AS, Li C, Eydoux C, Contreras JM, Morice C, Querat G, Gigante A, Perez Perez MJ, Jung ML, Canard B, Guillemot JC, Decroly E, Coutard B. 2019. Approved drugs screening against the nsP1 capping enzyme of Venezuelan equine encephalitis virus using an immuno-based assay. Antiviral Res 163:59-69.
24. Kaur R, Mudgal R, Narwal M, Tomar S. 2018. Development of an ELISA assay for screening inhibitors against divalent metal ion dependent alphavirus capping enzyme. Virus Res 256:209-218.
25. Bullard-Feibelman KM, Fuller BP, Geiss BJ. 2016. A Sensitive and Robust High-Throughput Screening Assay for Inhibitors of the Chikungunya Virus nsP1 Capping Enzyme. PLoS One 11:e0158923.
26. Feibelman KM, Fuller BP, Li L, LaBarbera DV, Geiss BJ. 2018. Identification of small molecule inhibitors of the Chikungunya virus nsP1 RNA capping enzyme. Antiviral Res 154:124-131.
27. Spuul P, Salonen A, Merits A, Jokitalo E, Kaariainen L, Ahola T. 2007. Role of the amphipathic peptide of Semliki forest virus replicase protein nsP1 in membrane association and virus replication. J Virol 81:872-83.
28. Mordecai EA, Paaijmans KP, Johnson LR, Balzer C, Ben-Horin T, de Moor E, McNally A, Pawar S, Ryan SJ, Smith TC, Lafferty KD. 2013. Optimal temperature for malaria transmission is dramatically lower than previously predicted. Ecol Lett 16:22-30.
29. Mordecai EA, Cohen JM, Evans MV, Gudapati P, Johnson LR, Lippi CA, Miazgowicz K, Murdock CC, Rohr JR, Ryan SJ, Savage V, Shocket MS, Stewart Ibarra A, Thomas MB, Weikel DP. 2017. Detecting the impact of temperature on transmission of Zika, dengue, and chikungunya using mechanistic models. PLoS Negl Trop Dis 11:e0005568.
30. Benelli G, Mehlhorn H. 2016. Declining malaria, rising of dengue and Zika virus: insights for mosquito vector control. Parasitol Res 115:1747-54.

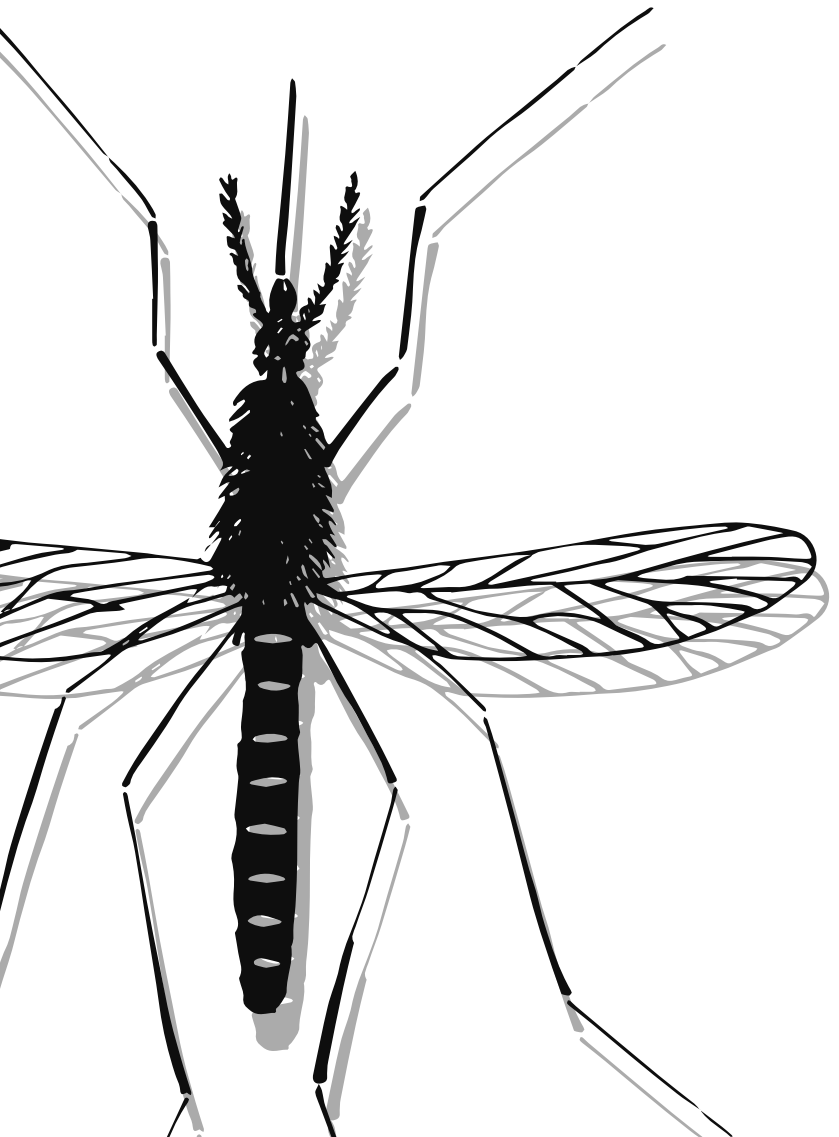

APPENDIX

English summary
Nederlandse samenvatting
List of publications
CV

English summary

This PhD thesis is dedicated to the development of novel antiviral agents against Chikungunya virus (CHIKV). CHIKV is a reemerging mosquito-borne virus causing an arthritis-like disease that is characterized by abrupt fever, malaise, and chronic joint and muscle pain. The high morbidity associated with Chikungunya fever and the negative impact on human health underscore the need to develop an effective antiviral therapy and other control measures. This PhD thesis presents a series of experimental studies focused on the identification of novel small molecules with CHIKV inhibitory activity and the elucidation of their mode of action. Importantly, the results in this thesis demonstrate that CHIKV nonstructural protein 1 (nsP1) represents a suitable target for antiviral drug development. CHIKV nsP1 is a multi-enzymatic protein involved in CHIKV RNA capping and in the attachment of the replication complex to the intracellular compartments where viral RNA synthesis occurs, the so-called 'spherules'. The cap structure plays many important roles in the CHIKV replication cycle. It protects viral mRNA from degradation by host exonucleases and from recognition by the host innate immune sensors, and it enables efficient translation of viral mRNAs by host ribosomes.

The introduction of this thesis (**Chapter 1**) provides a broad overview on CHIKV biology, replication cycle and pathogenesis. This chapter further discusses CHIKV evolution and spread, transmission by mosquito vectors, and disease manifestations including acute and chronic complications. It concludes with an overview of important control measures such as vector control, vaccine development and treatment with antiviral drugs and monoclonal antibodies. **Chapter 2** provides specific insights into the development of small-molecule CHIKV inhibitors, placing emphasis on the target(s) of these compounds, their modes of action, and mechanisms of antiviral drug resistance. Topics of interest related to CHIKV antiviral drug discovery, including the choice of cell lines and animal models for CHIKV antiviral drug research, are also discussed. **Chapters 3-6** of this thesis present in-depth experimental findings regarding the identification and the mode of action of CHIKV nsP1-targeting compounds. More specifically, the rational design, selection and validation of 6'fluorinated-aristeromycin and 6'-fluorinated-homoaristeromycin analogues as CHIKV inhibitors are described in **Chapter 3**. The identification and the mode of action of two adenosine analogues, 6'-β-fluoro-homoaristeromycin and 6'-fluoro-homoneplanocin A (FHNA), are discussed in **Chapter 4**. Furthermore, this chapter describes the identification of CHIKV nsP1 as the viral target of these compounds by selection of compound-resistant variants and

production of recombinant mutants by reverse genetics. The antiviral effect of FHNA was also supported by enzymatic assays with purified wild-type and mutant Semliki Forest virus (SFV) nsP1 for confirmation of target specificity. **Chapter 5** presents a study on other potent inhibitors of CHIKV replication belonging to the CHVB series. These compounds with novel chemical moieties strongly inhibit early stages of CHIKV replication in a similar manner to the previously described MADTP series. Selection of escape mutants and reverse genetics identified CHIKV nsP1 as the viral target of the CHVB compounds. Their antiviral activity was also demonstrated in enzymatic assays with purified Venezuelan Equine Encephalitis virus and SFV nsP1. **Chapter 6** describes the results of a first-of-its-kind molecular docking study with a CHIKV nsP1 cryo-EM structure and CHIKV nsP1 inhibitors. It demonstrates that the inhibitors can be grouped into different functional classes based on their modes of action. Using the oligomeric CHIKV nsP1 cryo-EM structure, the CHVB and MADTP compounds are predicted to bind at the active site of the capping domain, while FHNA is predicted to bind in a secondary binding pocket in the membrane binding and oligomerization domain. These findings provide the basis for further exploration of the precise binding and inhibitory activity of these inhibitors in CHIKV-infected cells. Lastly, **Chapter 7** places the results from these studies in the context of the published literature and discusses the latest developments in the field as well as some unexpected findings.

In conclusion, this PhD thesis demonstrates the potential for developing combination therapy consisting of small molecule inhibitors with different targets for prevention and treatment of CHIKV infections. Furthermore, combination therapy could increase the barrier to resistance as the rapid emergence of drug resistance still remains a major obstacle in the development of effective antiviral therapy. Last but not least, arboviruses such as CHIKV will continue to (re)emerge in the future due to their unpredictable epidemiology, substantiating the need for the development of antiviral treatment in addition to effective vaccines.

Nederlandse samenvatting

Het in dit proefschrift beschreven onderzoek is gericht op de ontwikkeling van nieuwe antivirale middelen tegen Chikungunya virus (CHIKV). CHIKV is een terugkerend probleem dat door muggen wordt overgedragen, en in mensen een op artritis lijkende ziekte veroorzaakt die gekenmerkt wordt door plotselinge koorts, algehele malaise en spier- en gewrichtspijn. De negatieve invloed op de menselijke gezondheid en de hoge morbiditeit geassocieerd met 'Chikungunya koorts', onderstrepen het belang van de ontwikkeling en het ter beschikking komen van effectieve antivirale therapieën en andere inperkingsmaatregelen. Dit proefschrift beschrijft een aantal experimentele studies gericht op het identificeren van nieuwe kleine moleculen die CHIKV replicatie remmen en het ontrafelen van de onderliggende moleculaire mechanismen. Een belangrijke conclusie is dat het niet-structurele eiwit 1 (nsP1) van CHIKV een geschikt doelwit is voor de ontwikkeling van antivirale middelen. Het CHIKV nsP1 is een eiwit met meerdere enzymatische activiteiten dat betrokken is bij CHIKV 'RNA capping' en het aanhechten van het replicatiecomplex aan intracellulaire compartimenten waar de RNA synthese plaatsvindt, de zogeheten 'spherules'. De structuur van de cap is belangrijk voor verschillende aspecten van de CHIKV replicatiecyclus. De cap zorgt ervoor dat het virale RNA niet wordt herkend door de aangeboren immuunrespons van de gastheer, en dat het RNA beschermd is tegen degradatie door exonucleasen van de gastheer. Bovendien is de cap essentieel voor de efficiënte translatie van virale mRNAs door gastheer ribosomen.

De introductie van dit proefschrift (**hoofdstuk 1)** geeft een algemeen overzicht van de biologie, de replicatiecyclus en de pathogenese van CHIKV. Dit hoofdstuk beschrijft bovendien de evolutie en verspreiding van CHIKV, de transmissie door muggenvectoren en de acute- en chronische complicaties na manifestatie van de door CHIKV veroorzaakte ziekte. Dit hoofdstuk sluit af met een overzicht van belangrijke mogelijke inperkingsmaatregelen, zoals het beperken van de muggenpopulaties, de ontwikkeling van vaccins en de behandeling van patiënten met antivirale geneesmiddelen en monoclonale antilichamen. **Hoofdstuk 2** biedt inzichten in de ontwikkeling van kleine moleculen die CHIKV replicatie remmen, waarbij de nadruk wordt gelegd op het doelwit van deze moleculen, hun werkingswijze en hoe deze invloed hebben op de ontwikkeling van resistentie tegen antivirale geneesmiddelen. Onderwerpen van belang voor het ontdekken van antivirale middelen tegen CHIKV, waaronder de keuze van cellijnen en diermodellen, worden tevens in dit hoofdstuk

beschreven. De **hoofdstukken 3-6** van dit proefschrift presenteren uitgebreid de experimentele bevindingen met betrekking tot de identificatie en werkingswijze van verschillende antivirale middelen die nsP1 als doelwit hebben. In het bijzonder beschrijft **hoofdstuk 3** het rationele ontwerp, de selectie en de validatie van 6'-β-fluoro-homoaristeromycin en 6'-fluoro-homoneplanocin A (FHNA) analogen als remmer van CHIKV. De identificatie en werkingswijze van deze twee adenosine analogen worden beschreven in **hoofdstuk 4**. Bovendien beschrijft dit hoofdstuk de identificatie van CHIKV nsP1 als doelwit voor deze antivirale middelen op basis van selectie van compound-resistente varianten, en productie van recombinante virusmutanten door middel van 'reverse genetics'. Het antivirale effect en de specificiteit van FHNA worden in dit hoofdstuk aangetoond door middel van enzymatische proeven die gebruik maken van opgezuiverd wildtype en mutant Semliki Forest virus (SFV) nsP1. **Hoofdstuk 5** beschrijft een onderzoek naar andere moleculen, behorende tot de CHVB series, die effectief de replicatie van CHIKV remmen. Deze remmers behoren tot een groep nieuwe chemische verbindingen en remmen de replicatie van CHIKV sterk in een vroeg stadium van infectie. Hun werkingswijze lijkt veel op die van de eerder gepubliceerde MADTP serie. Door de selectie van resistent geworden mutanten (escape mutants) en reverse genetics is aangetoond dat nsP1 het virale doelwit van CHVB is. Het antivirale effect van CHVB werd ook onderbouwd door middel van enzymatische proeven met gezuiverd nsP1 van Venzuelan Equine Encephalitis virus en SFV. In **hoofdstuk 6** worden de resultaten van een unieke moleculaire 'docking' studie beschreven, die gebruik maakt van de cryo-EM structuur van CHIKV nsP1 en CHIKV nsP1 remmers. Dit onderzoek toont aan dat de verschillende moleculen in verschillende functionele klassen kunnen worden ingedeeld op basis van hun werkingswijze. Door gebruik te maken van de oligomere cryo-EM structuur van CHIKV nsP1 wordt voorspeld dat de CHVB en MADTP compounds aan het katalytische centrum van het nsP1 capping domein binden, terwijl FHNA compounds voorspeld worden te binden aan een secundaire binding 'pocket' in de domeinen die betrokken zijn bij membraanbinding en oligomerizatie. Deze resultaten bieden de basis voor verder onderzoek naar de exacte binding die plaatsvindt en de manier waarop deze moleculen de CHIKV replicatie in geïnfecteerde cellen remmen. Tot slot plaatst **hoofdstuk 7** de resultaten van deze verschillende studies in de context van de gepubliceerde literatuur en bediscussieert daarbij de meest recente ontwikkelingen in het veld, alsook een aantal onverwachte bevindingen die gedaan zijn bij het onderzoek uitgevoerd gedurende dit promotietraject.

Samenvattend beschrijft dit proefschrift de potentie om een combinatietherapie te ontwikkelen om infecties met CHIKV te voorkomen en te behandelen, waarbij kleine moleculen die verschillende virale doelwitten hebben worden gecombineerd. Aangezien het snelle ontstaan van resistentie de ontwikkeling van effectieve antivirale therapieën kan bemoeilijken, zou een dergelijke combinatietherapie bovendien een extra barrière kunnen vormen voor dit soort complicaties. Arbovirussen als CHIKV zullen vanwege hun onvoorspelbare epidemiologie in de toekomst blijven opleven, wat de noodzaak voor de ontwikkeling van antivirale behandelingen naast effectieve vaccins onderstreept.

List of publications

Kovacikova K and van Hemert MJ. Small-Molecule Inhibitors of Chikungunya Virus: Mechanisms of Action and Antiviral Drug Resistance. Antimicrob Agents Chemother. 2020 Nov 17;64(12):e01788-20.

Abdelnabi R*, **Kovacikova K***, Moesslacher J, Donckers K, Battisti V, Leyssen P, Langer T, Puerstinger G, Quérat G, Li C, Decroly E, Tas A, Marchand A, Chaltin P, Coutard B, van Hemert M, Neyts J, Delang L. Novel Class of Chikungunya Virus Small Molecule Inhibitors That Targets the Viral Capping Machinery. Antimicrob Agents Chemother. 2020 Jun 23;64(7):e00649-20.
(* contributed equally)

Albulescu IC, White-Scholten L, Tas A, Hoornweg TE, Ferla S, **Kovacikova K**, Smit JM, Brancale A, Snijder EJ, van Hemert MJ. Suramin Inhibits Chikungunya Virus Replication by Interacting with Virions and Blocking the Early Steps of Infection. Viruses. 2020 Mar 17;12(3):314.

Kovacikova K, Morren BM, Tas A, Albulescu IC, van Rijswijk R, Jarhad DB, Shin YS, Jang MH, Kim G, Lee HW, Jeong LS, Snijder EJ, van Hemert MJ. 6'-β-Fluoro-Homoaristeromycin and 6'-Fluoro-Homoneplanocin A Are Potent Inhibitors of Chikungunya Virus Replication through Their Direct Effect on Viral Nonstructural Protein 1. Antimicrob Agents Chemother. 2020 Mar 24;64(4):e02532-19.

Shin YS, Jarhad DB, Jang MH, **Kovacikova K**, Kim G, Yoon JS, Kim HR, Hyun YE, Tipnis AS, Chang TS, van Hemert MJ, Jeong LS. Identification of 6'-β-Fluoro-Homoaristeromycin as a Potent Inhibitor of Chikungunya Virus Replication. Eur J Med Chem. 2020 Feb 1;187:111956.

Yoon JS, Kim G, Jarhad DB, Kim HR, Shin YS, Qu S, Sahu PK, Kim HO, Lee HW, Wang SB, Kong YJ, Chang TS, Ogando NS, **Kovacikova K**, Snijder EJ, Posthuma CC, van Hemert MJ, Jeong LS. Design, Synthesis, and Anti-RNA Virus Activity of 6'-Fluorinated-Aristeromycin Analogues. Med Chem. 2019 Jul 11;62(13):6346-6362.

Hussain S, Turnbull ML, Wise HM, Jagger BW, Beard PM, **Kovacikova K**, Taubenberger JK, Vervelde L, Engelhardt OG, Digard P. Mutation of Influenza A Virus PA-X Decreases Pathogenicity in Chicken Embryos and Can Increase the Yield ofReassortant Candidate Vaccine Viruses. J Virol. 2019 Jan 4;93(2):e01551-18.

Hwu JR, Gupta NK, Tsay SC, Huang WC, Albulescu IC, **Kovacikova K**, van Hemert MJ. Bis(benzofuran-thiazolidinone)s and Bis(benzofuran-thiazinanone)s as Inhibiting Agents for Chikungunya Virus. Antiviral Res. 2017 Oct;146:96-101.

Albulescu IC, **Kovacikova K**, Tas A, Snijder EJ, van Hemert MJ. Suramin Inhibits Zika Virus Replication by Interfering with Virus Attachment and Release of Infectious Particles. Antiviral Res. 2017 Jul;143:230-236

Curriculum Vitae

Kristina Kovacikova was born on 24 September 1991 in Zilina, Czechoslovakia (now Slovakia). She obtained Slovak-Spanish bilingual education at the Bilingual Secondary Grammar School in Zilina before starting her undergraduate studies in 2011. In June 2015, Kristina graduated from the University of Edinburgh, United Kingdom, with a first-class Bachelor of Science with Honors degree in Biomedical Sciences (Infectious Diseases). During her final year, she performed an internship at the Roslin Institute under the supervision of Dr Nikki Smith and Prof Paul Digard. In the Honors project, she investigated the antiviral effect of heat shock protein inhibitors on the replication of influenza A viruses. Between 2013 and 2014, Kristina participated in the International Exchange Program at the National University of Singapore and performed an internship at Dr Katja Fink's laboratory at the Agency for Science, Technology and Research (A*STAR). There, she worked on elucidating the role of B cells in protective immunity against dengue virus infection.

In September 2015, Kristina obtained a position as a PhD student within the Marie Skłodowska-Curie Initial Training Network ANTIVIRALS at the Leiden University Medical Center, the Netherlands, under the supervision of Dr Martijn van Hemert and Prof Eric Snijder. In her PhD research project, she studied the antiviral effect of chikungunya virus small molecule inhibitors on nonstructural protein 1. This research has led to the identification of novel chikungunya virus nonstructural protein 1-targeting compounds and characterization of their mechanisms of action. During her PhD research project, Kristina benefited from the excellent training program provided by both the academic and industrial partners of the ANTIVIRALS consortium. Since May 2020, Kristina has been continuing her scientific career as a postdoctoral researcher at the same department, focusing on the development of antiviral strategies against Severe acute respiratory syndrome coronavirus 2 in animal models. From June 2021, Kristina will join the German biopharmaceutical company CureVac as a Scientist Viral & Infectious Diseases where she will focus on developing mRNA vaccines against emerging viral pathogens.